



TECHNICAL WORKSHOP

Optimising steels microstructure and surface integrity to face new challenges in Additive Manufacturing



Funded by
the European Union

SuPreAM project has received funding from the European Union's
Research Fund for Coal and Steel (RFCS): project num. 101112346



Funded by
the European Union

Predictive simulation of finishing operations in steel Additive Manufacturing for optimal Surface integrity

SuPreAM and the Tribological Study on Burnished Surface of Additive Manufactured Metal

Adrián Travieso
Scientific Researcher, Eurecat Technology Centre
adrian.travieso@eurecat.org

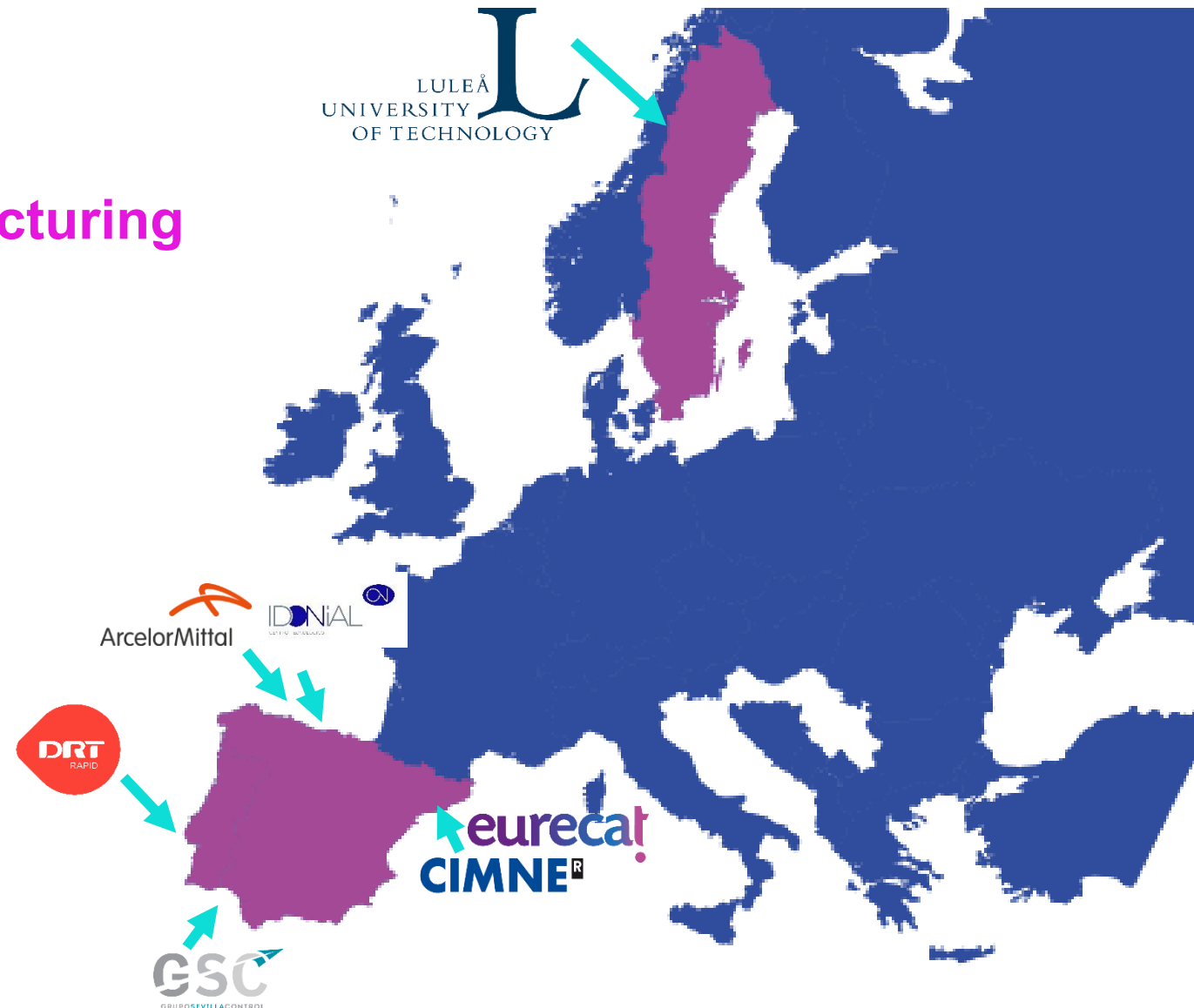
eurecat!

- 01** Project Overview
- 02** SuPreAM objectives
- 03** SuPreAM activities
- 04** WP5 - Surface integrity characterization
- 05** Vibration Assisted Ball Burnishing (VABB)
- 06** Results

Project overview

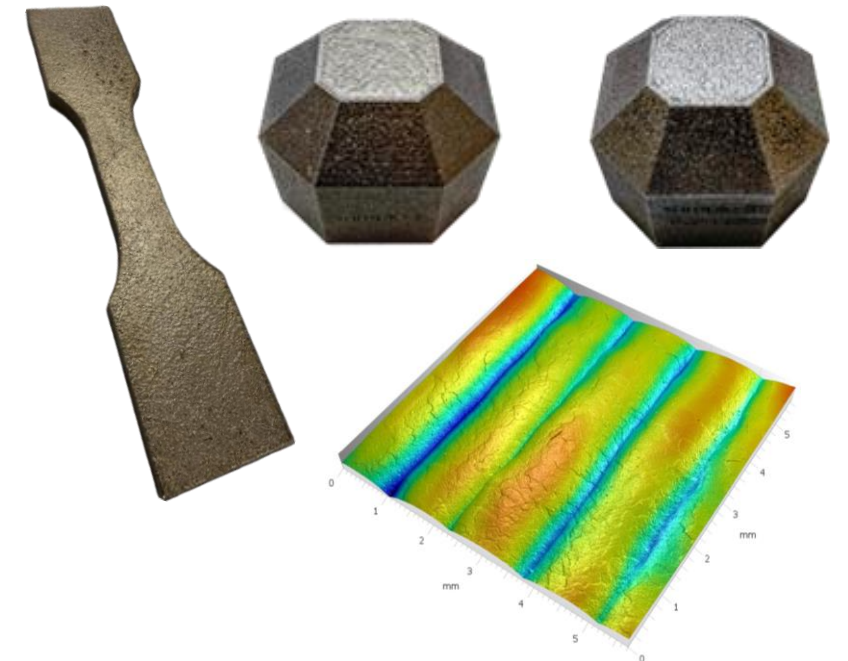
PREdictive simulation of finishing operations in steel Additive Manufacturing for optimal SURface integrity

- Coordinator: Eurecat Technology Centre
- Call: RFCS-2022
- Start date: 1st July 2023
- End date: 31st December 2026
- Total costs: 2 608 967.35 € (budget),
1 565 380.41 € (grant)



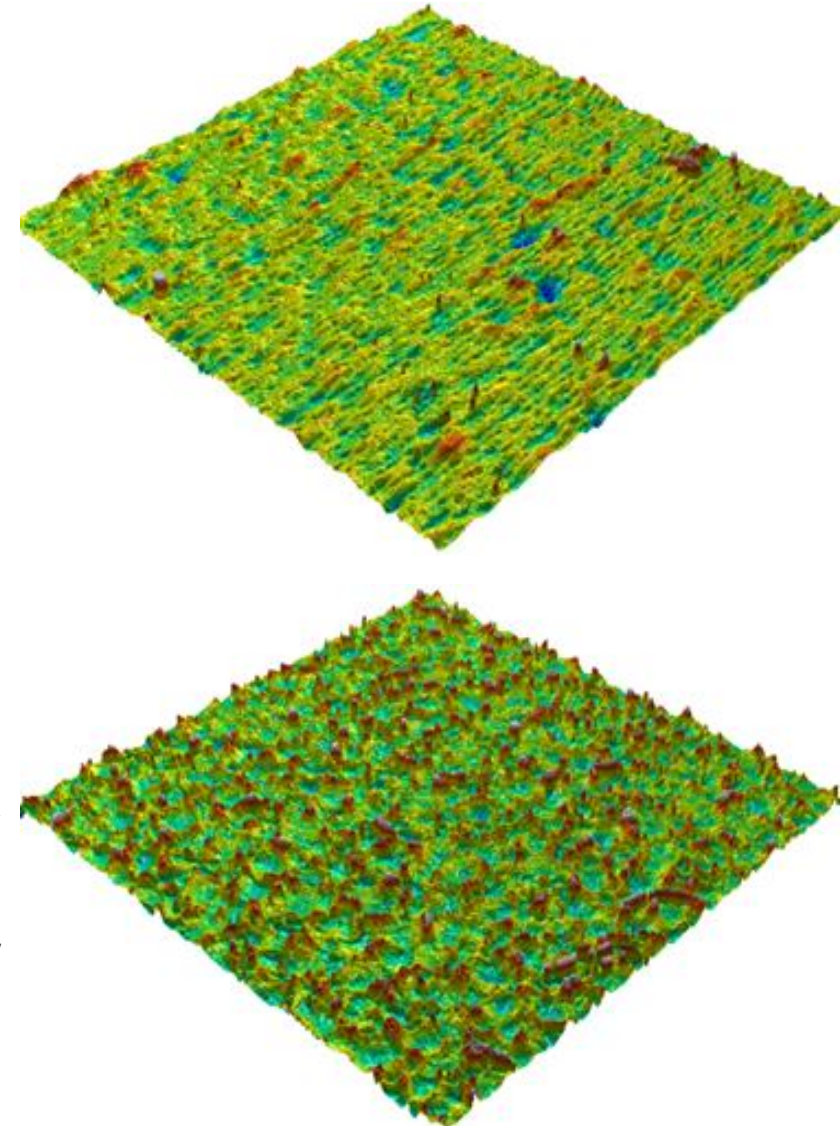
Challenge identification

- **Challenge 1:** Limited surface quality and dimensional accuracy of AMed steel components.
- **Solution 1:** SuPreAM develops a predictive model to quantify surface roughness and residual stresses, enabling targeted finishing strategies that enhance surface integrity and meet tight tolerance requirements.
- **Challenge 2:** Poor machinability of AMed steels due to inhomogeneities such as porosity and anisotropic microstructures.
- **Solution 2:** The project investigates tool wear mechanisms and cutting dynamics specific to AMed steels, optimizing machining parameters and tool selection to improve process reliability and part quality.



Challenge identification

- **Challenge 3:** High scrap rates and repeated reprocessing during finishing operations, increasing manufacturing costs.
- **Solution 3:** By identifying critical parameters affecting surface integrity and linking them to functional performance, SuPreAM enables first-time-right manufacturing, reducing scrap by up to 35% and defective parts below 2%.
- **Challenge 4:** Limited industrial knowledge on suitable finishing strategies (machining and polishing) for AMed components.
- **Solution 4:** SuPreAM will generate in-depth knowledge on how printing parameters, machining strategies, and polishing processes affect surface integrity—providing industry with clear guidelines for post-processing AMed steels.



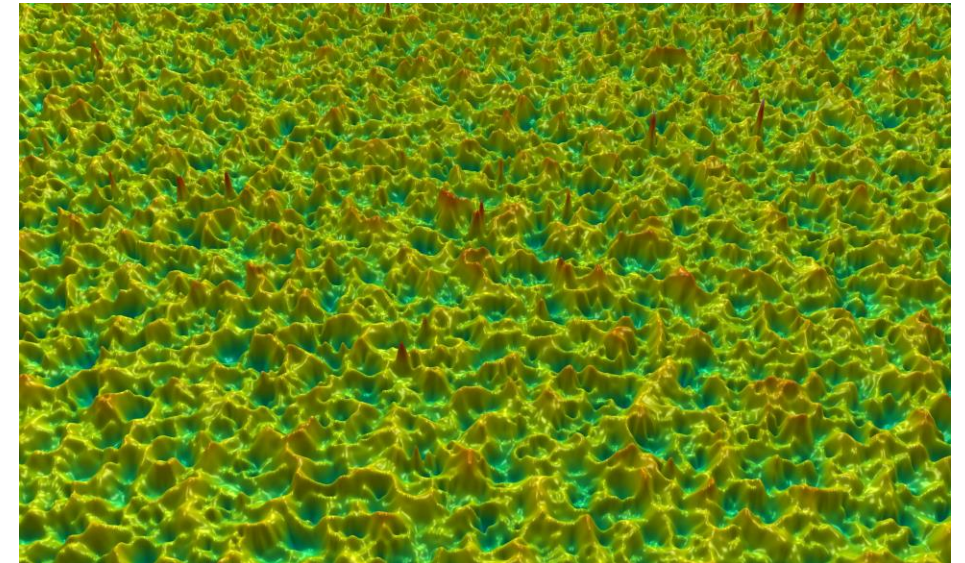
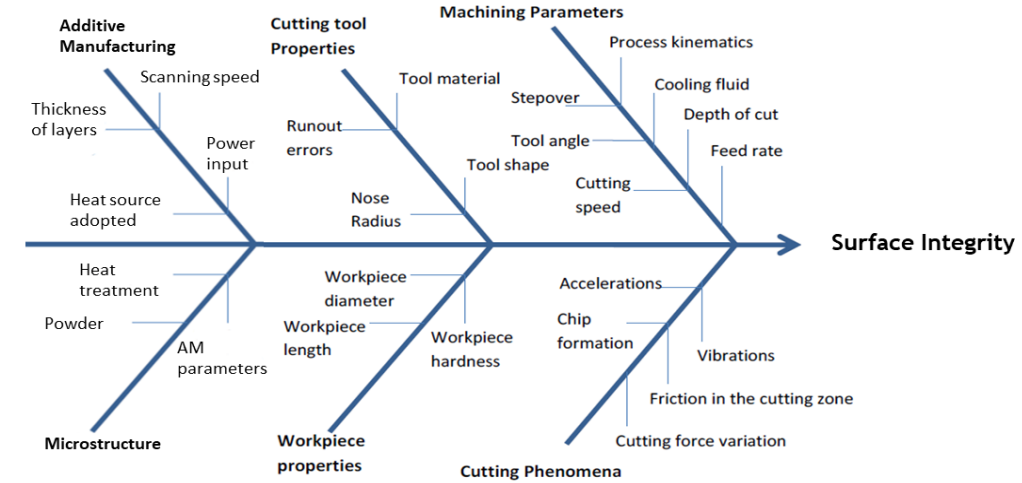
SuPreAM objectives

Our objectives

To **optimize the surface integrity** of Additive Manufactured and Machined steel components and to reduce manufacturing expenditures at the steel industrial sector through the **minimization of the material scrap up to 35%** and **reducing the number of re-processing loops** during finishing operations **keeping defective parts below 2%** of additive manufactured components.

The main objectives to be tackled to this purpose can be summarised as follows:

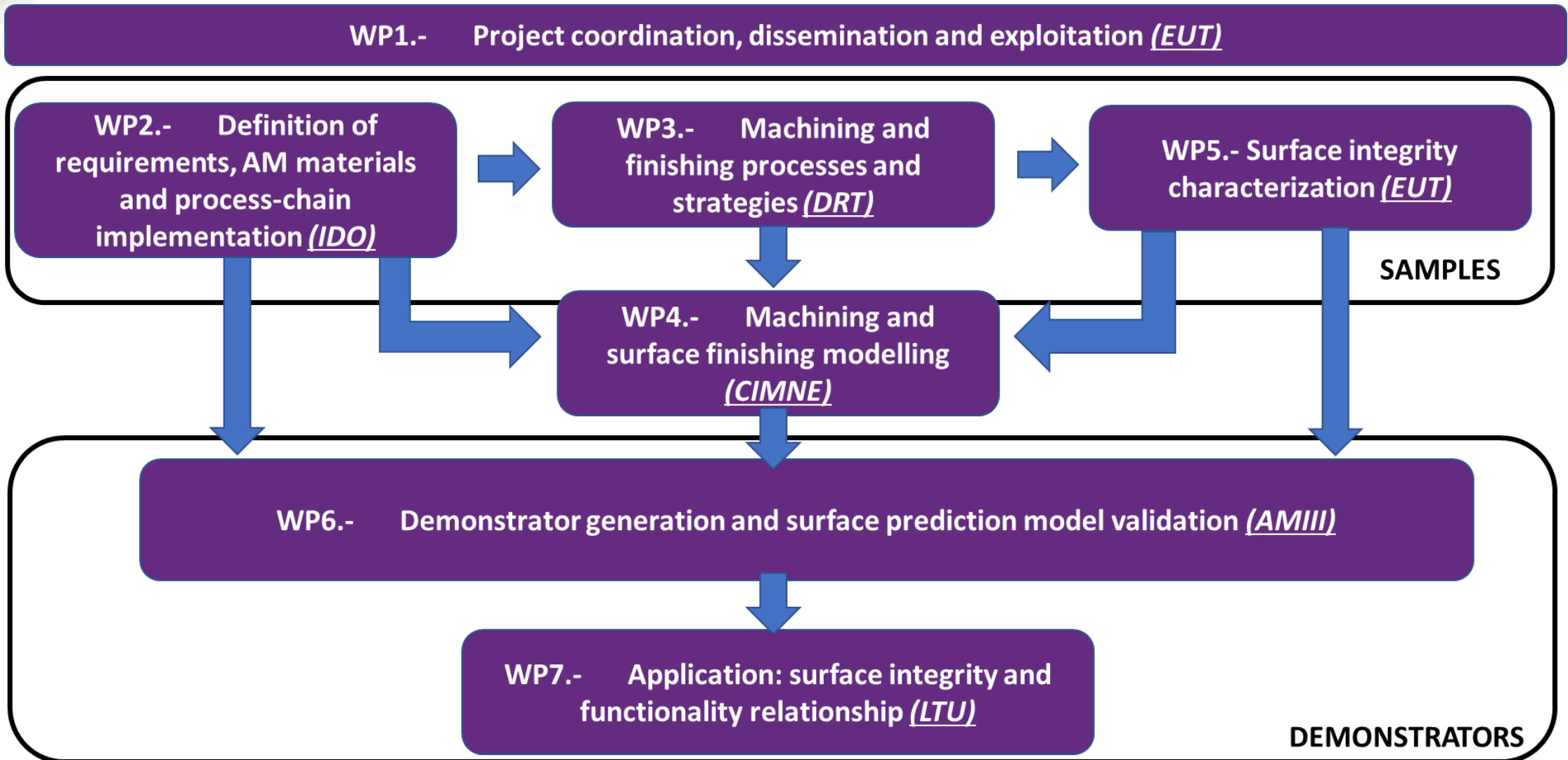
- **#OB1:** To develop and improve the performance and capabilities of a predictive simulation model of finishing operations in steel Additive Manufacturing (AM).
- **#OB2:** To optimize the surface integrity of steel additive manufactured (AMed) components.



Our objectives

- **#SO1:** To develop an in-house software module for the simulation of milling/turning and finishing processes based on particle finite element method (PFEM).
- **#SO2:** To develop an in-house software module for the simulation of the electrical discharge machining (EDM) process.
- **#SO3:** To evaluate steel grades for surface integrity optimization of AMed and machined parts and to implement novel lean maraging steel in AM.
- **#SO4:** To determine the influence of steel AM technology, machining strategies, machining process parameters and cutting tool materials on machinability and surface properties of AMed components.
- **#SO5:** To identify and describe the most significant AMed and machined component characteristics concerning surface topography, microstructure, metallurgical and mechanical properties through advanced characterization techniques.
- **#SO6:** To establish surface integrity and functionality relationship: identification of main parameters affecting surface integrity.

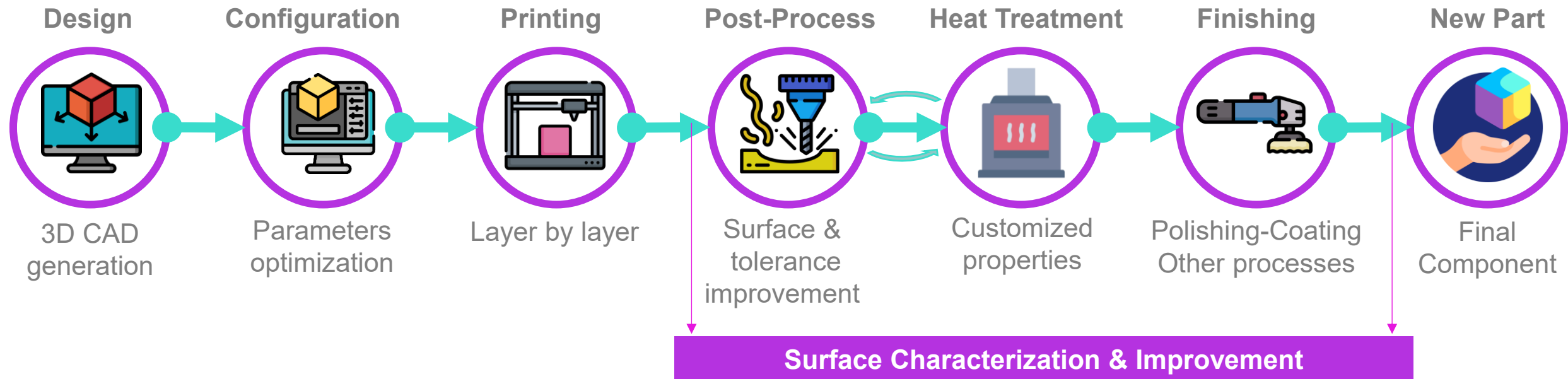
Activities



WP5 - Surface integrity characterization

Project Work Package (WP5)

WP5 Surface integrity characterization: AMed Machined samples will be characterized under the topics: surface topography, microstructural and metallurgical changes and mechanical changes. Specific tests will be designed to establish surface roughness and component functionality relationship. Cutting tools wear and failure mechanisms will be identified and characterized.





TECHNICAL WORKSHOP

Optimising steels microstructure and surface integrity to face new challenges in Additive Manufacturing



Funded by
the European Union

SuPreAM project has received funding from the European Union's
Research Fund for Coal and Steel (RFCS): project num. 101112346



Funded by
the European Union

Predictive simulation of finishing operations in steel Additive Manufacturing for optimal Surface integrity

3D Numerical Modelling of the Cutting Process: Recent Developments

PRESENTER NAME: Josep Maria Carbonell

COMPANY: CIMNE

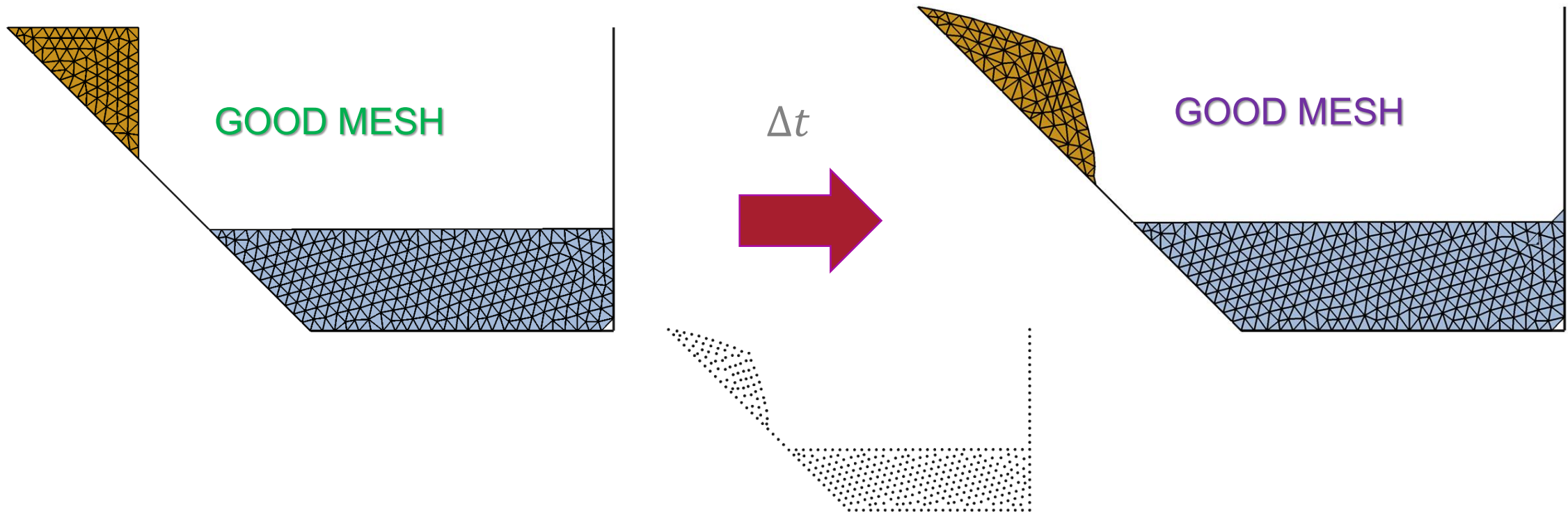
EMAIL: cpuigbo@cimne.upc.edu

CIMNE^R

International Centre
for Numerical Methods in Engineering

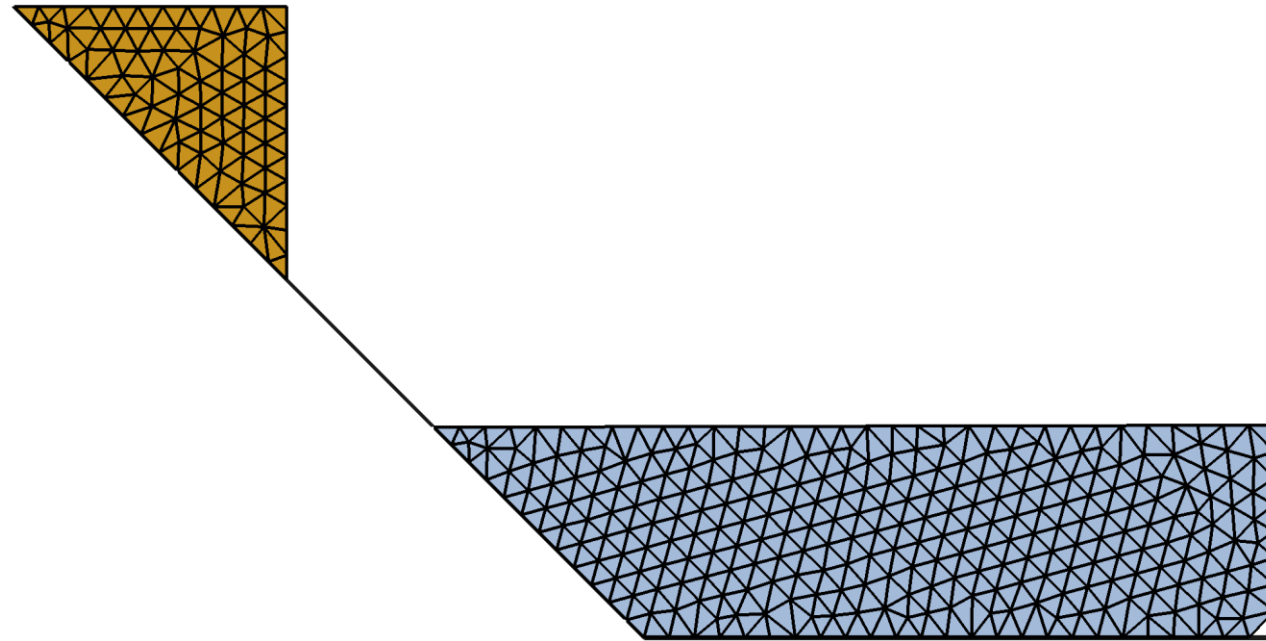
- 01** Key features of the PFEM
- 02** The PFEM applied to the modelling of Machining
- 03** Problems, solutions and examples
- 04** Conclusions and Future research lines

KEY FEATURES OF THE PFEM



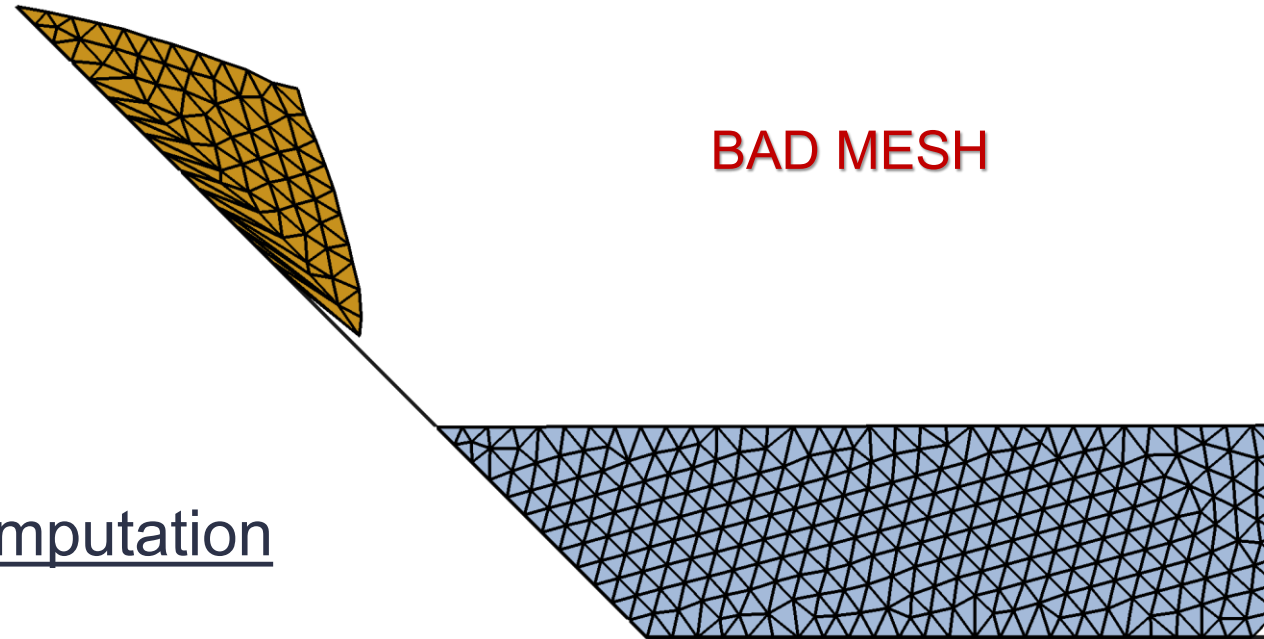
1

Mesh at t^n



2

Mesh at t^{n+1}
after FEM computation



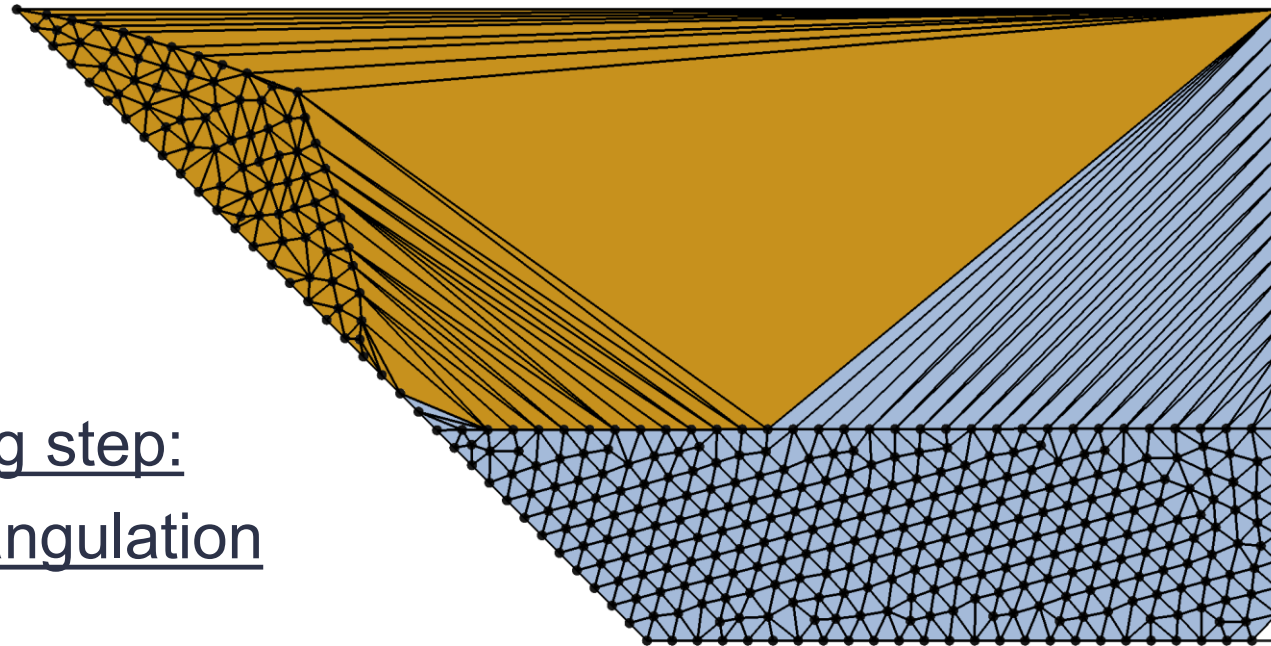
3

1st remeshing step:
Erase all elements,
maintain the nodes



4

2st remeshing step:
Delaunay triangulation



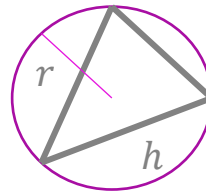
5

GOOD MESH

3st remeshing step:
Alpha Shape Method

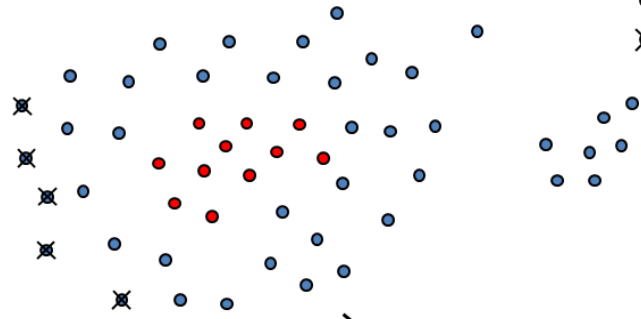
Erase element if:

$$r \geq \alpha \cdot h_{mean}$$

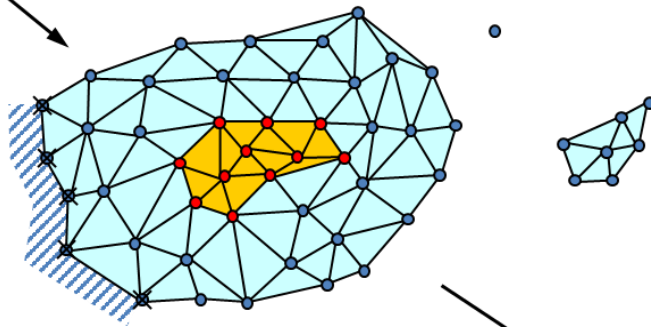


Initial cloud of nodes nC

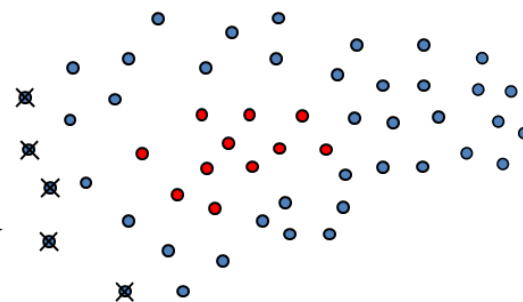
● Solid node
● Fluid node
✕ Fixed boundary node



Finite element mesh nM



New cloud of nodes ${}^{n+1}C$



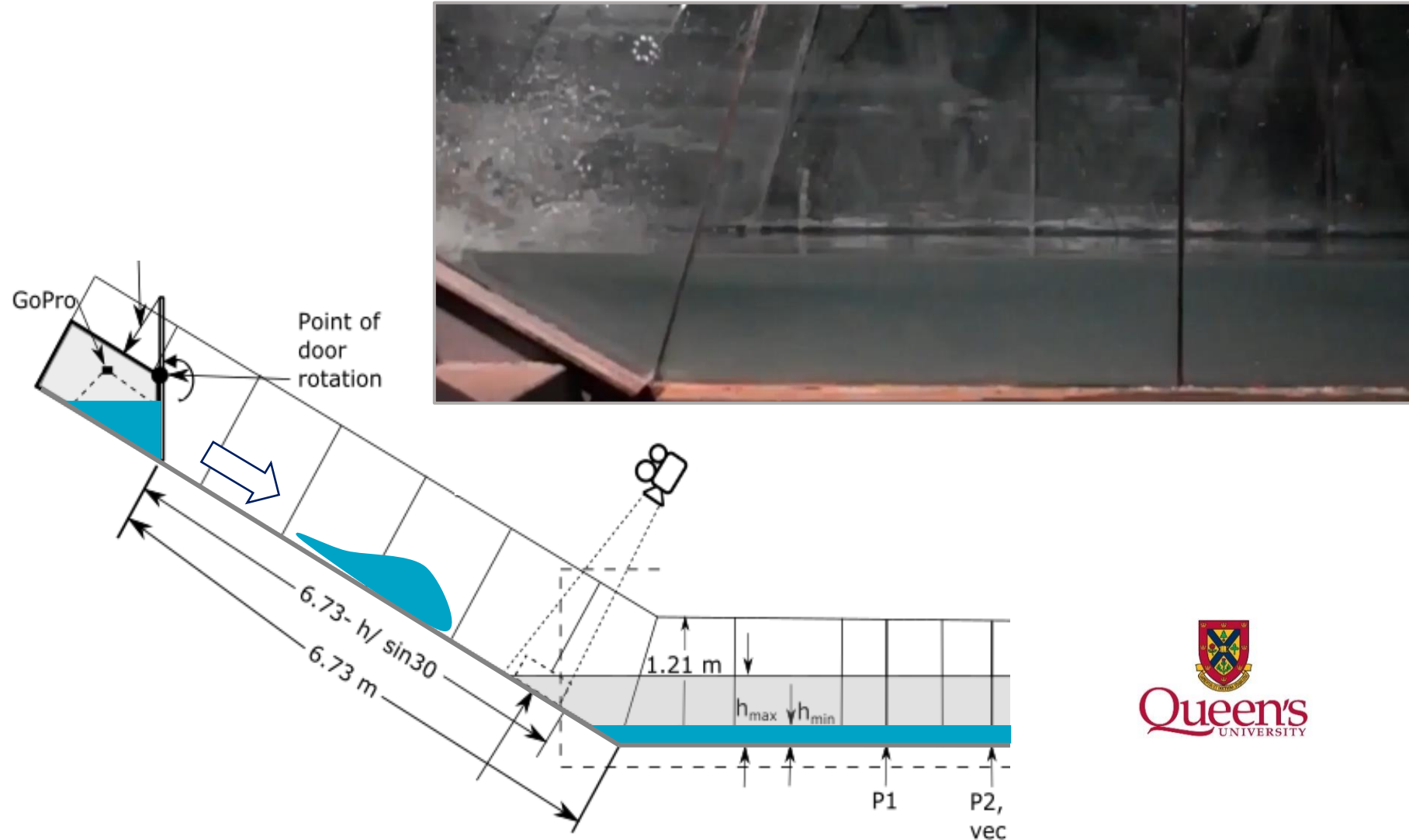
${}^n\mathbf{x}$,
 ${}^n\mathbf{u}$, ${}^n\mathbf{p}$

${}^{n+1}\mathbf{u}$, ${}^{n+1}\mathbf{p}$

${}^{n+1}\mathbf{x}$

Advantages:

- ✓ Allows to model severe changes of topology
- ✓ Uses standard **FEM theory** which means robustness and reliability in the solution
- ✓ Easy coupling with another techniques (e.g. FEM and DEM)



Mulligan, Franci, Celigueta, Take, *JGR, Oceans*, 2020





FLUID SOLVER

Navier Stokes equations for incompressible fluids (via FEM)

Linear momentum equations

$$\rho \dot{\mathbf{v}} - \operatorname{div}(\boldsymbol{\sigma}) - \mathbf{b} = \mathbf{0}$$

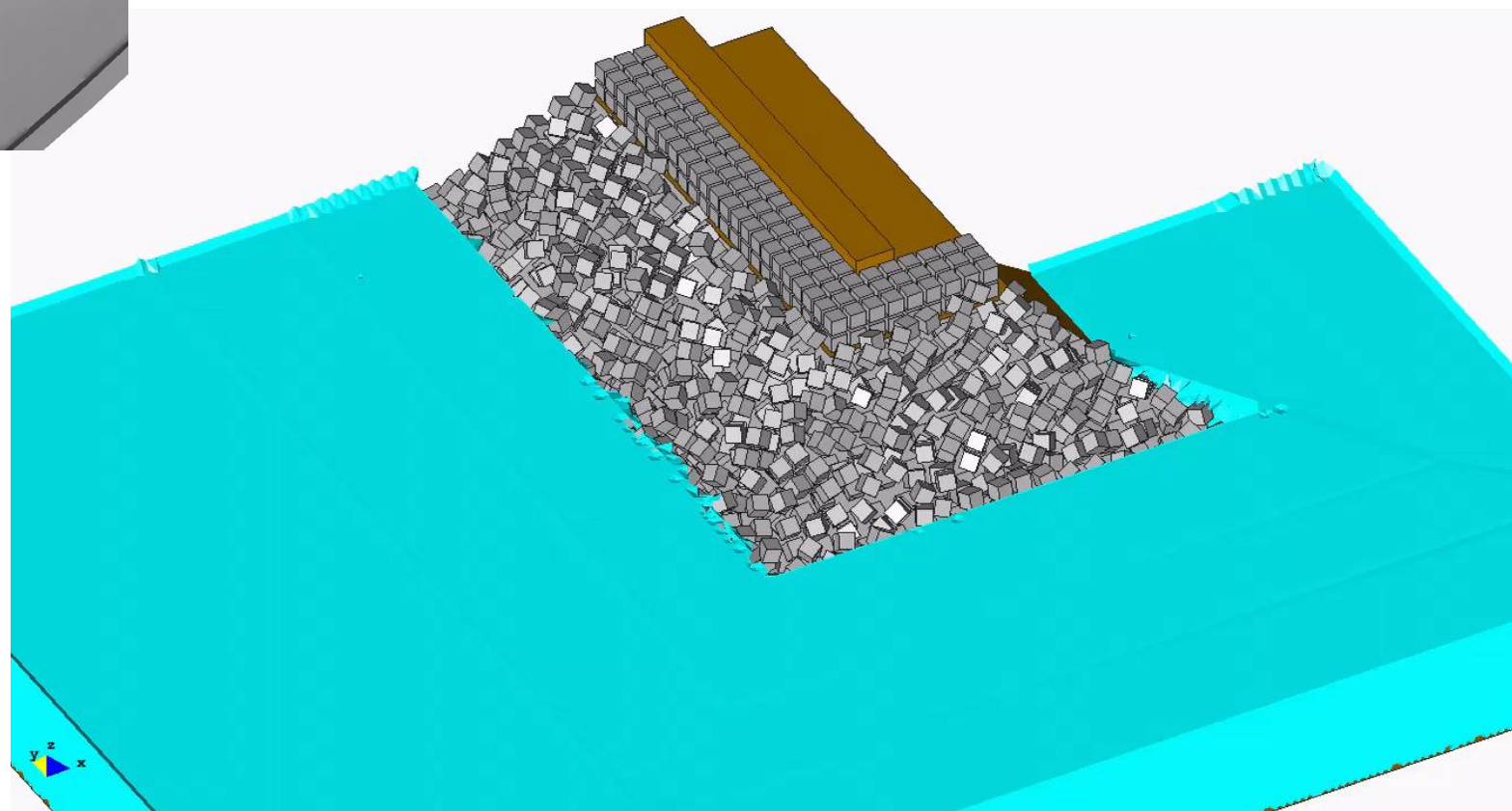
+ boundary conditions.

Continuity equation

$$\operatorname{div}(\mathbf{v}) = 0$$

→ incompressibility

☐ Fractional step predictor-multicorrector



- Governing equations for solids (via FEM):

Linear momentum equations

$$\rho \dot{\mathbf{v}} - \text{div}(\boldsymbol{\sigma}) - \mathbf{b} = \mathbf{0}$$

+ boundary conditions.

Continuity equation

$$\frac{1}{k} \dot{p} - \text{div}(\mathbf{v}) = 0$$

where k is the bulk modulus.

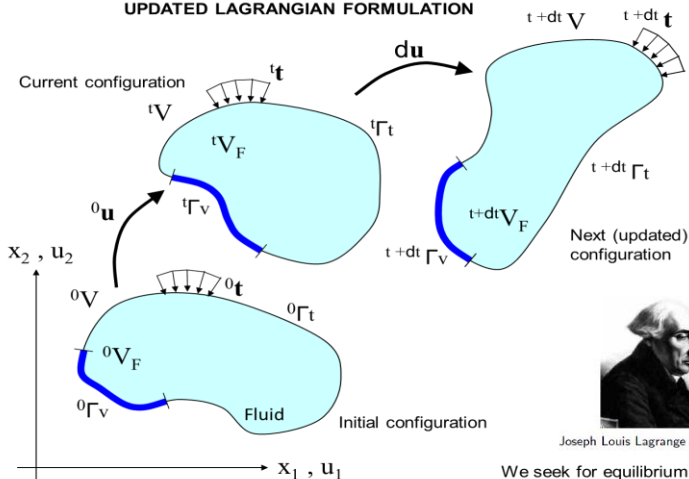
- Monolithic approach IMPLICIT (Lagrangian framework)
- Linear interpolation for displacement and pressure/jacobian
- Stabilization (PPP, FPL, FIC...)
- Hyper-elastoplasticity for solids
- Thermo-mechanical coupling:

Energy equation

$$\dot{e} + \text{div}(\mathbf{q}) = \mathcal{D}_{int} + r$$

Temperatures

UPDATED LAGRANGIAN FORMULATION



1. Isothermal elastoplastic problem

$$\dot{\mathbf{Z}} = \begin{bmatrix} \dot{\varphi} \\ \rho \dot{\mathbf{v}} \\ \dot{\theta} \end{bmatrix} = \begin{bmatrix} \mathbf{v}(\mathbf{x}, t) \\ \text{div}(\boldsymbol{\sigma}(\varphi, \theta, \lambda(\varphi, \theta))) \\ 0 \end{bmatrix} + \begin{bmatrix} 0 \\ \mathbf{b} \\ 0 \end{bmatrix}$$

2. Thermoplastic problem at a fixed configuration

$$\dot{\mathbf{Z}} = \begin{bmatrix} \dot{\varphi} \\ \rho \dot{\mathbf{v}} \\ \dot{\theta} \end{bmatrix} = \begin{bmatrix} 0 \\ 0 \\ -\text{div}(\mathbf{q}(\varphi, \theta, \lambda(\varphi, \theta))) + \mathcal{D}_{int} \end{bmatrix} + \begin{bmatrix} 0 \\ 0 \\ r \end{bmatrix}$$

$$\mathbf{F} = \mathbf{F}^e \mathbf{F}^p$$

1. Free energy function.

$$\hat{\psi} = \hat{T}(\theta) + \hat{M}(\theta, J^e) + \hat{U}(J^e) + \hat{W}(\bar{\mathbf{b}}^e) + \hat{K}(\bar{e}^p, \theta)$$

2. kirchhoff stress.

$$\begin{aligned}\boldsymbol{\tau} &= J^e p \mathbb{1} + \mathbf{s} \\ p &:= \left[-3 \alpha \kappa \frac{(1 - \ln(J^e))}{J^e} (\theta - \theta_0) + \kappa \ln(J^e) \right] \\ \mathbf{s} &:= \mu \operatorname{dev}(\bar{\mathbf{b}}^e)\end{aligned}$$

and the entropy

$$\begin{aligned}\eta &= \eta^p - \eta^e + \eta^t \\ \eta^e &:= -\partial_\theta \hat{T}(\theta) \\ \eta^t &:= -\partial_\theta \hat{M}(\theta, J^e) - \partial_\theta \hat{K}(\bar{e}^p, \theta)\end{aligned}$$

3. *Von Mises* yield criterion.

$$\Phi(\boldsymbol{\tau}, \bar{e}^p, \theta) = \|\operatorname{dev}(\boldsymbol{\tau})\| - \sqrt{\frac{2}{3}} (\sigma_y + \beta) \leq 0$$

4. Evolution equations $\lambda > 0, \quad \Phi \leq 0, \quad \lambda \Phi = 0$

$$\begin{aligned}\mathcal{L}_v \bar{\mathbf{b}}^e &= -2 \lambda J^{-\frac{2}{3}} \frac{1}{3} \operatorname{tr}(\bar{\mathbf{b}}^e) \mathbf{n} \\ \dot{\bar{e}}^p &= -\lambda \partial_\beta \Phi(\boldsymbol{\tau}, \bar{e}^p, \theta) \\ \dot{\eta}^p &= \lambda \partial_\theta \Phi(\boldsymbol{\tau}, \bar{e}^p, \theta)\end{aligned}$$

Allows the usage of:

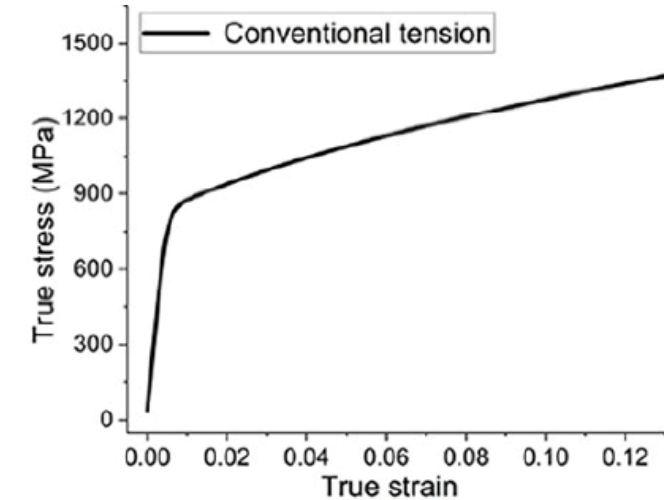
- Linear Elastic
- Hypo-Elastic
- Hyper-Elastic
- +
- Plasticity Models

- ✓ Advanced constitutive models used in the classical FEM.
- ✓ It allows the material modelling of any kind.
- ✓ It can include continuous damage and fracture

JOHNSON-COOK

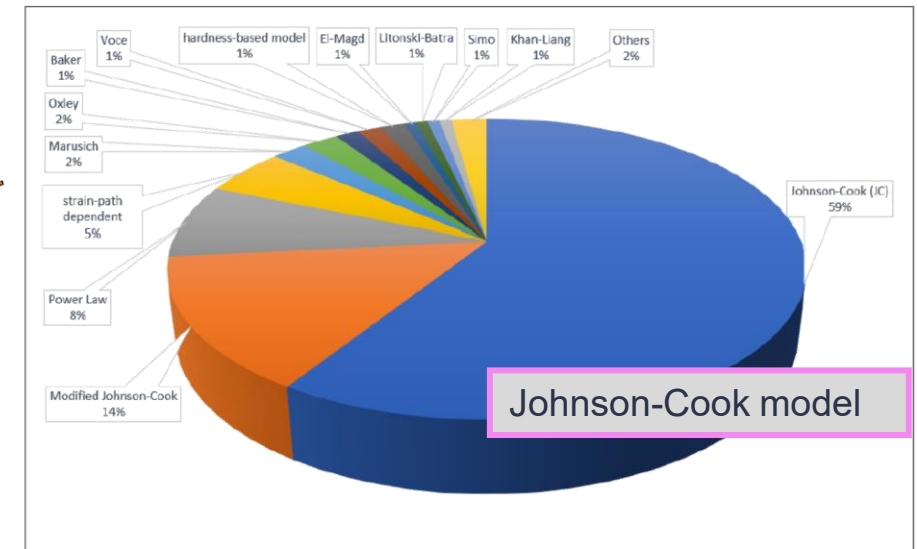
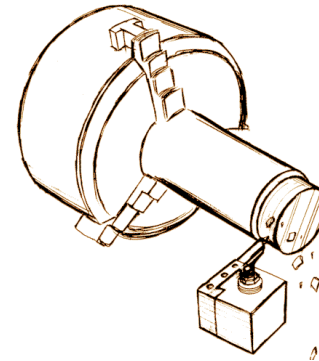
$$\sigma = [C_1 + C_2 \varepsilon_p^n] \left[1 + C_3 \ln \frac{\dot{\varepsilon}_p}{\dot{\varepsilon}_0} \right] \left[1 - \left(\frac{T - T_0}{T_m - T_0} \right)^m \right]$$

Fitting parameter in JC model by conventional tensile tests



Johnson-Cook (JC) constitutive model [1] as the base model:

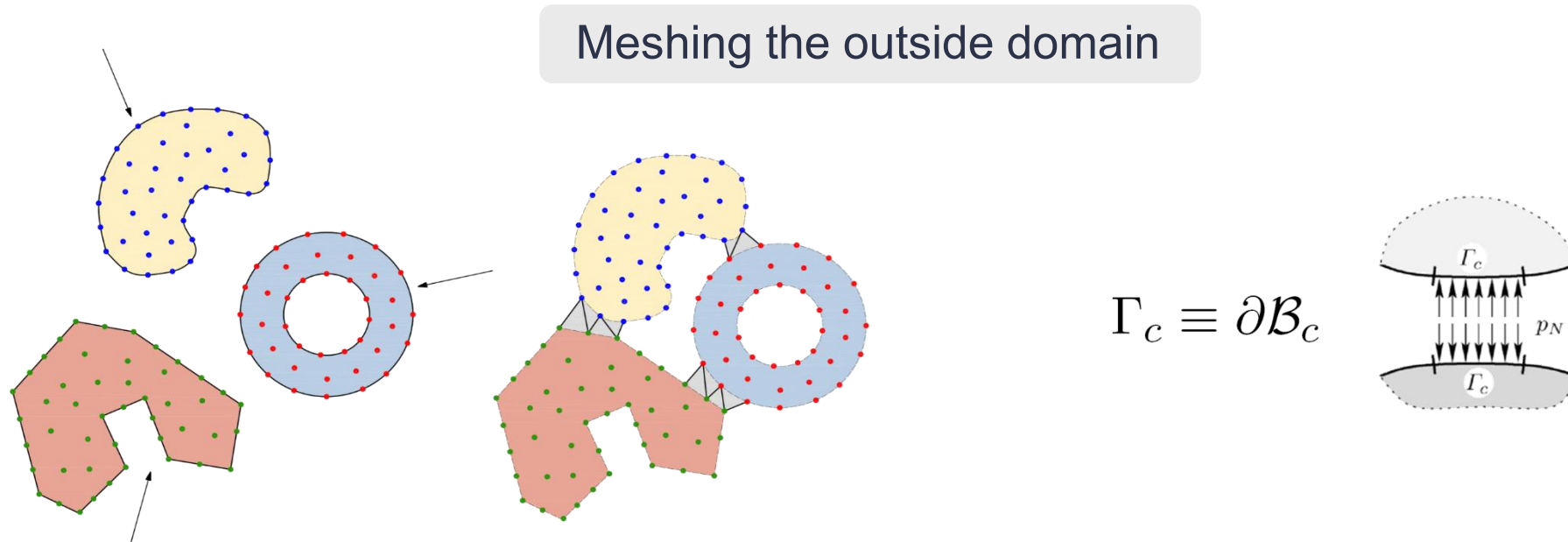
- ❑ The most used model in machining literature: The data is widely available
- ❑ Strain, strain rate and temperature dependent: Appropriate for machining
- ❑ Few number of parameters: easy to calibrate



[1] Johnson, Gordon R. "A constitutive model and data for materials subjected to large strains, high strain rates, and high temperatures." Proc. 7th Int. Sympo. Ballistics (1983): 541-547.

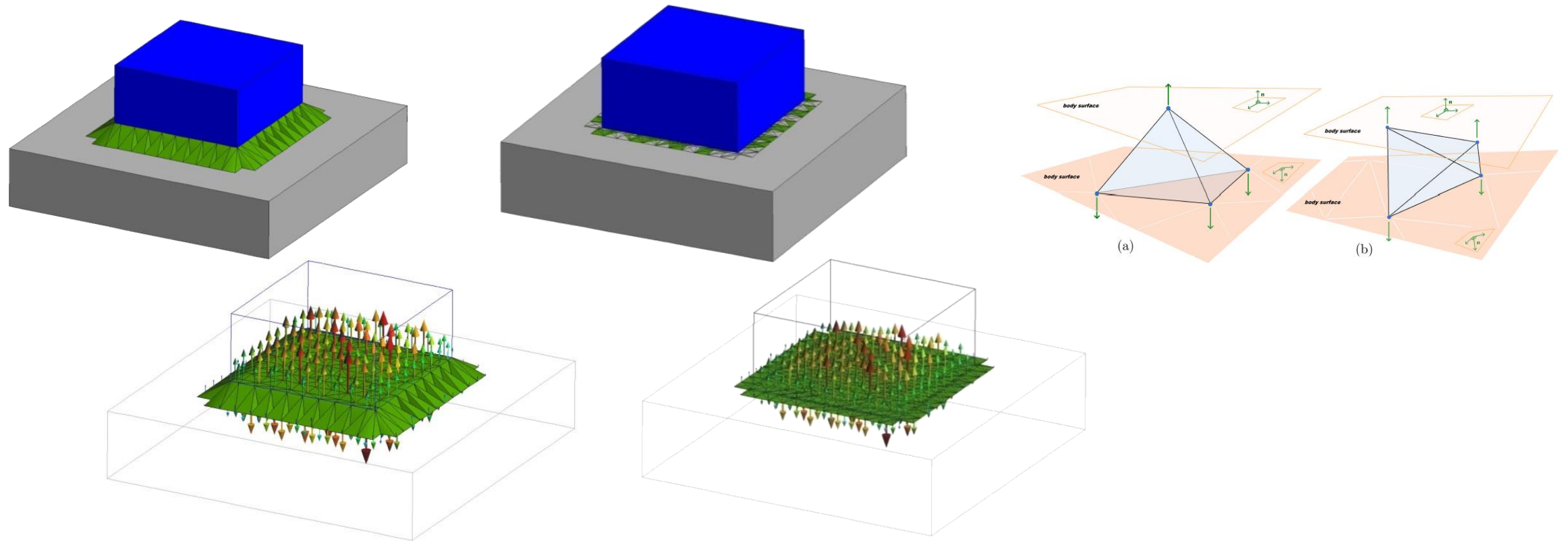
Figure 3 The distribution of the phenomenological models in the literature of the conventional machining applications

- **Detection** of contact and **active set**
- An **ancillary interface mesh** is created by the Delaunay tessellation using alpha-shapes



$$\sum_{\gamma=1}^2 \left\{ \int_{\varphi(\mathcal{B}^\gamma)} \boldsymbol{\sigma}^\gamma \cdot \nabla^S \boldsymbol{\eta}^\gamma dv - \int_{\varphi(\mathcal{B}^\gamma)} \rho^\gamma \bar{\mathbf{b}}^\gamma \cdot \boldsymbol{\eta}^\gamma dv - \int_{\varphi(\partial \mathcal{B}_\sigma^\gamma)} \bar{\mathbf{t}} \cdot \boldsymbol{\eta}^\gamma d\Gamma \right\} + \boxed{C_c} = 0$$

- Based on the interface mesh generated between the shrunk contacting domains.



- Condensed Lagrange Multipliers or Penalty approach

(Hartmann et al.)



|CONTACT FORCE| (kN)

— 0.050758

— 0.045118

— 0.039478

— 0.033839

— 0.028199

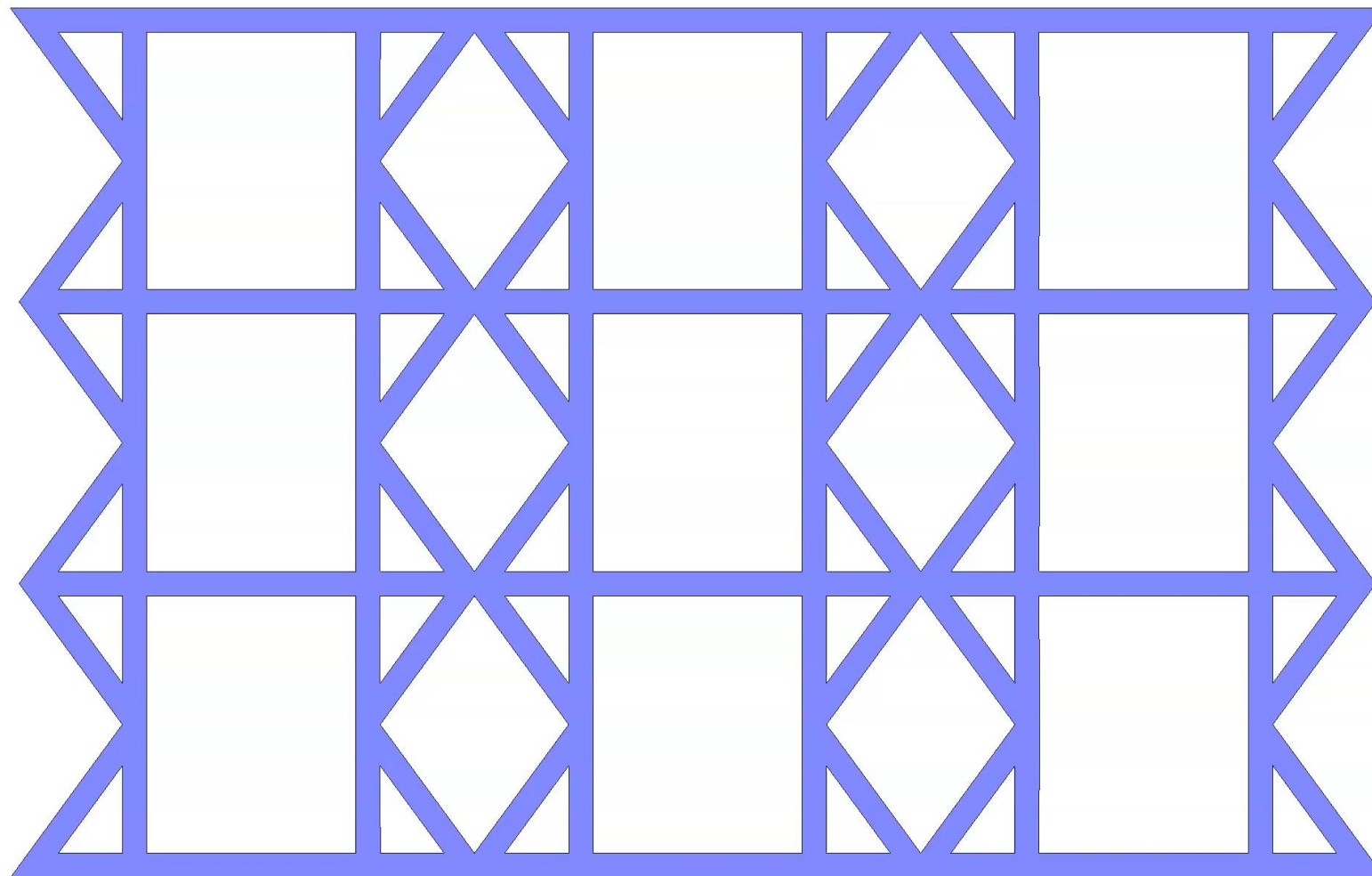
— 0.022559

— 0.016919

— 0.01128

— 0.0056398

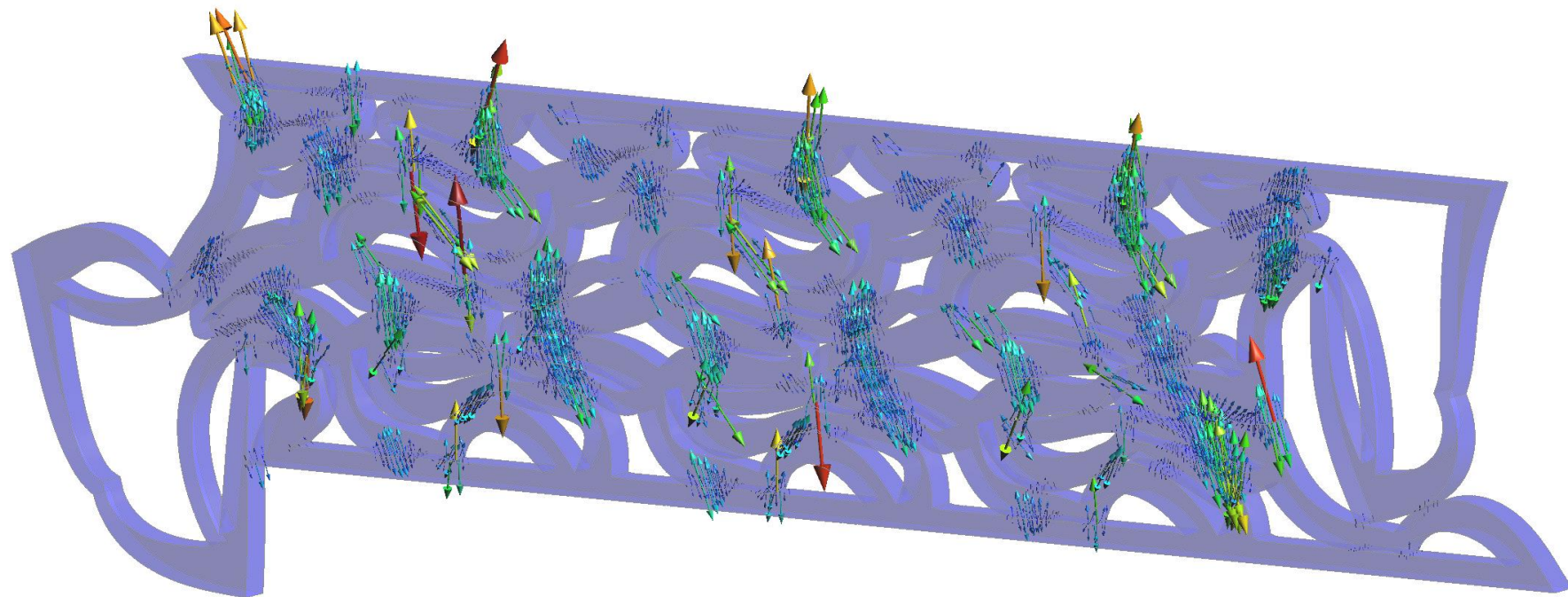
— 0



step 0.001

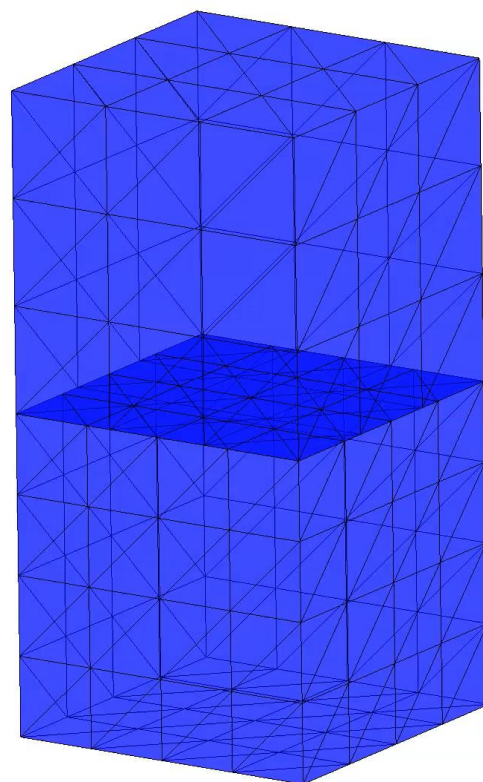


|CONTACT FORCE| (N)



step 0.922

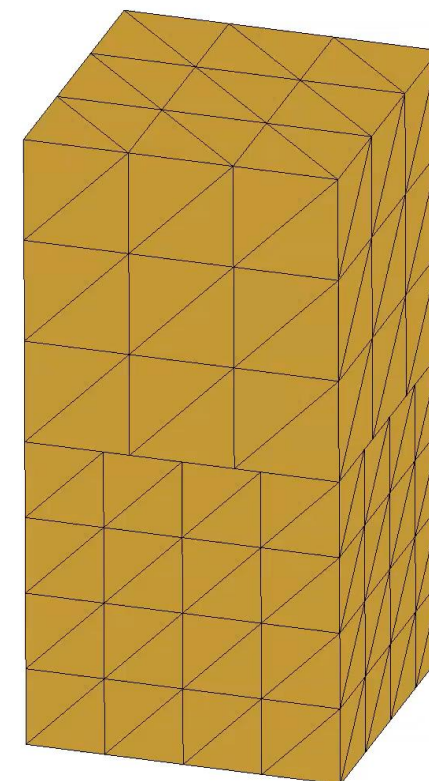
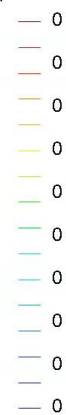
Display Vectors of .



step 0

Display Vectors of CONTACT FORCE (kN), |CONTACT FORCE| factor 0.001799424.

|CONTACT FORCE|



step 0

Display Vectors of CONTACT FORCE (kN), |CONTACT FORCE| factor 0.003387454.

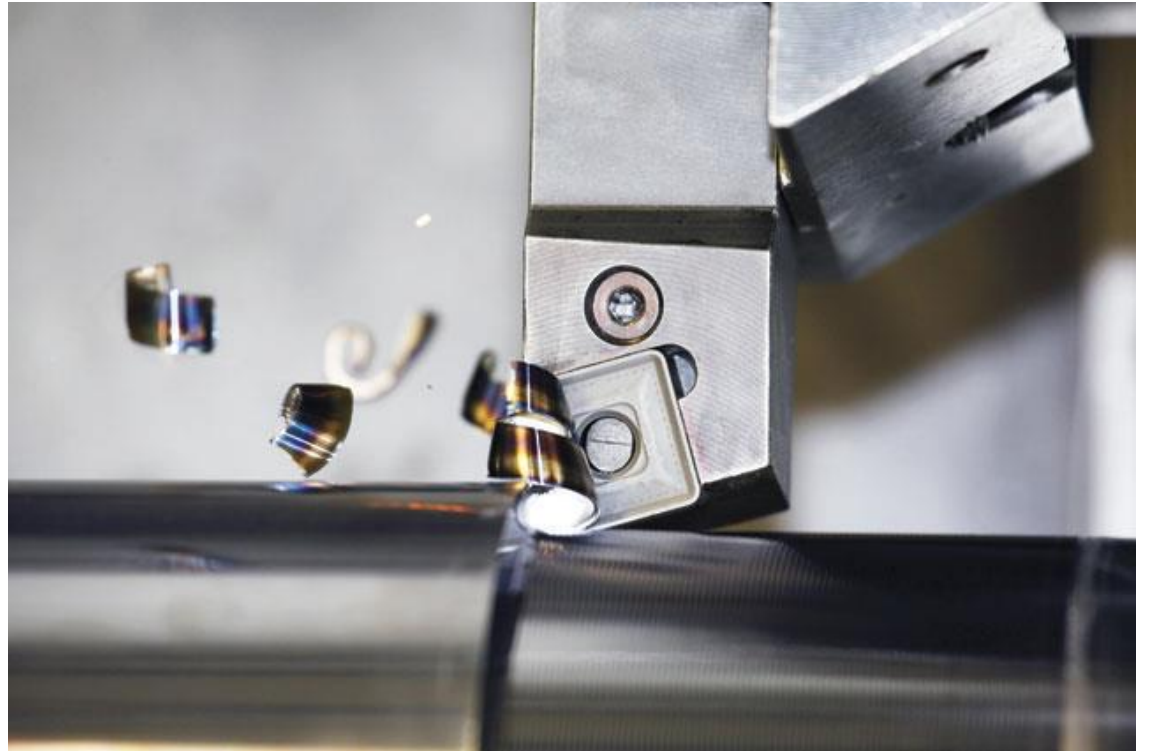
|CONTACT FORCE| (kN)

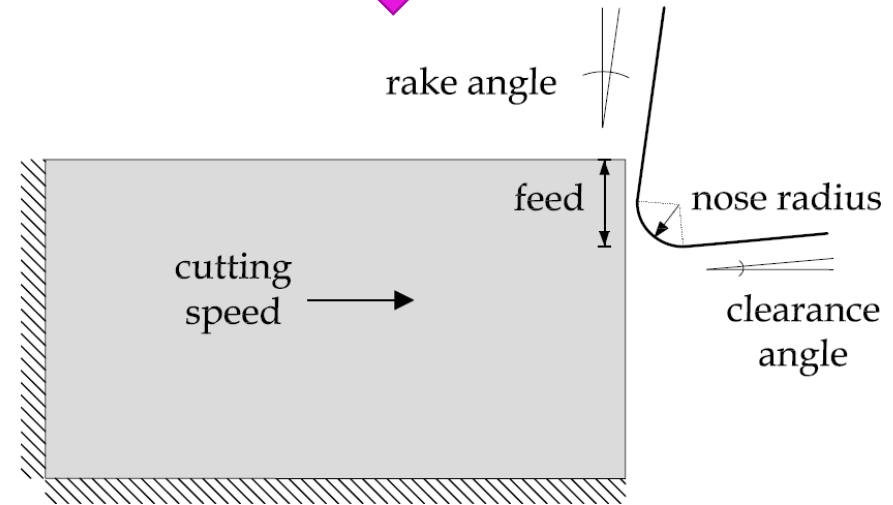
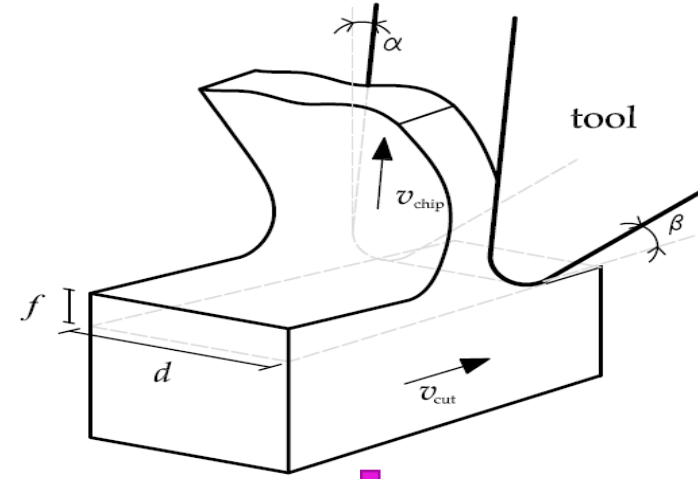
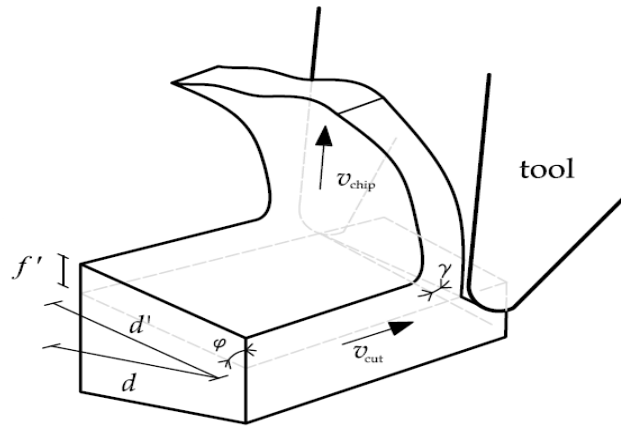
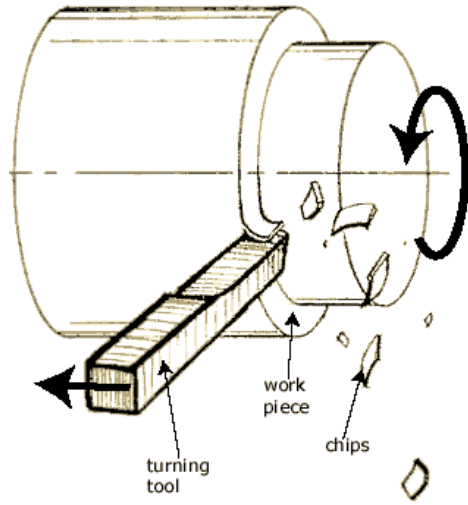


PROBLEM OF INTEREST : MACHINING

- MACHINING / CUTTING METAL

Material is cut by means of a cutting tool detaching the material and producing different types of chips

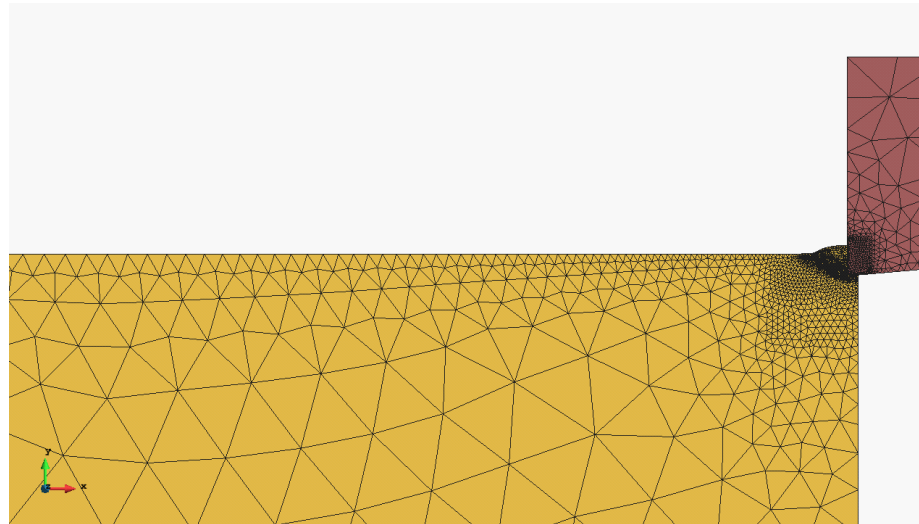




- **Continuous chip:** Johnson-Cook plasticity model

$$\sigma = [C_1 + C_2 \varepsilon_p^n] \left[1 + C_3 \ln \frac{\dot{\varepsilon}_p}{\dot{\varepsilon}_0} \right] \left[1 - \left(\frac{T - T_0}{T_m - T_0} \right)^m \right]$$

DEFORMABLE
TOOL



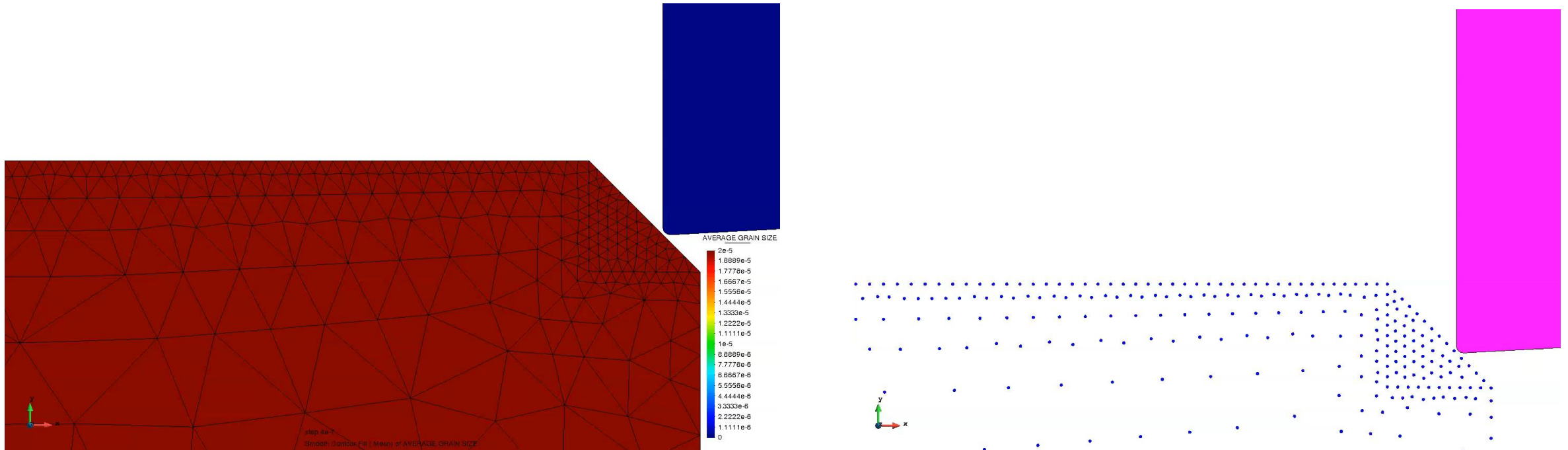
TEMPERATURE



RIGID TOOL

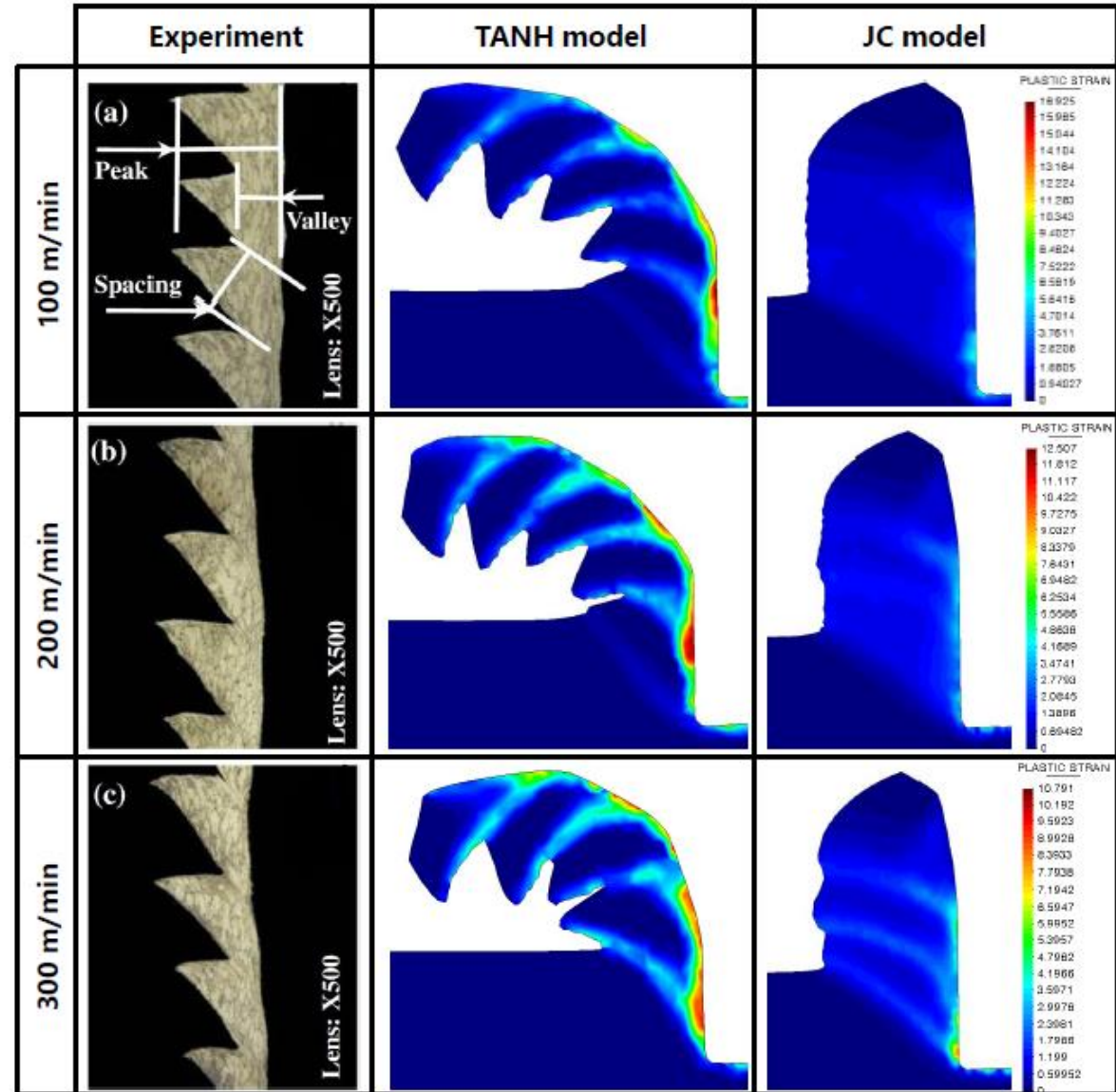
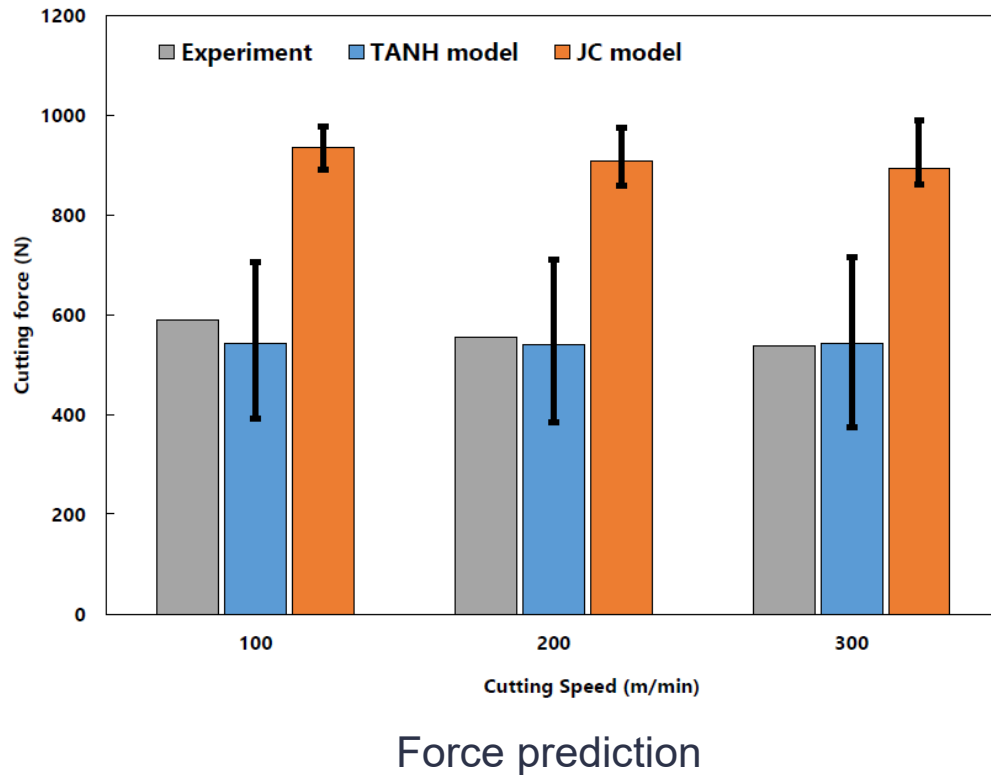


- **Segmented chip:** Modified Johnson-Cook plasticity model (TANH)

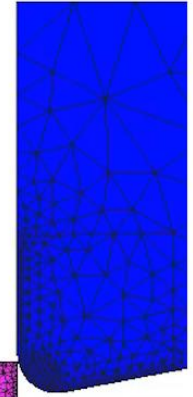
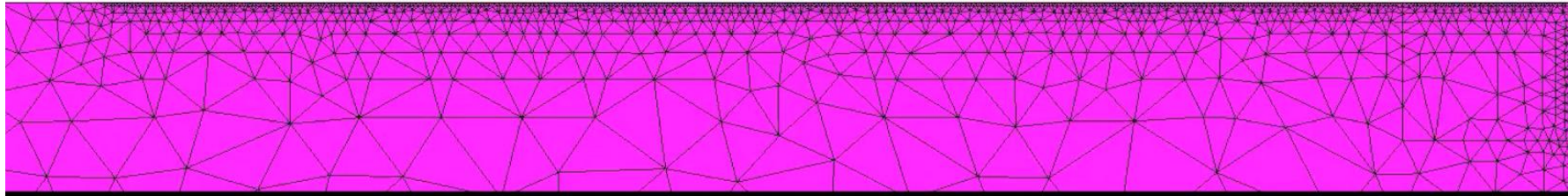


- Adaptive insertion of particles

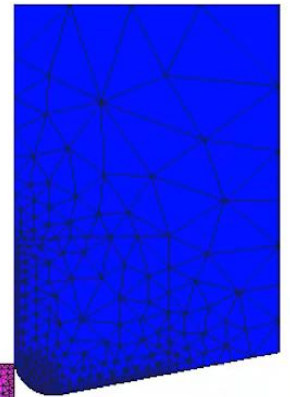
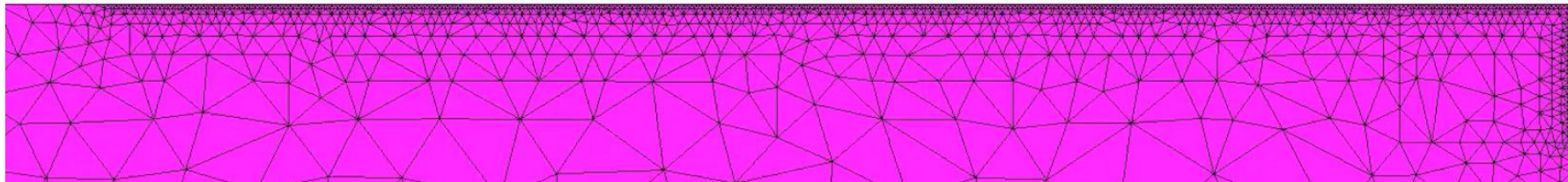
$$\sigma = \left[C_1 + C_2 \varepsilon_p^n \left(\frac{1}{\exp(\varepsilon_p^a)} \right) \right] \left[1 + C_3 \ln \frac{\dot{\varepsilon}_p}{\dot{\varepsilon}_0} \right] \left[1 - \left(\frac{T - T_0}{T_m - T_0} \right)^m \right] \left[D + (1 - D) \left[\tanh \left(\frac{1}{(\varepsilon_p + p)^r} \right) \right]^s \right]$$



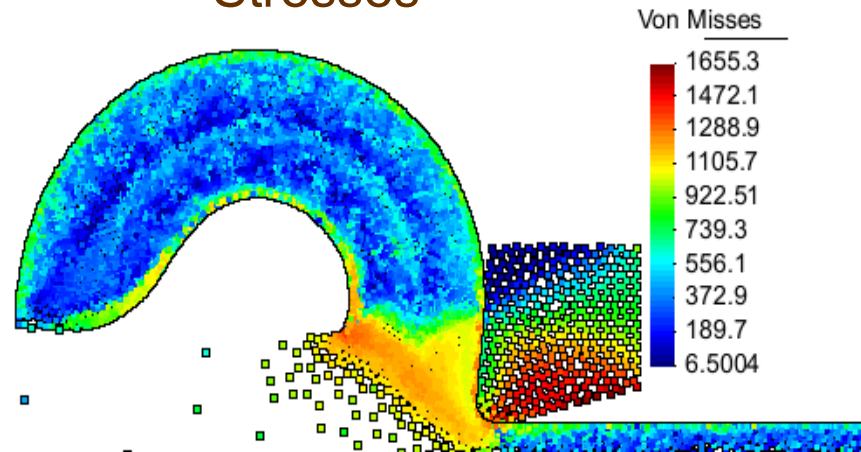
Conventional machining



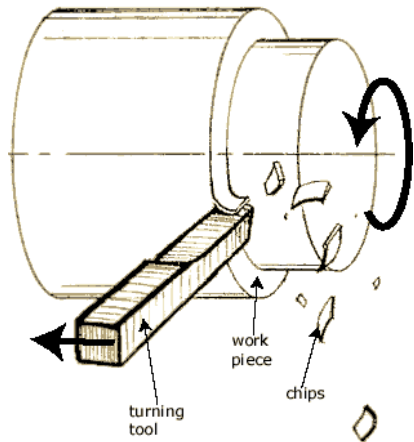
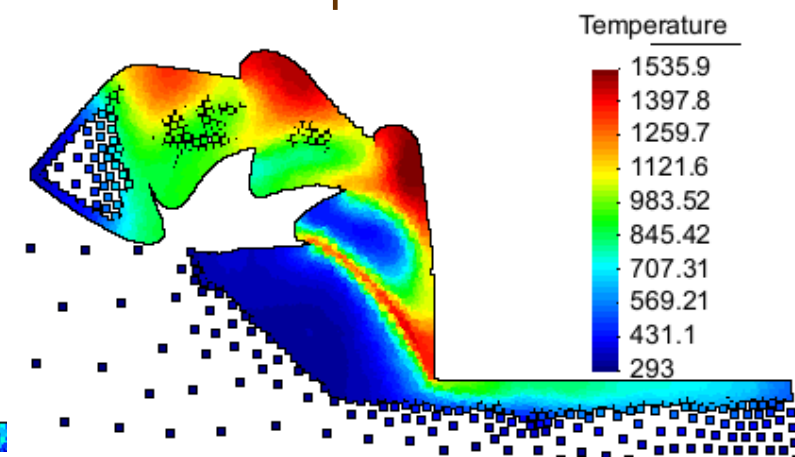
Vibration-assisted
machining



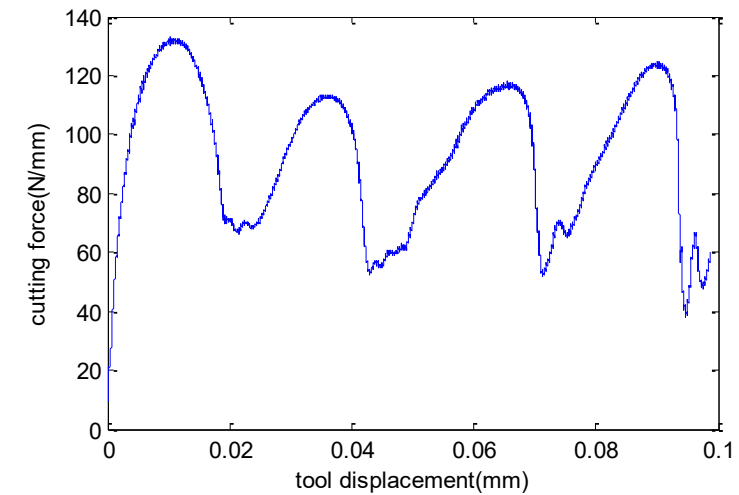
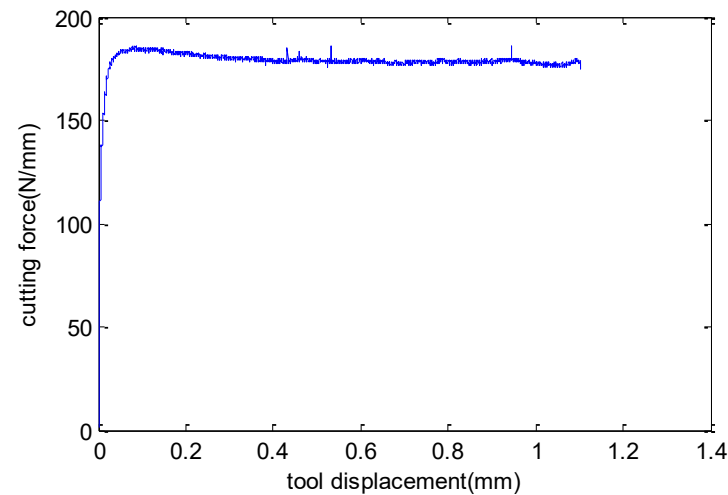
✓ Stresses

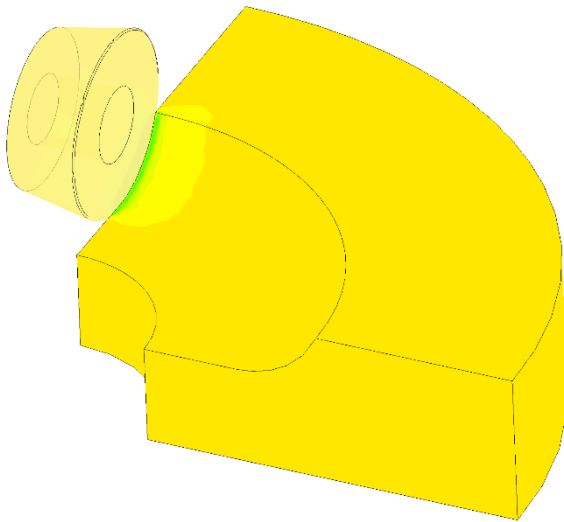
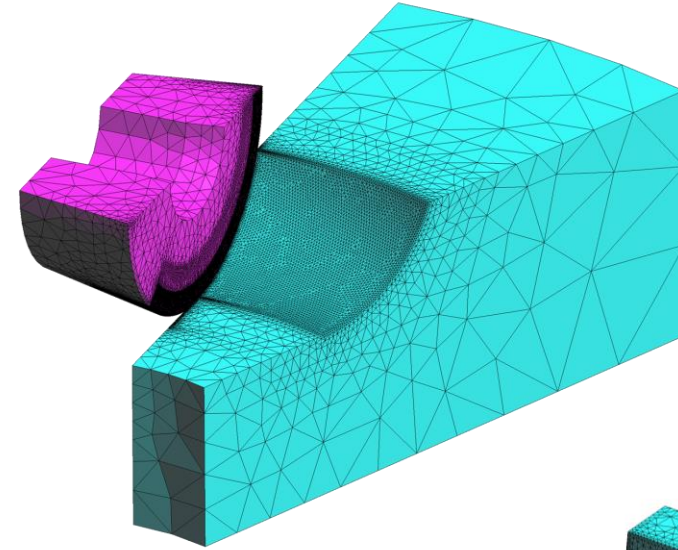


✓ Temperatures

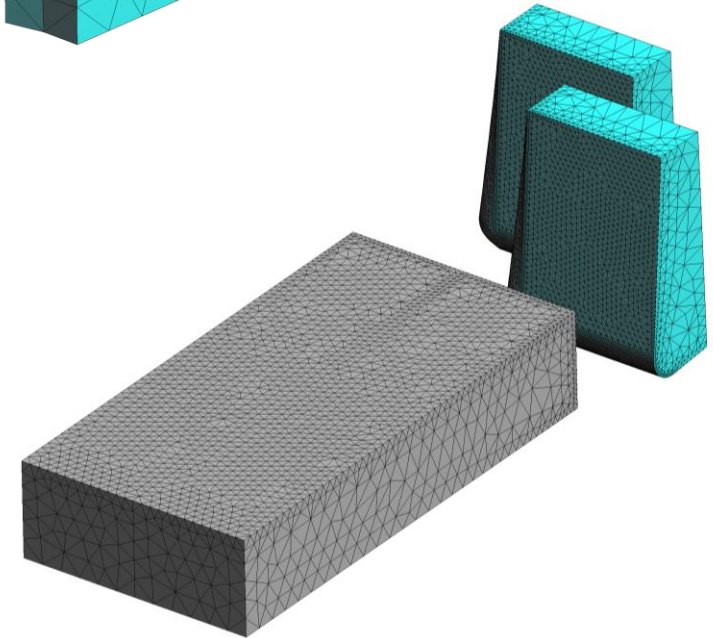
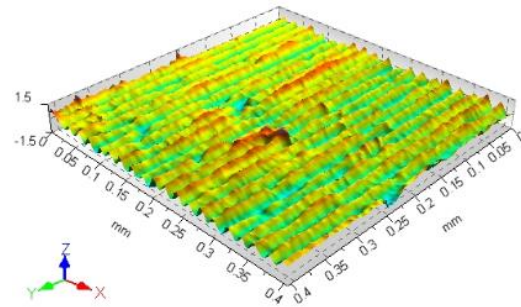


✓ Cutting and Feed forces



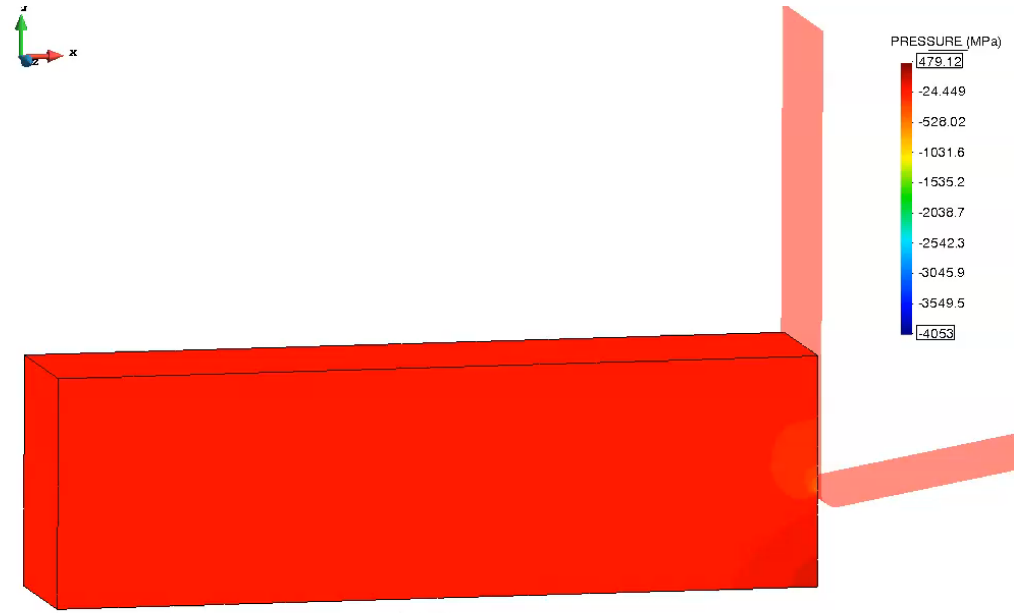
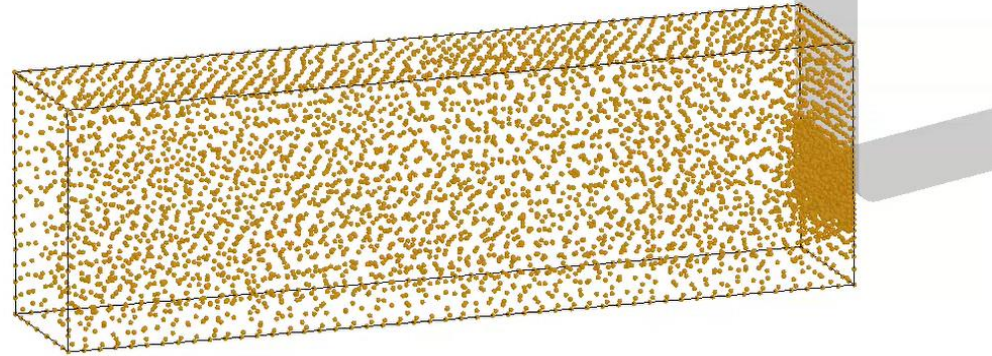


Computationally very expensive

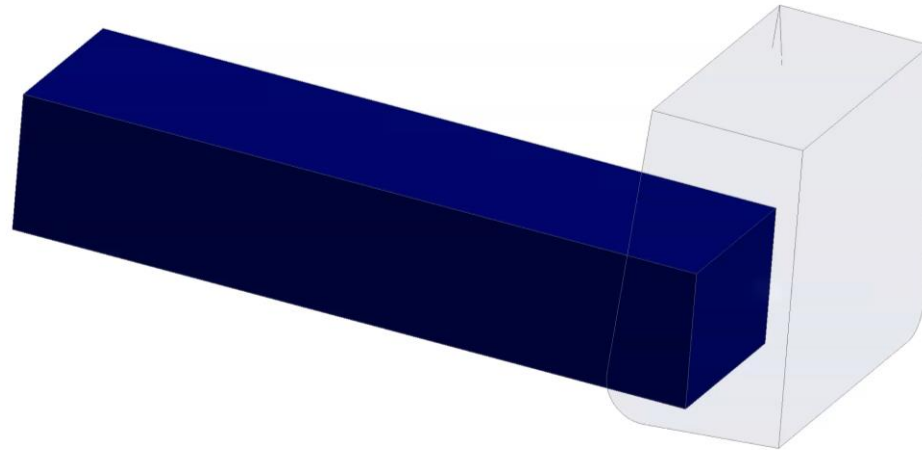
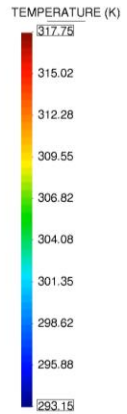




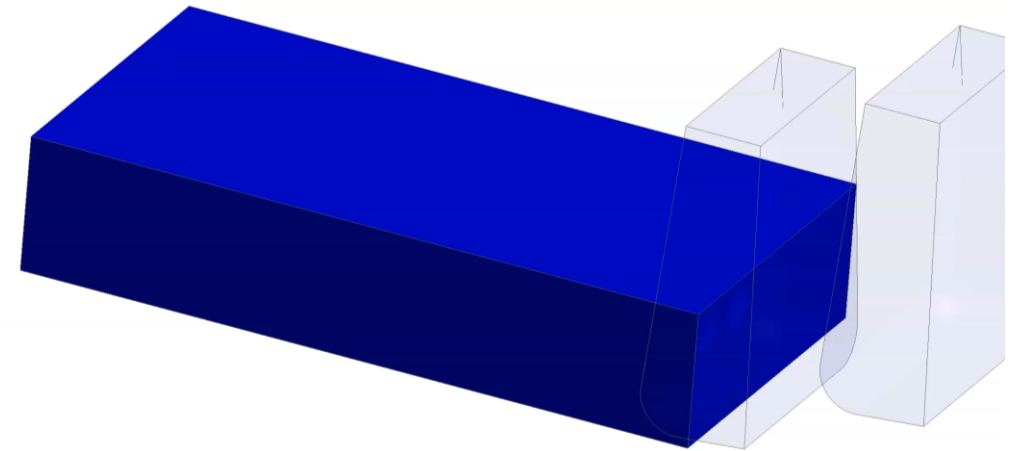
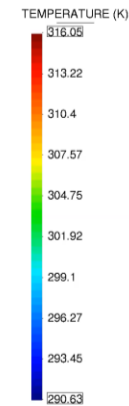
3D MODELLING



step 8e-7
Contour Fill of PRESSURE (MPa).



step 2e-08
Contour Fill of TEMPERATURE (K).



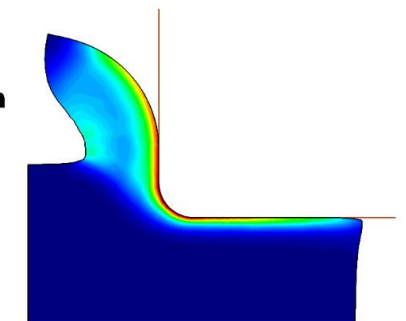
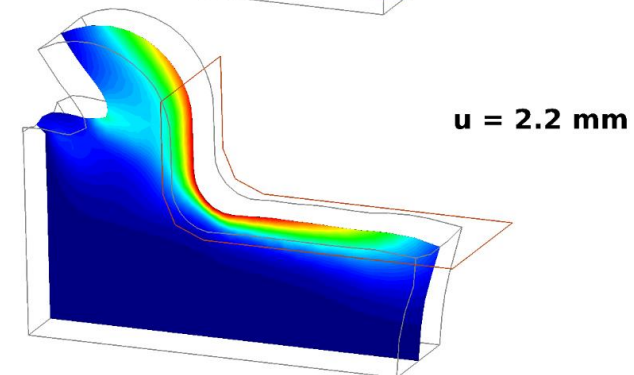
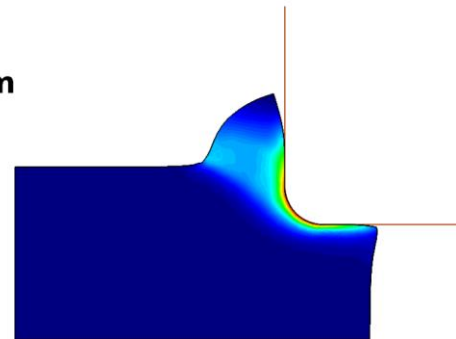
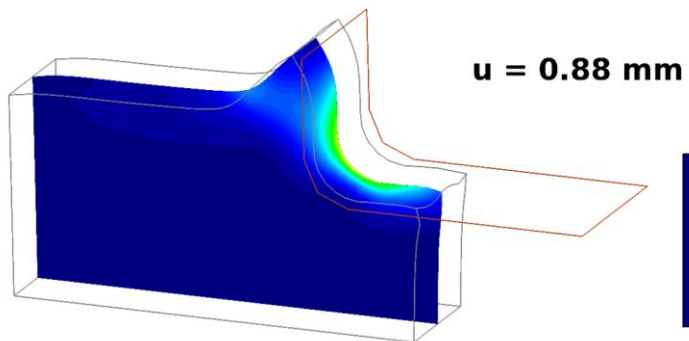
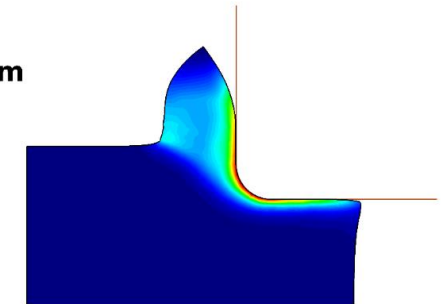
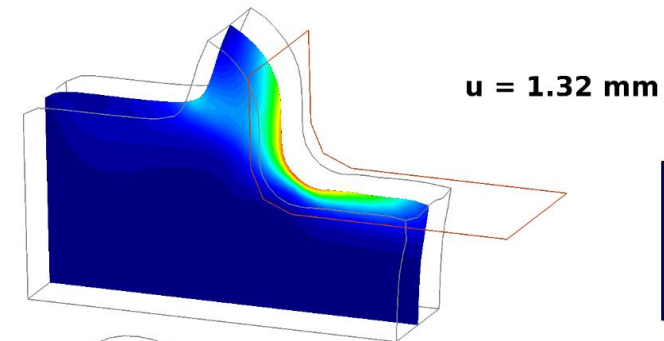
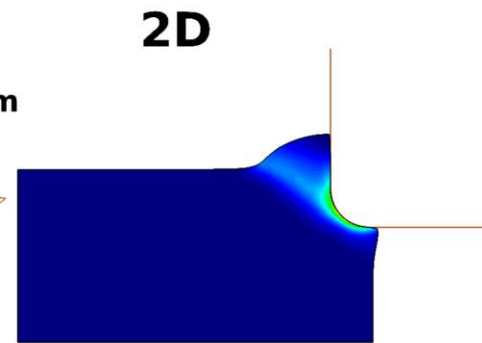
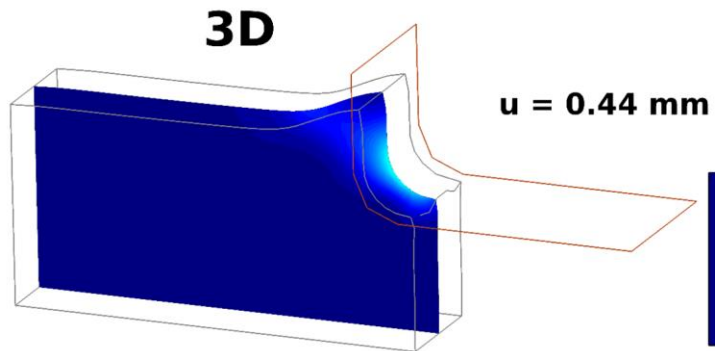
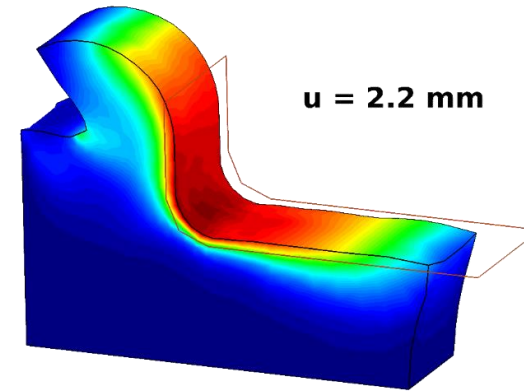
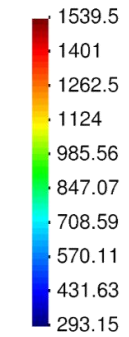
step 1e-07
Contour Fill of TEMPERATURE (K).

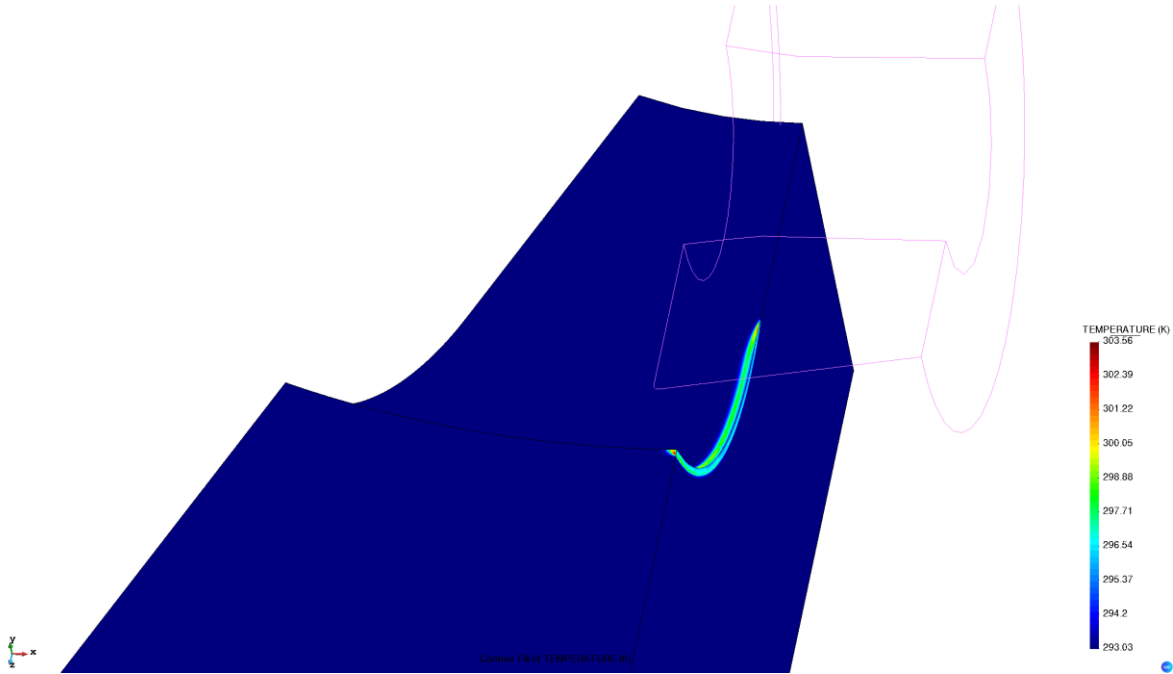
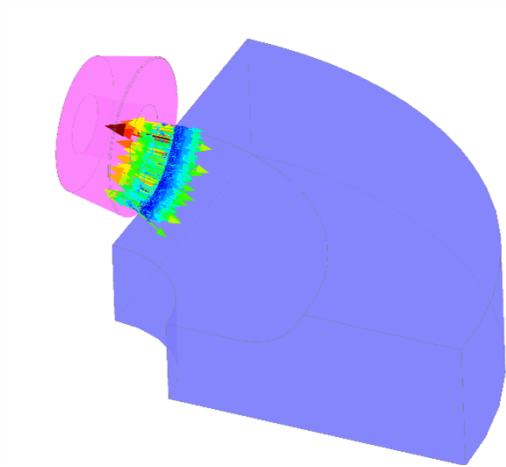
- Machining test: 2D model vs 3D model



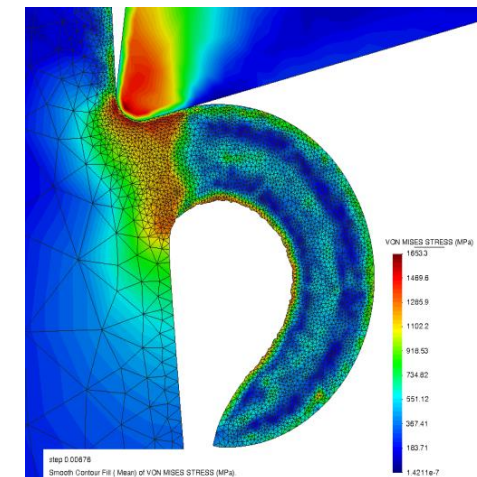
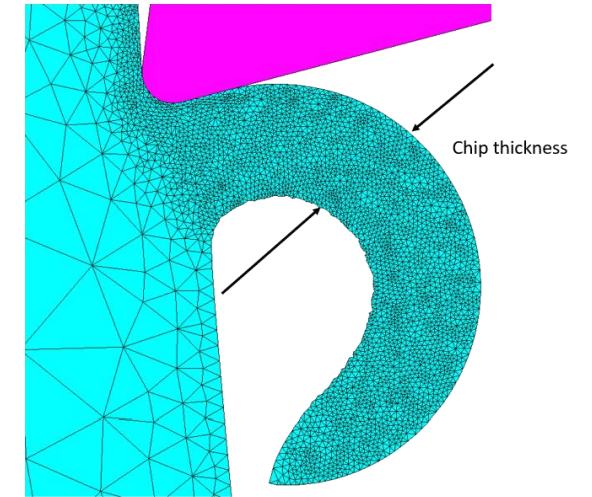
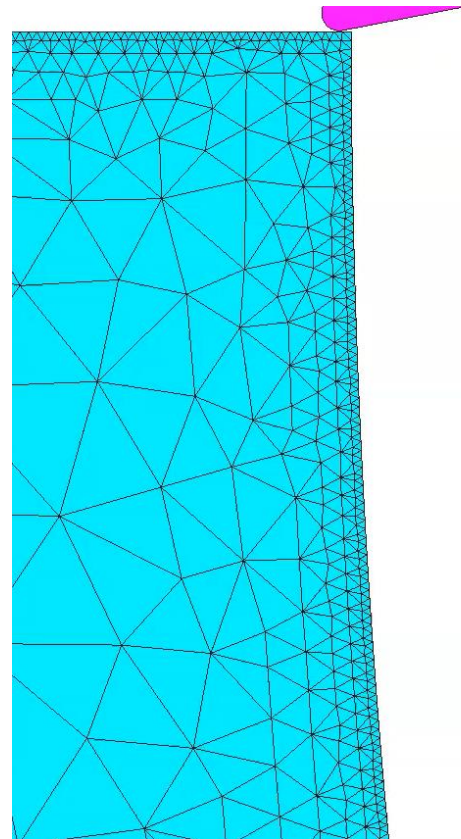
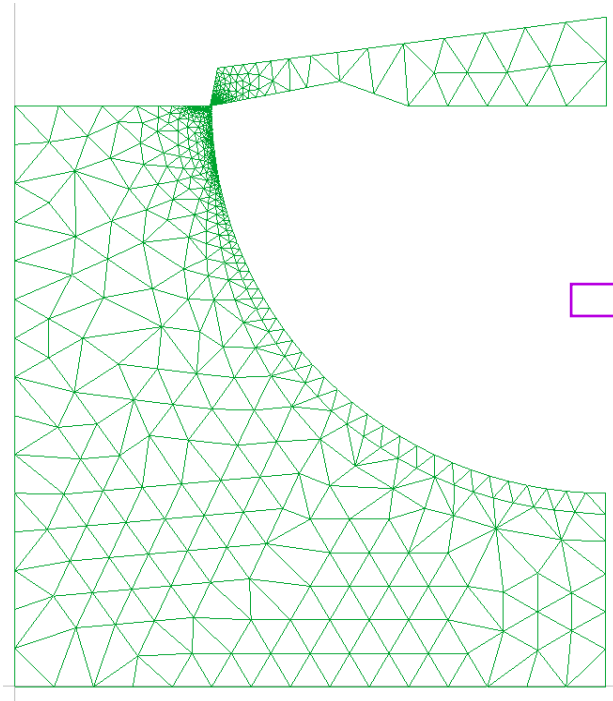
Funded by
the European Union

Temperature (K)



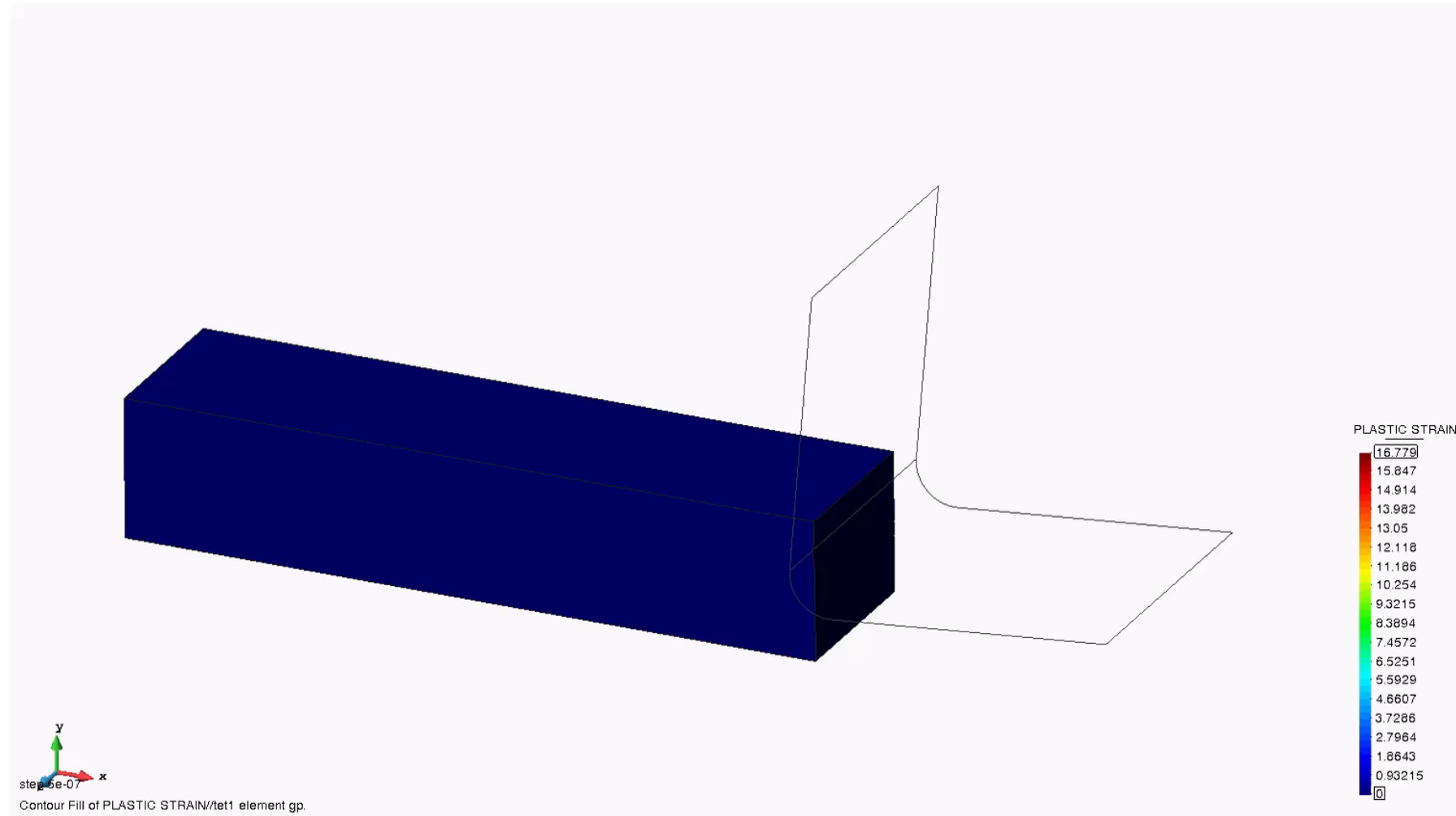


- 2D Modeling



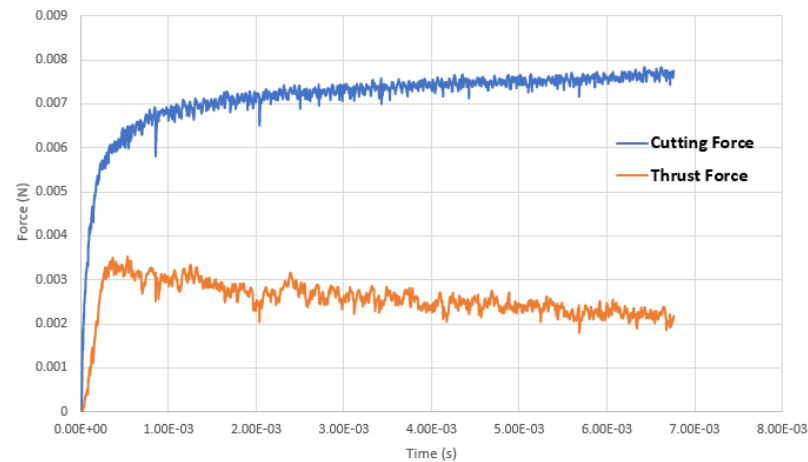
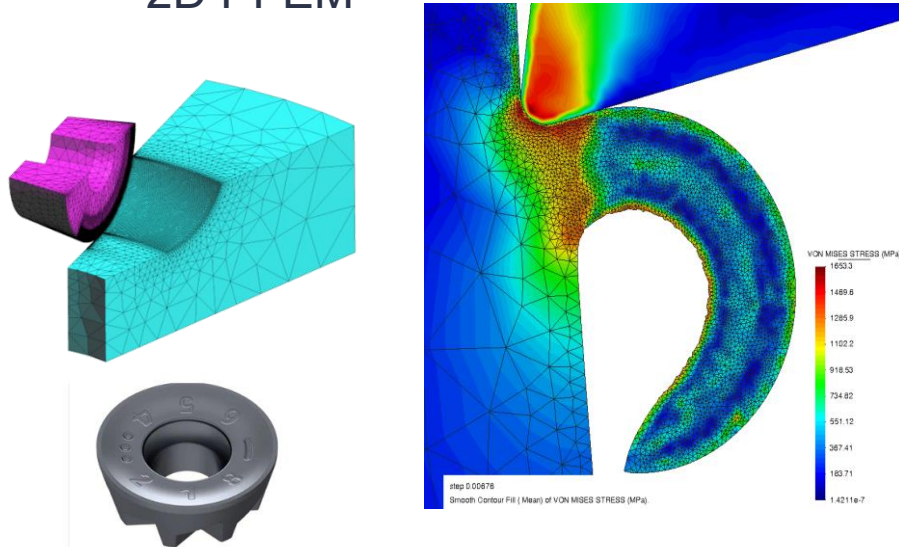
3hr simulation

- 3D Modeling

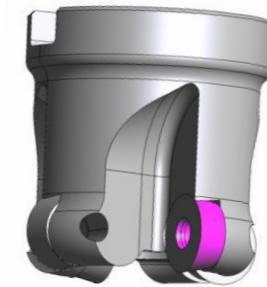


20 h simulation

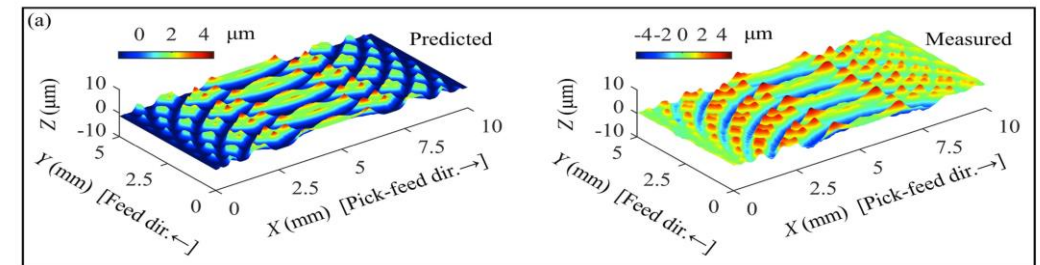
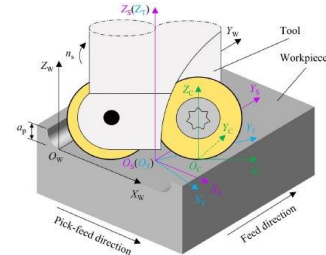
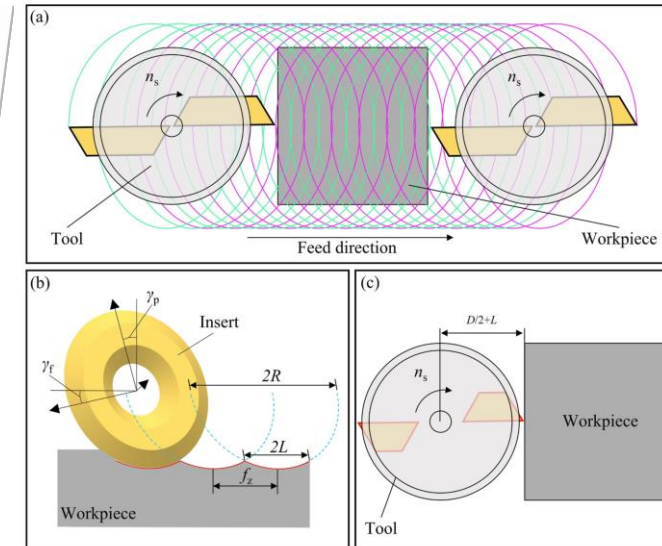
- 2D PFEM



- 3D surface topography model



+



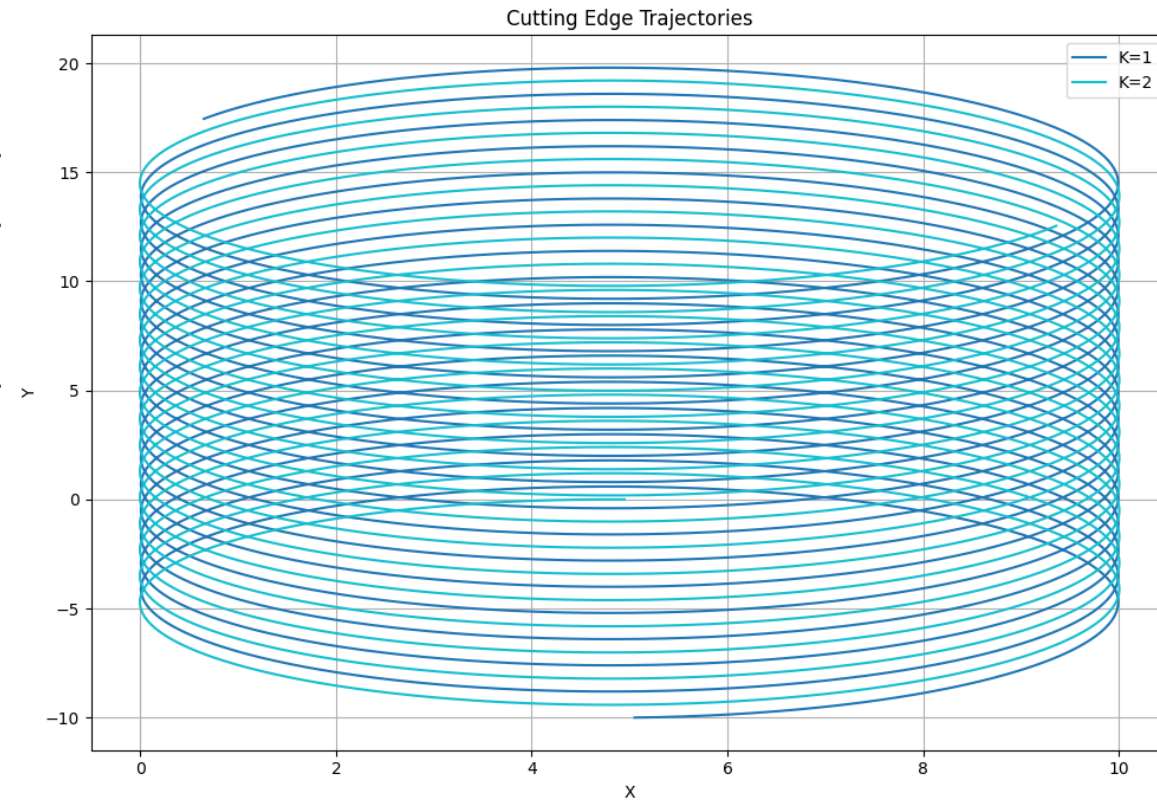
[1] Wang, Jianing, et al. "A high efficiency 3D surface topography model for face milling processes." *Journal of Manufacturing Processes* 107 (2023): 74-87.

Surface topography:

Cutting parameters.

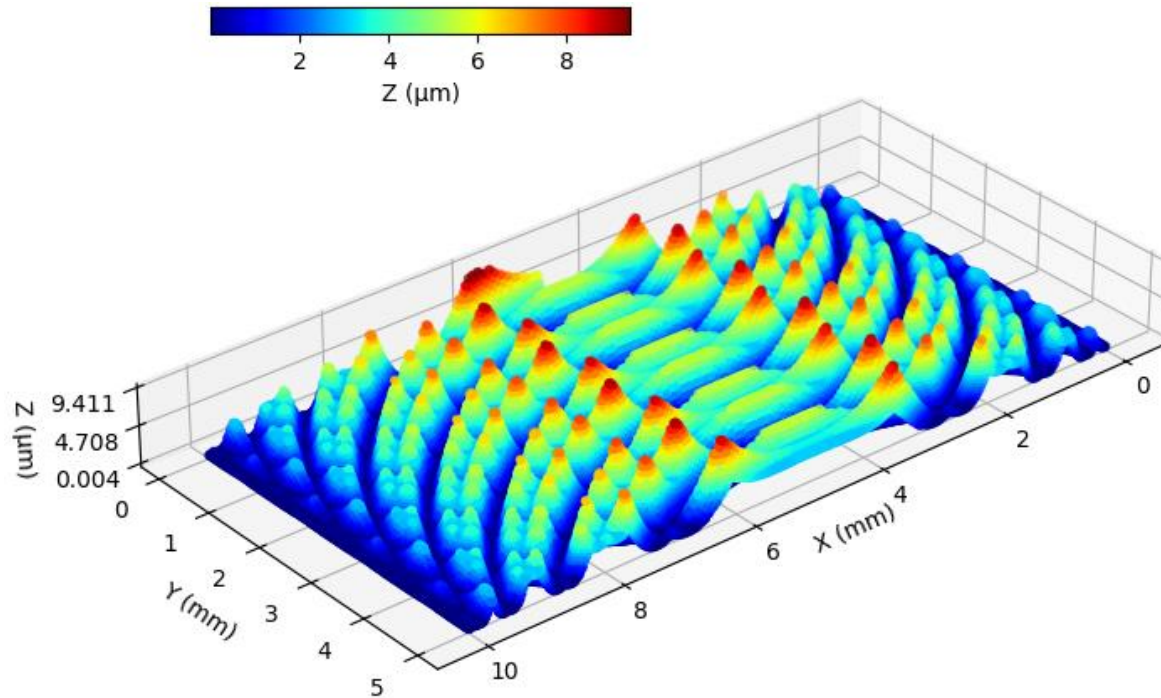
No.	v_c (m/min)	f_z (mm/tooth)	a_p (mm)
A1	170	0.6	0.5
A2	200	0.4	0.4
A3	230	0.5	0.3

A1

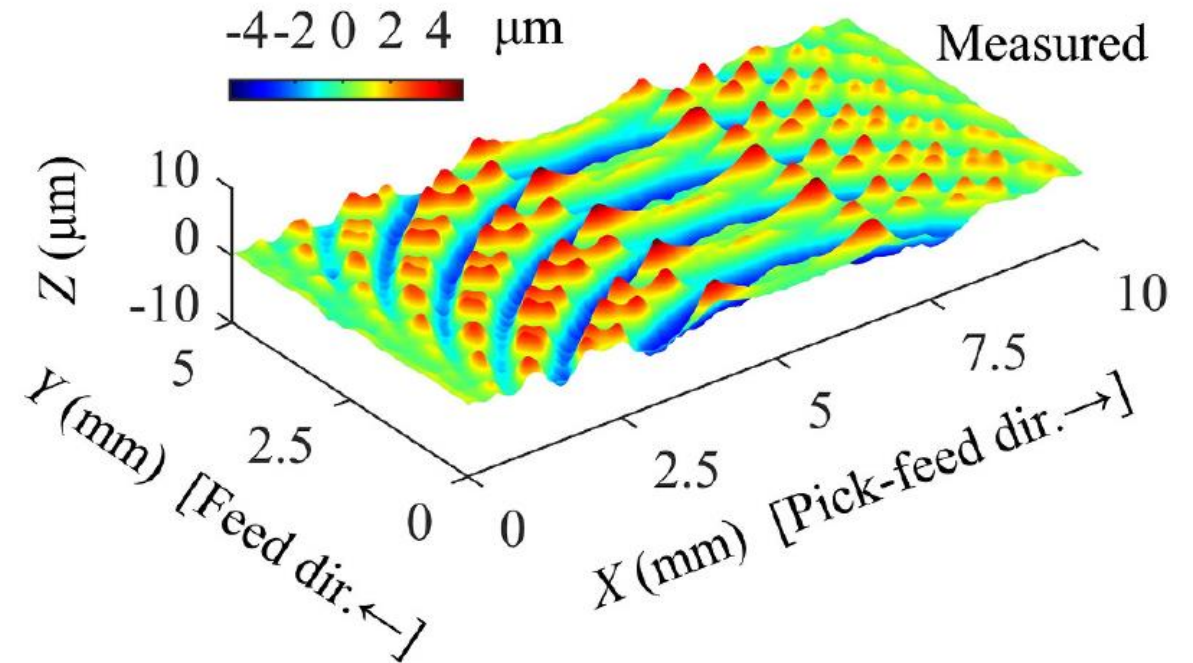


Surface topography: A1

Modeling



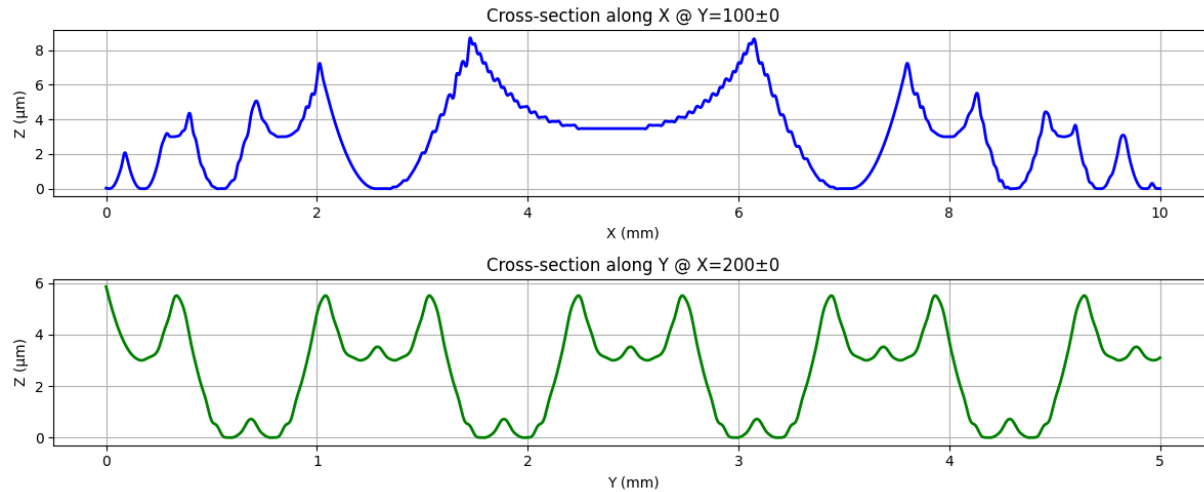
Experiment [1]



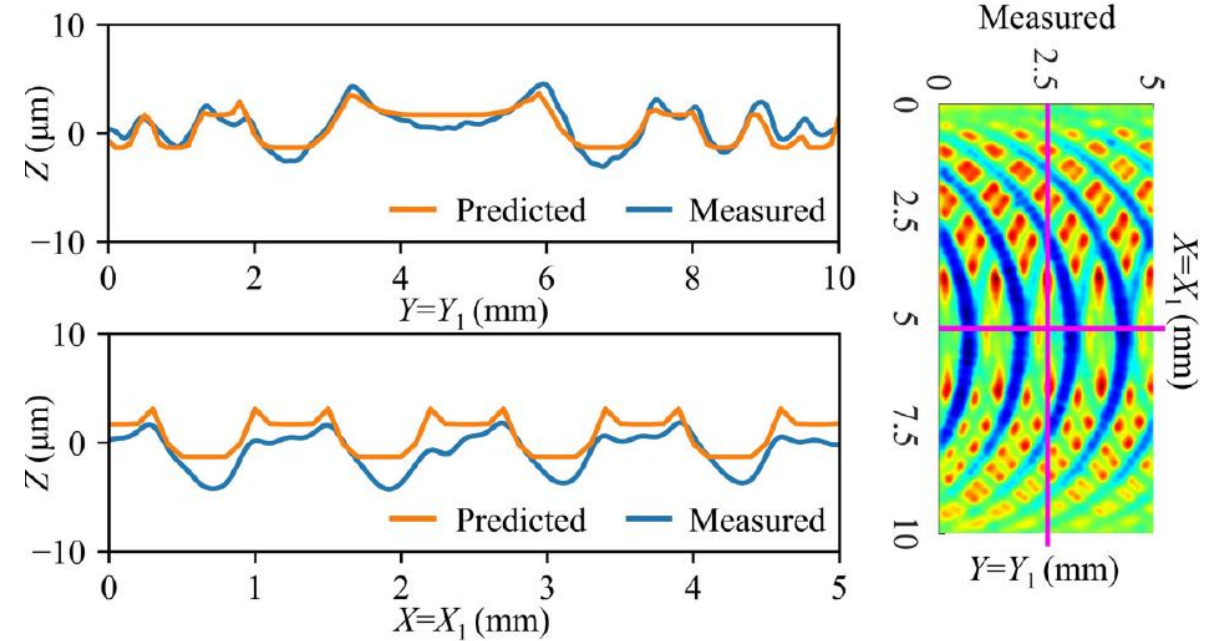
Wang, Jianing, et al. "A high efficiency 3D surface topography model for face milling processes." *Journal of Manufacturing Processes* 107 (2023): 74-87.

2D surface roundness contour line: A1

Modeling



Experiment [1]



Wang, Jianing, et al. "A high efficiency 3D surface topography model for face milling processes." *Journal of Manufacturing Processes* 107 (2023): 74-87.

- ✓ **PFEM allows for the study of machining by direct simulation:**
 - ✓ The **modelling material deformations** and **contact**
 - ✓ Determining **cutting forces** and **temperatures**, including:
 - The **thermo-mechanical material** behaviour.
 - The **frictional heat generation**, effects of **lubrication** and refrigeration.
 - The effects of **coating** and **wear** on the cutting tool.
- ✓ **Current research is focused in:**
 - Robust and efficient **3D PFEM** modelling
 - **Hybrid model : 2D/3D PFEM** model + **3D surface topography** model

Thank you for your attention

Josep Maria Carbonell Puigbó
cpuigbo@cimne.upc.edu

CIMNE[®]
International Centre
for Numerical Methods in Engineering

Dr. Hadi Bakhshan - Dr. Fernando Rastellini – Prof. Eugenio Oñate



TECHNICAL WORKSHOP

Optimising steels microstructure and surface integrity to face new challenges in Additive Manufacturing



Funded by
the European Union

SuPreAM project has received funding from the European Union's
Research Fund for Coal and Steel (RFCS): project num. 101112346



TECHNICAL WORKSHOP

Optimising steels microstructure and surface integrity to face new challenges in Additive Manufacturing



Funded by
the European Union

SuPreAM project has received funding from the European Union's
Research Fund for Coal and Steel (RFCS): project num. 101112346



Funded by
the European Union

Predictive simulation of finishing operations in steel Additive Manufacturing for optimal Surface integrity

Adaptive Numerical Simulation of Electro Discharge Machining finishing operations using an Embedded Approach.

Joan Baiges
Associate Research Professor, CIMNE
joan.baiges@upc.edu

CIMNE^R

01 Introduction

02 EDM Governing equations

03 Numerical approximation

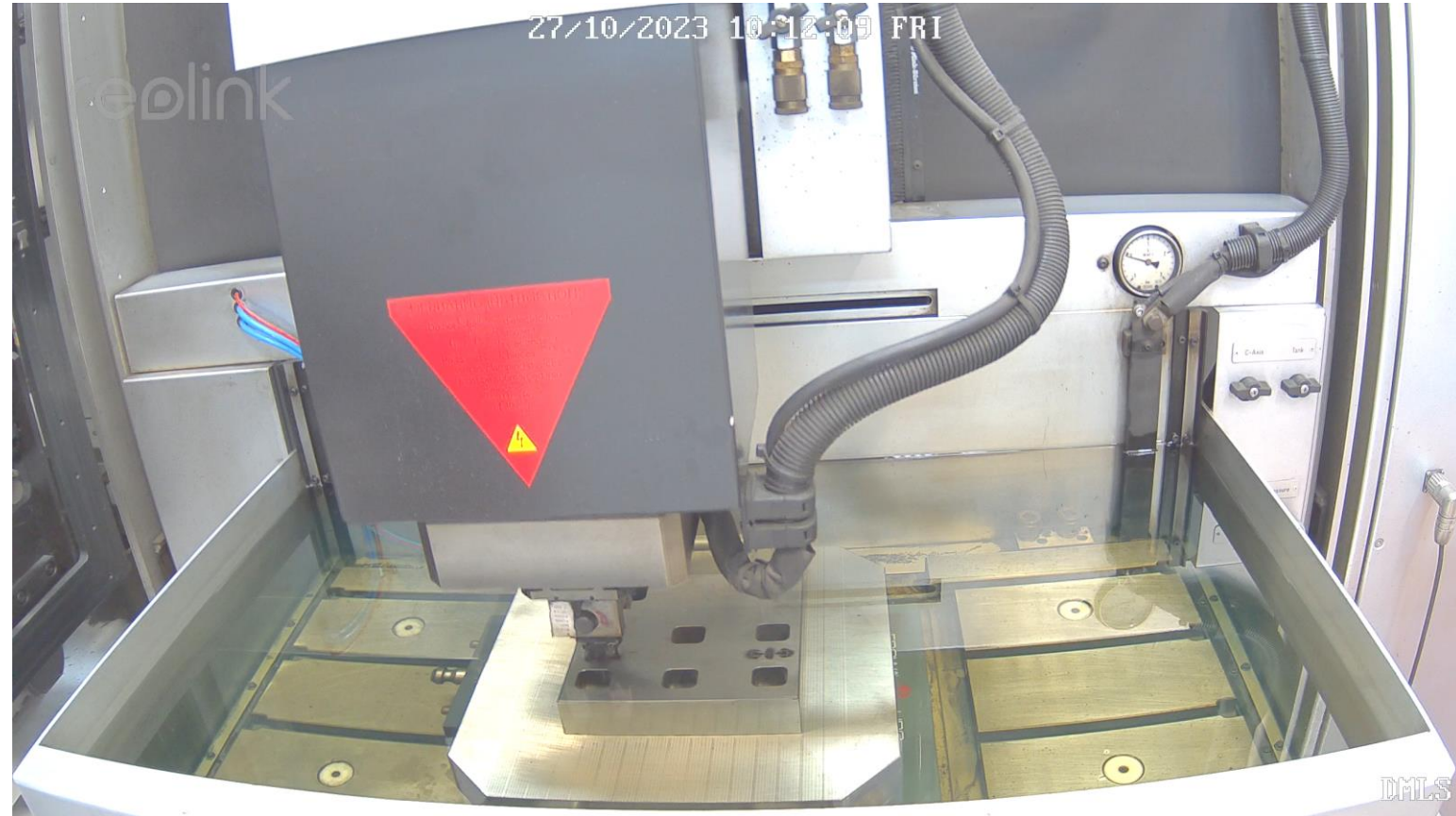
04 Numerical examples

05 Conclusions

Motivation

- EDM (Electro Discharge Machining) is essential for machining hard, conductive materials in aerospace, automotive, and medical industries.
- Surface finishing operations require high precision, but traditional simulation methods are computationally expensive.
- Standard FEM needs body-fitted meshes and frequent remeshing to capture evolving material geometries.
- There is a need for robust, scalable simulations that can accurately handle multi-spark, transient effects in EDM.

Motivation



Objectives

- Develop a numerical framework for simulating EDM surface finishing based on:
 - Embedded Finite Element Method (FEM) to avoid remeshing.
 - Adaptive Mesh Refinement (AMR) to concentrate computational effort where needed.
 - Ghost stabilization for numerical robustness near cut elements.
- Validate the approach through comparison with experimental data.
- Demonstrate applicability to large-scale simulations with multi-spark interactions.

Thermal model for EDM

- Transient Heat Equation

$$\rho c \partial_t T + \nabla \cdot (k \nabla T) = \mathbf{f} \quad \text{in } \Omega$$

$$T = \bar{T} \quad \text{in } \Gamma_D$$

$$q = \bar{q} \quad \text{in } \Gamma_N$$

- Nonlinear due to temperature-dependent properties.
- Purely thermal model: no fluid or plasma dynamics.
- Material removal triggered by boiling point T_b .

EDM Governing equations - Boundary conditions

- On boundaries not affected by the spark heat input, convective and radiative heat flux:

$$q = h(T - T_{\infty}) + \epsilon\sigma(T^4 - T_{\infty}^4) \quad \text{on } \Gamma_S,$$

- On the spark boundary, a Gaussian heat flux:

$$q(r) = q_0 \exp\left(-4.5 \left(\frac{r}{R_{pc}}\right)^2\right) \quad \text{on } \Gamma_E,$$

$$q_0 = \frac{4.57 F_c V I}{\pi R_{pc}^2},$$

$$R_{pc} = (2.04 \times 10^{-3}) \cdot I^{0.43} \cdot t_{on}^{0.44}.$$

- Once the material reaches the boiling point, it is removed from the computational domain

EDM Governing equations - Boundary conditions

- Energy distribution ratio:

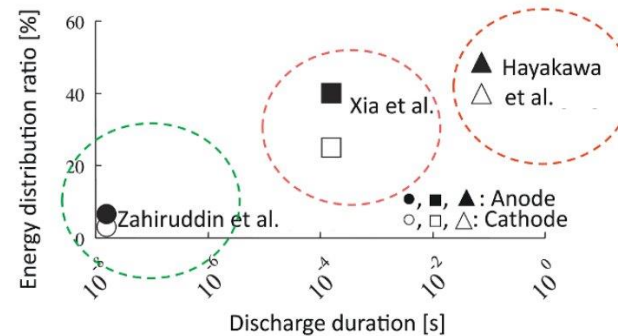


Fig. 15: Energy distribution into anode and cathode, taken from Hinduja and Kunieda [1].

Authors	Concept	F_c (%)	F_a (%)
Van Dijck [55]	Thermo-physical model with disc heat source	50	50
Pandey and Jilani [37]	Constant cathode boiling temperature condition	50	50
DiBitonto et al. [7]	Point heat source with photoelectric effect	18.3	-
Patel et al. [60]	Disc heat source with photoelectric effect	-	8
Xia et al. [48]	Temperature measurements: single, multiple sparks	25 - 34	40 - 48
Revaz et al. [49].	Temperature measurement: single, multiple sparks	10 - 15	-
Zahiruddin and Kunieda [62]	Micro-EDM with small energy discharges, T_{ON} : 70 ns	-	10.37
Singh [52] [52]	Temperature measurements: multiple sparks	6 - 27	-
Zhang et al. [63]	Gaussian heat source, validated for single craters	44	-
Shabgard et al. [64]	Gaussian heat source, plasma flushing efficiency	4 - 9	4 - 36
Zhang et al. [53]	Metallographic analysis of craters to derive energy input	42 - 60	36 - 50
Maradia et al. [42]	Expanding disc heat source, different electrode and workpiece materials, single spark analysis	15 - 45	28 - 36

01 Introduction

02 EDM Governing equations

03 Numerical approximation

04 Numerical examples

05 Conclusions

Numerical approximation – Embedded finite element method

- Time discretization using a backward differences scheme:

$$\delta_t f^{n+1} = \sum_{j=0}^k \alpha_j f^{n+1-j},$$

- BDF2:

$$\alpha_0 = \frac{3}{2\delta t}, \quad \alpha_1 = -\frac{2}{\delta t}, \quad \alpha_2 = \frac{1}{2\delta t}.$$

- Galerkin variational form of the problem:

$$\langle v, \rho c \partial_t T \rangle + (\nabla v, k \nabla T) = (v, f) + \langle v, \bar{q} \rangle \quad \forall v \in V_0,$$

$$T = \bar{T} \quad \text{on } \Gamma_D.$$

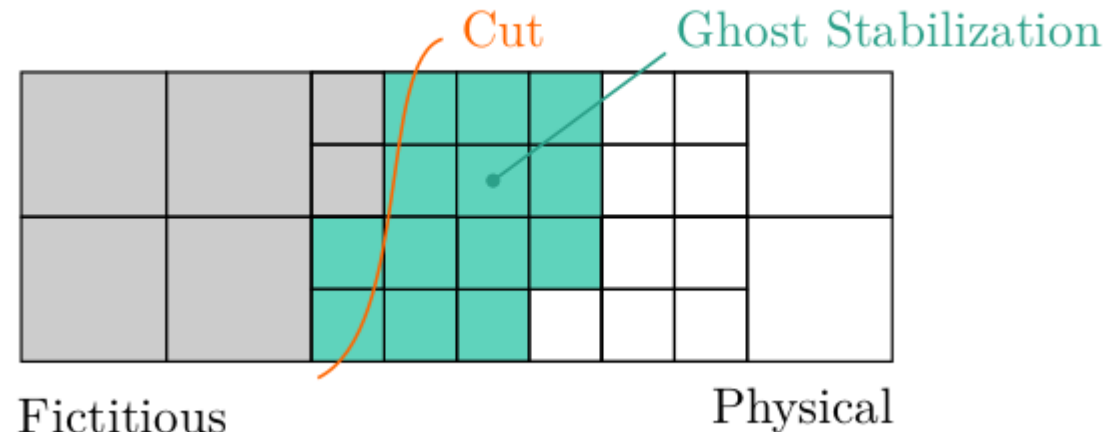
Numerical approximation – Embedded finite element method

- Ghost stabilization terms for small cuts instabilities:

$$\sum_{K \in \Omega_h^{\text{cut}}} \varepsilon_K \langle \nabla v_h, P_h^\perp(\nabla T_h) \rangle_K,$$

$$P_h^\perp := I - P_h,$$

$$\varepsilon_K = c_1 k,$$



Numerical approximation – Final stabilized formulation

Given $T_h^0, \dots, T_h^n \in V_h$, find $T_h^{n+1} \in V_h$ such that

$$\begin{aligned} & \langle v_h, \rho c \delta_t T_h^{n+1} \rangle + (\nabla v_h, k \nabla T_h^{n+1}) \\ & + \sum_{K \subset \Omega_h^{\text{cut}}} \varepsilon_K \langle \nabla v_h, P_h^\perp(\nabla T_h^{n+1}) \rangle_K = (v_h, f^{n+1}) + \langle v_h, \bar{q}^{n+1} \rangle \end{aligned}$$

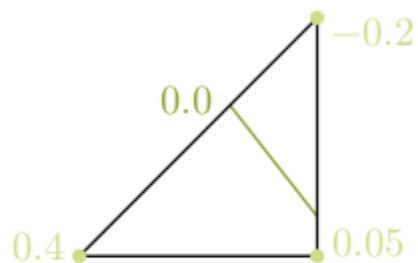
for all $v_h \in V_{h,0}$.

Numerical approximation – Level set function and element subintegration

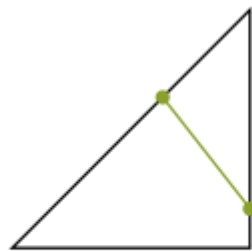
- A level set function is used to define the active domain of the problem:

$$\phi_h^{n+1} = \max_{t \in [0, t^{n+1}]} T(t) - T_b,$$

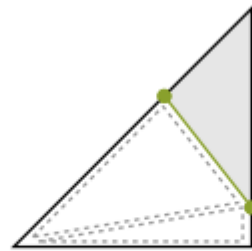
$$\phi_h^{n+1} \leq 0,$$



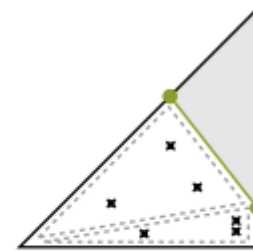
(a) Discrete Level Set



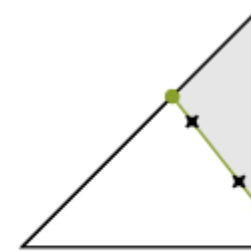
(b) Intersection Points



(c) Sub-Integration Cells



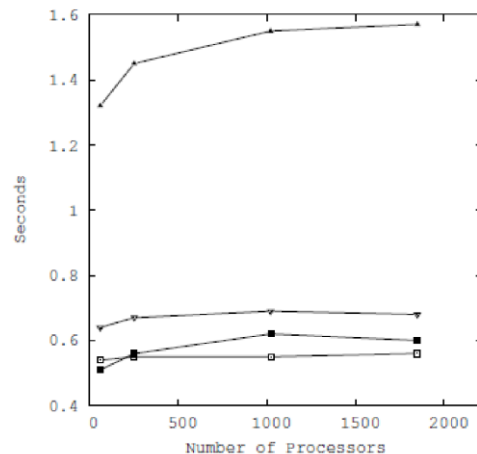
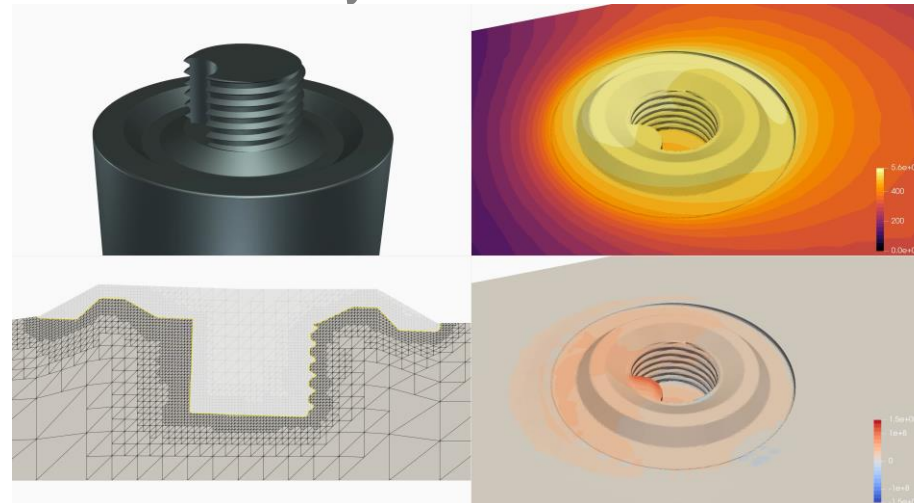
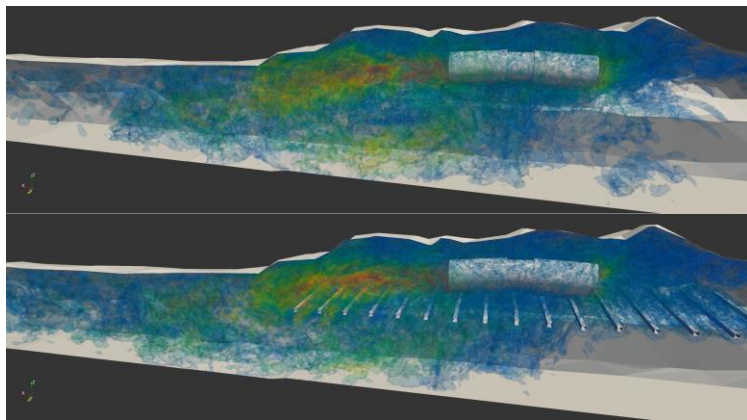
(d) Volume Integration Points



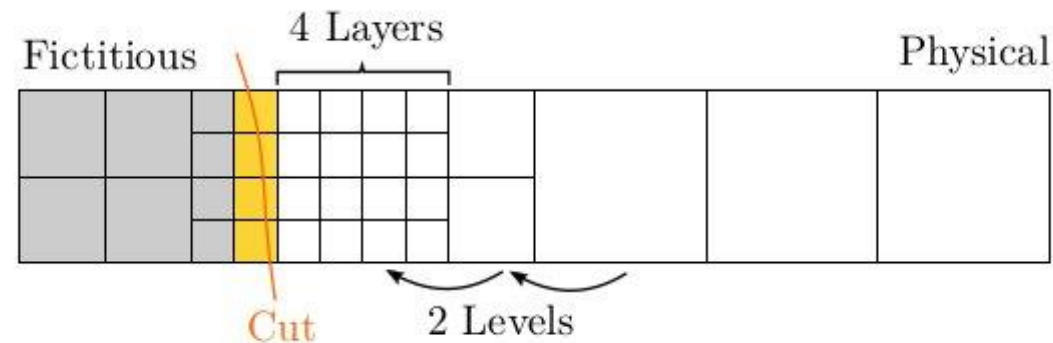
(e) Surface Integration Points

Numerical approximation – Adaptive mesh refinement strategy and refinement criteria

- We use our in-house adaptive refinement library Refficientlib

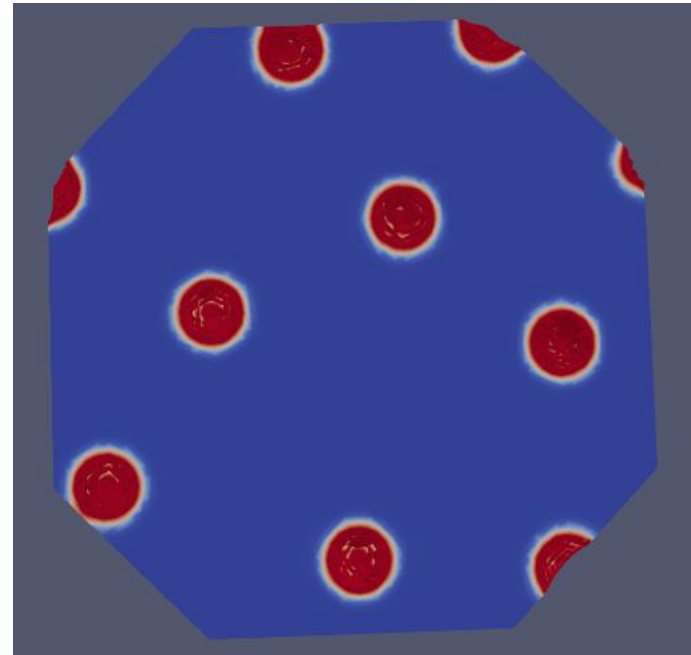


- Geometrical refinement criteria:



Numerical approximation – Parallelization and simultaneous sparks simulation

- MPI based parallelization, domain decomposition with adaptivity, load rebalancing
- Electrode is represented by means of a CAD file, and from there a distance function to the electrode for each node is built (OCCT library)
- Position of the next spark is based on a minimum distance of the active nodes to the electrode (easy to parallelize through gather and scatter operations).
- To accelerate simulation time, multiple sparks if they are sufficiently separated and do not affect each other, can be simulated (more involved to parallelize)



01 Introduction

02 EDM Governing equations

03 Numerical approximation

04 Numerical examples

05 Conclusions

Numerical examples – Single spark simulation



Available online at www.sciencedirect.com

ScienceDirect

Procedia Manufacturing 26 (2018) 617–628

Procedia
MANUFACTURING

www.elsevier.com/locate/procedia

46th SME North American Manufacturing Research Conference, NAMRC 46, Texas, USA

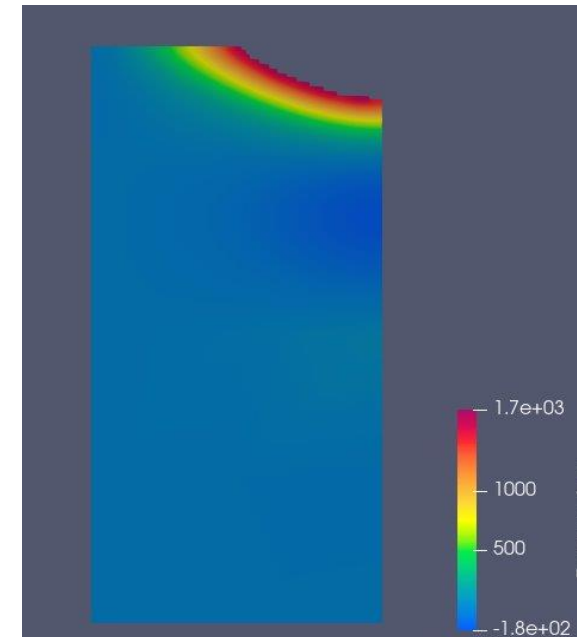
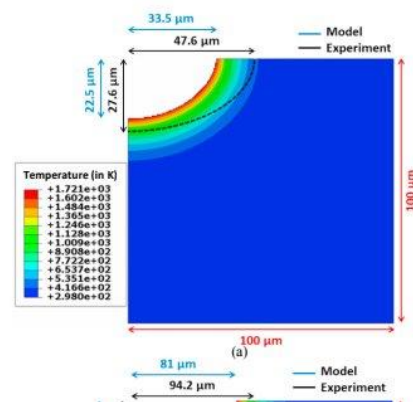
FE Modeling for Single Spark in EDM Considering Plasma Flushing Efficiency

S. Jithin^a, Ajinkya Raut^a, Upendra V. Bhandarkar^a, Suhas S. Joshi^{a,*}

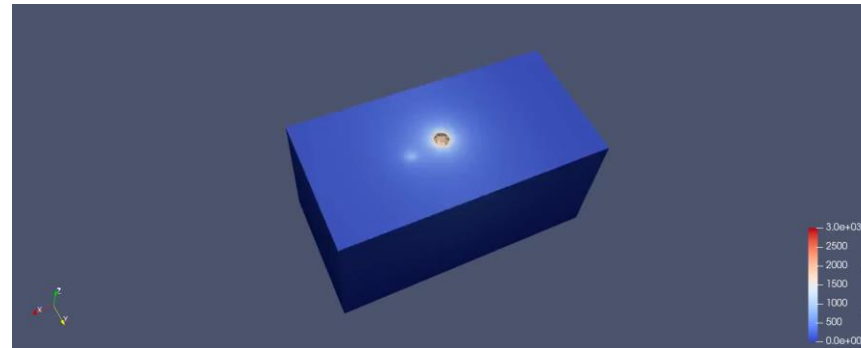
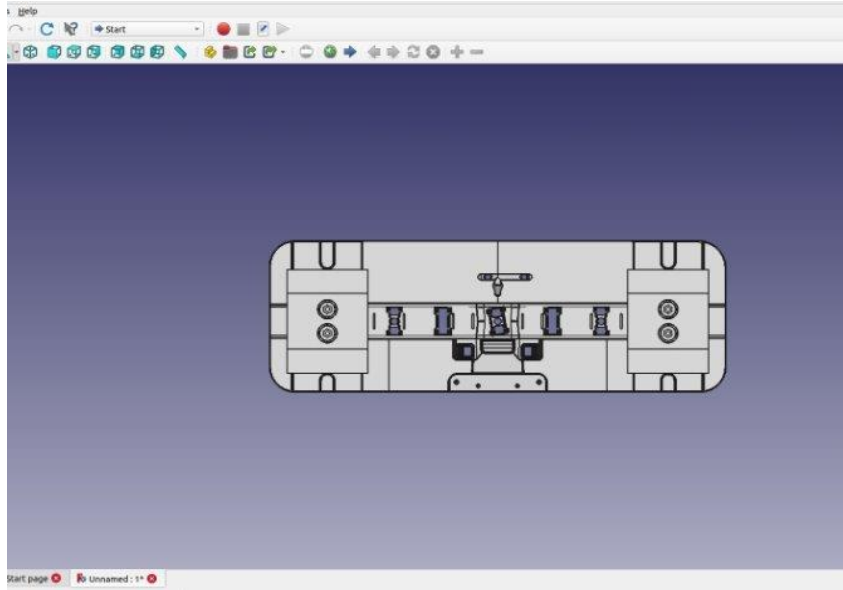
^aDepartment of Mechanical Engineering, Indian Institute of Technology Bombay, Mumbai – 400076, India

* Corresponding author. Tel.: +91-22-25767527
E-mail address: ssjoshi@iitb.ac.in

Abstract



Numerical examples – Multiple spark simulation (single spark at a time)



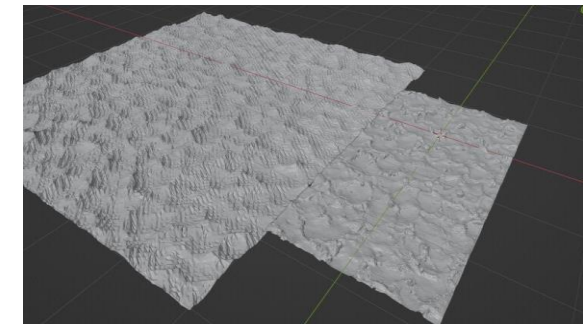
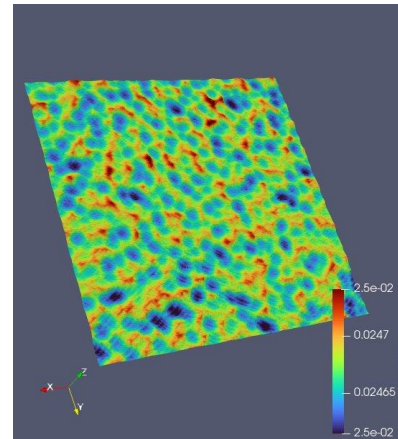
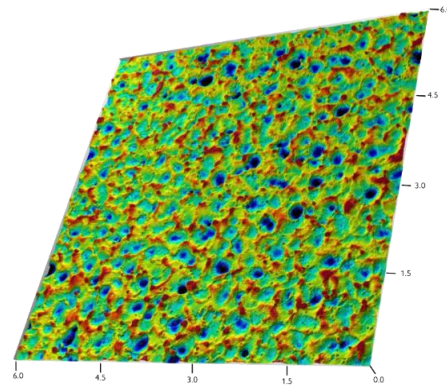
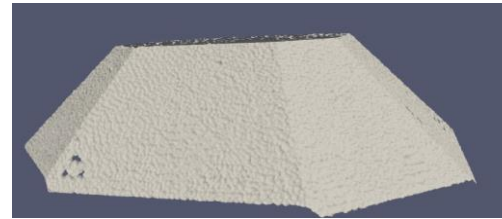
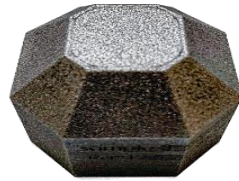
Numerical examples – Part-scale simulation

- Part-scale simulation run on the LUMI supercomputer
- 22 time steps per TOn / TOff, 3000 time steps in total
- 500 simultaneous sparks
- 30+ million element mesh (6 levels of adaptive refinement close to the surface).
- Run on 256 processors



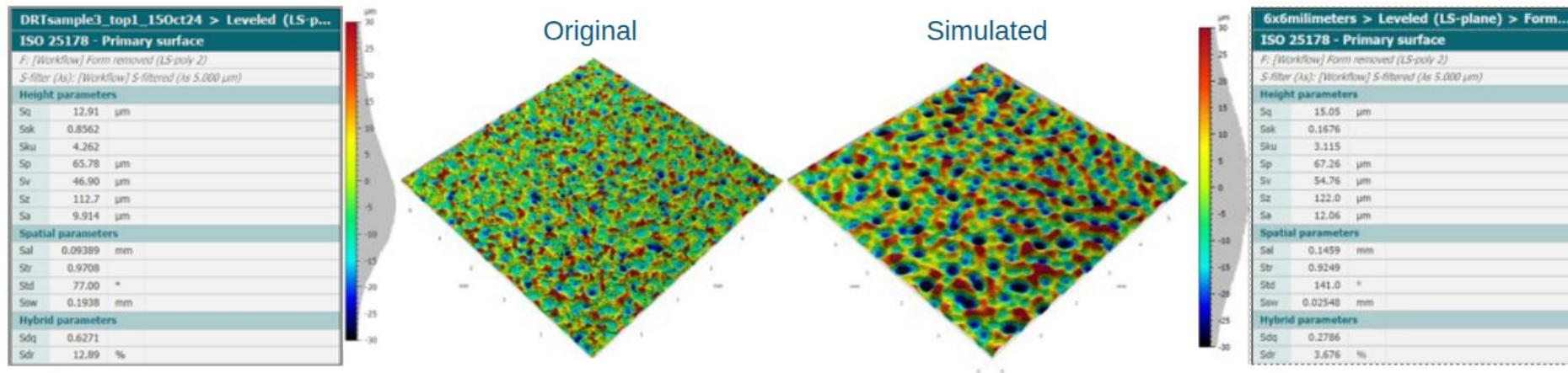
Numerical examples – Part-scale simulation

- Comparison against experimental results from DRT



Numerical examples – Part-scale simulation

- Comparison against experimental results from DRT

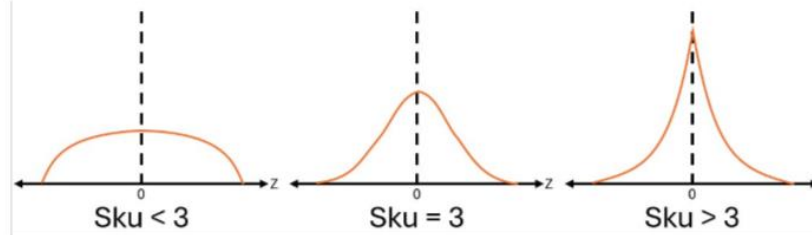


Analysis:

Peaks are thinner and sharper in the original surface, associated with Sku value.

The original surface has a lower Sz value, which indicates the difference between the highest peak and deepest valley.

The original surface has a lower Sv value, which represents the maximum depth of valleys below the mean line (considered in absolute value).



Assumption + Suggestion (No SME comment):

- EDM sparks may be removing up more material.
- Smaller EDM sparks might help to improve the result.
- The surface may also improve if the mesh size is reduced, so that the difference between the mesh planes is not interpreted as flat surfaces and the peaks are more noticeable.

01 Introduction

02 EDM Governing equations

03 Numerical approximation

04 Numerical examples

05 Conclusions

Conclusions - overview

An efficient algorithm for EDM process simulation has been presented

- ✓ Thermal simulation
- ✓ Level set based on eliminating boiled volume
- ✓ Embedded finite element method
- ✓ Ghost stabilization
- ✓ Adaptive mesh refinement
- ✓ Coupling with geometrical representation of the electrode by means of CAD
- ✓ Simultaneous simulation of multiple sparks (sufficiently separated)

Numerical results have been presented

- ✓ Single spark validation
- ✓ Part-scale simulation

The presented strategy is capable of properly representing the EDM process

Next steps will include further calibration, residual stress evaluation

Conclusions - references

- J. Baiges, H. Venghaus, M. Dias. **Adaptive Numerical Simulation of Electro Discharge Machining finishing operations using an Embedded Approach.** In preparation, 2025
- J. Baiges and C. Bayona. **RefficientLib: An efficient load-rebalanced adaptive mesh refinement algorithm for high performance computational physics meshes.** SIAM Journal of Scientific Computing 2017



TECHNICAL WORKSHOP

Optimising steels microstructure and surface integrity to face new challenges in Additive Manufacturing



Funded by
the European Union

SuPreAM project has received funding from the European Union's
Research Fund for Coal and Steel (RFCS): project num. 101112346



Funded by
the European Union

Predictive simulation of finishing operations in steel Additive Manufacturing for optimal Surface integrity

Material characterisation and surface roughness prediction

Simon Larsson

Associate Professor at the Division of Solid Mechanics, Luleå University of Technology

simon.larsson@ltu.se



Material characterisation

Introduction

- Characterisation of Additively manufactured materials at elevated strain-rates and temperatures.
- Calibration of constitutive model.

Constitutive model – Johnson-Cook

$$\sigma = \underbrace{(A + B \cdot \varepsilon^n)}_{\text{Plastic deformation}} \cdot \underbrace{\left(1 + C \cdot \ln\left(\frac{\dot{\varepsilon}}{\dot{\varepsilon}_0}\right)\right)}_{\text{Strain-rate dependency}} \cdot \underbrace{\left(1 - \left(\frac{T - T_0}{T_m - T_0}\right)^m\right)}_{\text{Thermal softening}}$$

Material constants

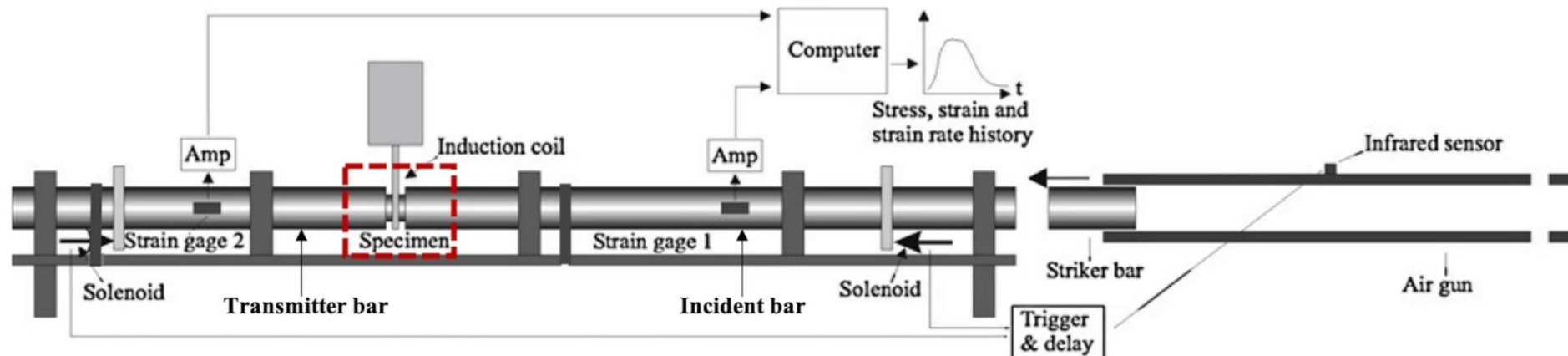
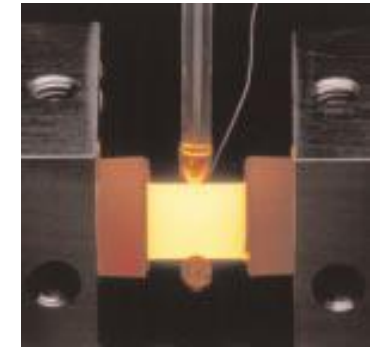
A	Initial yield strength
B	Flow stress effect
n	Flow stress effect
C	Strain-rate effect
m	Thermal softening effect

Variables

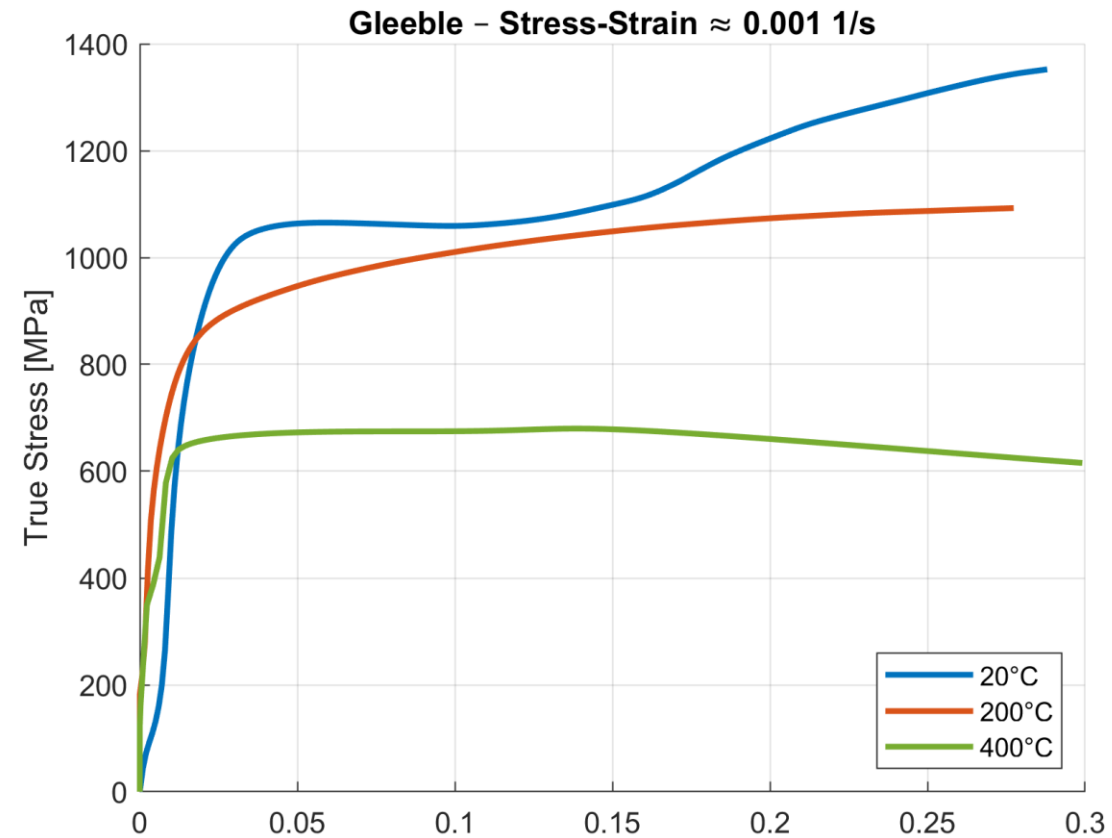
ε	Equivalent plastic strain
$\dot{\varepsilon}$	Plastic strain-rate
$\dot{\varepsilon}_0$	Reference plastic strain-rate
T	Temperature
T_0	Reference temperature
T_m	Melt temperature

Experimental setups

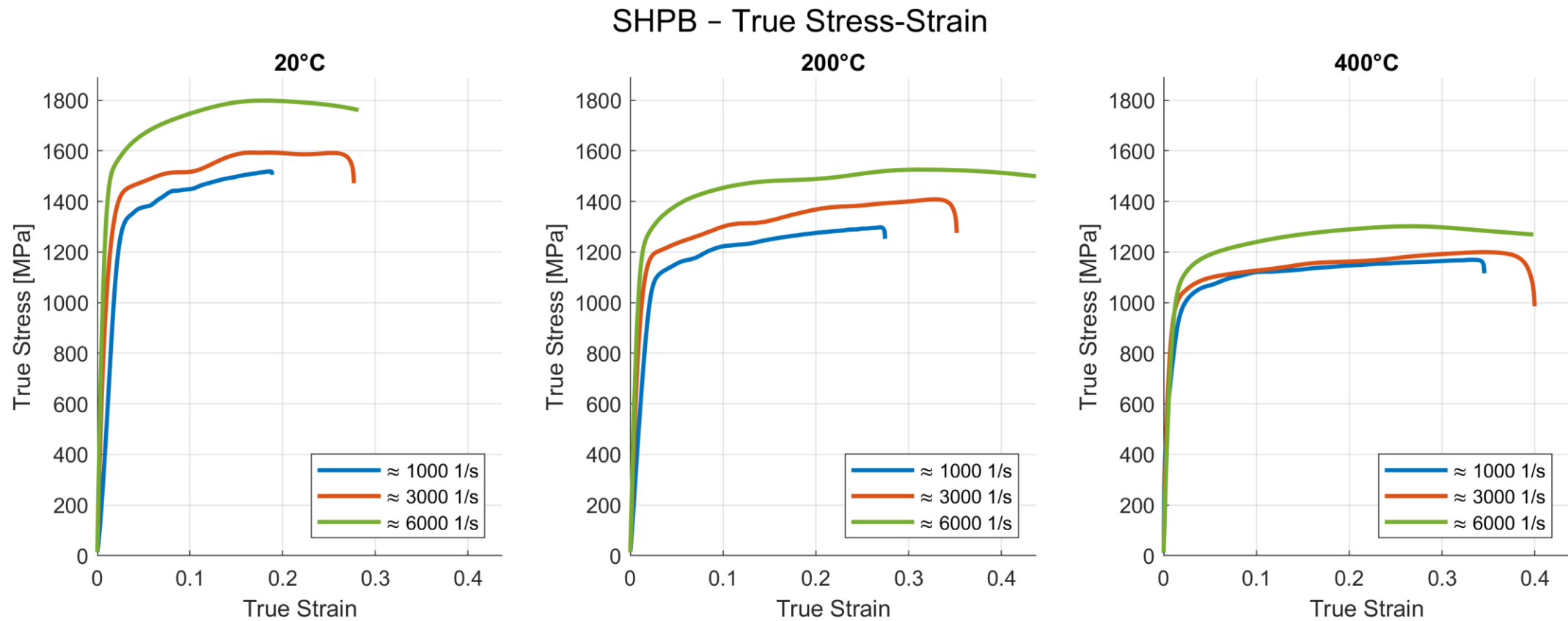
- Compressive testing of cylindrical samples
- Low strain-rate: Gleeble 3800 GTC
- High strain-rate: split-Hopkinson pressure bar (SHPB)
- 3 Temperatures: 20°C, 200°C and 400°C
- 4 Strain-rates: quasi-static, 1000 s⁻¹, 3000 s⁻¹ and 6000 s⁻¹



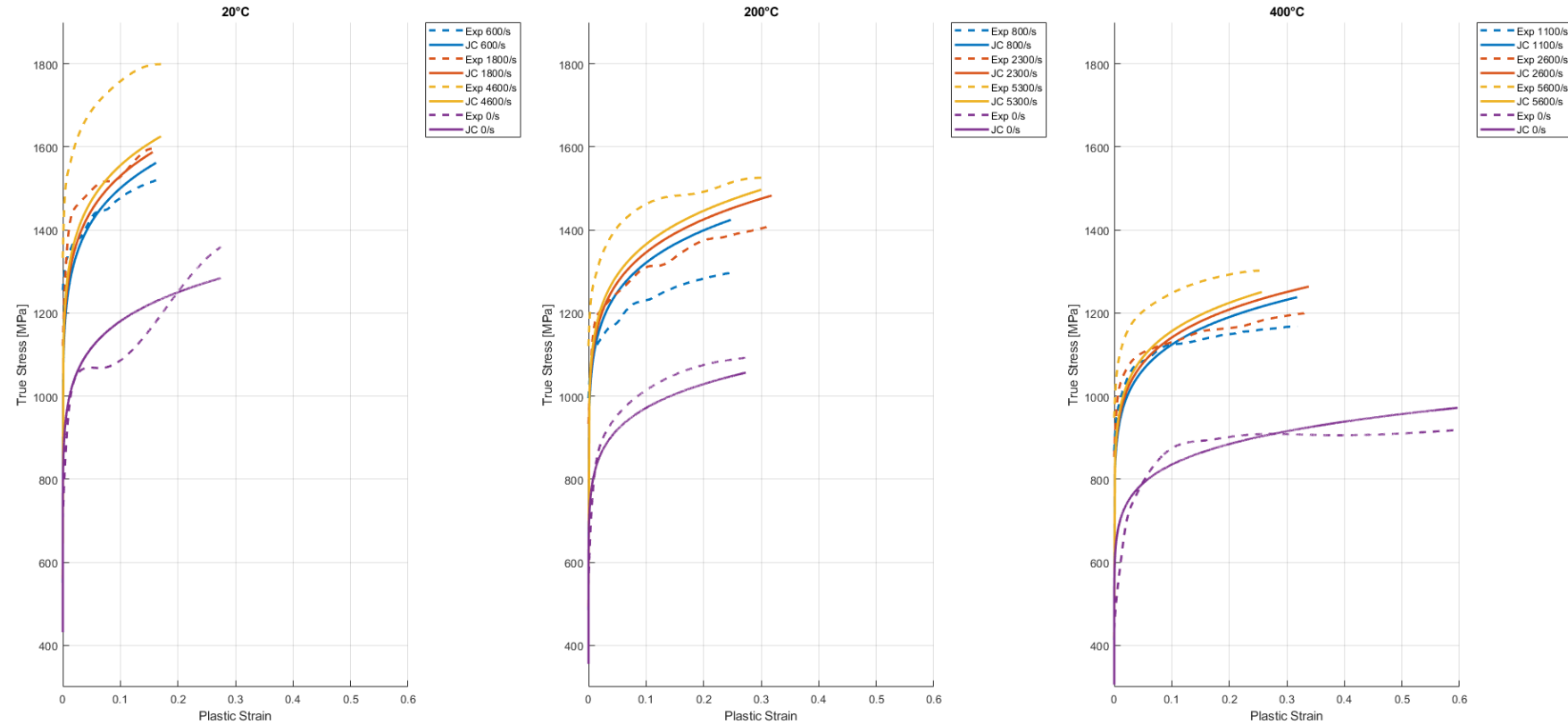
Experimental results – quasi-static compression



Experimental results – elevated strain-rates

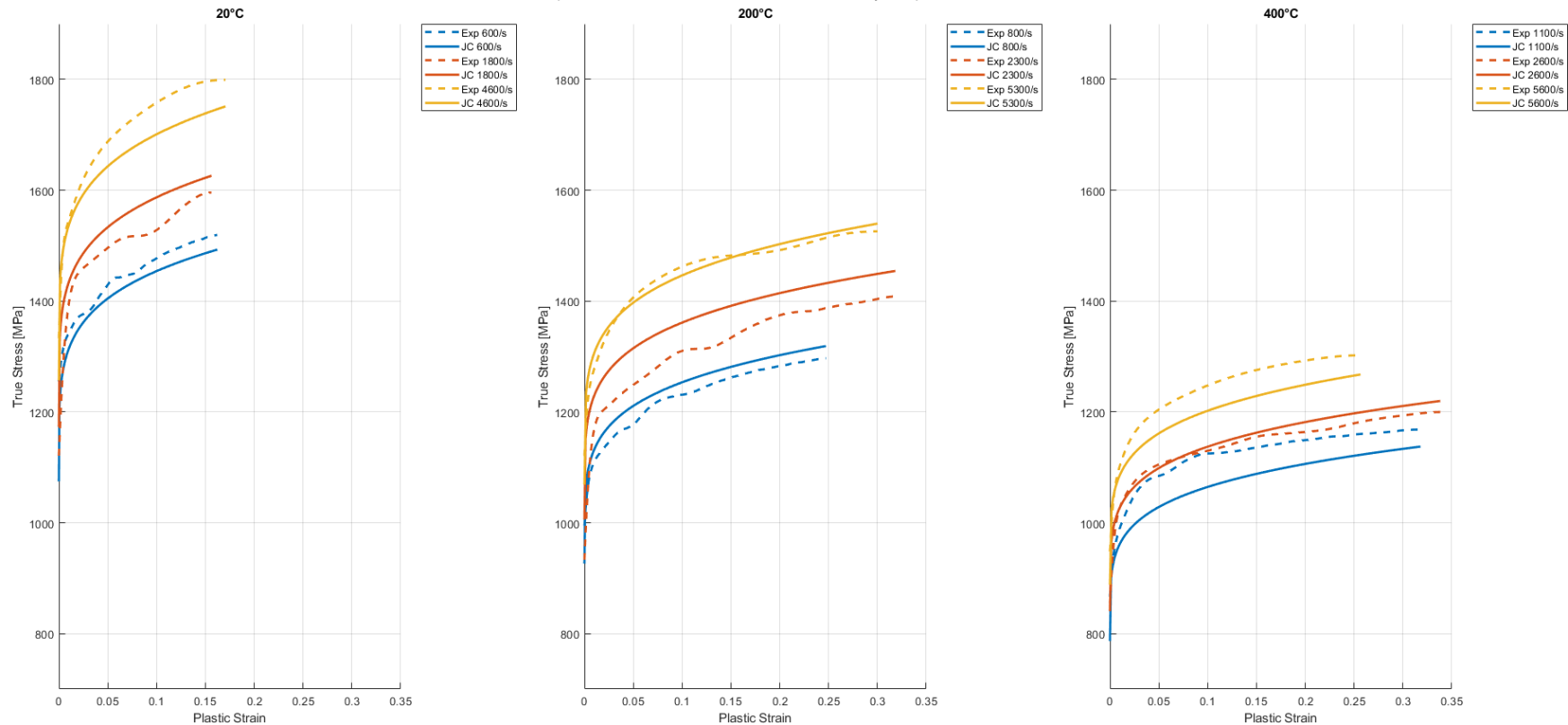


Model calibration – combined SHPB and Gleeble fitting



Parameter	A	B	n	C	m
Value	486.32	1132.56	0.128	0.0202	0.984

Model calibration – SHPB fitting



Parameter	A	B	n	C	m
Value	501.94	281.74	0.201	0.1784	0.869

Conclusions

- Fitting based on both SHPB and Gleeble did not yield satisfactory accuracy across entire dataset.
- Fitting based on SHPB provide significantly improved accuracy.

Surface roughness prediction

Introduction

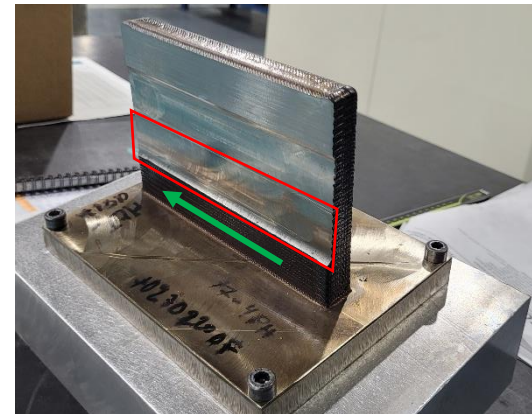
Predicting Surface Roughness in Milling

- Surface roughness is critical for product quality, tool life, and process efficiency
- Predictive models can help optimize parameters without excessive experiments.
- **Goal:** Predict S_a (arithmetic mean height) and S_q (RMS height) from simple machining parameters.

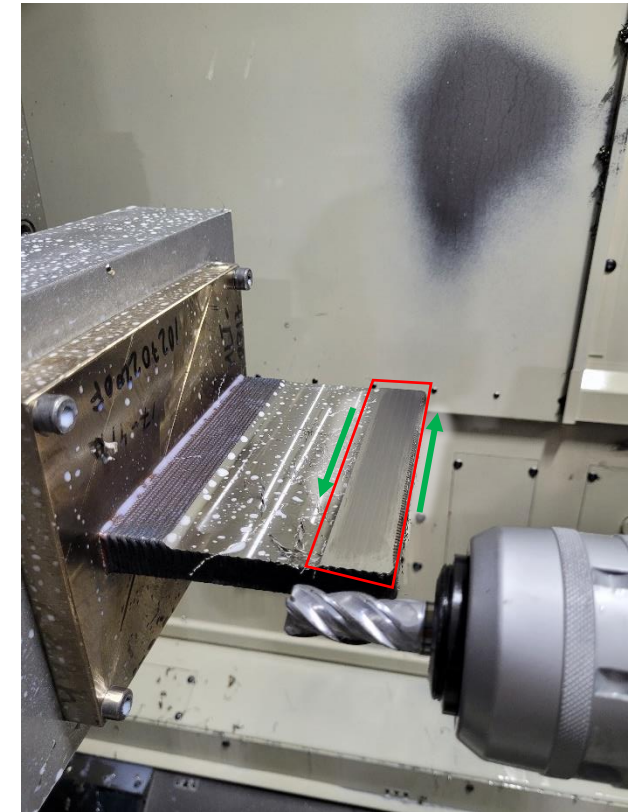
Experiments & Data Collection

- Machining of 2 sample parts, each tested under:
 - End milling (smooth & aggressive conditions)
 - Face milling (smooth & aggressive conditions)
- Parameters recorded:
 - Depth of cut (axial or radial)
 - Feed rate
 - Spindle speed (fixed ~995 rpm)
 - Mean spindle load (Nm)
- Surface roughness measured: S_a , S_q (μm)
- Dataset: 8 experimental cases total

Milling case	Depth of cut (mm)	Feed rate (mm/min)	Spindle load (Nm)	S_a (μm)	S_q (μm)
End milling – aggressive	2.0	500	4.06	0.61	0.83
End milling – smooth	1.0	500	0.70	0.69	0.82
Face milling – aggressive	2.5	125	5.26	1.18	1.42
Face milling – smooth	0.5 ($\times 4$ passes)	1990	6.47	0.30	0.38



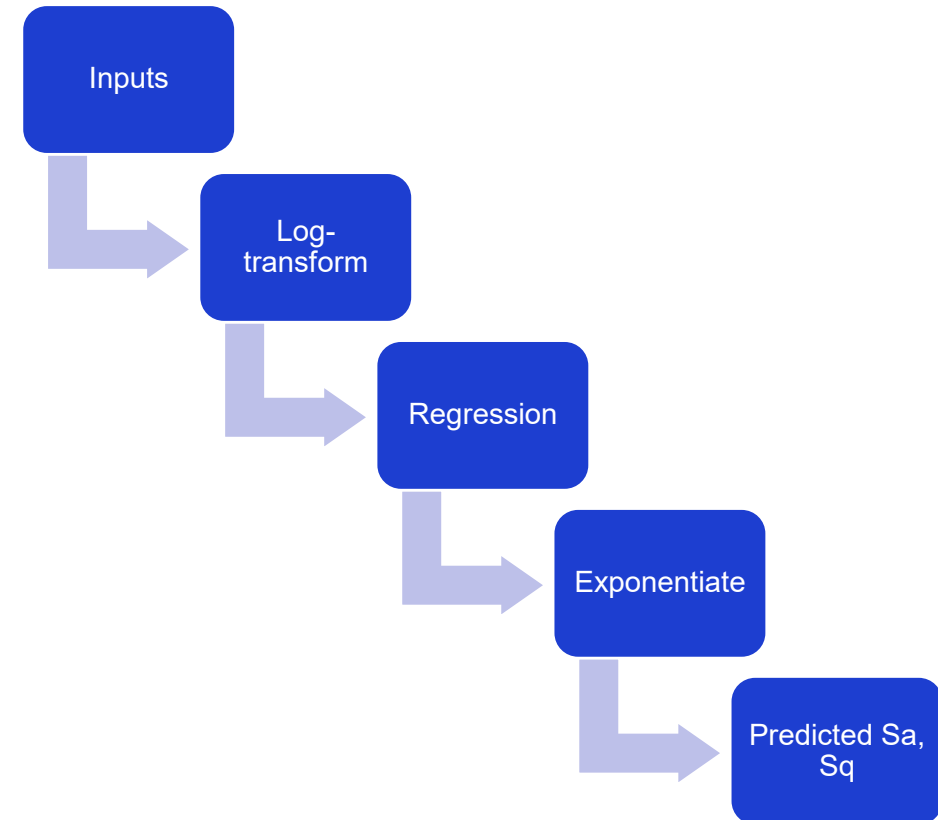
Face milling



End milling

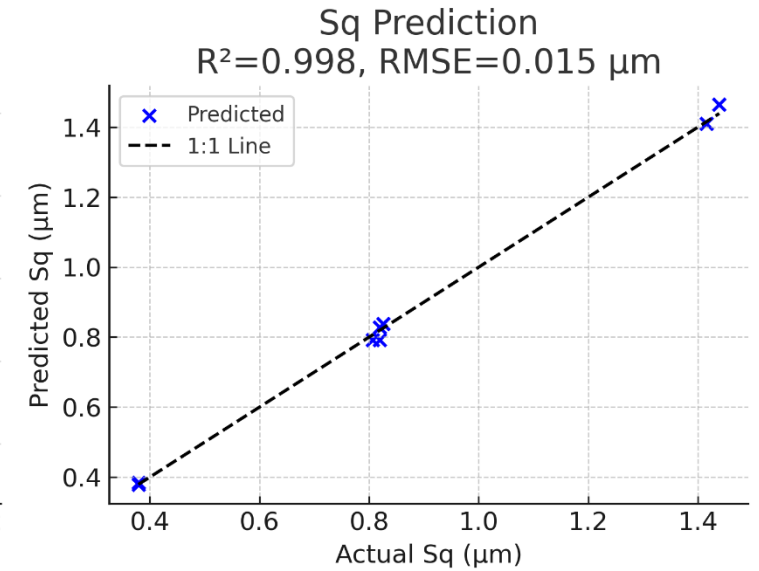
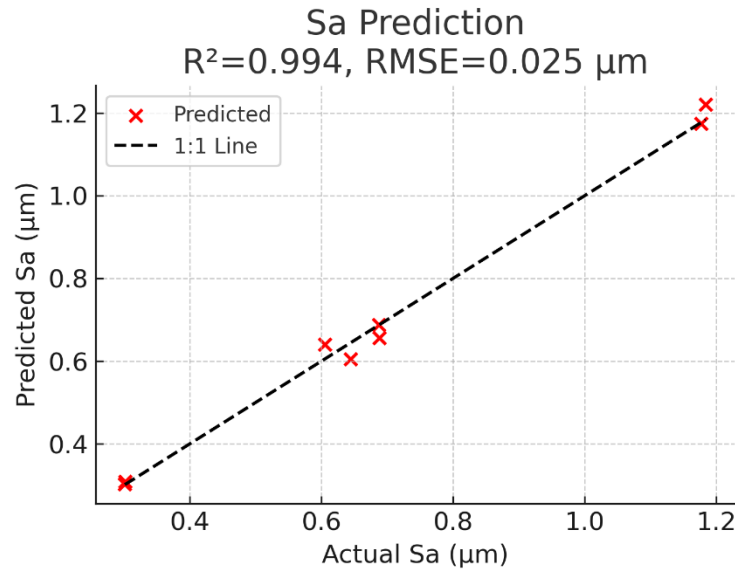
Model development

- Predictors:
 - $\log(\text{depth of cut})$
 - $\log(\text{feed rate})$
 - Spindle load
- Responses:
 - $\log(Sa)$, $\log(Sq)$
- Linear regression structure:
$$\log(Sa) = \beta_0 + \beta_1 \log(d) + \beta_2 \log(f) + \beta_3 L_s$$
$$\log(Sq) = \gamma_0 + \gamma_1 \log(d) + \gamma_2 \log(f) + \gamma_3 L_s$$
- Predictions are exponentiated back to μm scale.
- Implemented in Python (scikit-learn).
- Missing spindle load \rightarrow replaced by mean spindle load.



Results and model performance

- Performance (training data):
 - Sa model:
 $R^2 = 0.994$, RMSE = 0.025 μm
 - Sq model:
 $R^2 = 0.998$, RMSE = 0.015 μm
- Model captures main trends well despite very small dataset (8 samples)



Predicted vs Actual values for Sa and Sq.
Dashed line = perfect agreement.

Conclusions & next steps

- A simple linear regression model can predict surface roughness from basic milling parameters.
- Good fit on limited dataset.
- Handles missing inputs (spindle load).
- **Limitations:** only 8 samples → risk of overfitting.
- Possible next steps:
 - Collect more data (different tools, materials, conditions).
 - Try ridge regression or leave-one-out validation.
 - Extend model to include spindle speed, tool wear, and material effects.



TECHNICAL WORKSHOP

Optimising steels microstructure and surface integrity to face new challenges in Additive Manufacturing



Funded by
the European Union

SuPreAM project has received funding from the European Union's
Research Fund for Coal and Steel (RFCS): project num. 101112346



TECHNICAL WORKSHOP

Optimising steels microstructure and surface integrity to face new challenges in Additive Manufacturing



Funded by
the European Union

The NewAIMS project has received funding from the European Union's Research Fund for Coal and Steel (RFCS): project num. 101112371





New approach to Additive Manufacturing of Microstructurally Optimised Steels

Conceptualisation, study and demonstration of strategies to obtain cost-effective high-performance steel in metal 3D printing processes

Eduard Garcia-Llamas, Dr.

EURECAT



Funded by
the European Union

- 01** Introduction
- 02** NewAims Project
- 03** NewAims in Practice
- 04** Expected Outcomes

Introduction



Opening Question

Jet engine



Intricate structures



Medical implants



Image 1 and 2: <https://www.shutterstock.com/es/search/3d-printed-metal-parts>

Image 3: <https://3dwithus.com/3d-printing-in-medicine>

What is Additive Manufacturing?

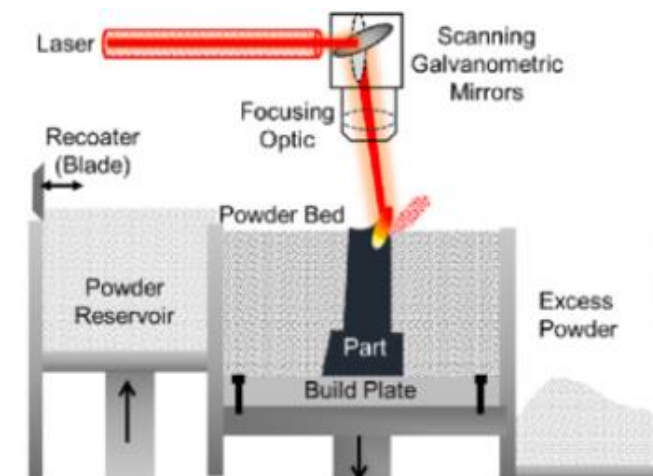
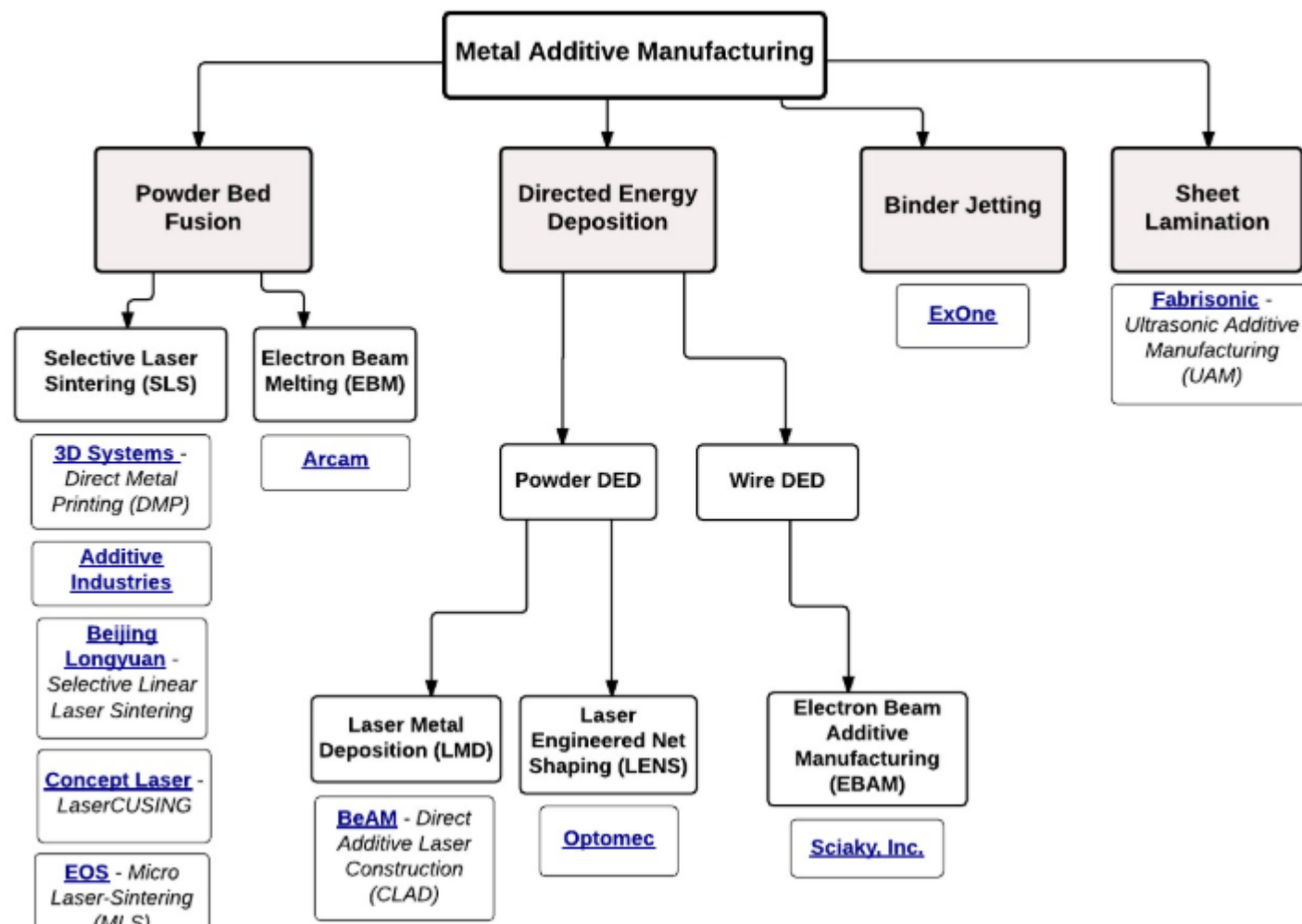
Traditional manufacturing



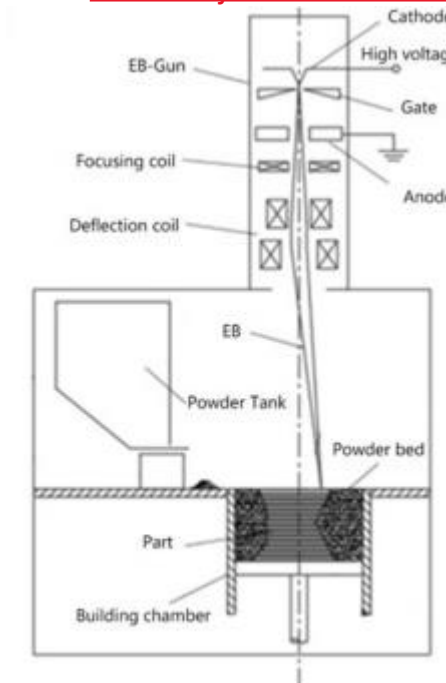
3D Additive manufacturing



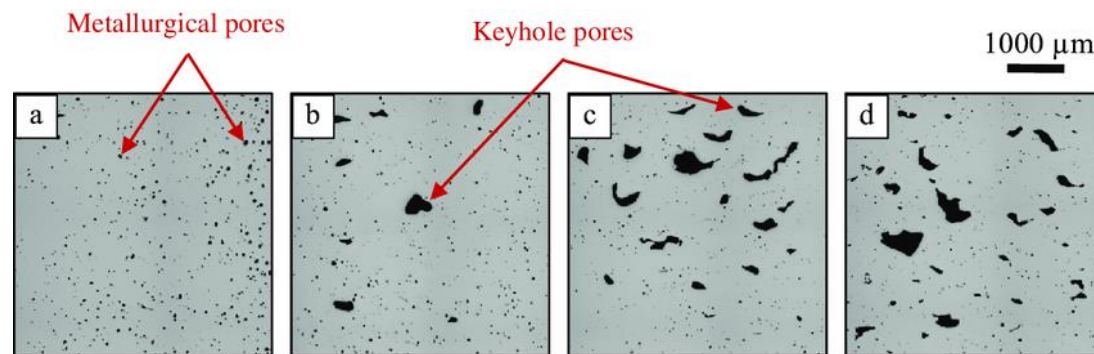
AM Technologies Overview



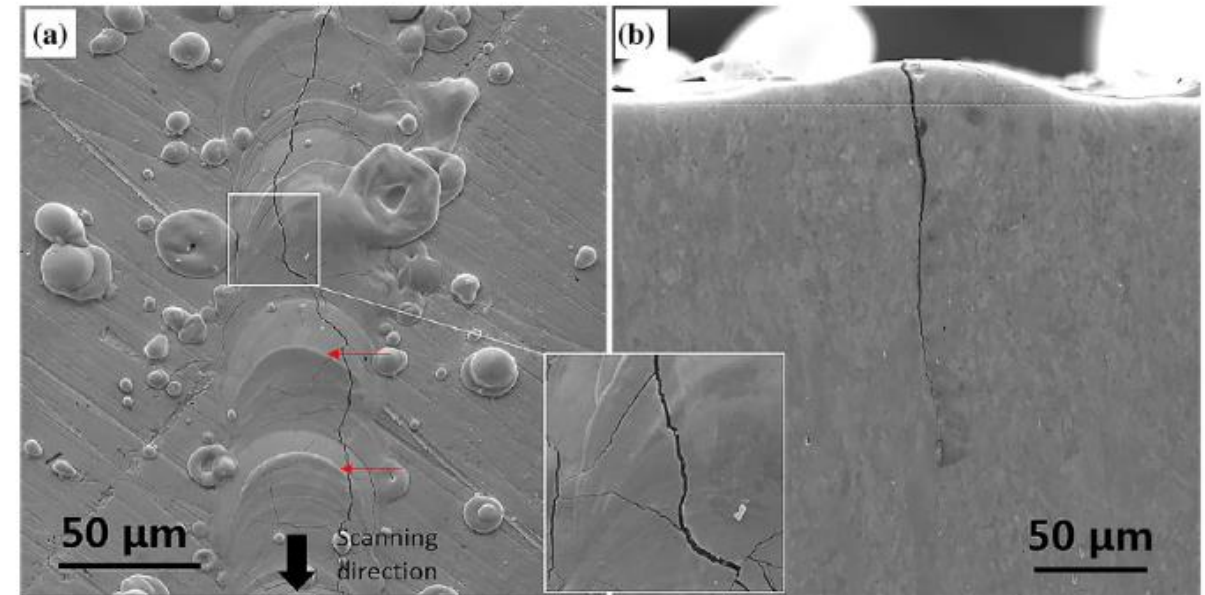
DOI:[10.1016/j.matdes.2022.111351](https://doi.org/10.1016/j.matdes.2022.111351)



The Challenges of AM



Nesma T. Aboulkhair*, Marco Simonelli, Luke Parry, Ian Ashcroft, Christopher Tuck, Richard Hague. 3D printing of Aluminium alloys: Additive Manufacturing of Aluminium alloys using selective laser melting. Progress in Materials Science, Volume 106, December 2019, 100578



Dian-Zheng Wang, Kai-Lun Li, Chen-Fan Yu, Jing Ma, Wei Liu, Zhi-Jian Shen. Cracking Behavior in Additively Manufactured Pure Tungsten[J]. Acta Metallurgica Sinica(English Letters), 2019, 32(1): 127-135 <https://doi.org/10.1007/s40195-018-0752-2>

NEWAIMS PROJECT



Additive Manufacturing & NEWAIMS Project

3D Printing advantages:

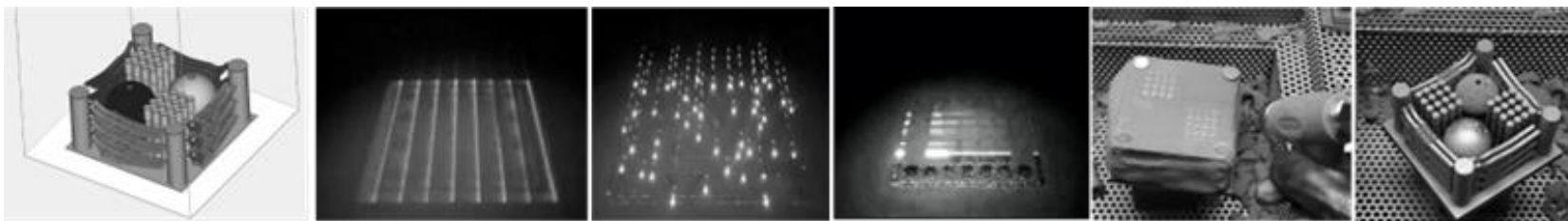
- Enables design optimization and limited-series production.
- Particularly suitable for hot forming tools.
- Industrial benefits: Hot stamping, die casting, plastic injection molding.
- Allows free-form cooling channels not possible with conventional (subtractive) methods.

Current limitations:

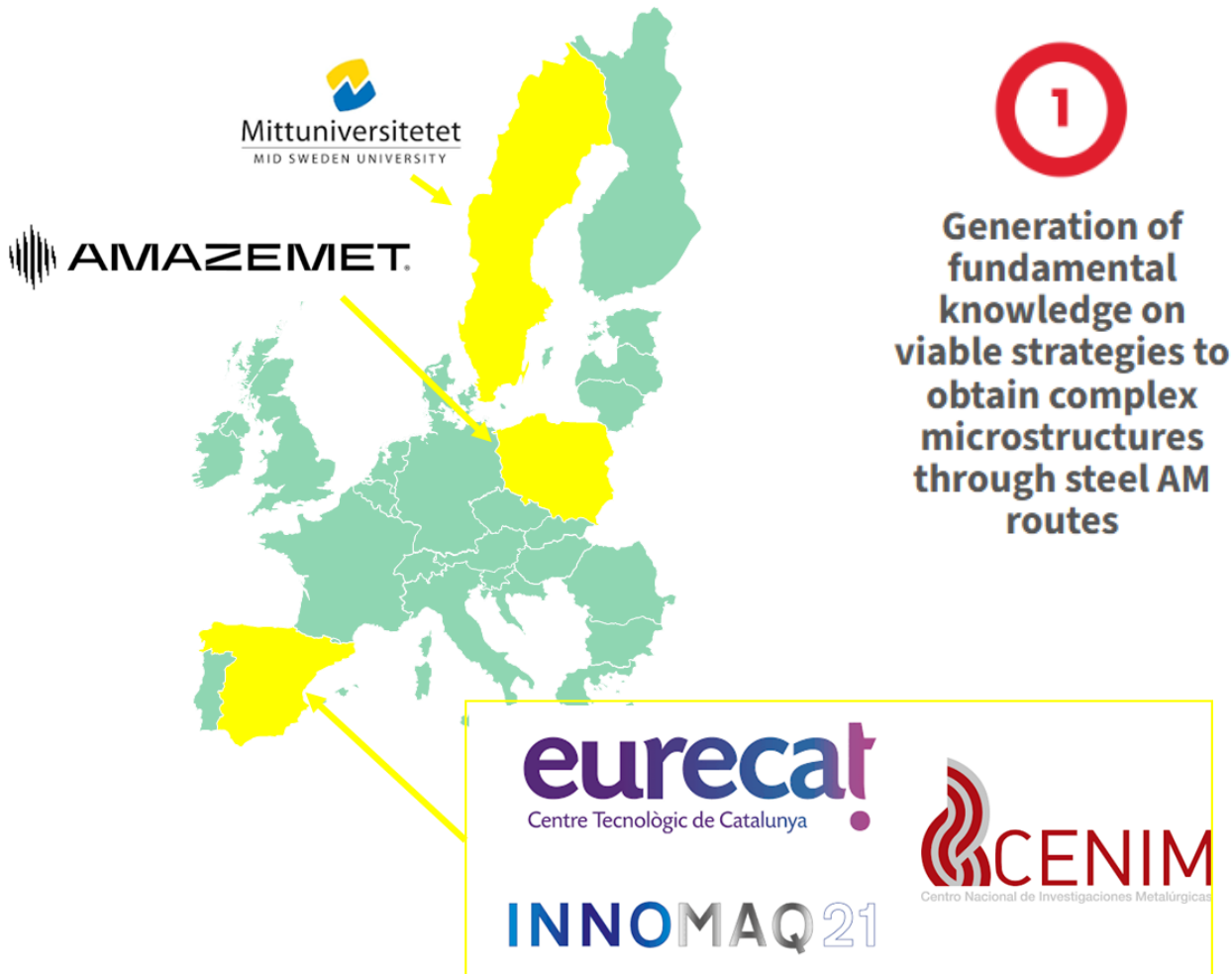
- Limited selection of printable materials.
- Hot work tool steels often require expensive superalloys or high-alloy steels (e.g., Maraging grades).
- Even premium materials may be inferior in durability to conventional tool steels.

NEWAIMS objective:

- Develop cost-effective, high-performance steels for metal 3D printing



NEWAIMS Pillars and Partners



1

Generation of fundamental knowledge on viable strategies to obtain complex microstructures through steel AM routes

2

Development of high-performance tool steel grades specifically designed for Powder bed Fusion

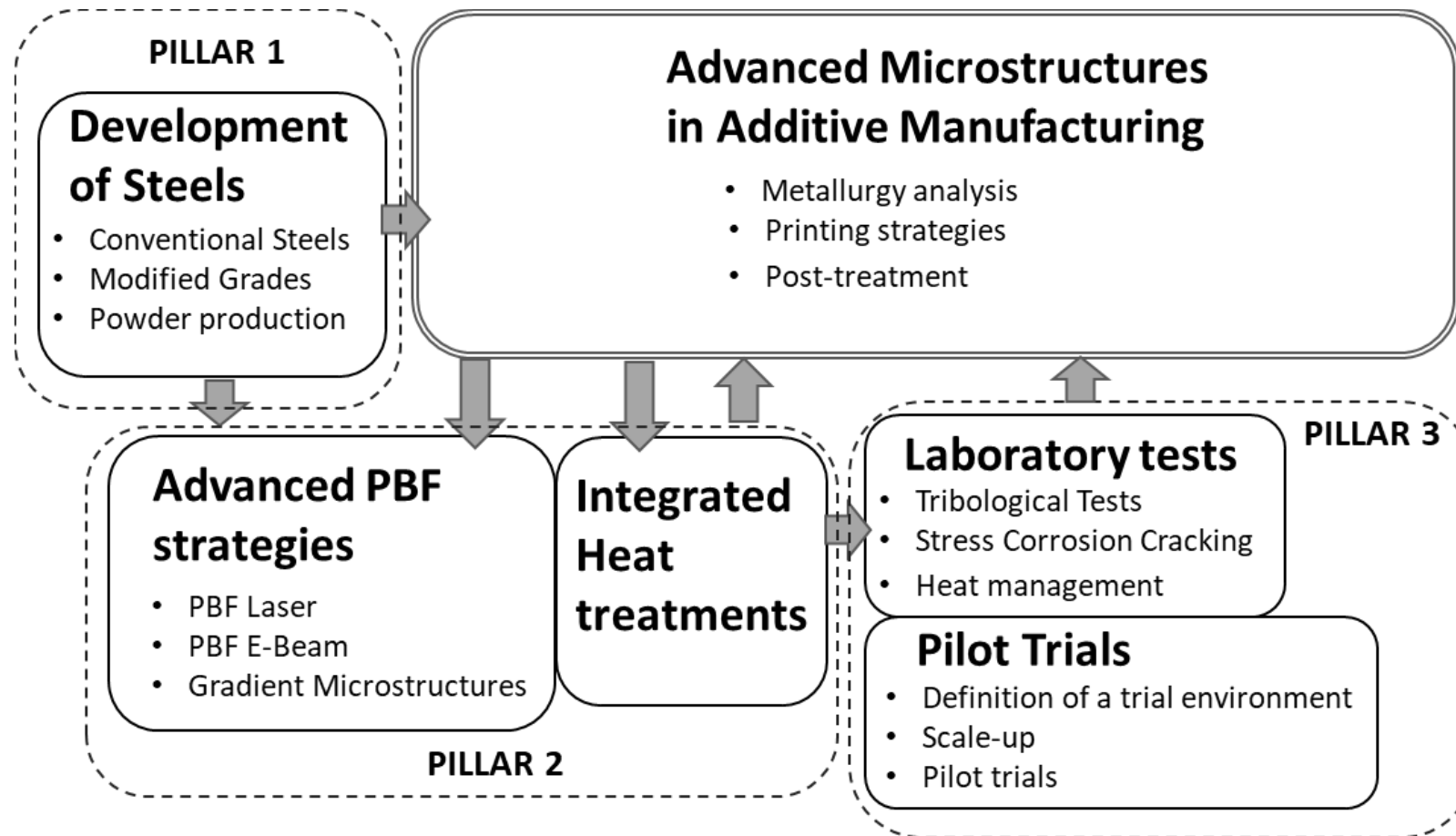
3

Development and demonstration of temperature-enhanced AM materials using complex microstructures in high-C steel

4

Achievement of material performance rivalling wrought material with AM

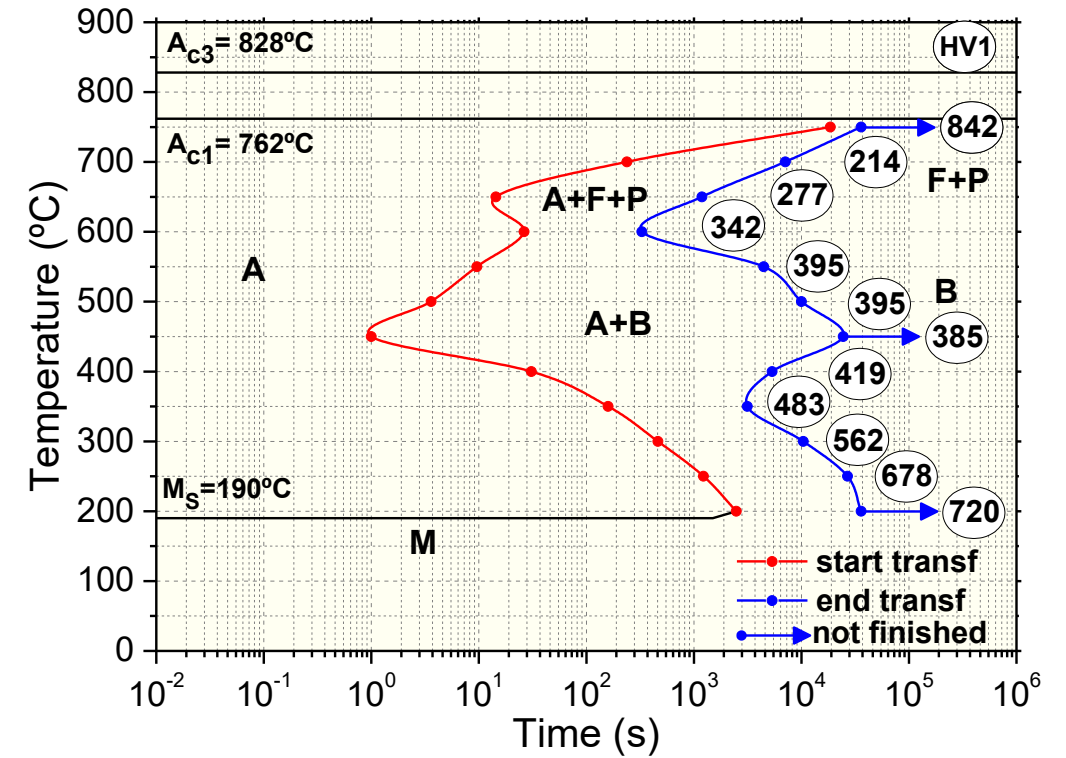
Project structure



NewAIMS in Practice



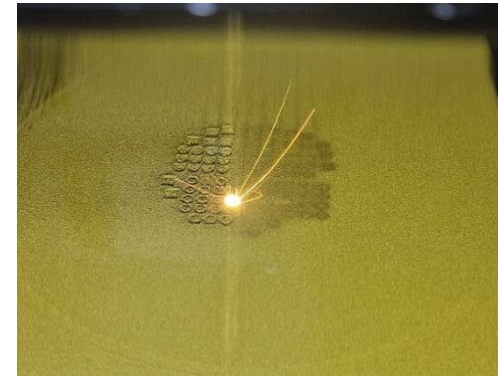
Microstructural Analysis via Dilatometry



L-PBF Additive manufactured samples



Aconity MINI



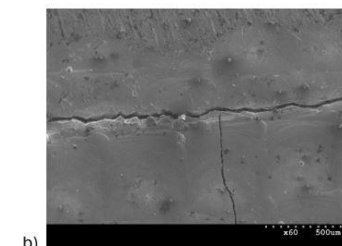
L-PBF Additive manufactured samples



Additive Manufacturing Observations

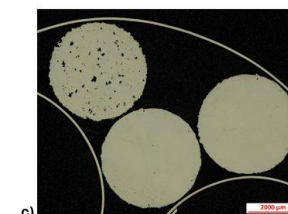
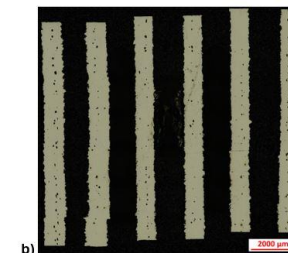
Room-temperature builds:

- Caused cracking and delamination due to high thermal gradients



Preheating (350 °C):

- Optimized laser power and scan speed
- Eliminated major defects



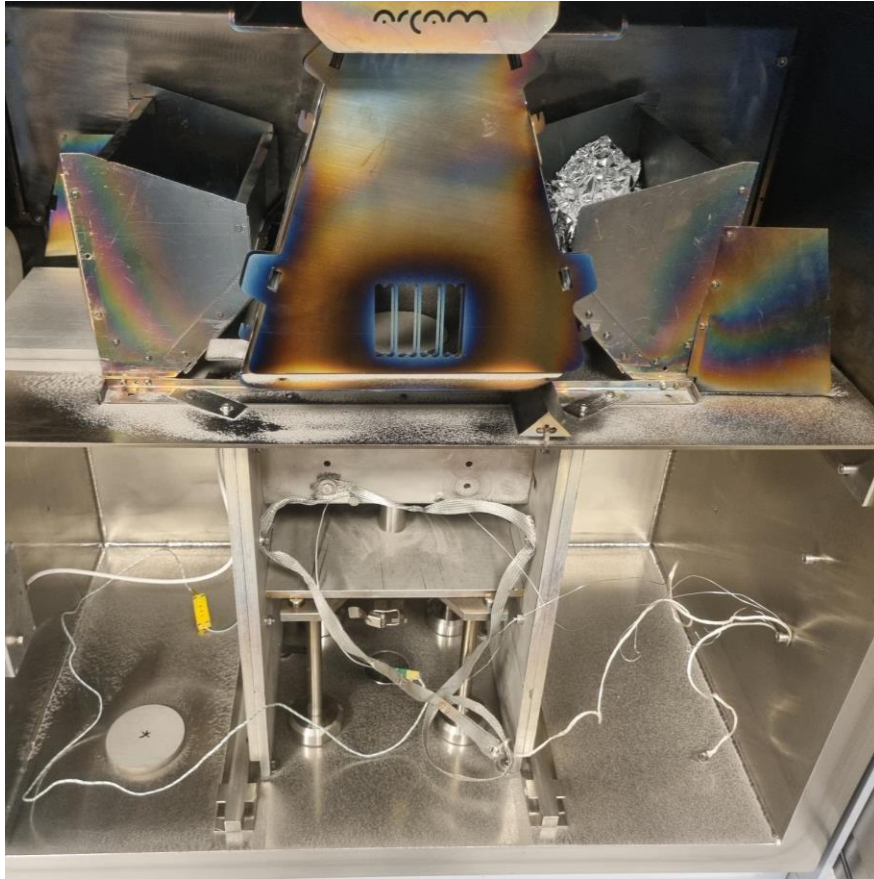
Material-specific observations:

- HTCS® : keyhole-induced porosity

Outcome:

- Crack-free builds achieved
- Highlights importance of thermal control and process tuning

E-PBF Additive manufactured samples



Modified Arcam S12 EB-PBF system (3 kW electron gun, 60 kV, partial He pressure 2×10^{-3} mbar)

Ø90 mm build tank with gravity-fed hopper and integrated rake

Samples built on 60×60×10 mm 304 stainless steel plates

Temperature monitored via K-type thermocouple

Expected Outcomes



Outcomes and Impact

- Development of two new high-performance steels specifically designed for Additive Manufacturing (AM).
- Production of demonstrator tooling parts to validate performance.
- Establishment of a clear link between process, microstructure, and performance, which is essential for industrial adoption.
- Expected Impact
 - Enables stronger, more reliable, and cost-effective steel components for AM.
 - Boosts Europe's manufacturing competitiveness and supports sustainability by reducing material waste.
 - Accelerates the industrial use of AM, particularly in tooling and automotive sectors.



TECHNICAL WORKSHOP

Optimising steels microstructure and surface integrity to face new challenges in Additive Manufacturing



Funded by
the European Union

The NewAIMS project has received funding from the European Union's Research Fund for Coal and Steel (RFCS): project num. 101112371





TECHNICAL WORKSHOP

Optimising steels microstructure and surface integrity to face new challenges in Additive Manufacturing



Funded by
the European Union

The NewAIMS project has received funding from the European Union's Research Fund for Coal and Steel (RFCS): project num. 101112371



New approach to Additive Manufacturing of Microstructurally Optimised Steels

Phase Transformations in Additively Manufactured Steels

Francisca G. Caballero

Spanish National Centre for Metallurgical Research (CENIM-CSIC)



Funded by
the European Union

Phase Transformations in Additively Manufactured Steels

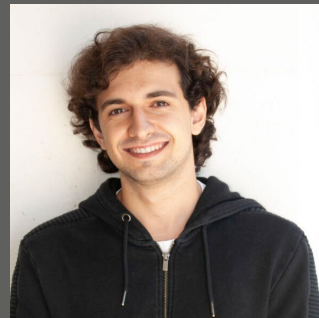
CSIC Team:



Ana Santana
FPU23/00285



Nisrine Elhamouchi



Guillermo Larrosa



In collaboration with:

Adriana Eres-Castellanos, Los Alamos National Lab, NM, USA

Jonathan D. Poplawsky, Oak Ridge National Laboratory, TN, USA.

Aleksandra Królicka, Politechnika Wroclawska Univ., PL.



Acknowledge funding sources:

European Commission, Research Fund for Coal and Steel Programme. Ref. RFCS-2022-101112371.
Center for Nanophase Materials Sciences-DOE Office of Science User Facility, Ref. CNMS2022-B-01449 and CNMS2024-B-02594.

- 01** Revealing the complexity of non-equilibrium, and non-uniform microstructures formed during LPBF process of Maraging steels.
- 02** Precipitation of intermetallic phases and austenite growth/reversion during ageing of LPBF Maraging steels.

01 Revealing the complexity of non-equilibrium, and non-uniform microstructures formed during LPBF process of Maraging steels.

02 Precipitation of intermetallic phases and austenite growth/reversion during ageing of LPBF Maraging steels.

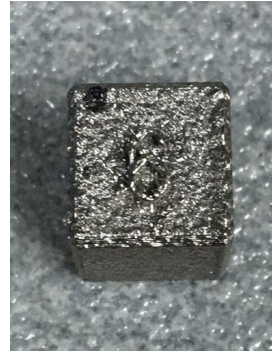
Laser Powder Bed Fusion of Maraging Steel

EOS cylinders (Ref. Material)

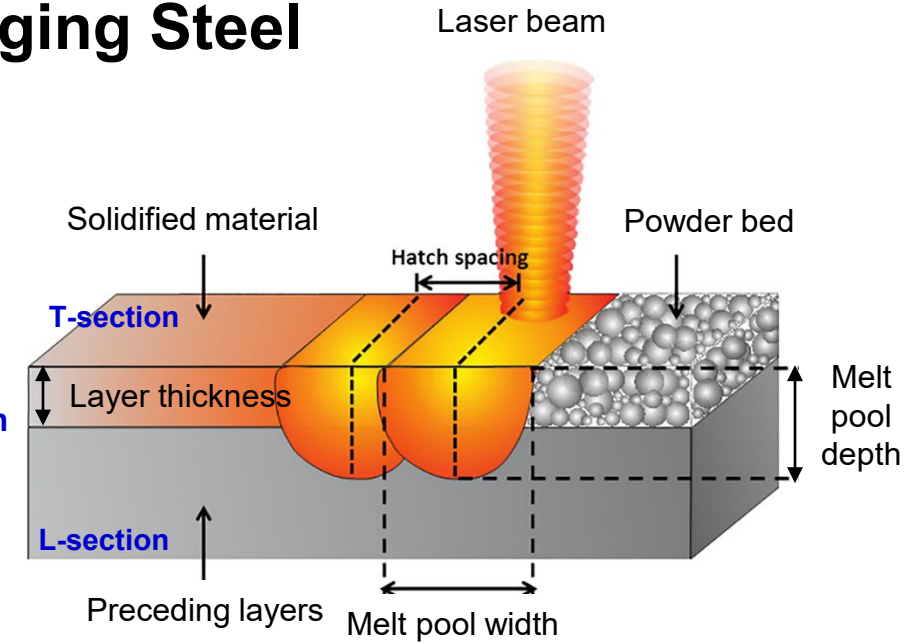


Under N² atmosphere
Volume rate of 3 mm³/s
Continuous Wave Emission
Layer thickness: 40 μm
Hatch spacing: 100 μm
Hatch angle: 67°

RENISHAW cubes

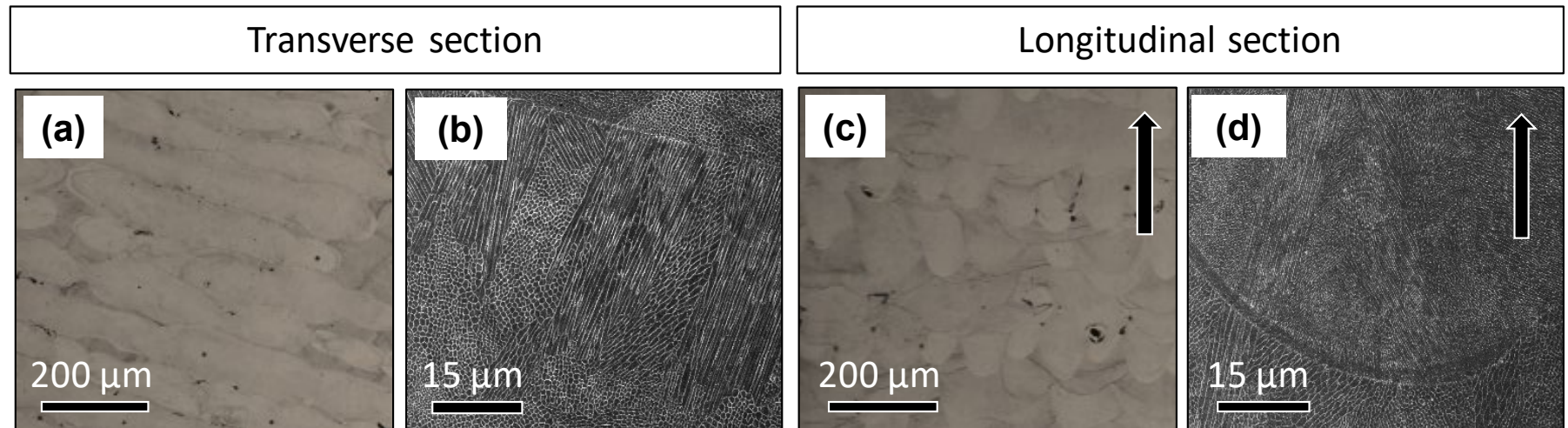


Under Ar atmosphere
Laser power: 250 W
Laser speed: 1000 mm/s
Continuous & Pulsed Wave Emission
Layer thickness: 50 and 100 μm
Hatch spacing: 80 μm
Hatch angle: 67°



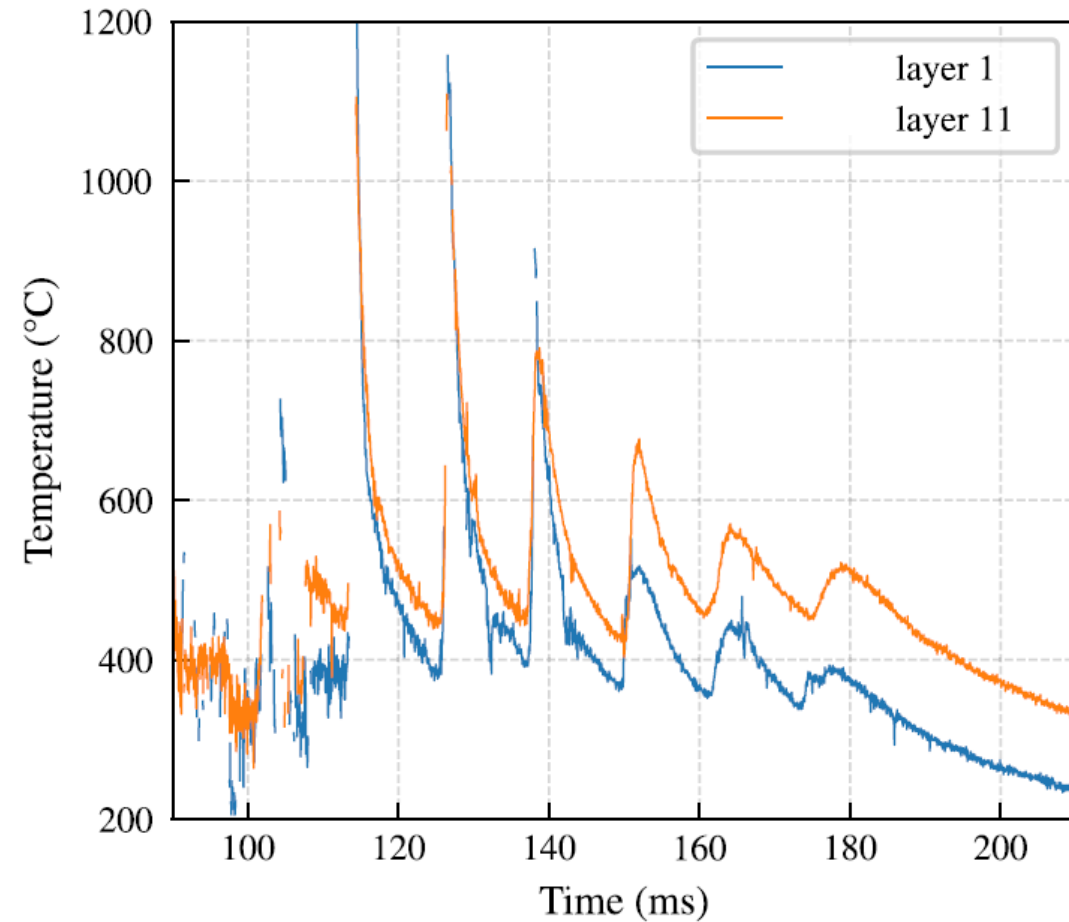
Element	Wt. %
Fe	66.38
Ni	18.35
Co	8.64
Mo	5.45
Ti	0.87
Cr	0.15
Si	0.11
Mn	0.05

Renishaw - 100 μm - PW laser

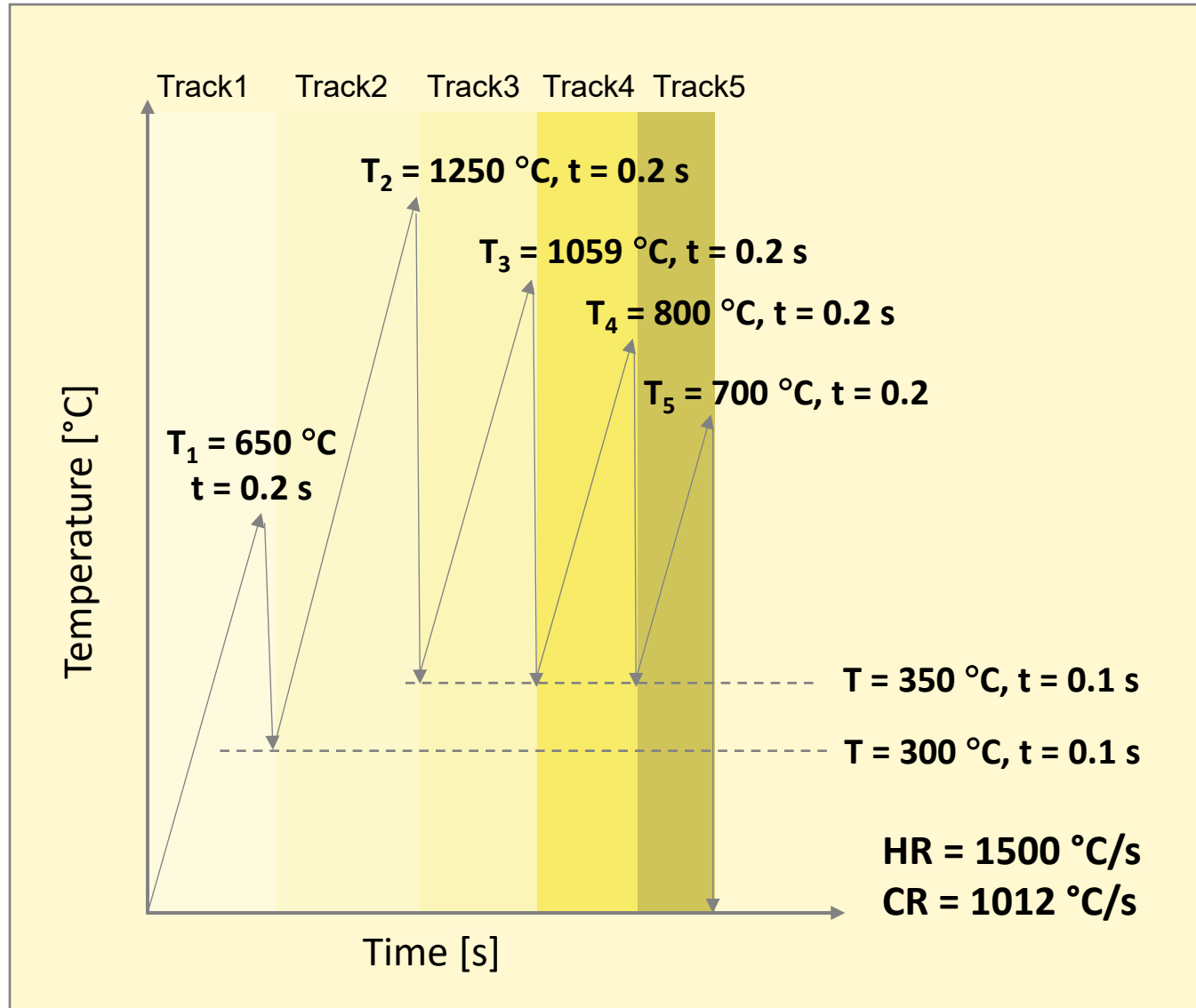


Thermal history experienced by the material during the build process

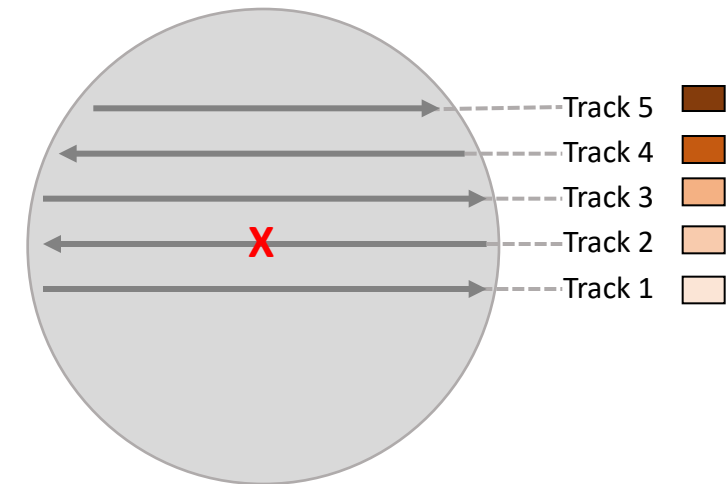
Temperature profiles for layers 1 and 11 based on measurements using *operando* X-ray diffraction



Thermal history experienced by the material during the build process

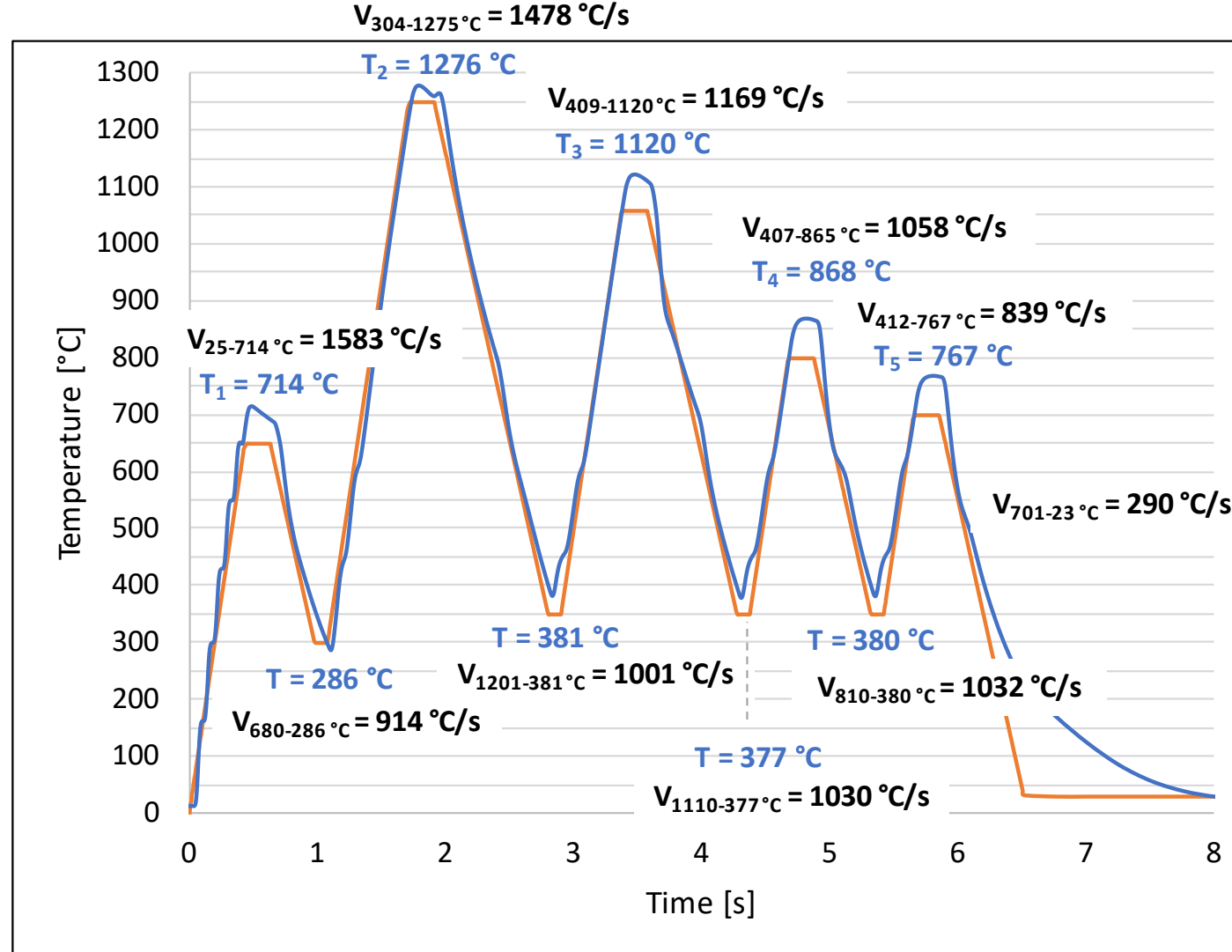


Last printed layer



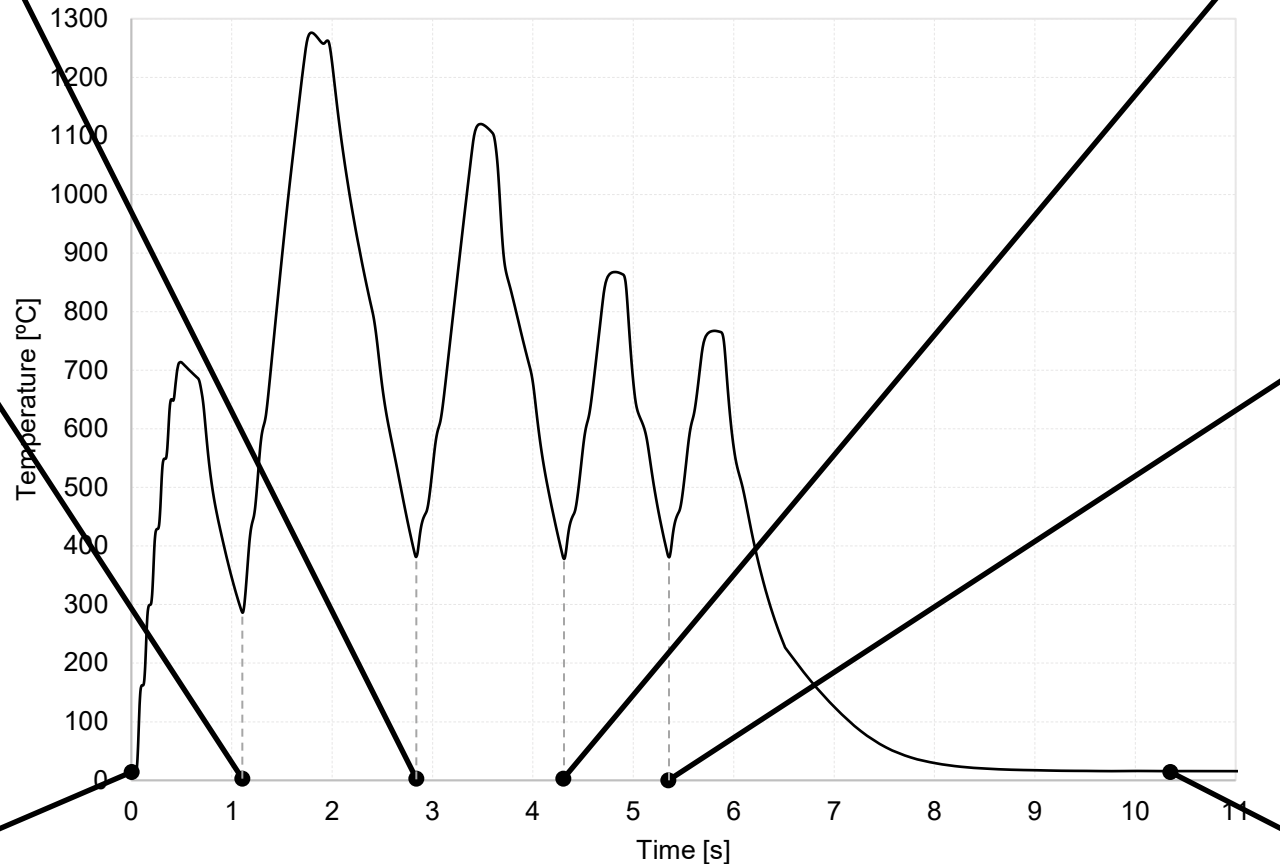
Scheel et al., Additive Manufacturing Letters 6 (2023) 100150
Ji et al., Journal of Materials Processing Tech. 301 (2022) 117452
Ashby et al., Additive Manufacturing 53 (2022) 102669

Thermal history experienced by the material during the build process

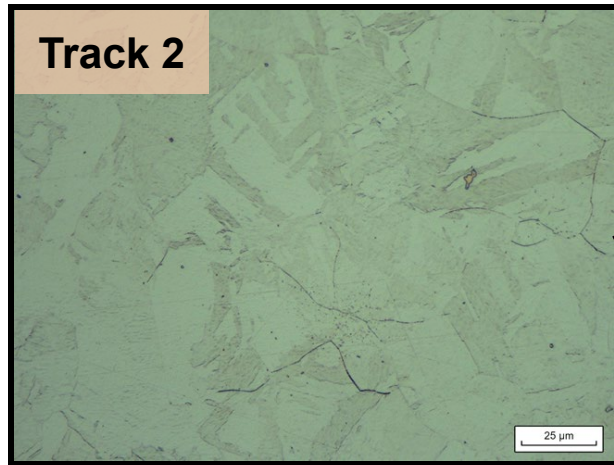


BAHR DIL 805A Quenching Dilatometer. Hollow cylindrical samples. Maraging Steel. As-cast material

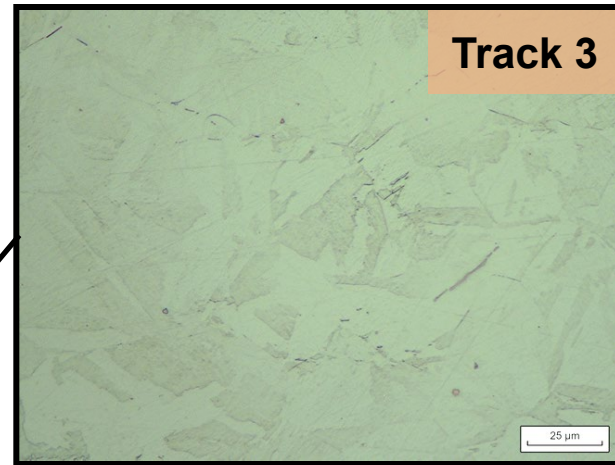
Microstructure evolution of as-cast Maraging steel under LPBF thermal history



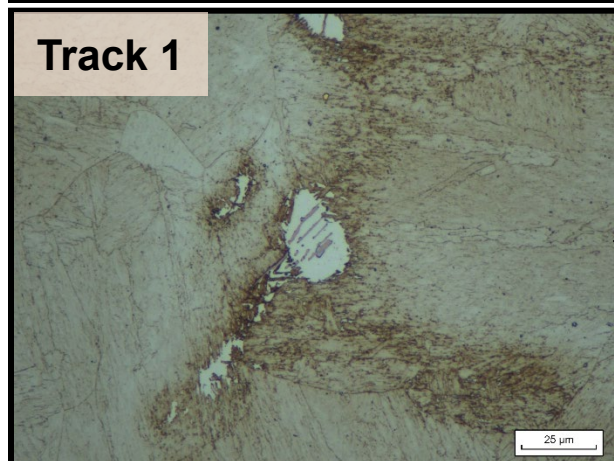
Track 2



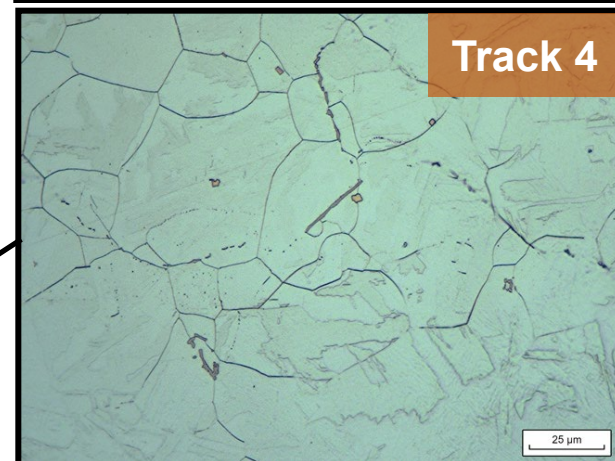
Track 3



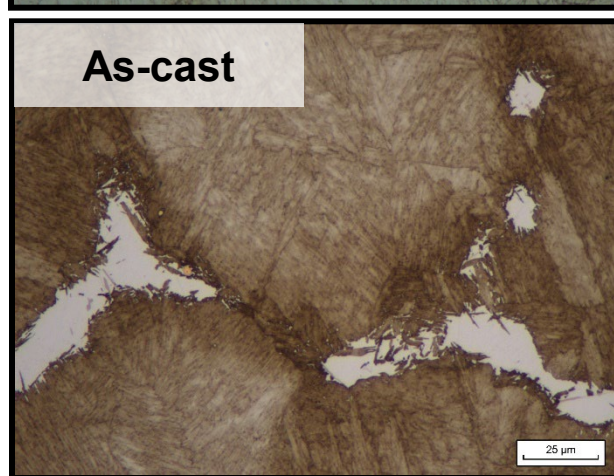
Track 1



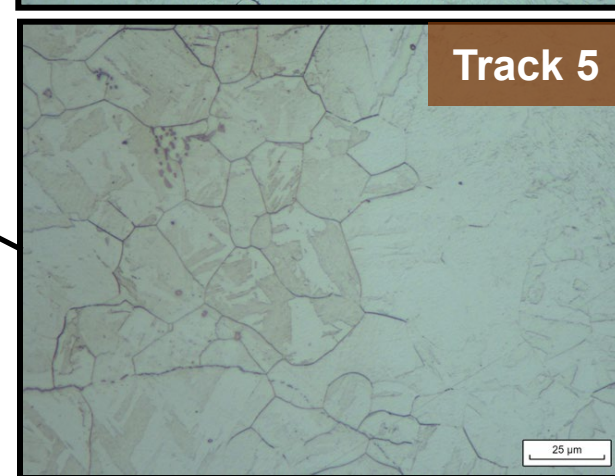
Track 4



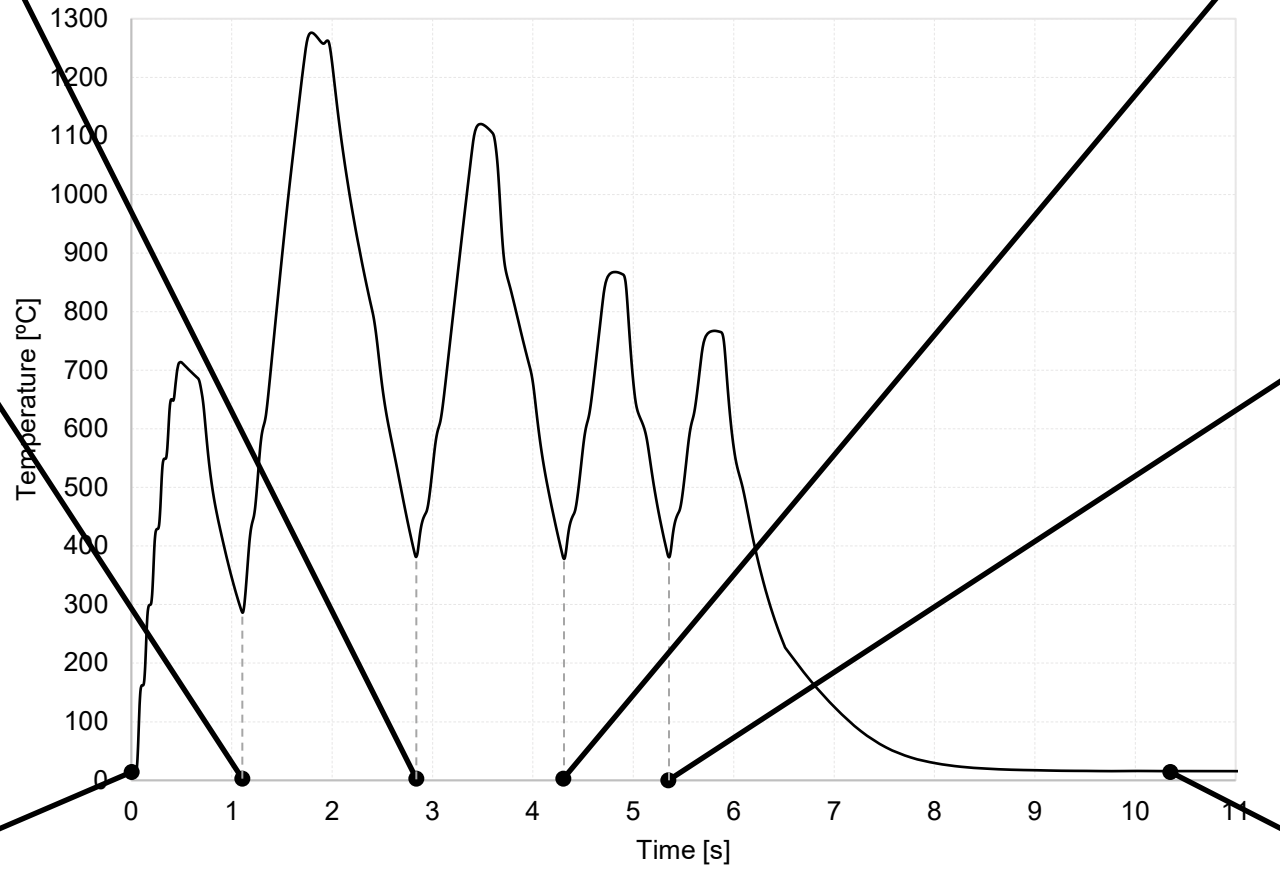
As-cast



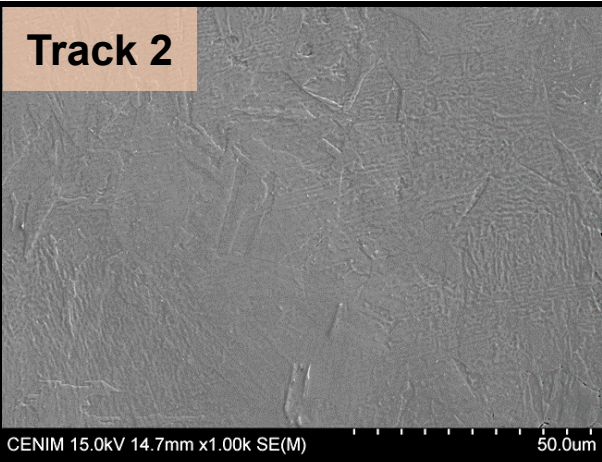
Track 5



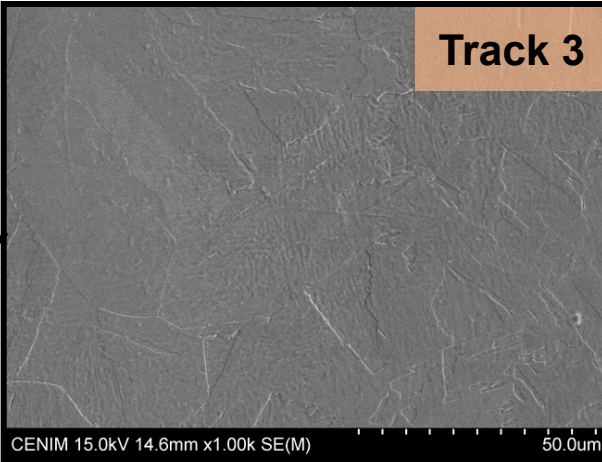
Microstructure evolution of as-cast Maraging steel under LPBF thermal history



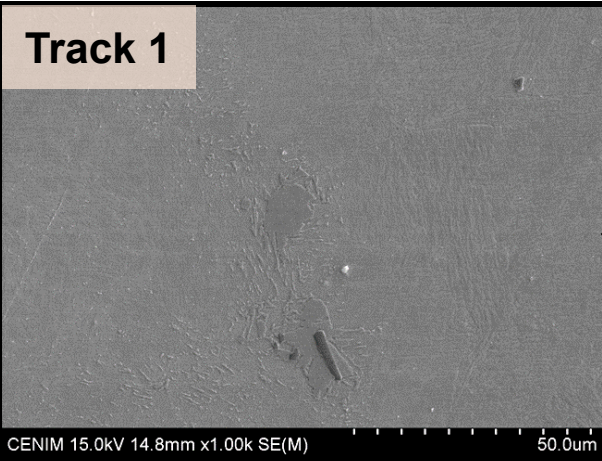
Track 2



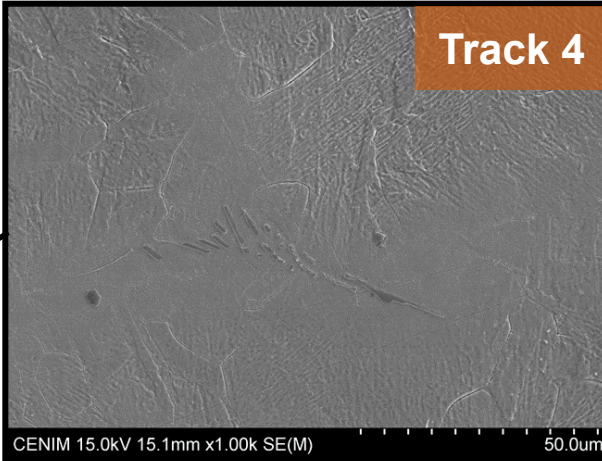
Track 3



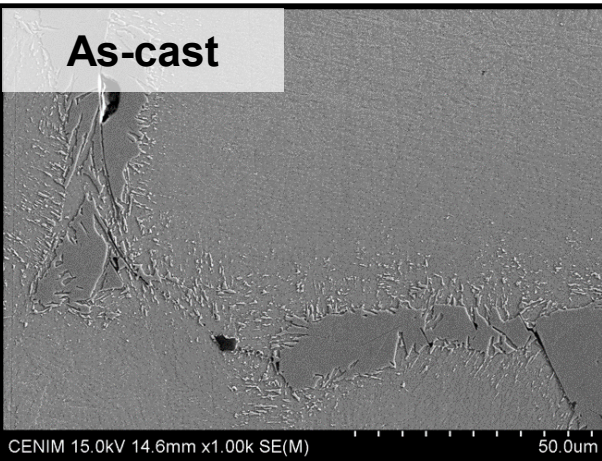
Track 1



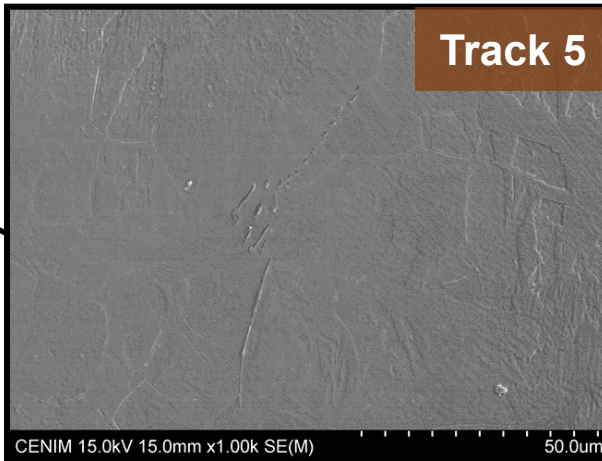
Track 4



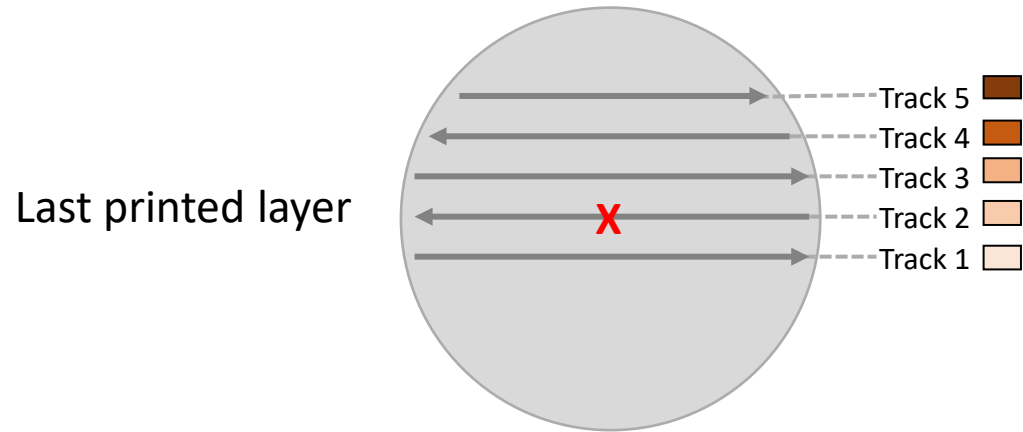
As-cast



Track 5

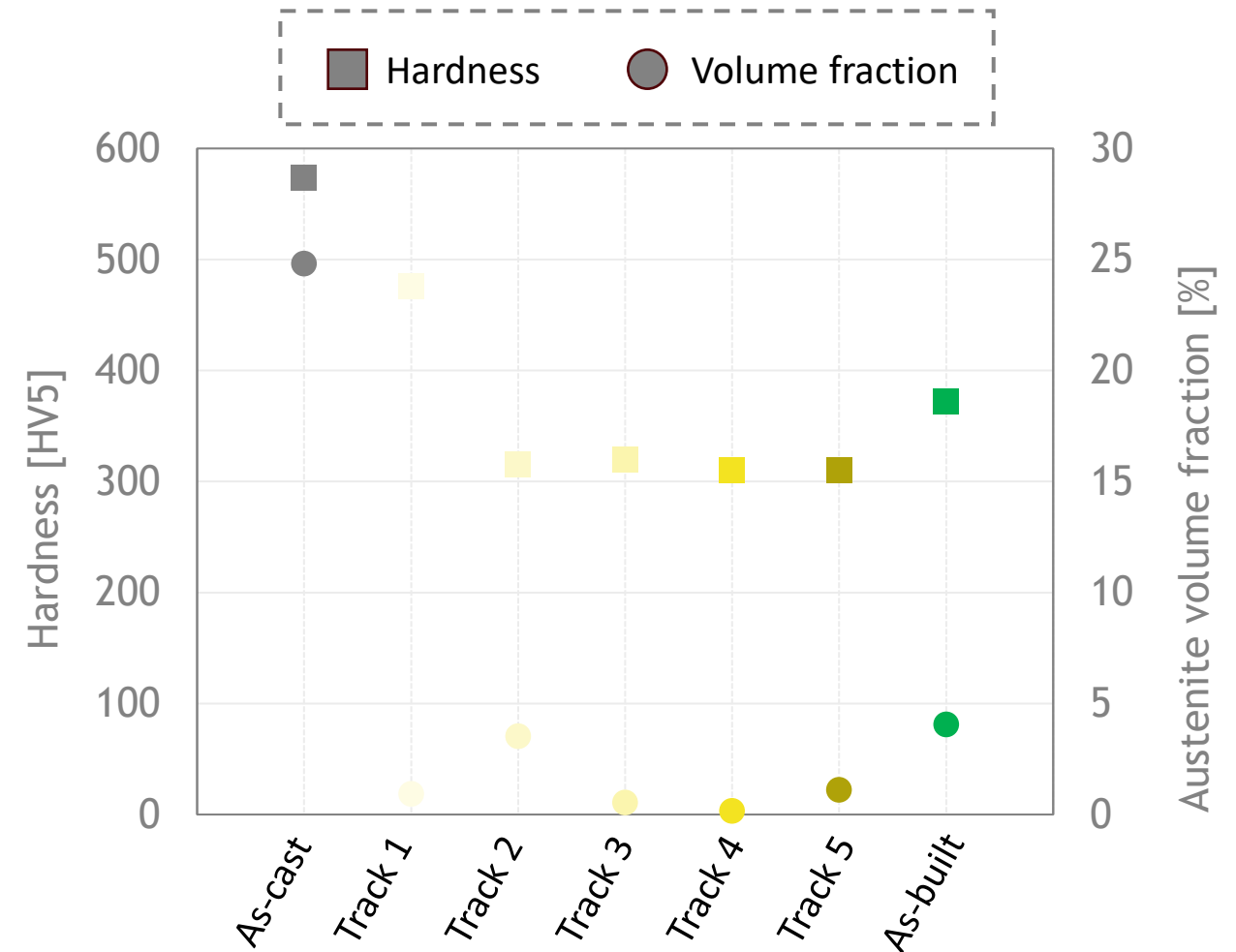


Microstructure evolution of as-cast Maraging steel under LPBF thermal history

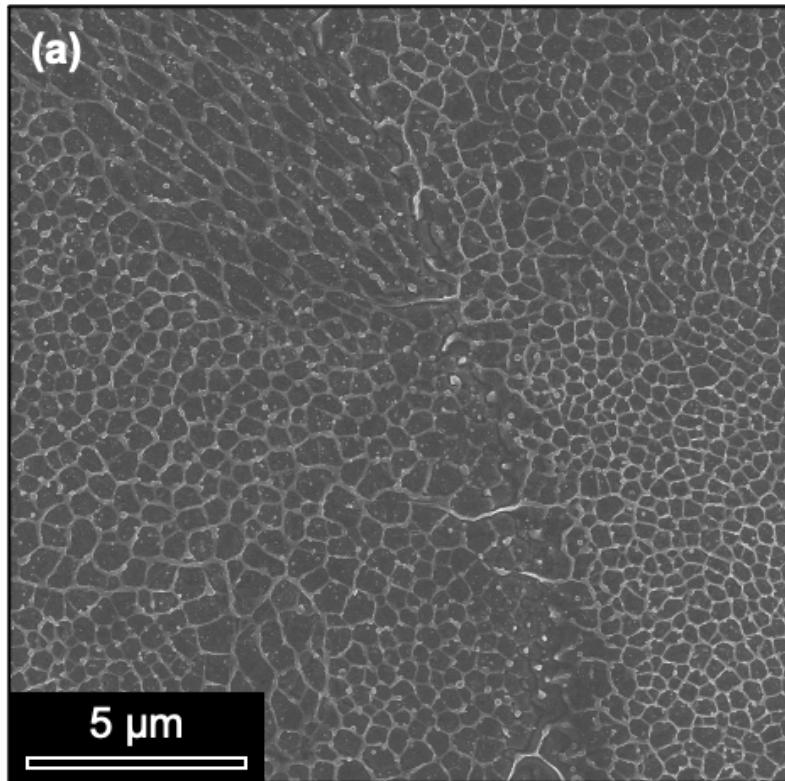


Sample	Volume percentage (%)		HV5
	BCT	FCC	
As-cast	75	25	574
Track 1	99	1	476
Track 2	96	4	315
Track 3	99	1	320
Track 4	99	1	310
Track 5	99	1	310
As-built	96	4	372*

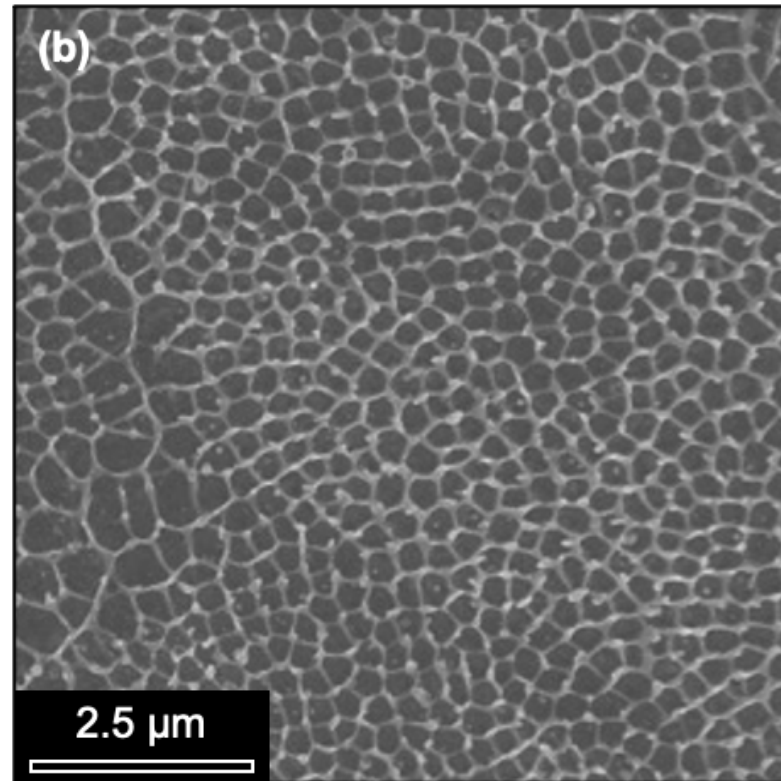
*value from the intermediate T section of the sample



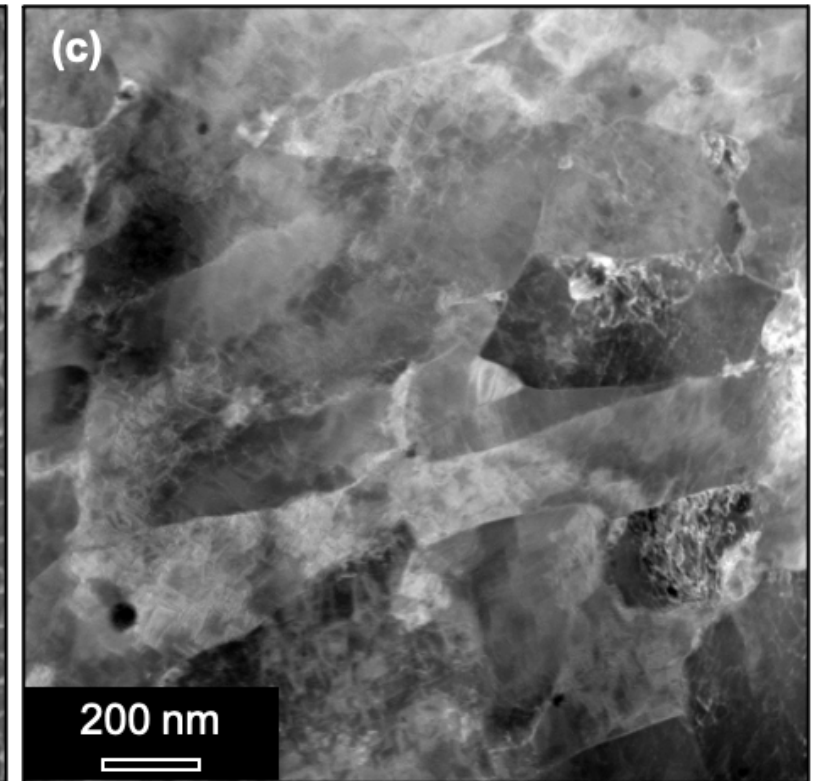
Transverse section



Low magnification SE image in SEM



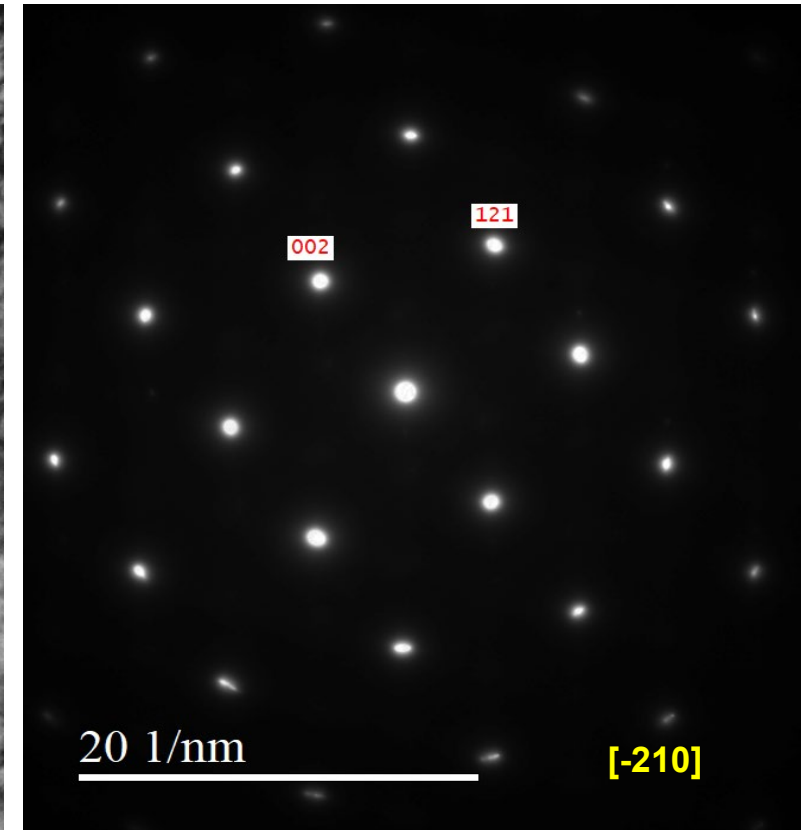
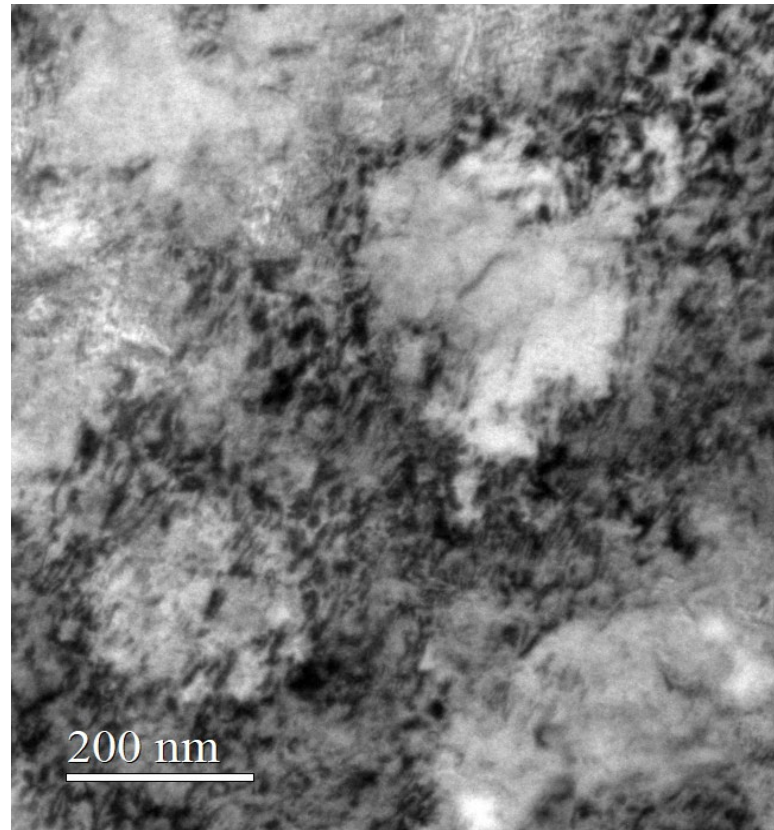
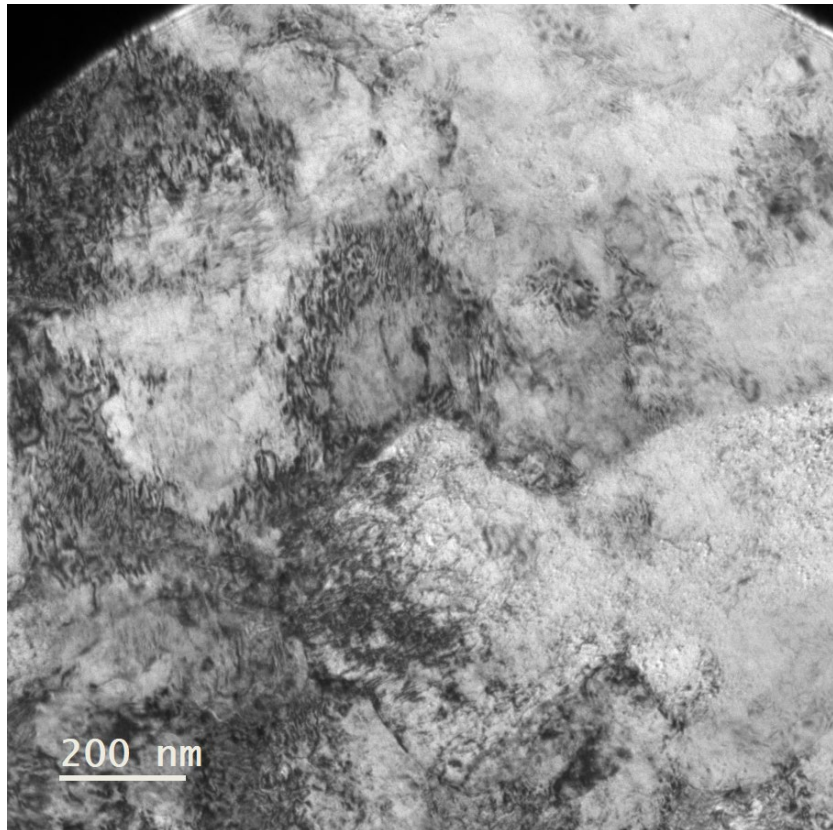
High magnification SE image in SEM

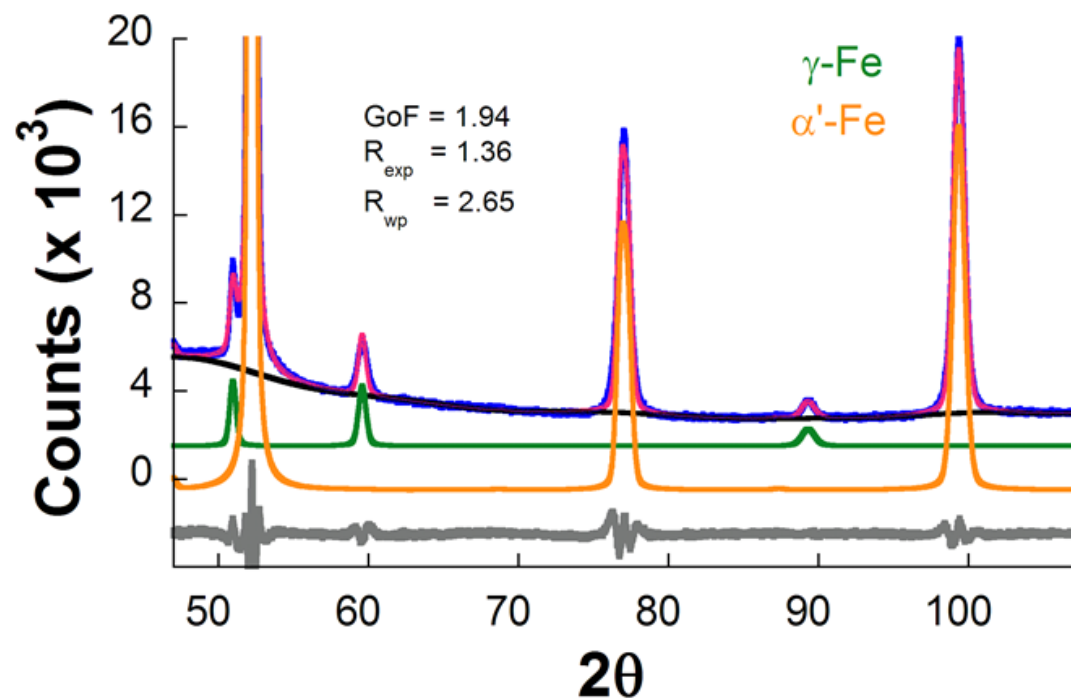


BF image in TEM

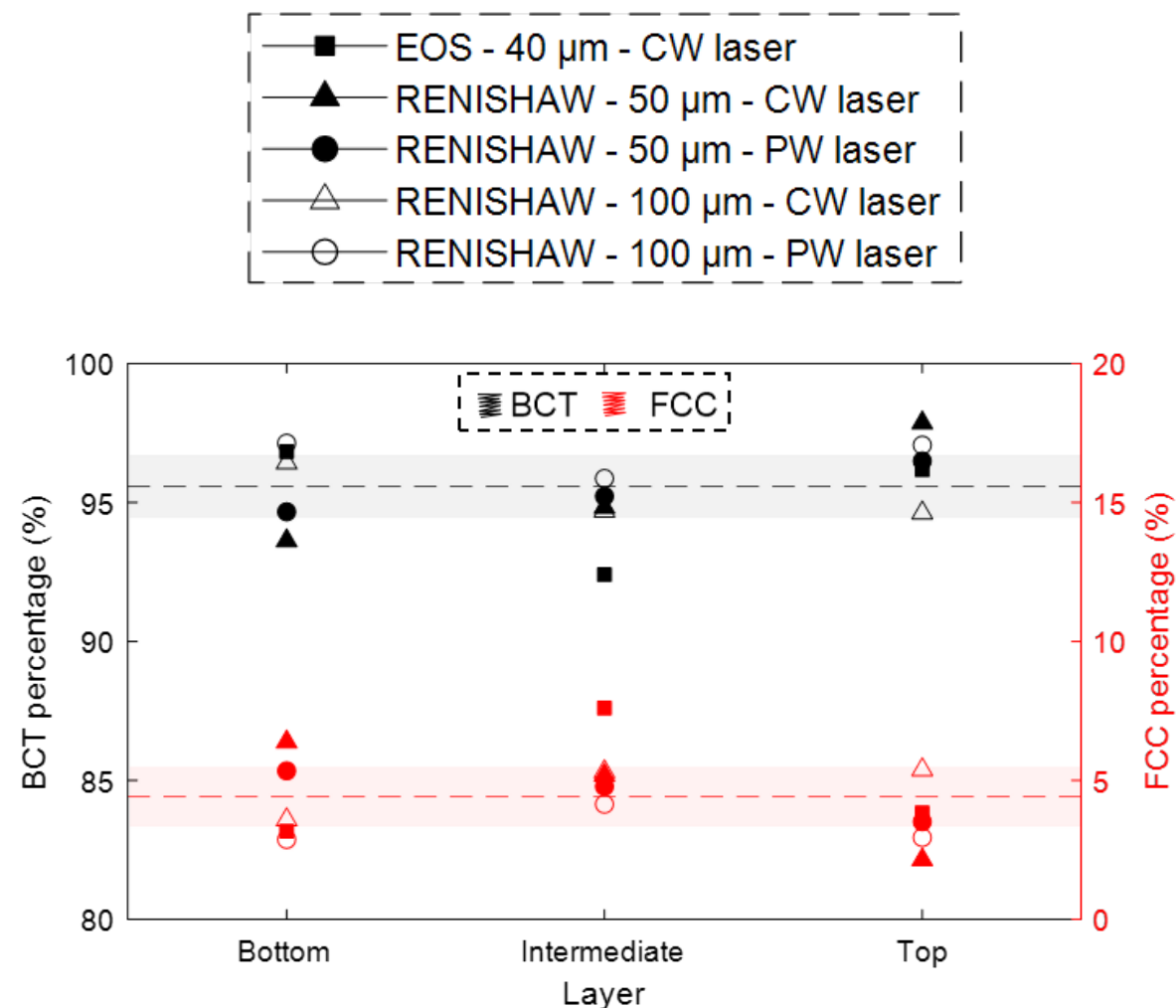
Layer thickness is a key parameter to modify the solidification cell size of the as-built samples.

Transverse section

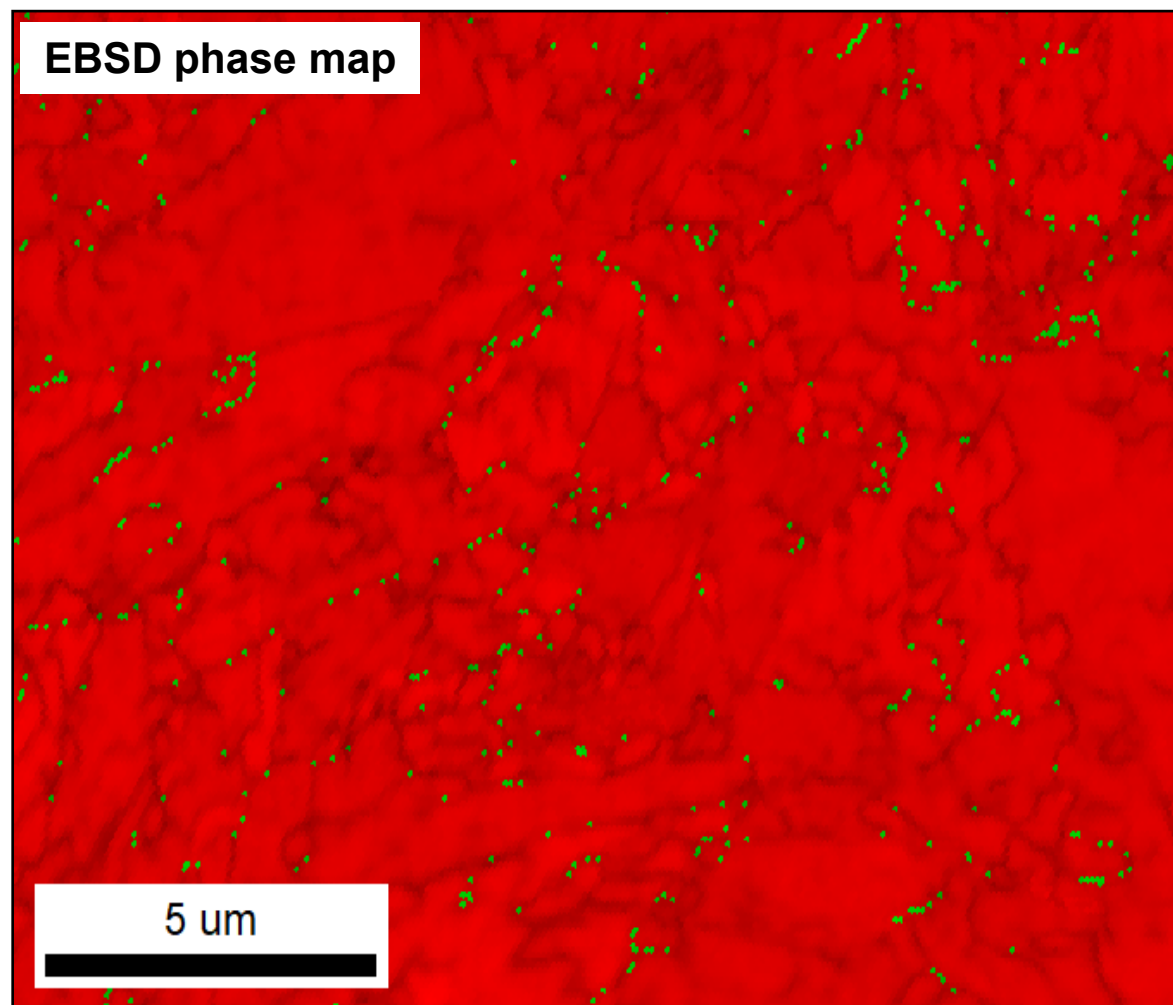




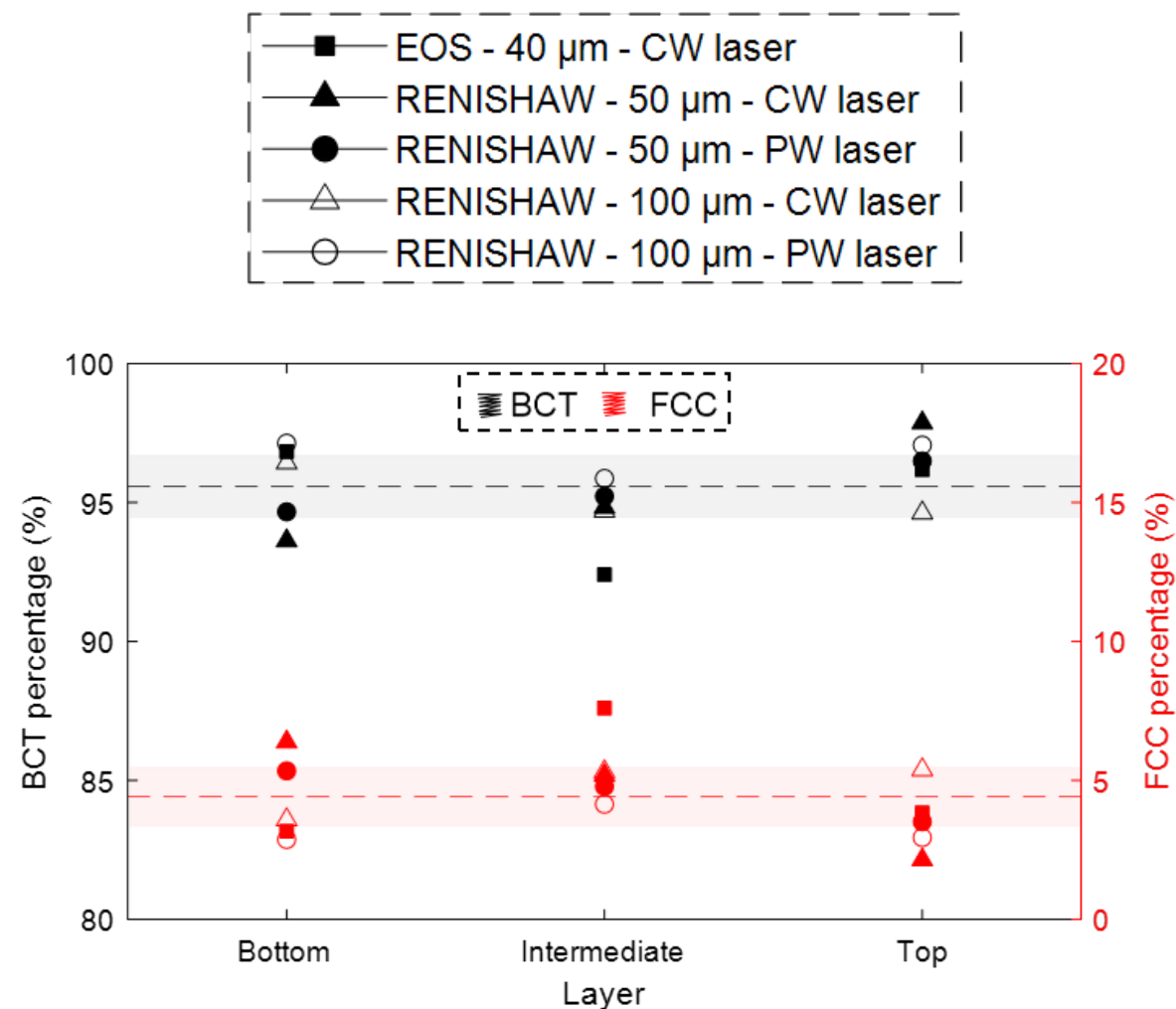
Rwp: weighted summation of residual of the least squares fit,
Rexp: statistically expected least squares fit,
GoF: goodness of fit (sometimes referred as chi-squared);
GoF=Rwp/Rexp; a GoF=1.0 means a perfect fitting.



■ BCC ■ FCC

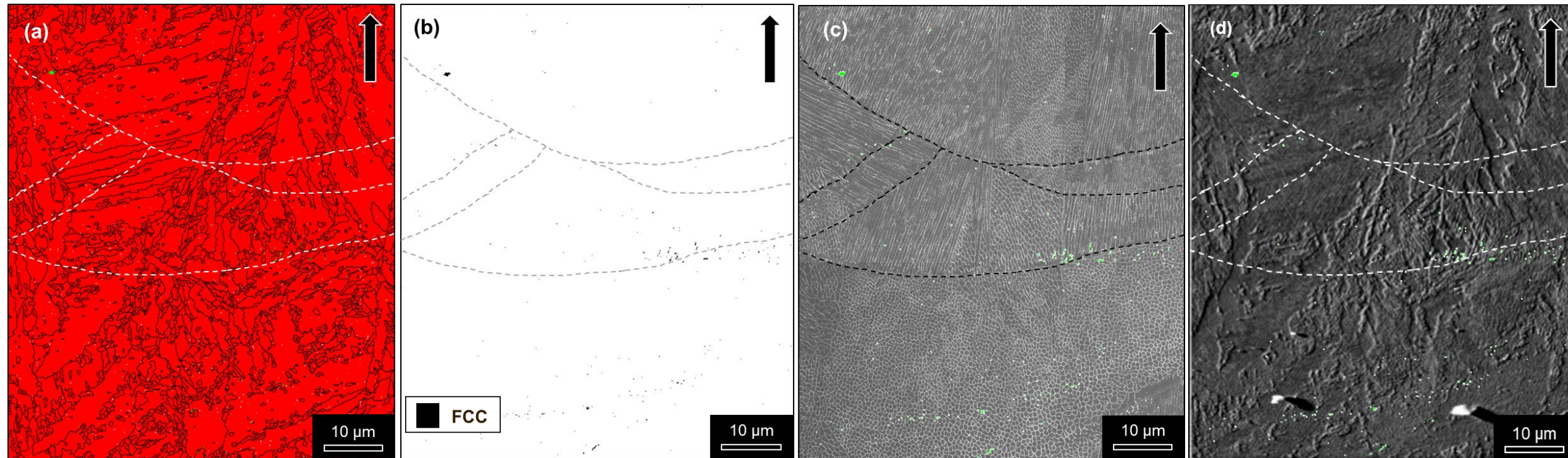


Step size = 0.08 μm



■ BCC ■ FCC

Longitudinal section



EBSD phase distribution map
with retained austenite, BCT
and high angle grain
boundaries

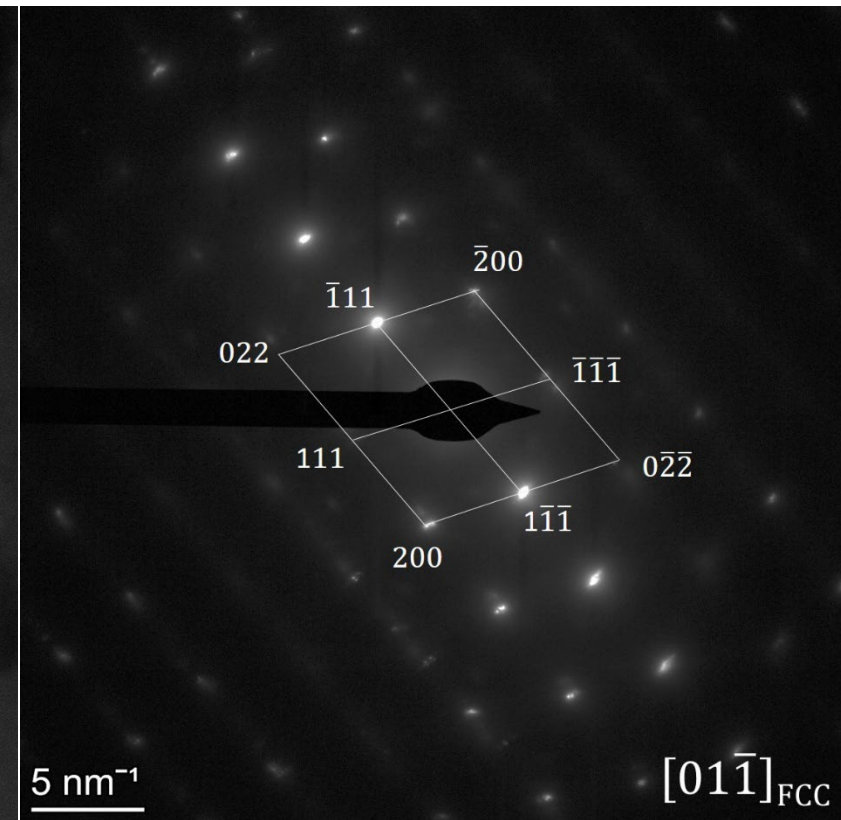
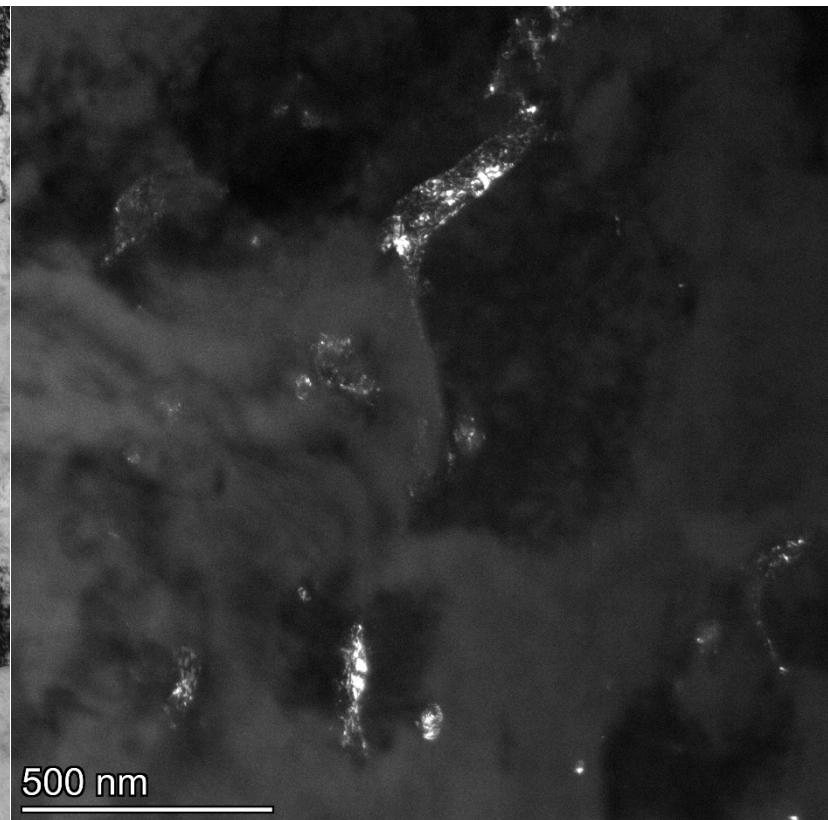
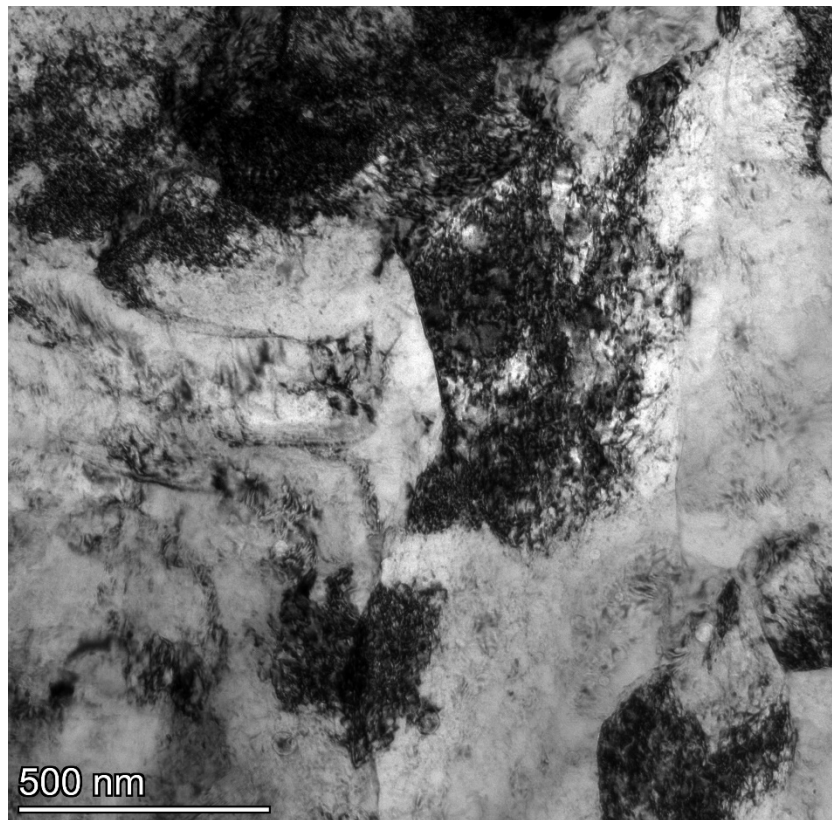
FCC phase distribution

SE image with the FCC
phase overlaid

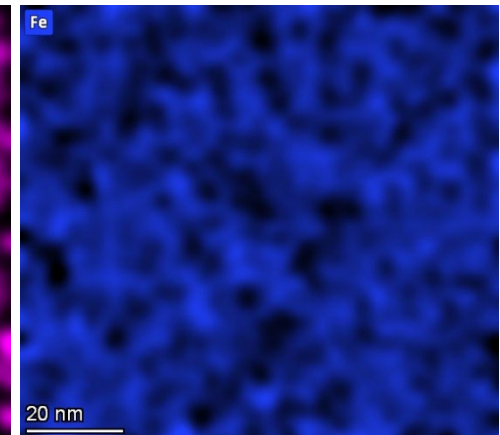
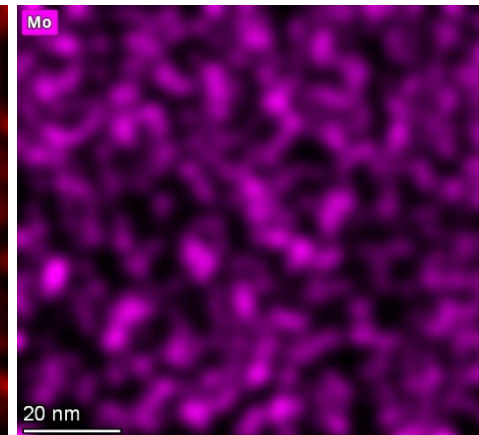
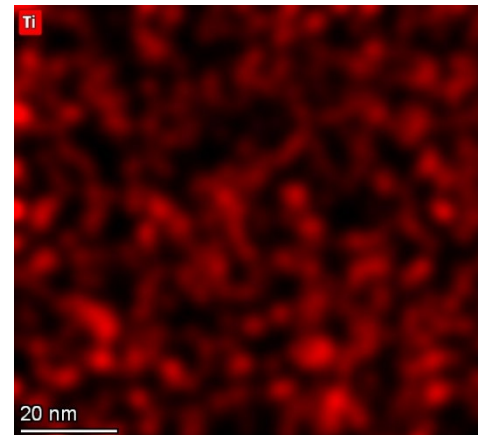
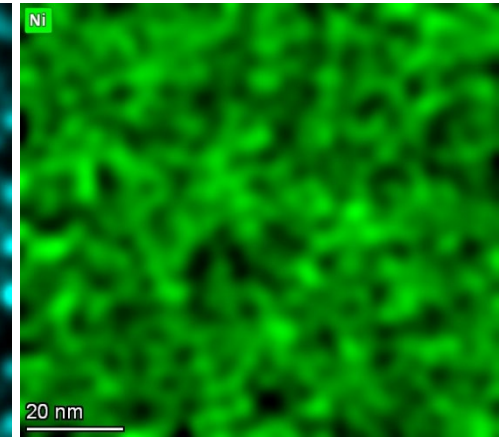
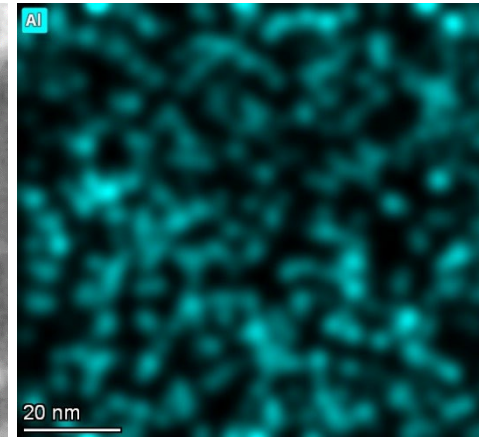
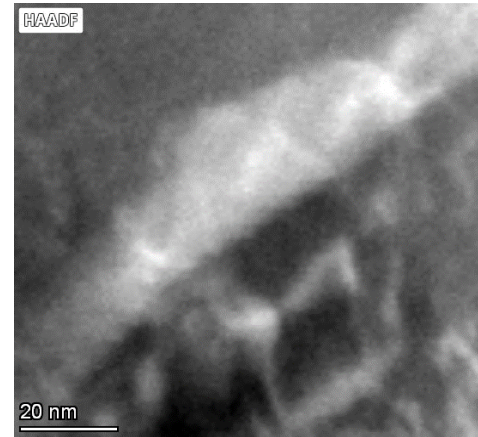
BSE micrograph with FCC
phase overlaid

Step size = 0.2 µm

Transverse section

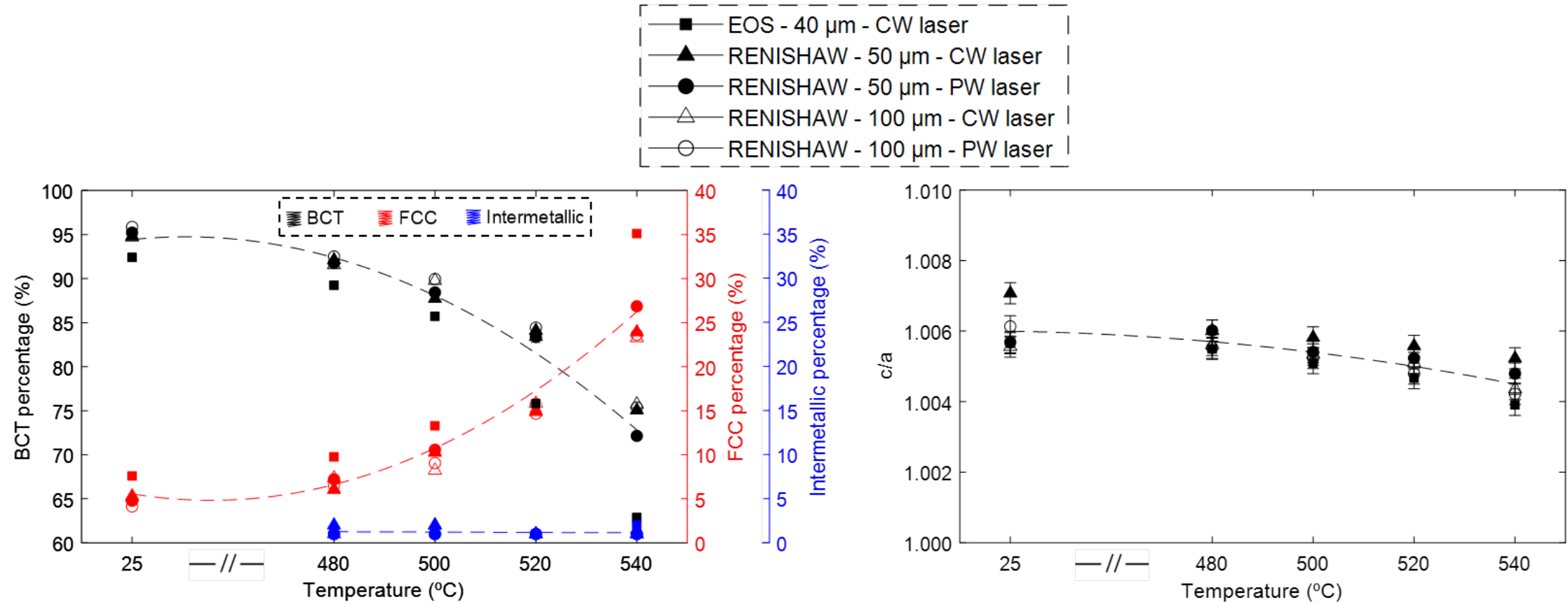


Austenite at celular boundaries

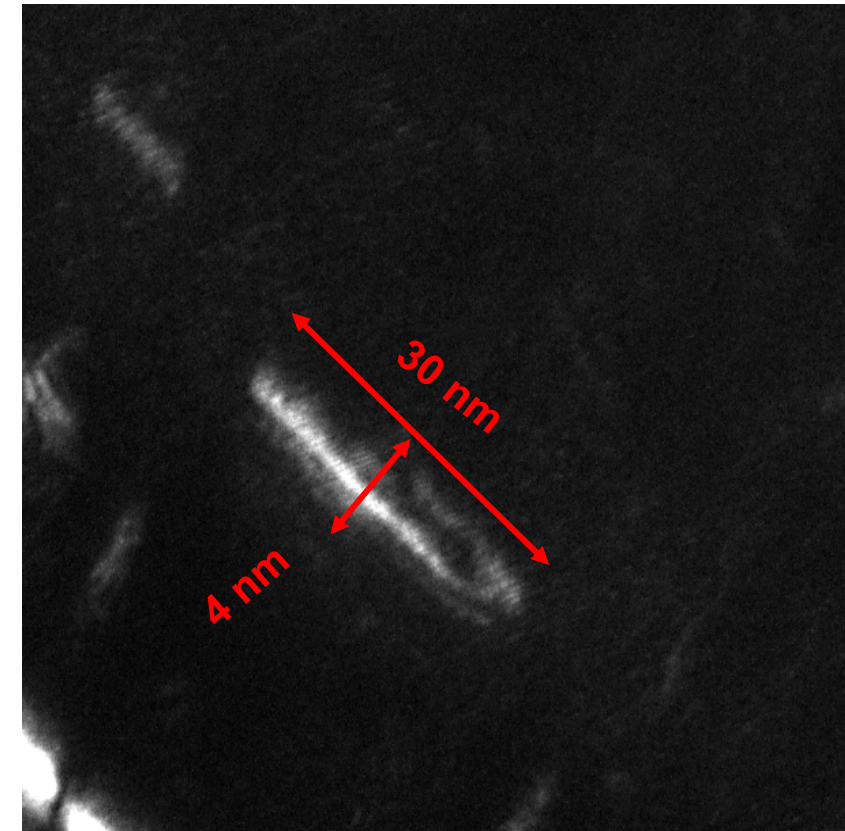
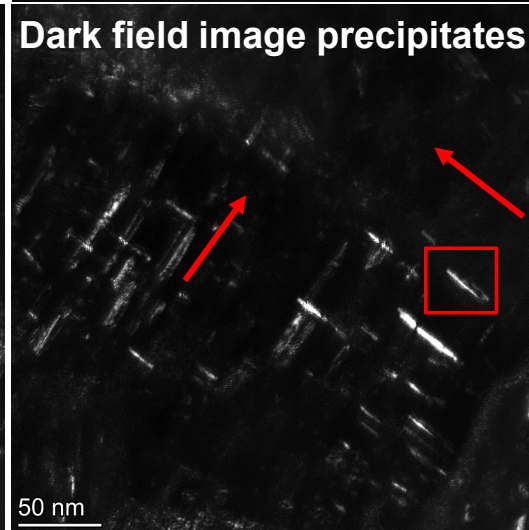
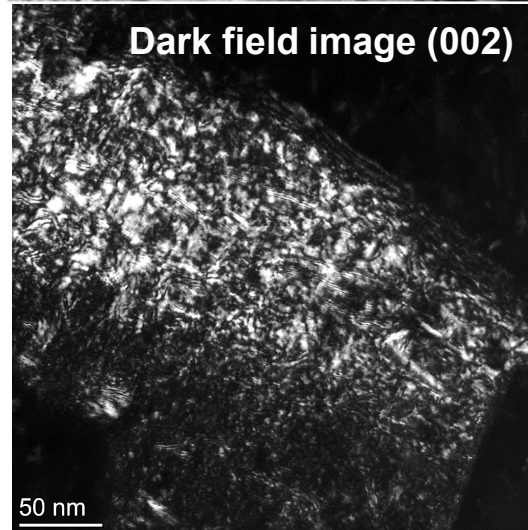
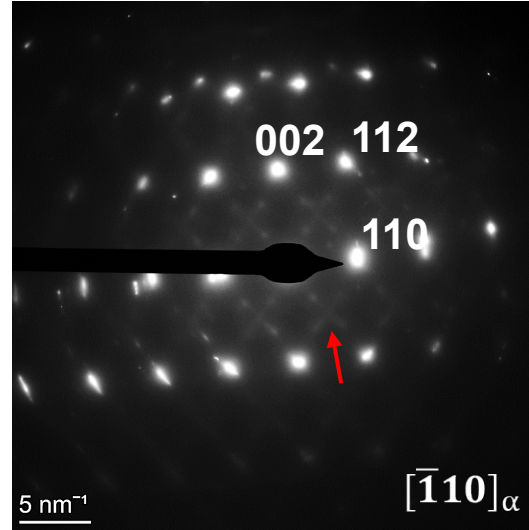
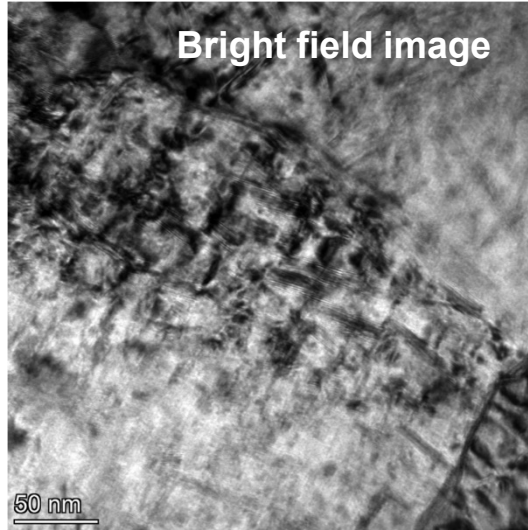


01 Revealing the complexity of non-equilibrium, and non-uniform microstructures formed during LPBF process of Maraging steels.

02 Precipitation of intermetallic phases and austenite growth/reversion during ageing of LPBF Maraging steels.

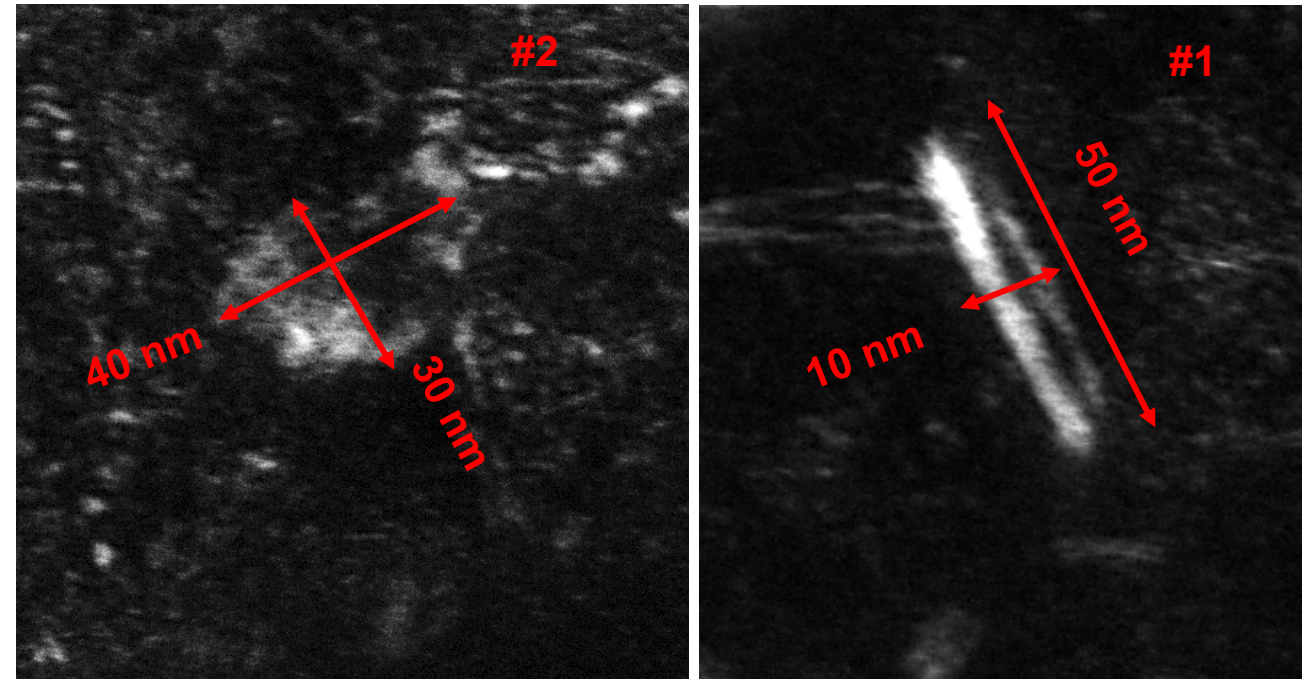
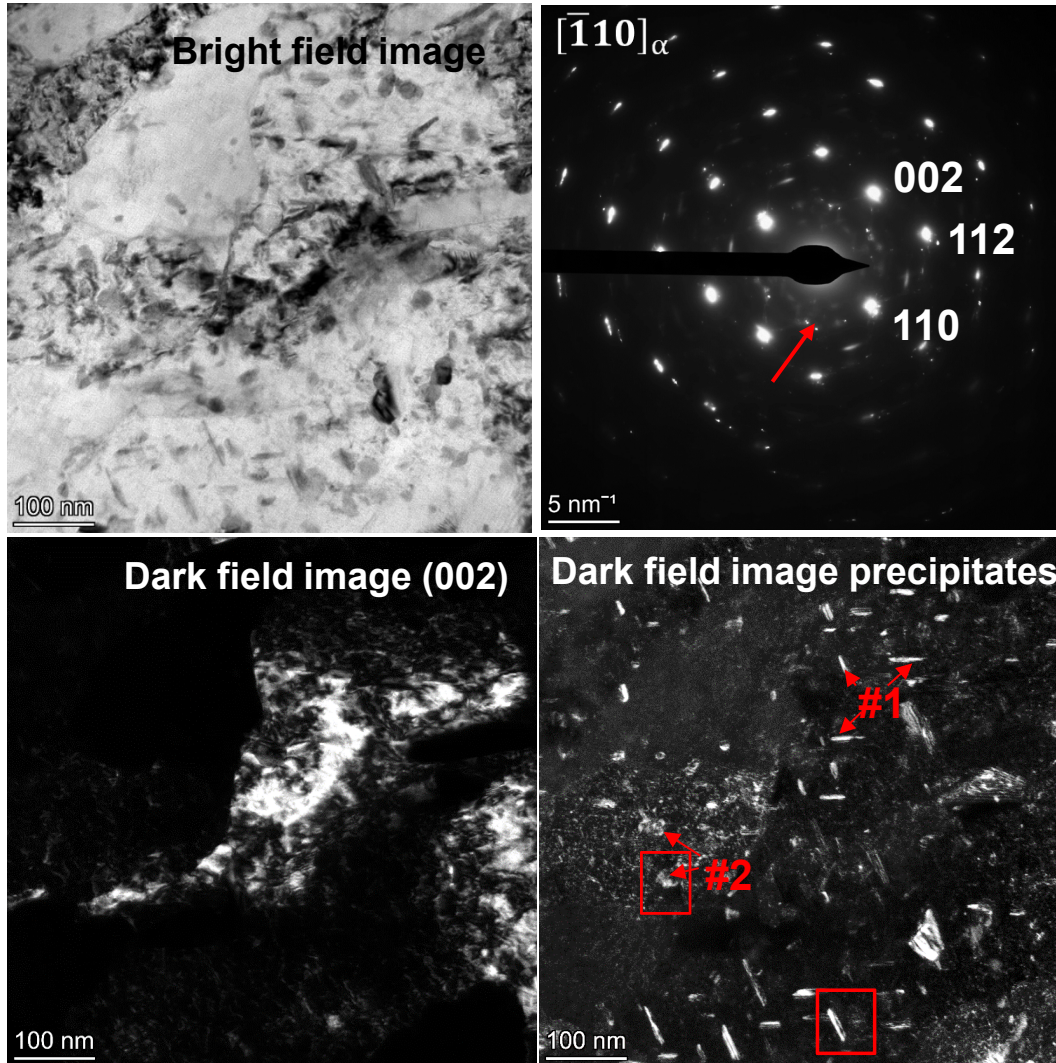


Precipitation Processes during Aging – $T_{ag} = 480\text{ }^{\circ}\text{C}$



Ni, Ti enriched rod-like particles

Precipitation Processes during Aging – $T_{ag} = 540\text{ }^{\circ}\text{C}$



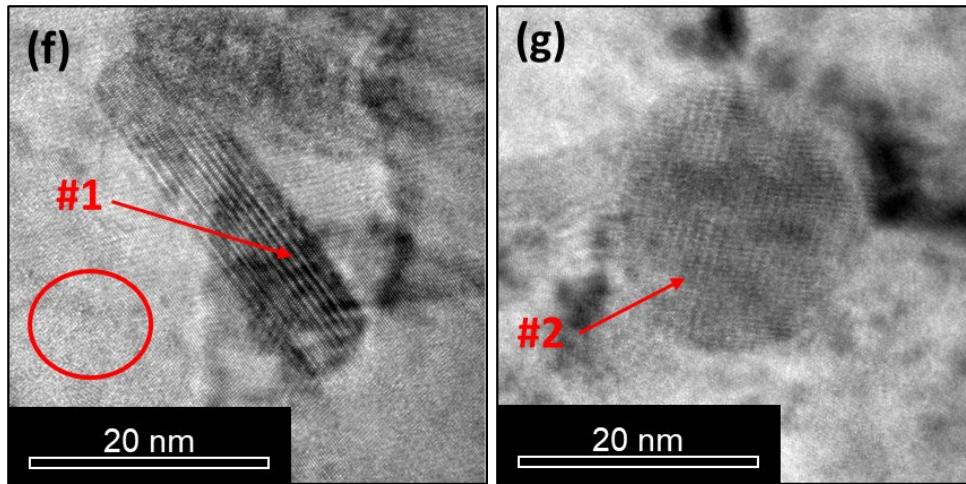
#1: Ni, Ti enriched rod-like phases
#2: Mo enriched spherical phases

Precipitation Processes during Aging – $T_{ag} = 540\text{ }^{\circ}\text{C}$

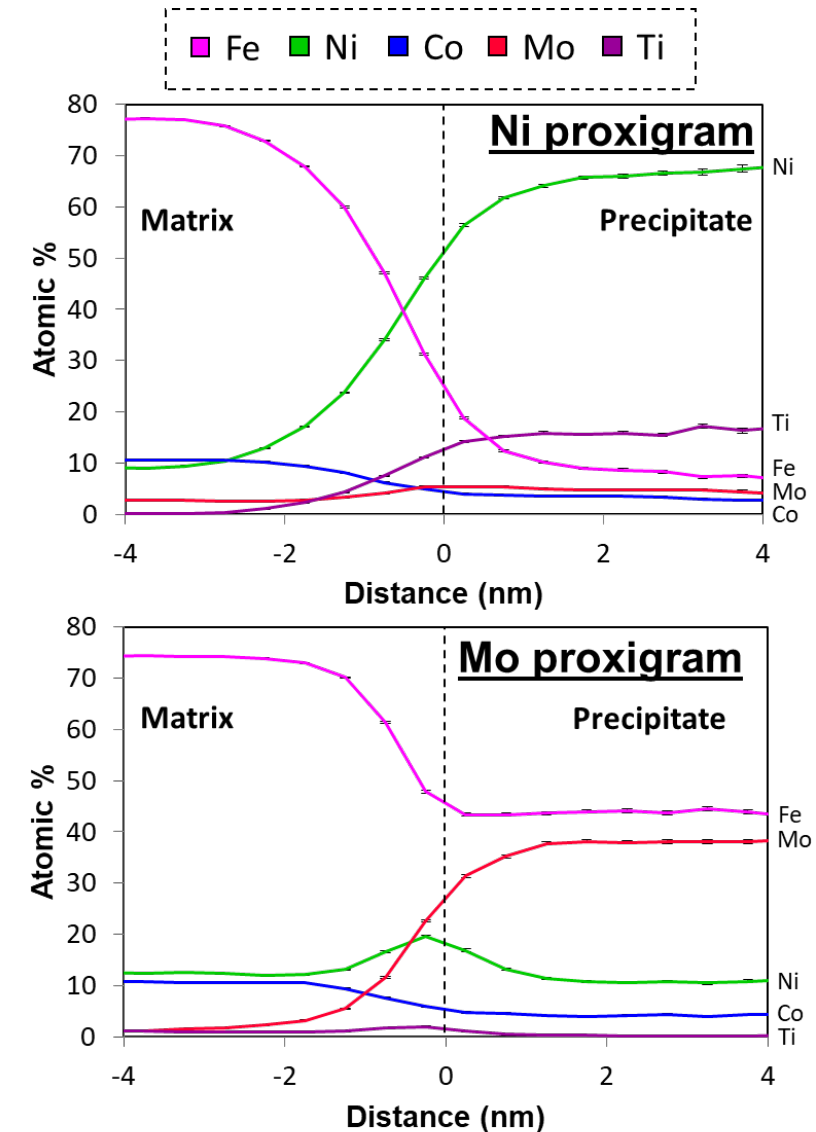
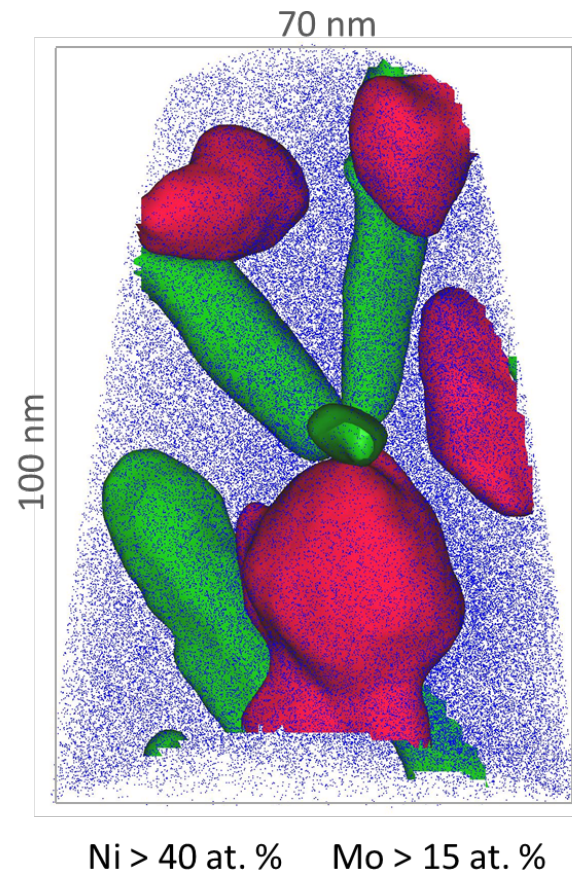


Funded by
the European Union

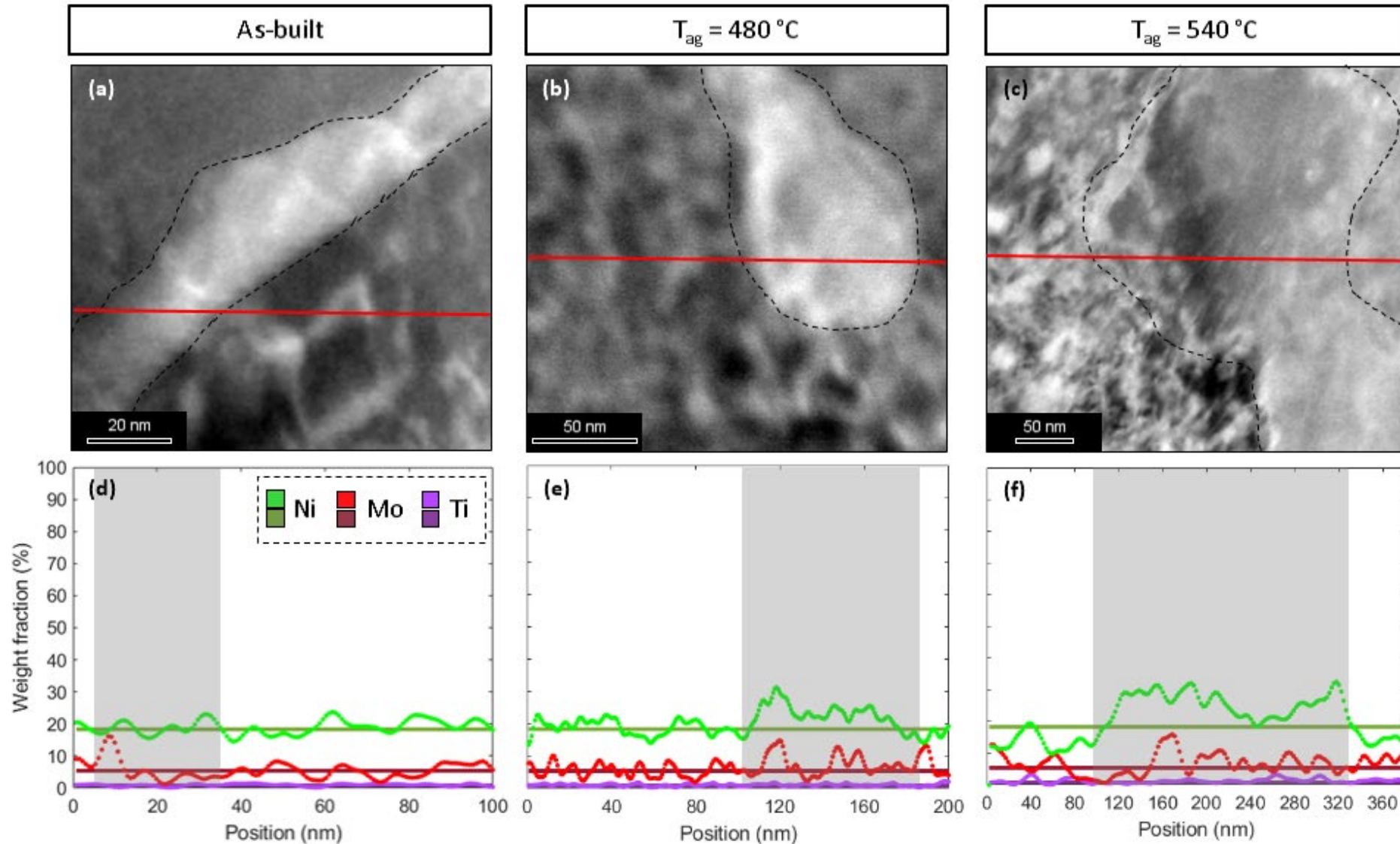
Ni, Ti enriched rod-like
and Mo enriched
spherical phases

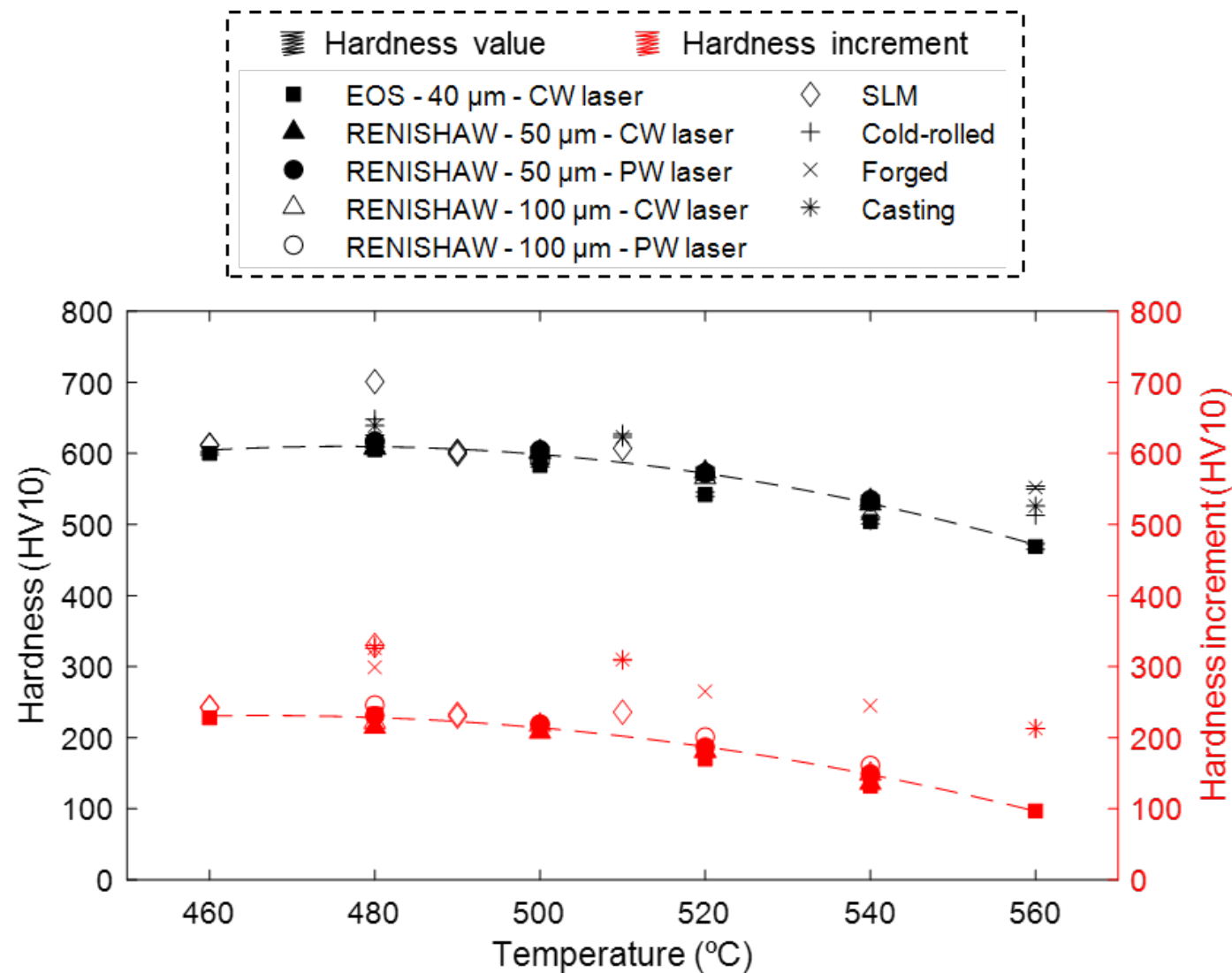


Ni, Ti enriched rod-like and Mo
enriched spherical phases



Transverse section



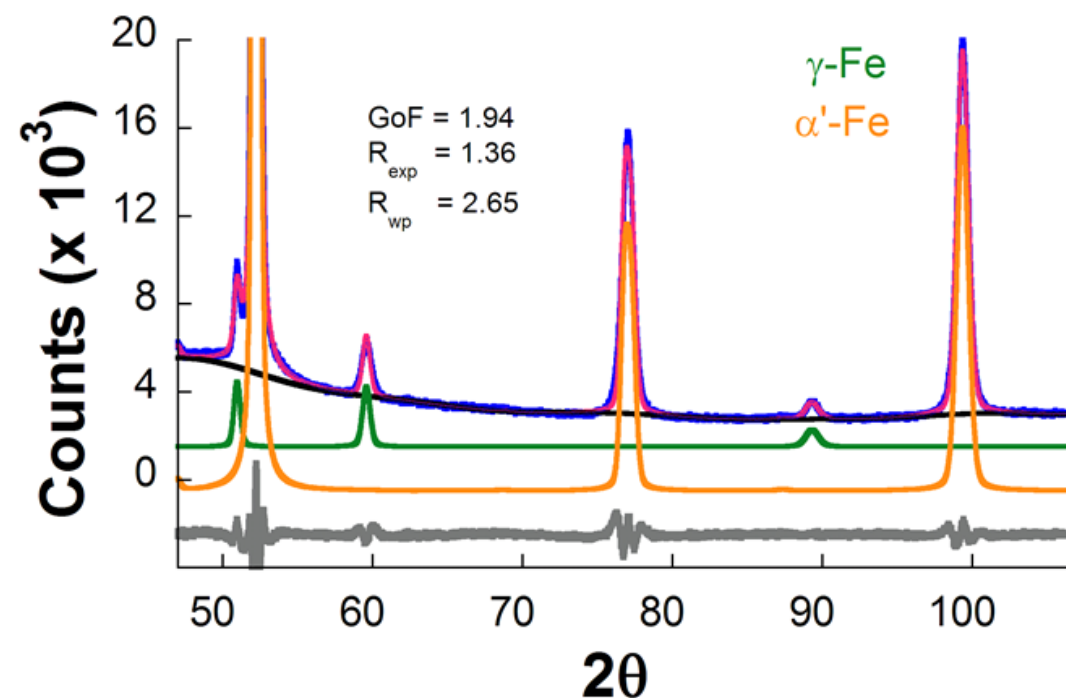
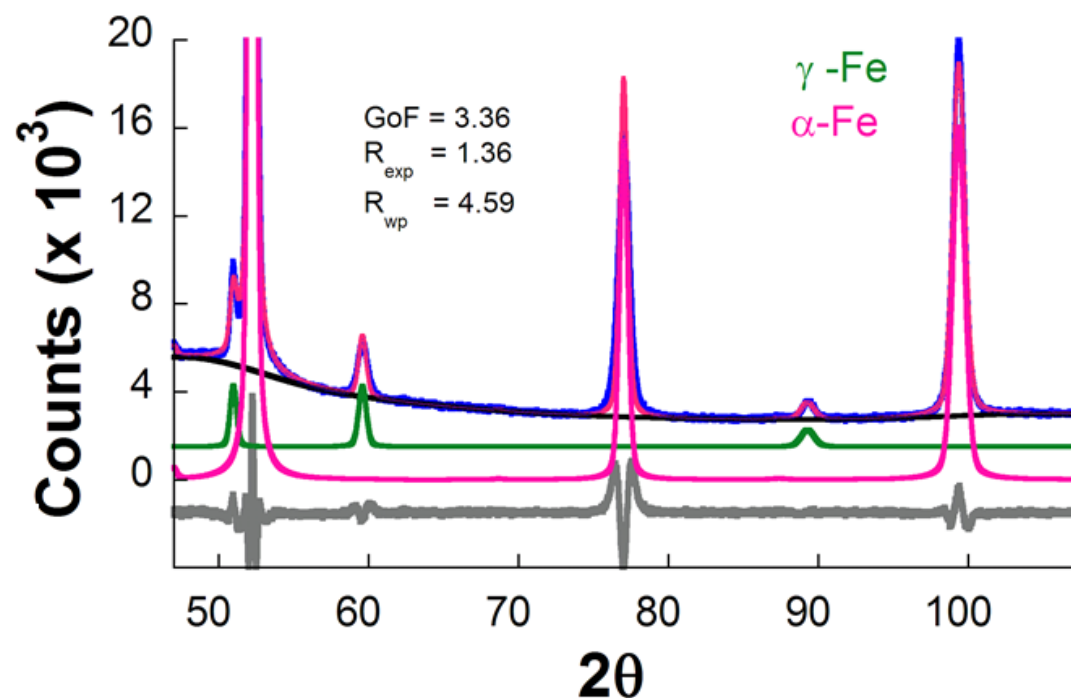


Remarks

- ✓ Refined cellular microstructure is a unique feature in alloys fabricated by laser powder bed fusion. Results evidenced **the importance of layer thickness as a key parameter to modify the solidification cell size of the as-built samples.**
- ✓ Additive manufacturing of Maraging steels results in **complex microstructures formed by a tetragonal martensitic matrix and a heterogeneous distribution of retained austenite.**
- ✓ The **high dislocation density in combination with solute segregation** in the as-fabricated material can promote **the precipitation of intermetallic phases** that are responsible for the high strength.
- ✓ **It is not clear if the austenite growth/reversion and the precipitation of the intermetallic phases during ageing occur as competitive or collaborative phase transformations.**

Thanks for your attention

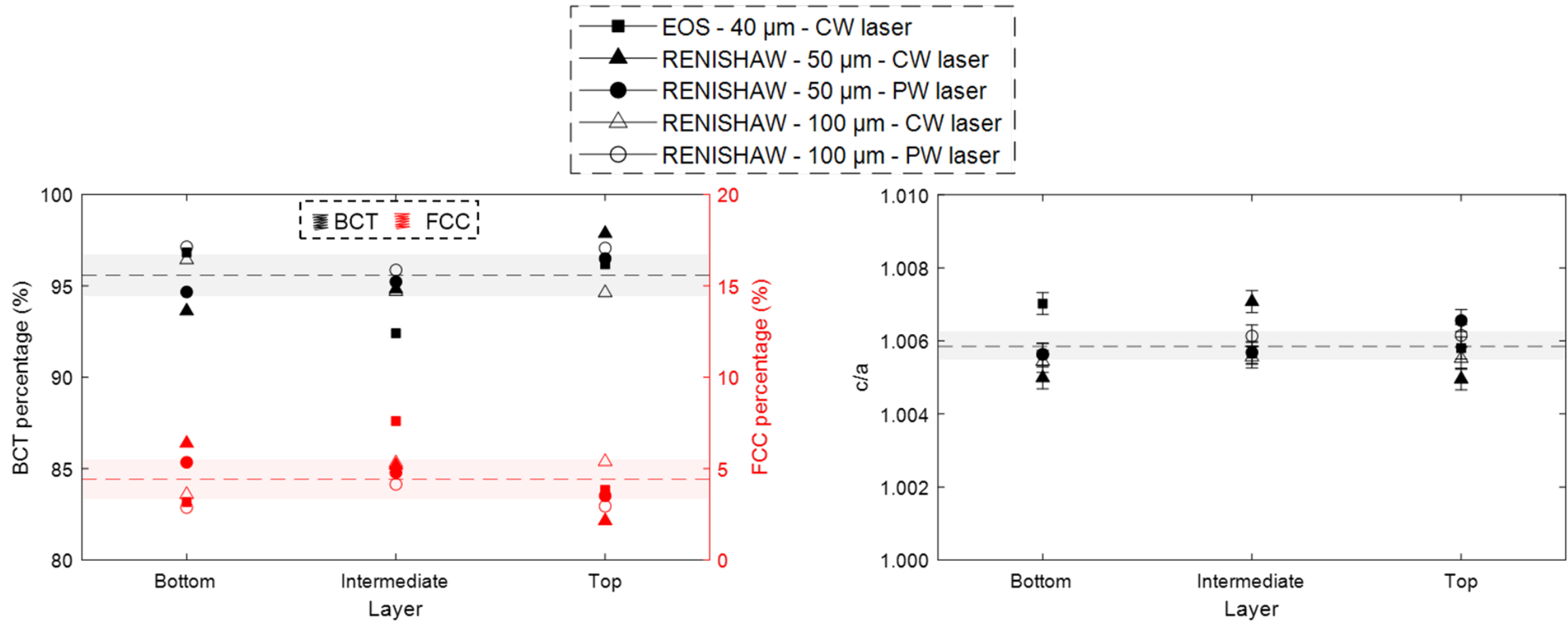




Rwp: weighted summation of residual of the least squares fit,

Rexp: statistically expected least squares fit,

GoF: goodness of fit (sometimes referred as chi-squared); $GoF = R_{wp}/R_{exp}$; a $GoF = 1.0$ means a perfect fitting.

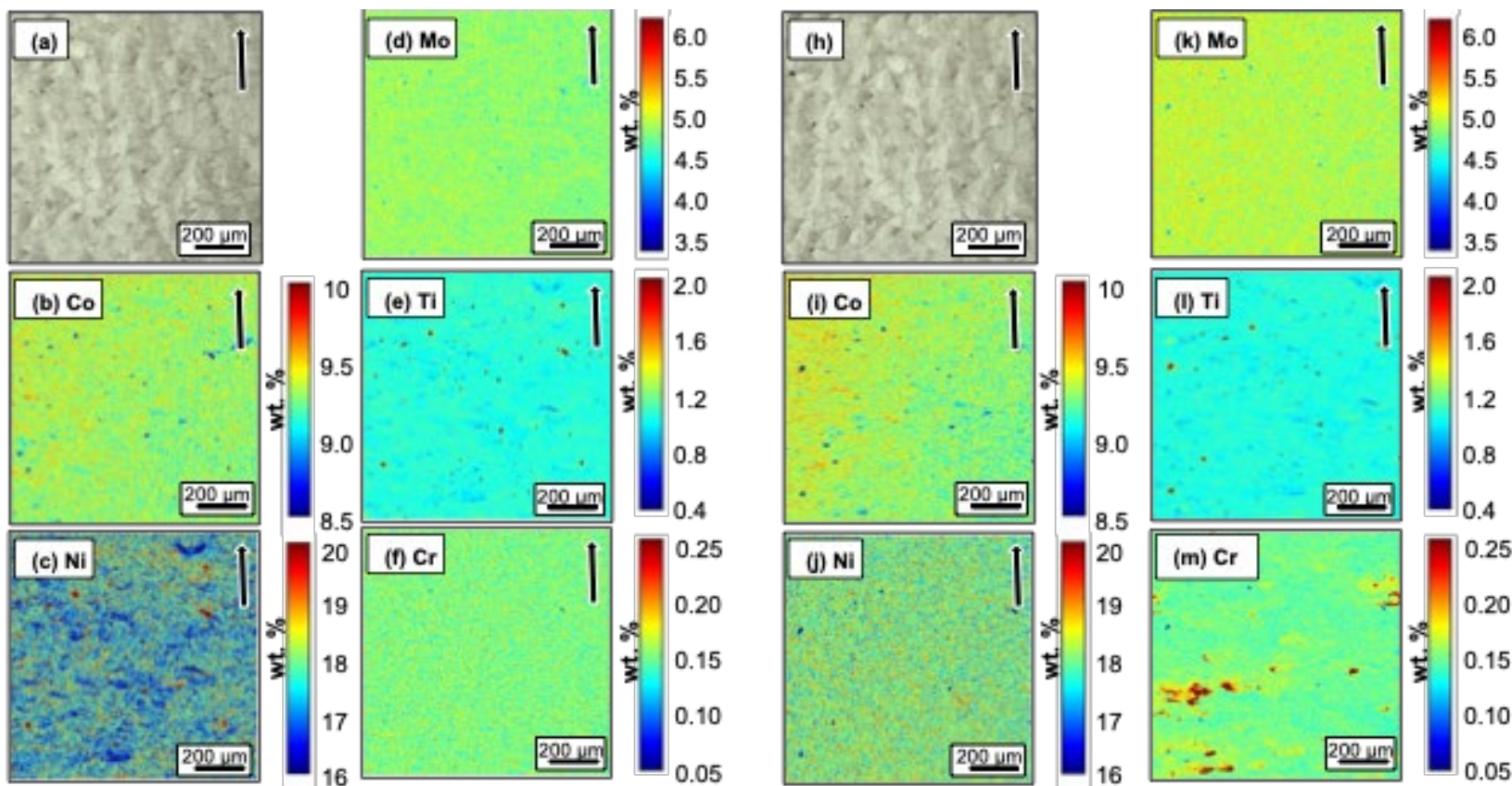


Longitudinal section

EOS - 40 μm - CW laser mode

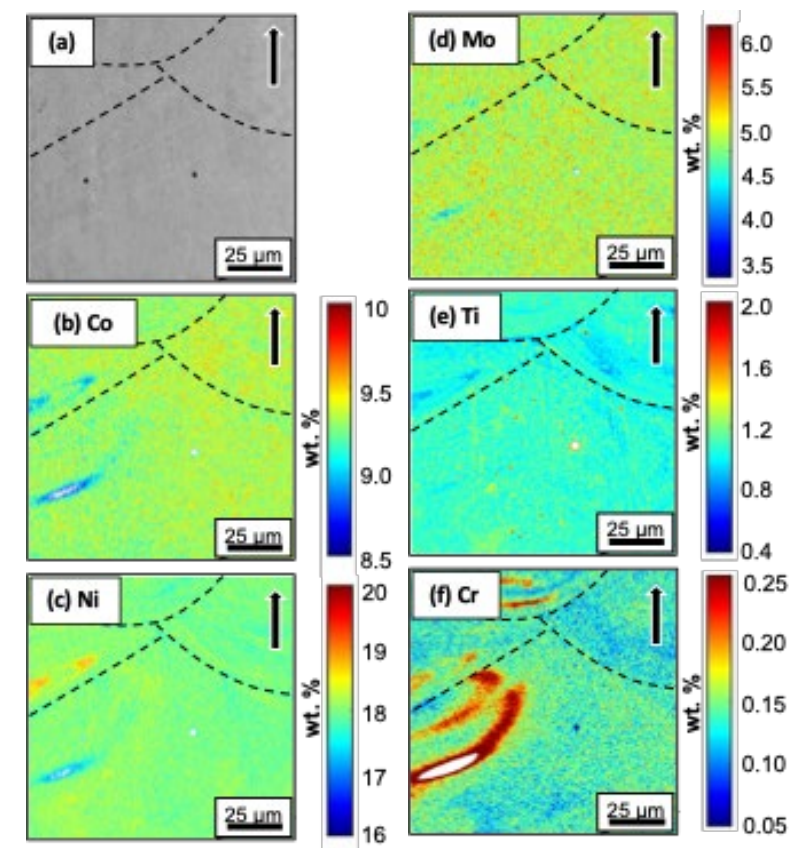
Additive Manufacturing 94 (2024) 104494

Low magnification

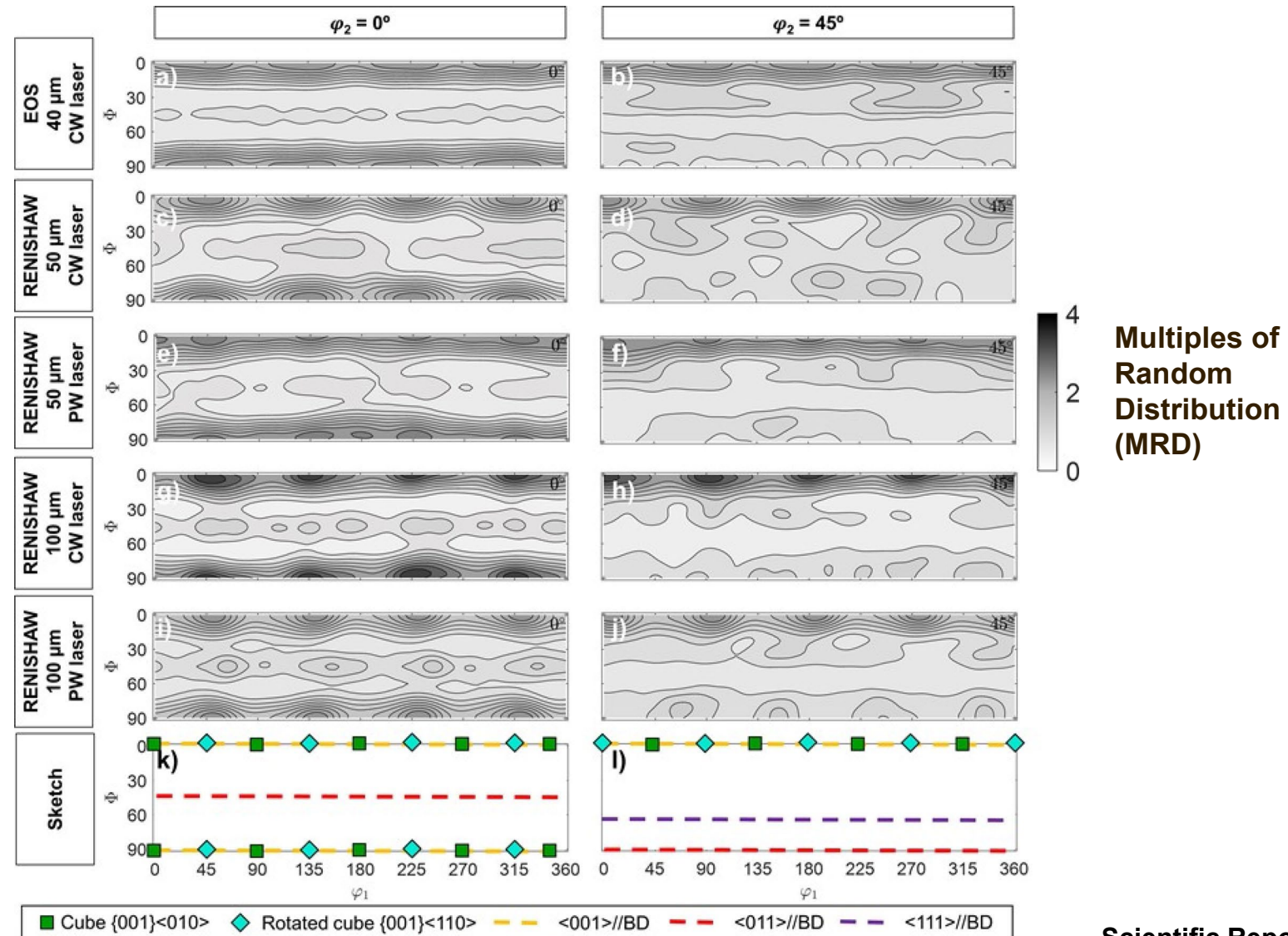


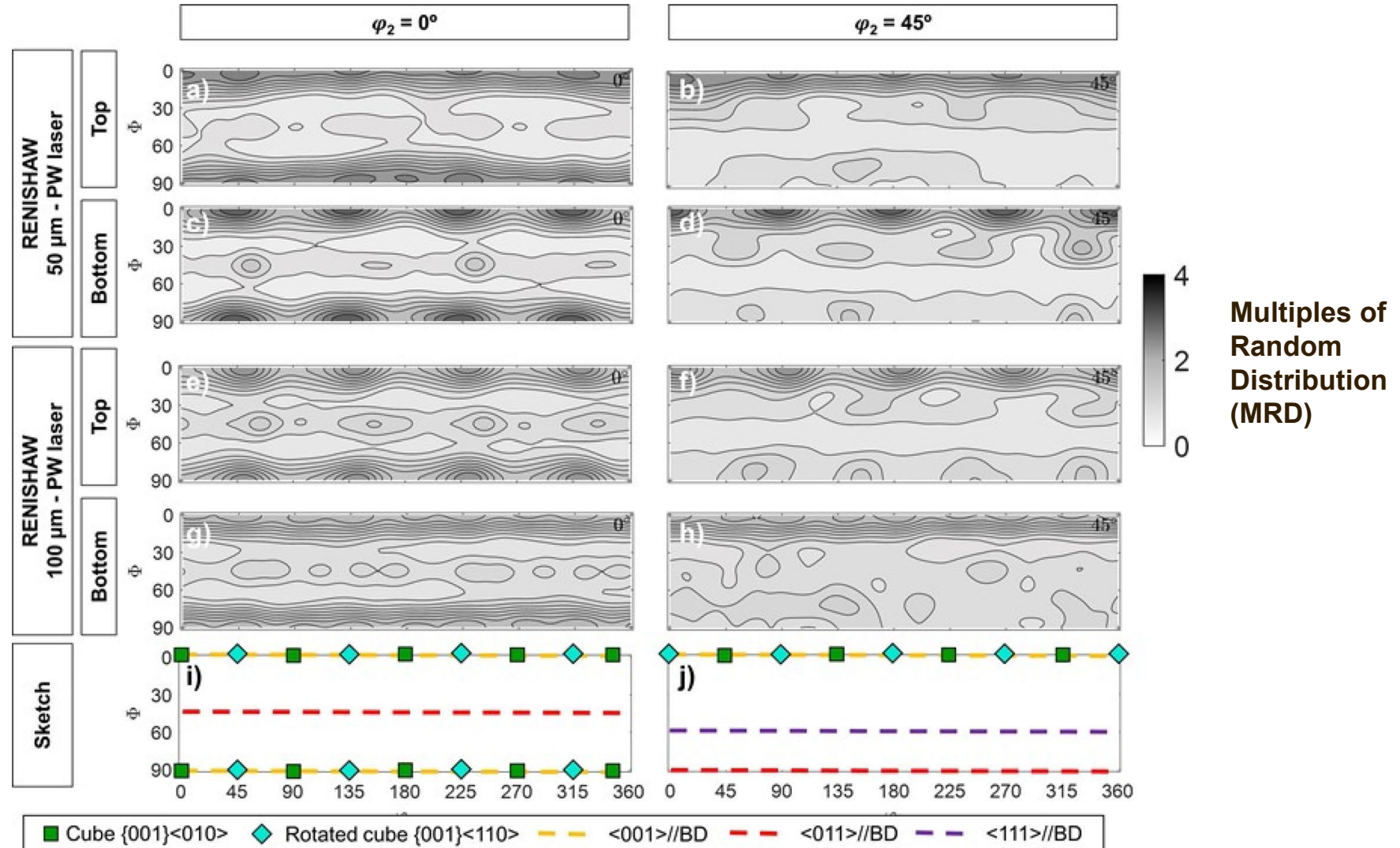
Area: 1000 μm x 1000 μm ; Step size: 1 μm

High magnification



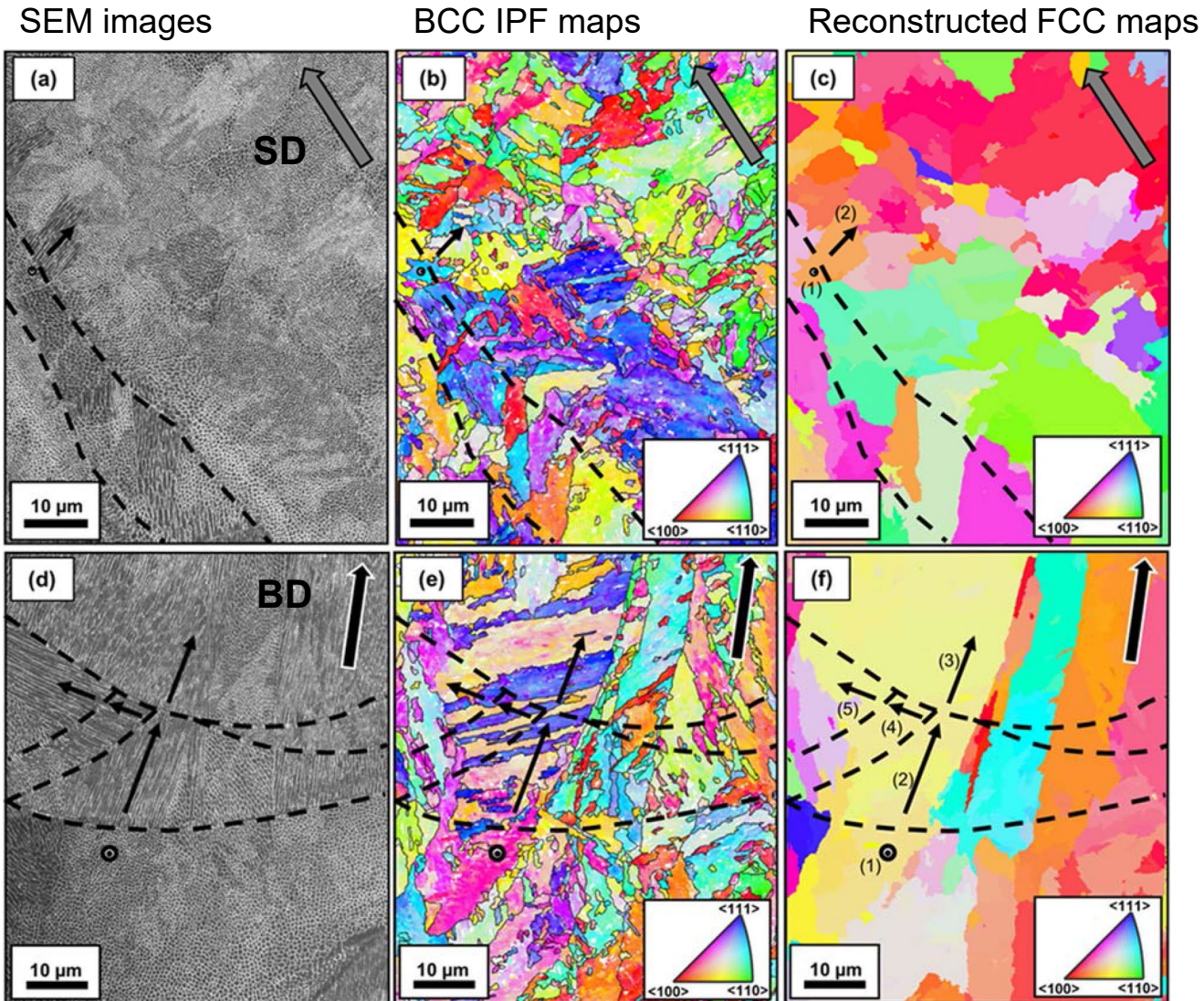
Area: 100 μm x 100 μm ; Step size: 0.1 μm

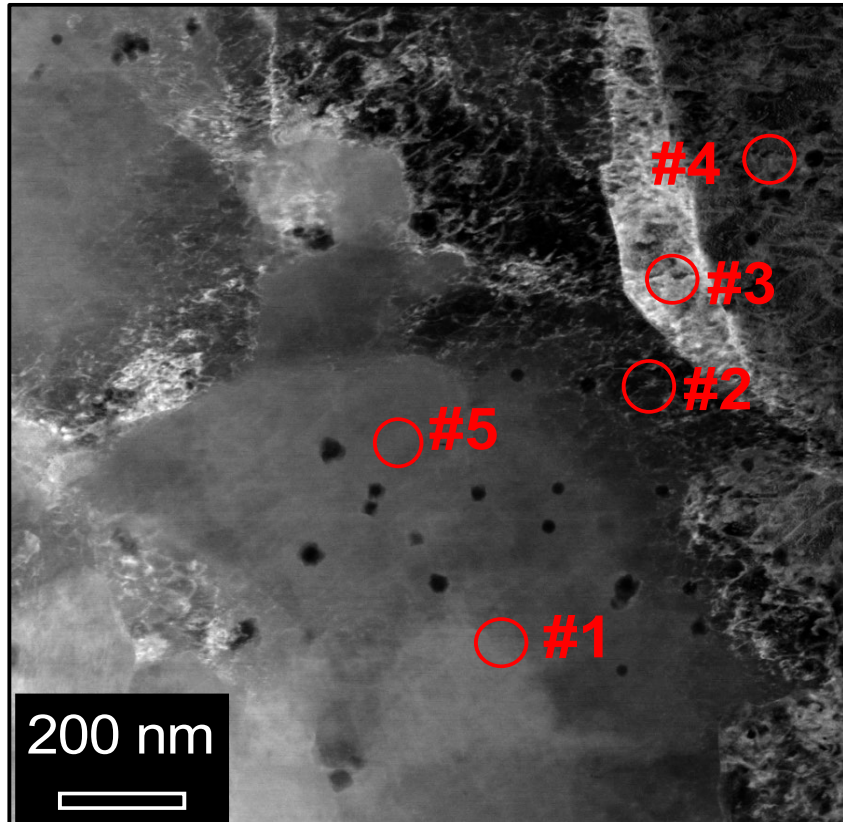




EOS - 40 μm - CW laser mode

Transverse section





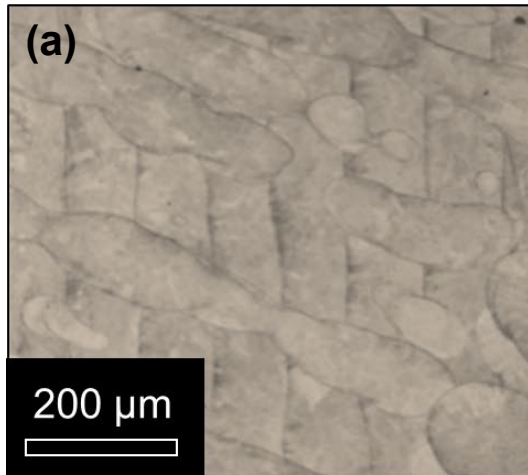
Chemical composition (at. %)						
	Al	Ti	Cr	Fe	Ni	Mo
Matrix #1	0.18	0.88	0.25	76.79	18.16	3.74
Intercellular #2	0.15	0.84	0.21	75.46	19.03	4.31
Intercellular #3	0.07	0.75	0.21	76.48	18.71	3.78
Intercellular #4	0.21	0.78	0.23	76.00	18.54	4.24
Matrix #5	0.11	0.61	0.20	76.98	18.23	3.87

EOS - 40 μm - CW laser mode

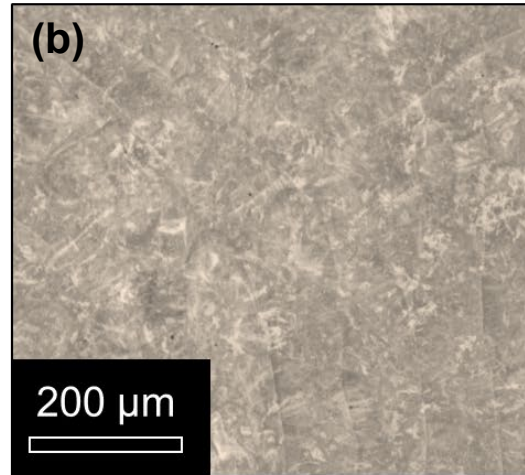
Transverse section

LOM

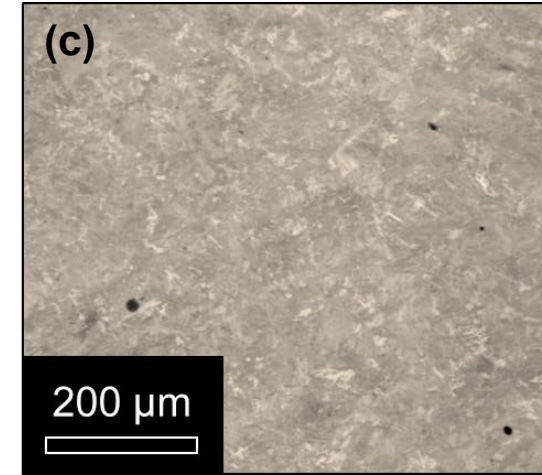
As-built



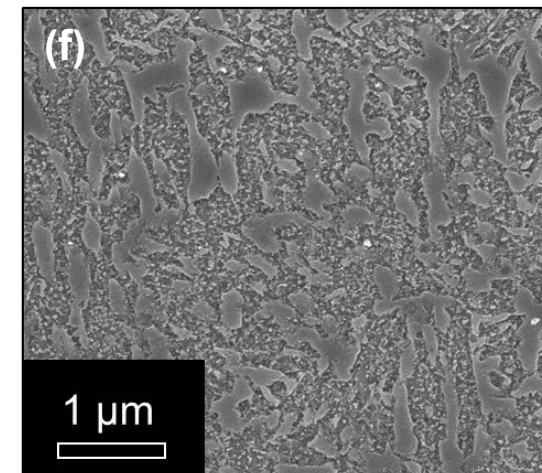
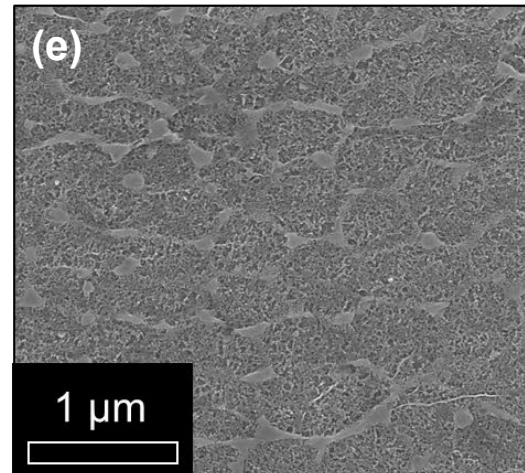
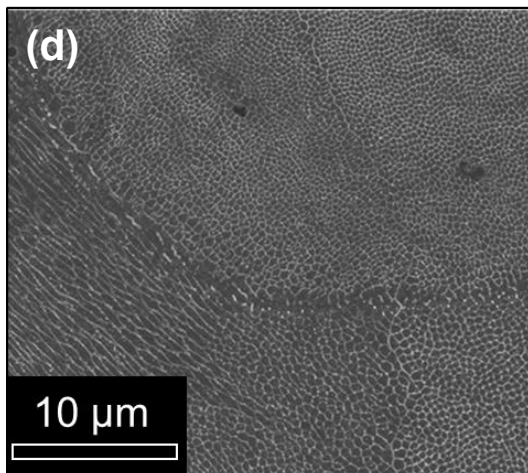
Tag = 480 °C



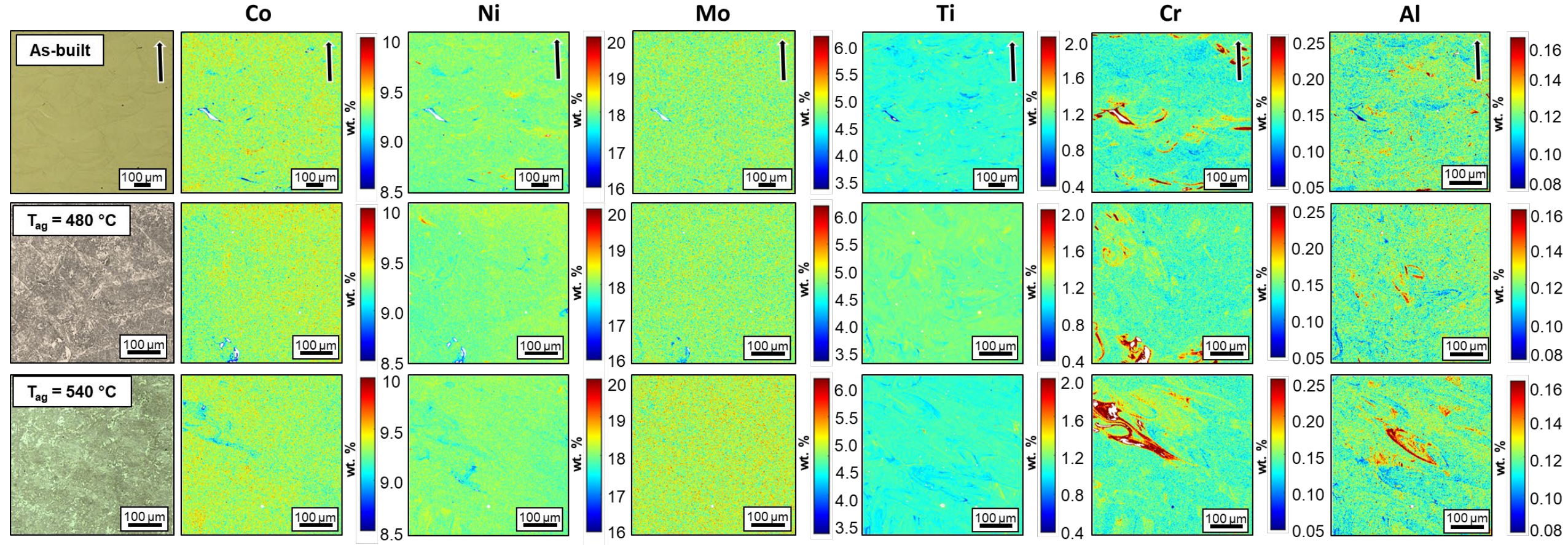
Tag = 540 °C



SEM



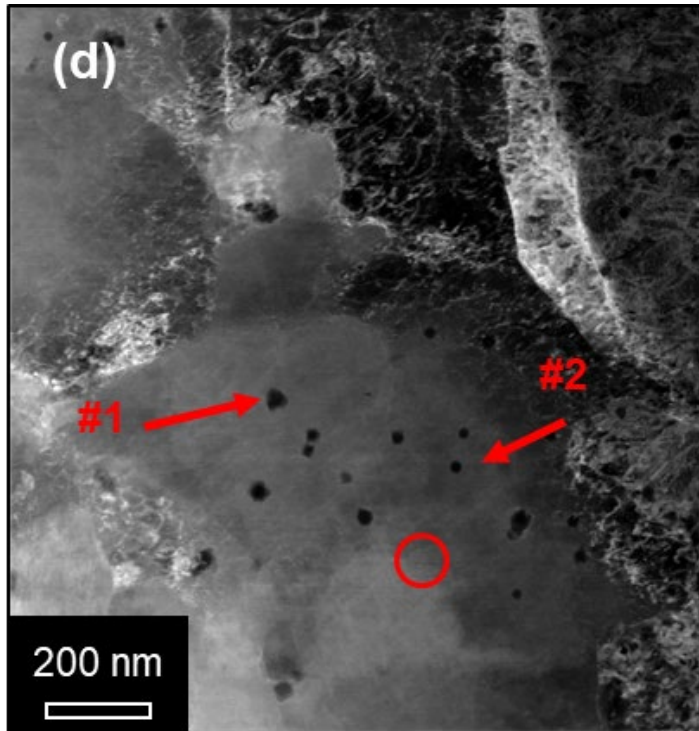
As-built = Longitudinal section; T_{ag} 480 and 540 °C = Transverse section



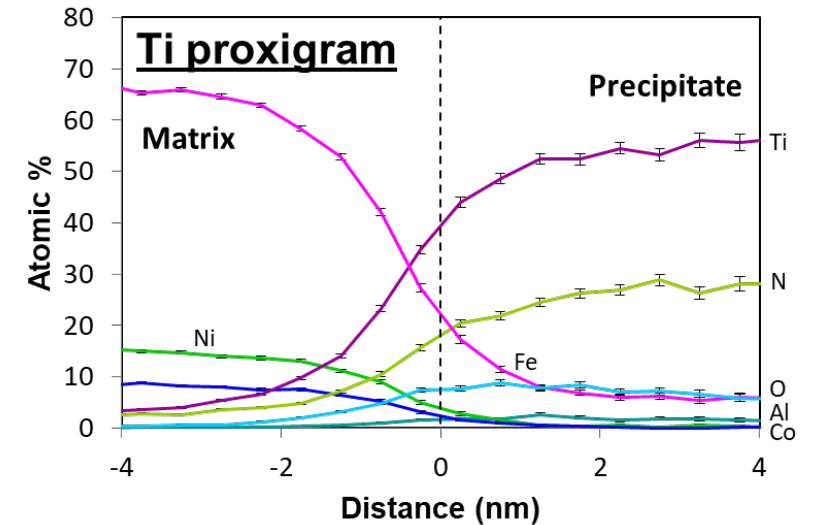
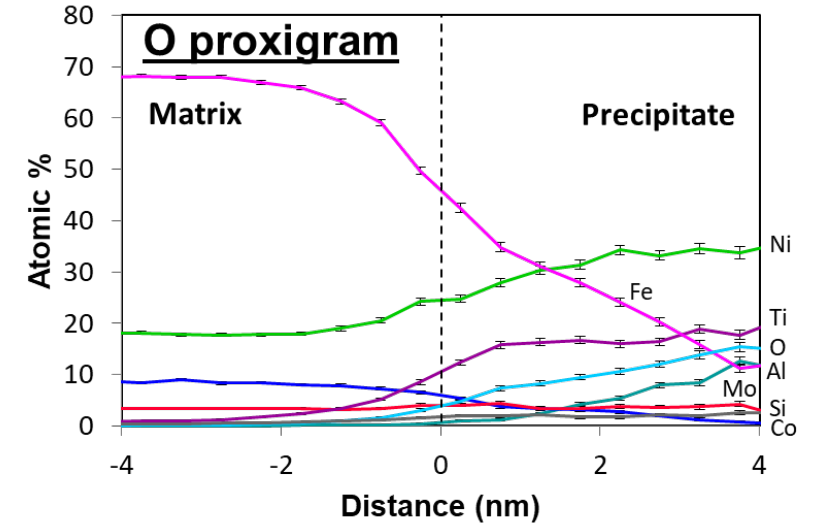
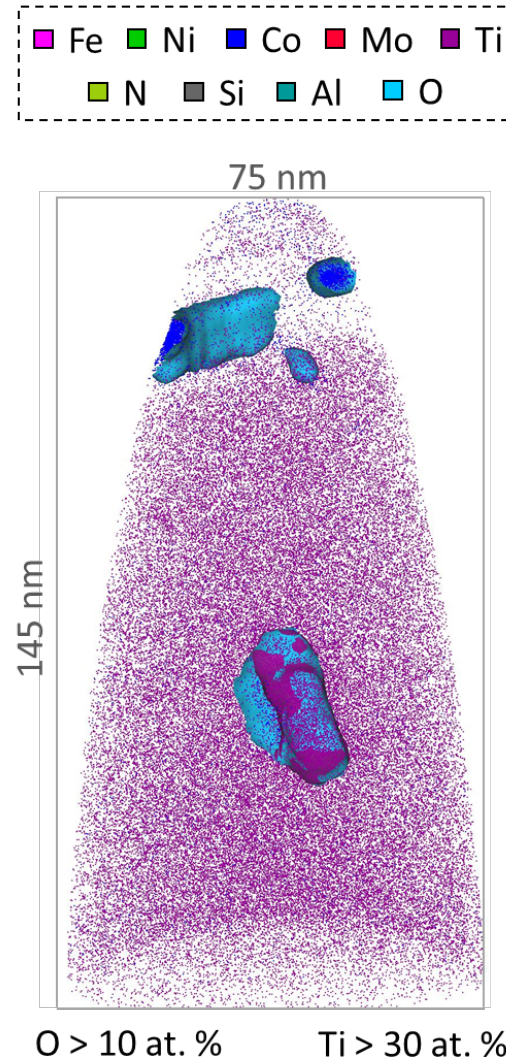
Area: 500 mm x 500 mm; Step size: 0.5 mm

Ti and Al enriched particles

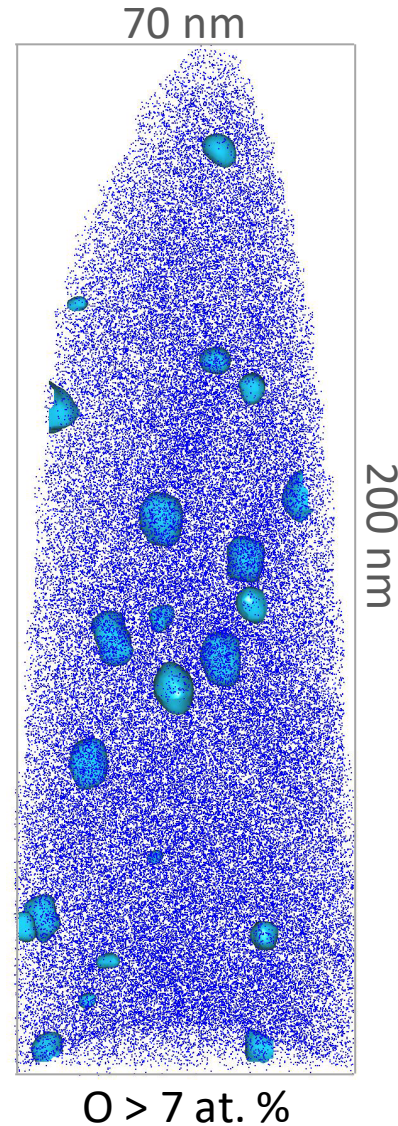
EOS - 40 μm - CW laser mode



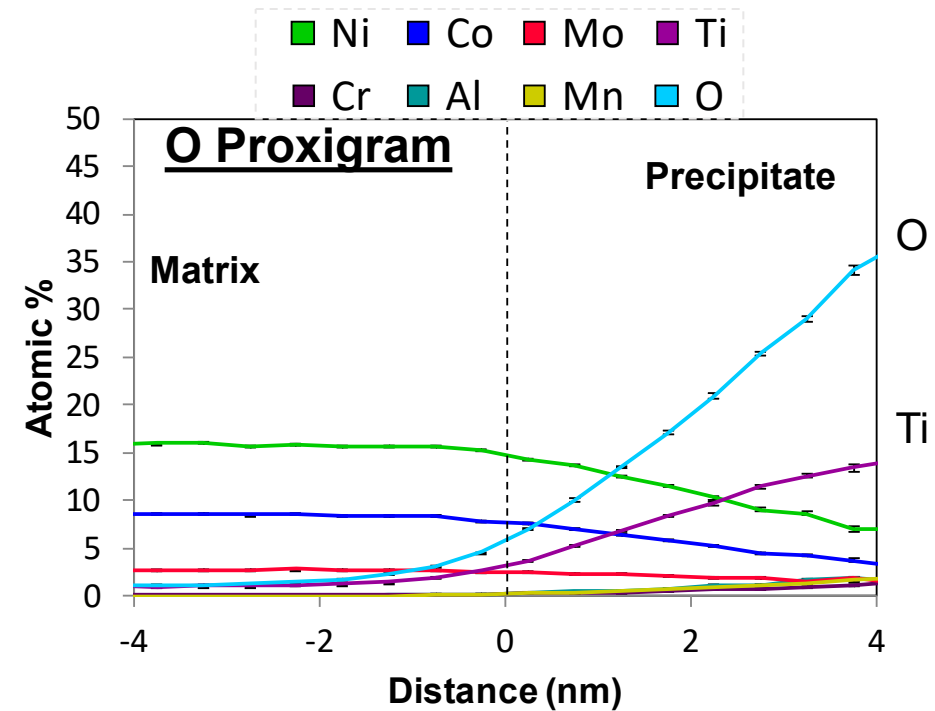
Randomly distributed Ti and
Al enriched particles



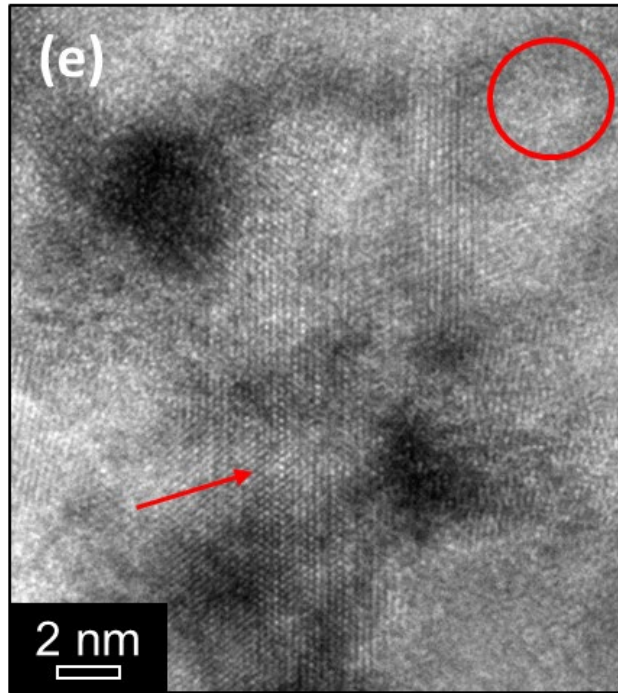
EOS - 40 μm - CW laser mode



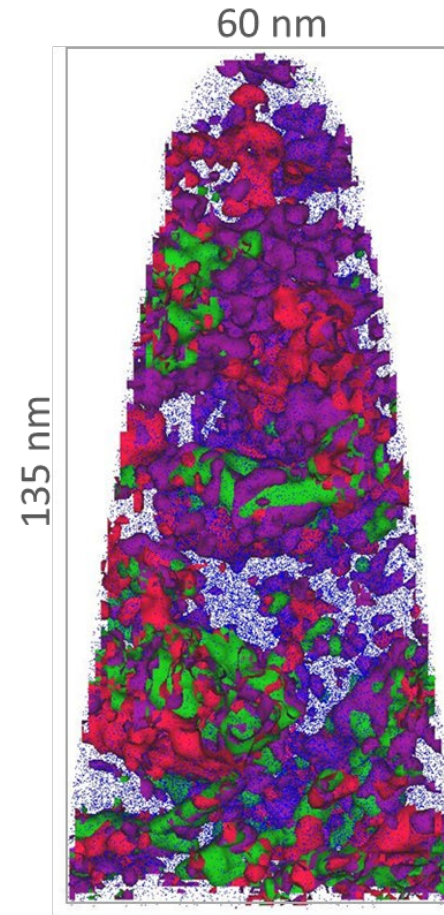
Spherical Ti oxides (TiO and TiO₂)



EOS - 40 μm - CW laser mode



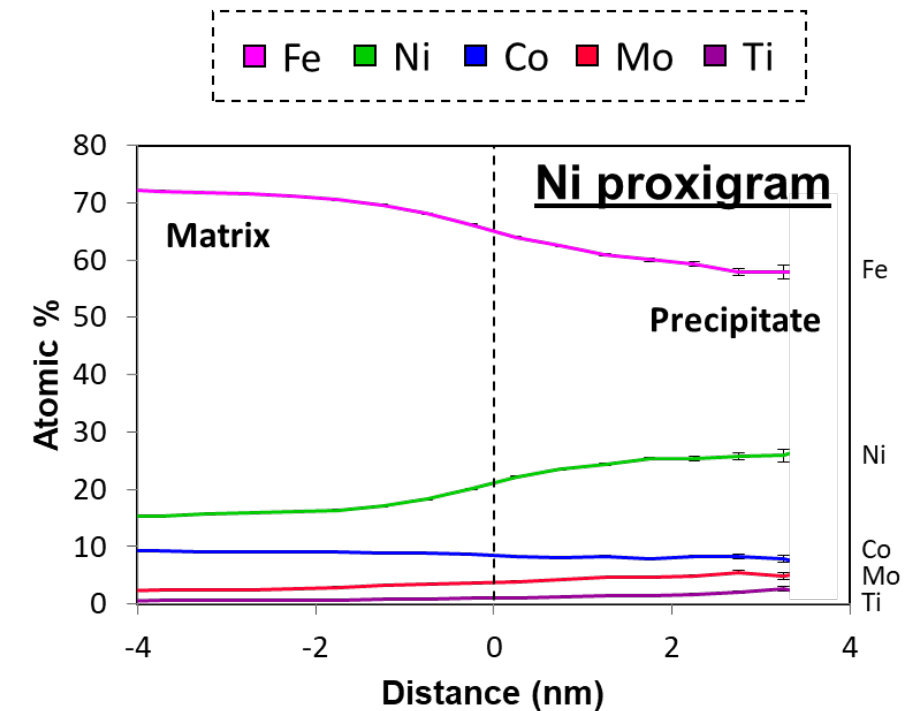
Ni, Ti enriched rod-like particles



Ni > 20 at. % Mo > 4 at. %

Ti > 1 at. %

Clusters enriched in Ni, Ti and Mo





TECHNICAL WORKSHOP

Optimising steels microstructure and surface integrity to face new challenges in Additive Manufacturing



Funded by
the European Union

The NewAIMS project has received funding from the European Union's Research Fund for Coal and Steel (RFCS): project num. 101112371





New approach to Additive Manufacturing of Microstructurally Optimised Steels

Revolutionising Steel: Advances in Additive Manufacturing Technologies

Gonzalo Varela Castro

INNOMAQ21, S.L.

INNOMAQ21



Funded by
the European Union

- 01** Intro
- 02** Tool steels in AM: HTCS steels
- 03** Powder production for AM
- 04** AM technologies
- 05** Challenges, future trends and research in AM of tool steels

Revolutionising Steel: Advances in Additive Manufacturing Technologies



01 Intro

- The global tool steel market is valued at approximately EUR6.0-7.0 billion in 2030, with steady growth fueled by automotive, aerospace, and energy sectors.
- Service life of tooling has decreased by 15-20% over the last decade due to more demanding process conditions, underscoring the importance of both efficient fabrication and effective re-manufacturing strategies.
- Conventional machining routes
 - Difficult to produce complex shapes and internal cooling channels (casting, forging, and machining).
 - Subtractive processes cause high material waste and lengthen production cycles.
 - Repair is challenging due to metallurgical bonding issues, leading to frequent need for full part replacement.
- Additive Manufacturing (AM) adoption in tool steels supports efficiency gains and cost reduction in high-demand industrial applications:
 - Design freedom
 - Conformal cooling channels
 - Enhance tool performance
 - Materials

02 Tool Steels in Additive Manufacturing

Widely used tool steels in AM and key features

- Cold-work tool steels (<200 °C)
C, Cr, Mo, V, W, Nb: O-series, A-series, D-series
Cold forging dies, stamping dies, cutting tools, blades and punches
O1, A2, D2, ...
- Hot-work steels
C*, Cr, Mo, W, Co: H-series, W-series
Die casting dies and molds, Al-Mg-Zn injection, hot forging, extrusion dies, hot shearing
H11, H13, ...
- High-speed steels (HSS)
C, Cr, Mo, V, W, Co: M-series, T-series
Cutting, drilling, and machining, saw blades, punches and dies, end mills
T1, M2, ...

Key handicaps in AM:

- High cracking susceptibility, porosity
- Microstructural issues
- Poor printability and limited grades
- Extensive post-processing requirements

Key features:

- High hardness and wear resistance
- Thermal stability at elevated temperatures
- Good toughness and fatigue resistance
- Hardening and tempering, surface treatments (e.g. nitriding and hard coating)
- Abrasive/adhesive wear

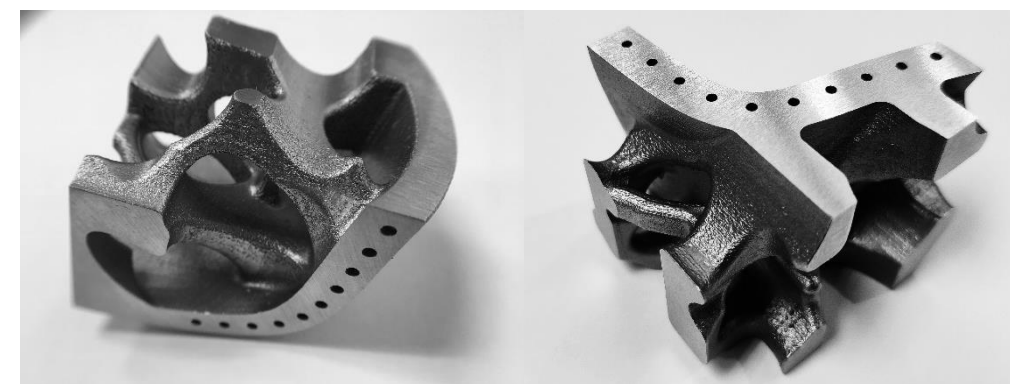


Figure 1. Demo dies (CCC's+TO)

02 High Thermal Conductivity Steels

What are High Thermal Conductivity Steels (HTCS)?

- HTCS are tool steels engineered to maximize heat dissipation:
 $>50-70 \text{ W}\cdot\text{m}^{-1}\cdot\text{K}^{-1}$ ($20-30 \text{ W}\cdot\text{m}^{-1}\cdot\text{K}^{-1}$ for conventional tool steels)
- Thermal conductivity depends on electron and phonon transport in both metal and hardening phases, influenced by their volume fractions and microstructure. Scattering effects from impurities, defects, and lattice distortions reduce thermal conductivity by disrupting phonon-electron flow and crystal regularity.
- Reduced thermal gradients in tooling, lower thermal fatigue, distortion, and reduce cycle times!
- Expanding applications in injection molding, die casting, electronics, and aerospace tooling.
- Emerging research focuses on processing challenges and microstructure-property control.

<https://rovalma.com/application/hot-stampingpress-hardening/>

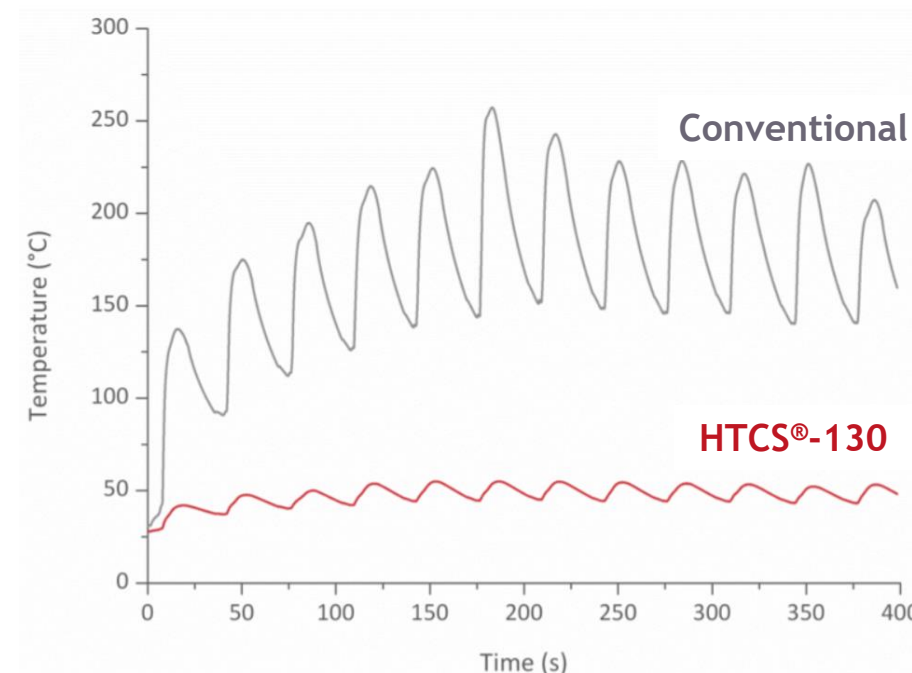


Figure 2. Examples of tool steel performance.

03 Powder Production for AM

Powder Production for Additive Manufacturing

- Gas atomization is the dominant method to produce high-quality metal powders for AM, ensuring round/spherical particles with controlled size distribution.
- Powder morphology, size, surface texture impacts flowability, packing density, and final part quality.
- Key compositional control (O, N, C): defects (melt&sol).
- Advanced powders with tailored microalloying enable functional properties for specific AM tool steels.

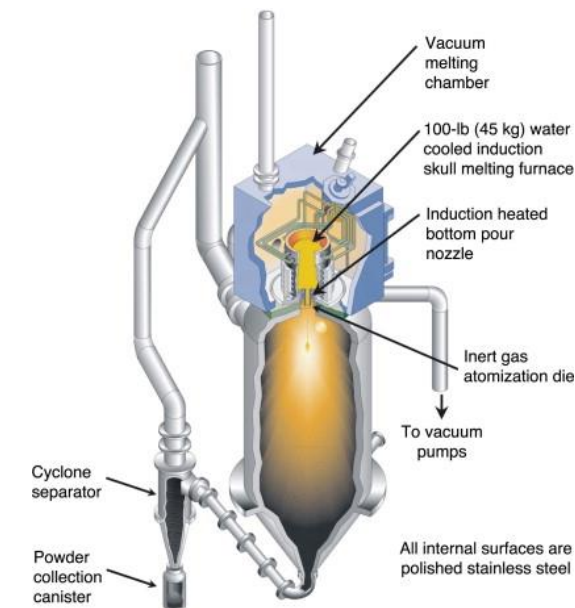


Figure 3. Close-coupled gas atomizer.

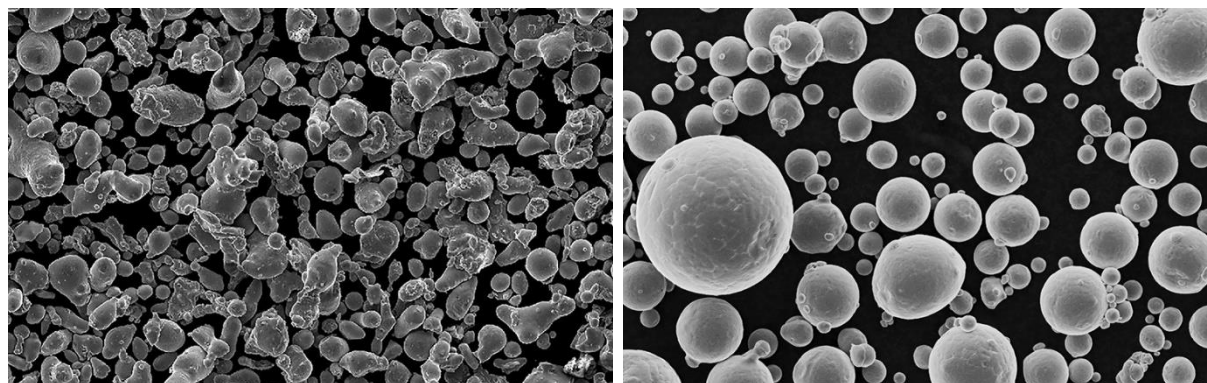


Figure 4. Powder morphologies.

04 Additive Manufacturing technologies

Key technologies

- POWDER BED FUSION-LASER (L-PBF)
 - Selective Laser Melting/Sintering (SLM/S)
 - Direct Metal Laser Sintering (DMLS)
 - Electron Beam Melting (EBM)
- DIRECT ENERGY DEPOSITION (DED)
 - Laser Engineered Net Shaping (LENS)

90 % of tool steels!

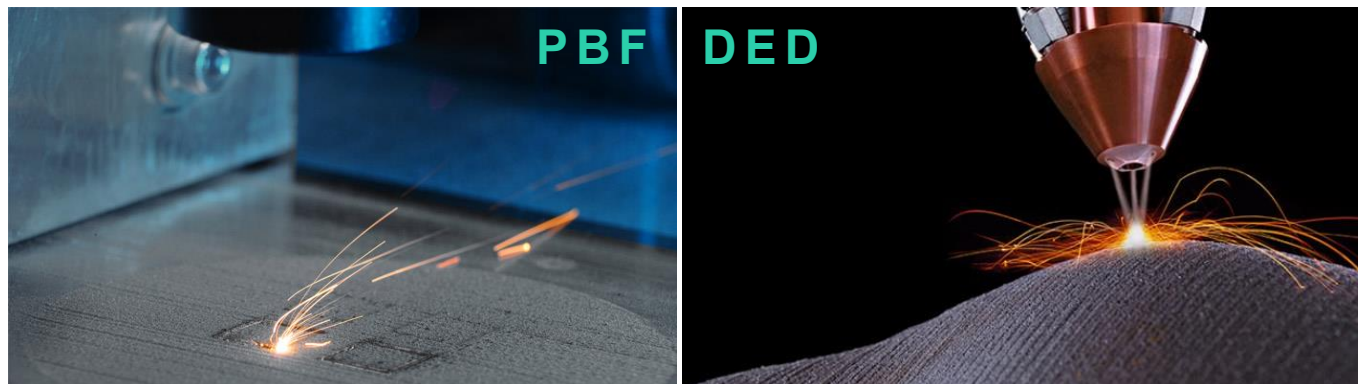


Figure 5. PBF and DED technologies.

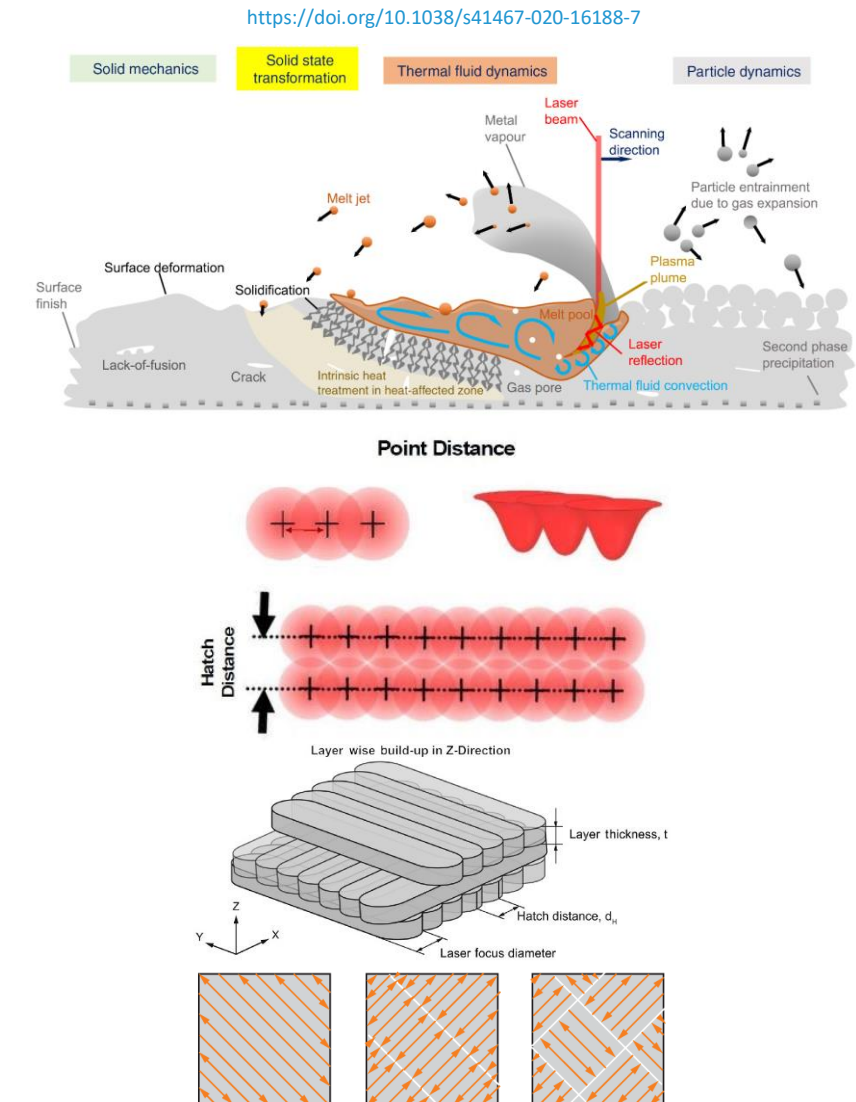


Figure 6. Multi-scale-physics phenomena. 9

05 Future, trends and research

Steel sector: emissions

https://reports.weforum.org/docs/WEF_Net_Zero_Industry_Tracker_2024.pdf

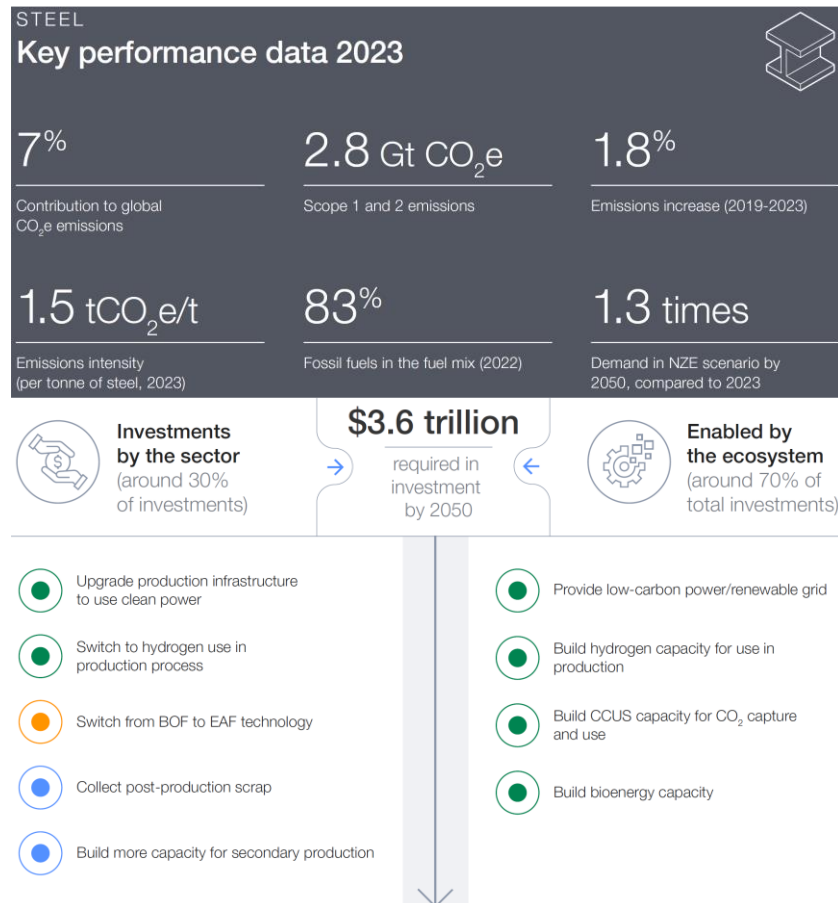


Figure 7. Steel sector's performance.

Short-term:

- CCS/CCUS

Long-term:

- Direct reduced iron in electric arc furnaces (H₂-DRI)
- Increased scrap steel use/raw materials

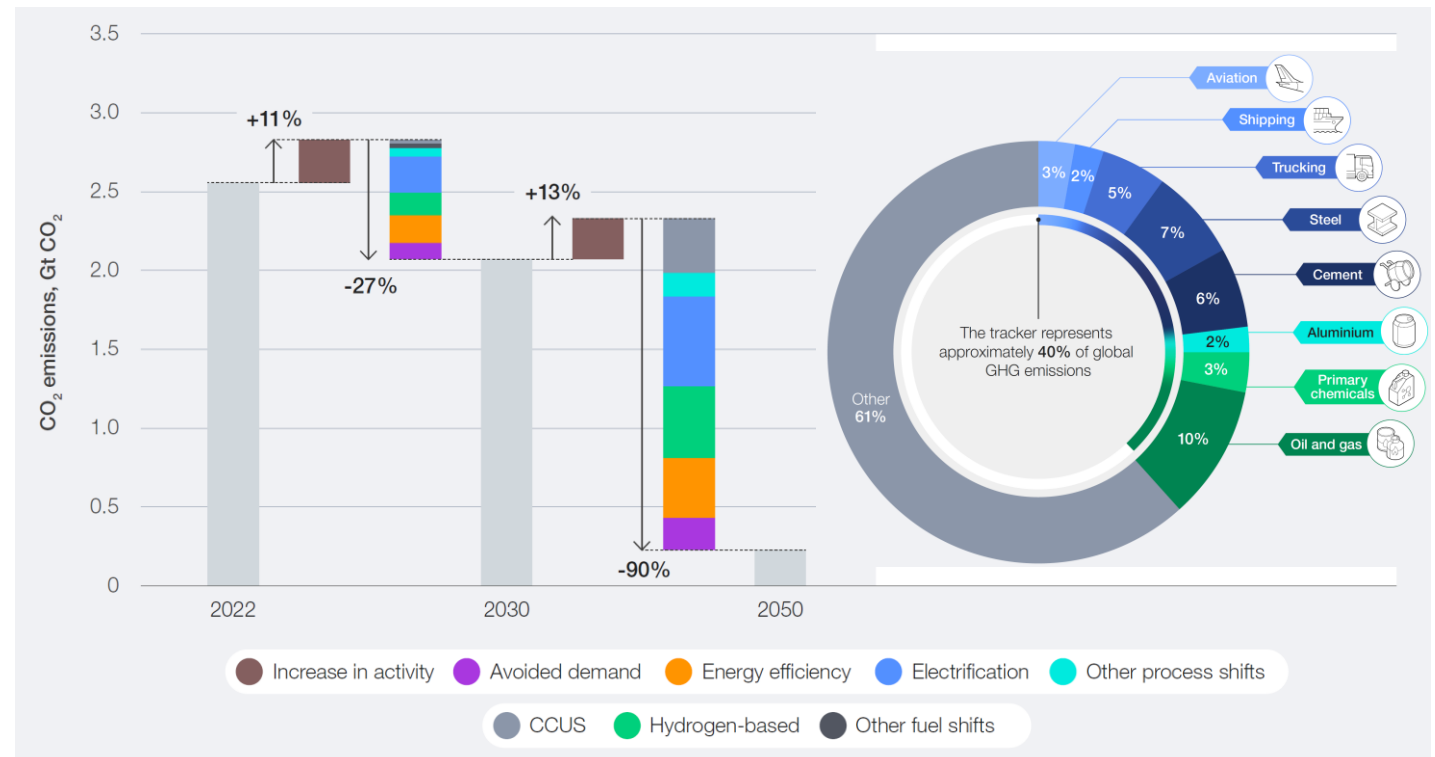


Figure 8. Decarbonization levers.

05 Future, trends and research

How can contribute?

AM plays a well-known role in Industry 5.0:

MAM high performance materials + added functionalities

- Virtually freedom of design, complexity for free.
- Highly efficient CCC's features.
- DfAM: lightweight design (lattice) + TO + GD.
- Consolidation of multiple components.

Raw material usage:

- Optimized alloys or grades for example in terms of mechanical properties (microstructure), thermal conductivity, cost, and energy consumption of production.
- Optimized steel production: decreasing consumption of rare alloying elements, including critical raw materials (Cr, Co, Mo, V, and more).
- Minimizing alloying element reliance via waste reduction.
- Increased tool lifetime (thermal shock or thermal fatigue).
- Reducing frequency's tool replacement.

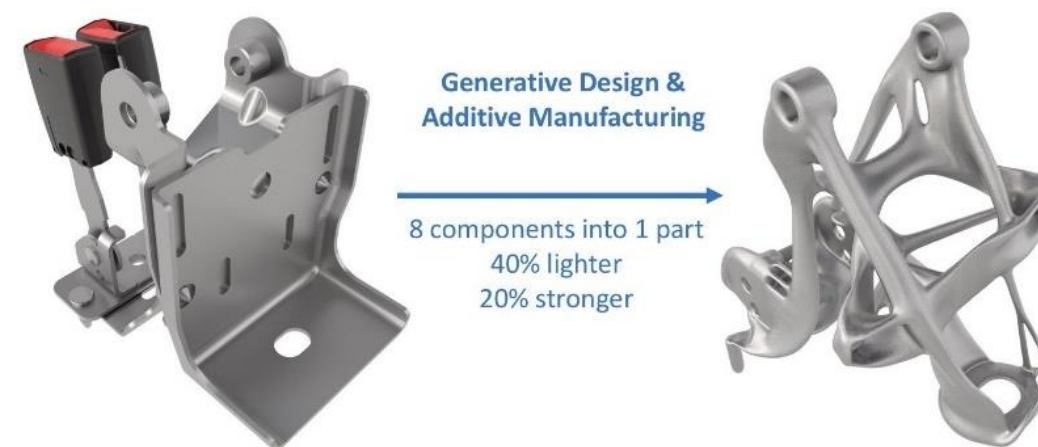


Figure 9. Example of GD and AM.

Superior mat/process, superior sustainability outcomes!

05 Future, trends and research

Research trends

- Advanced Alloy Design (pre): predict printability/enhance reliability, crack and defect prevention (ML).
- Microstructure Control via Process Parameters (in situ): **NewAIMS!!!**
- Microstructural Modification Strategy (post): crystal structure, matrix, lattice, defects, martensite, non-cellular/dendritic μ -structure, solid solution atoms and dislocations heat carriers, e.g. electrons and phonons, anisotropy. HIP reducing pores, defects, microcracks.

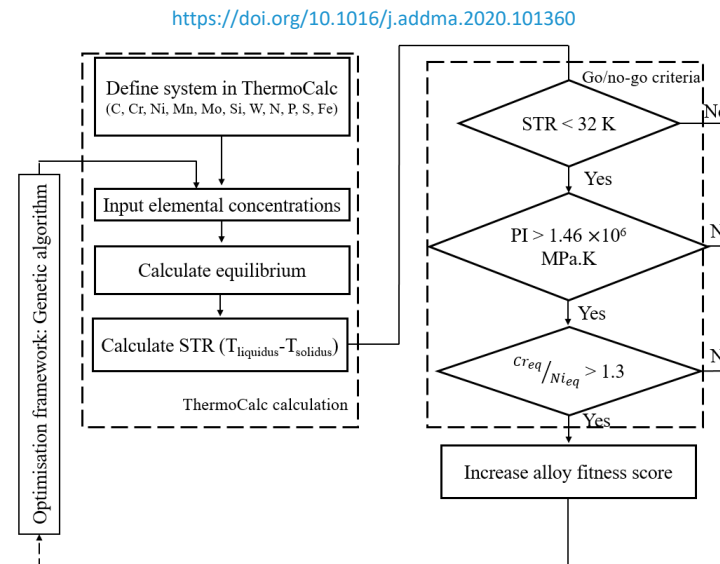


Figure 10. Algorithm for thermodynamic calculations and criteria evaluation.

05 Future, trends and research

Research trends

- Advanced Alloy Design (pre): predict printability/enhance reliability, crack and defect prevention (ML).
- Microstructure Control via Process Parameters (in situ): **NewAIMS!!!**
- Microstructural Modification Strategy (post): crystal structure, matrix, lattice, defects, martensite, non-cellular/dendritic μ -structure, solid solution atoms and dislocations heat carriers, e.g. electrons and phonons, anisotropy. HIP reducing pores, defects, microcracks.

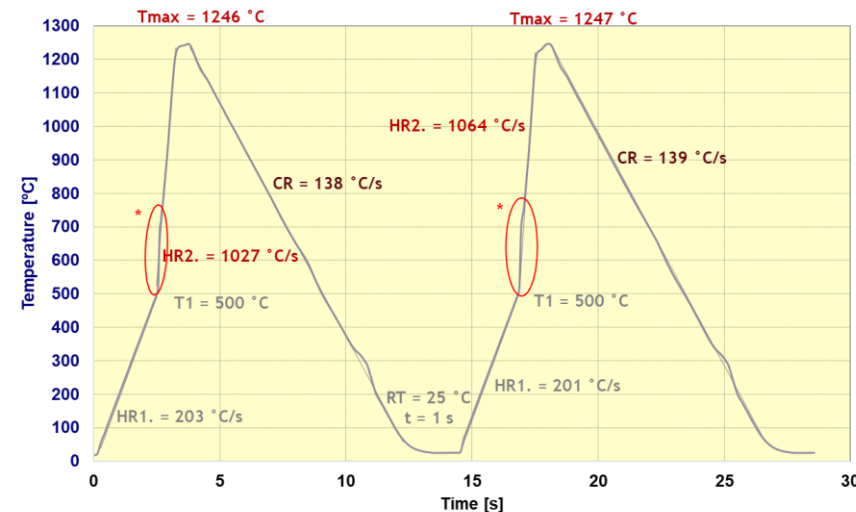
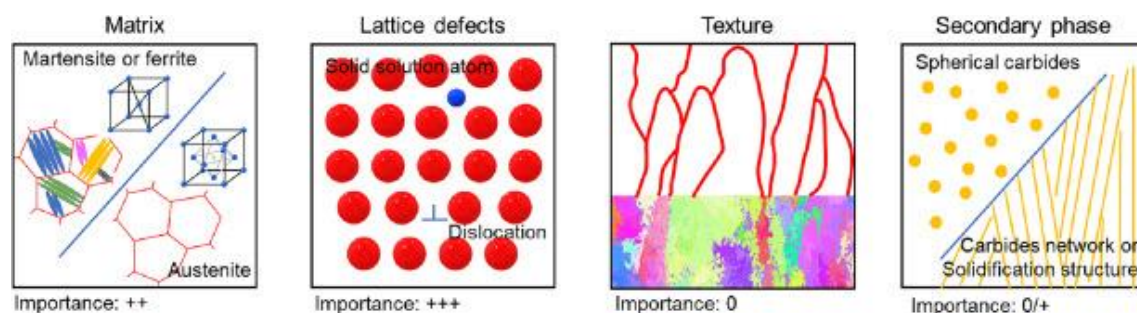


Figure 11. Preliminary research (NewAIMS).

05 Future, trends and research

Research trends

- Advanced Alloy Design (pre): predict printability/enhance reliability, crack and defect prevention (ML).
- Microstructure Control via Process Parameters (in situ): **NewAIMS!!!**
- Microstructural Modification Strategy (post): crystal structure, matrix, lattice, defects, martensite, non-cellular/dendritic μ -structure, solid solution atoms and dislocations heat carriers, e.g. electrons and phonons, anisotropy. HIP reducing pores, defects, microcracks.



<https://doi.org/10.1016/j.matchar.2024.113917>

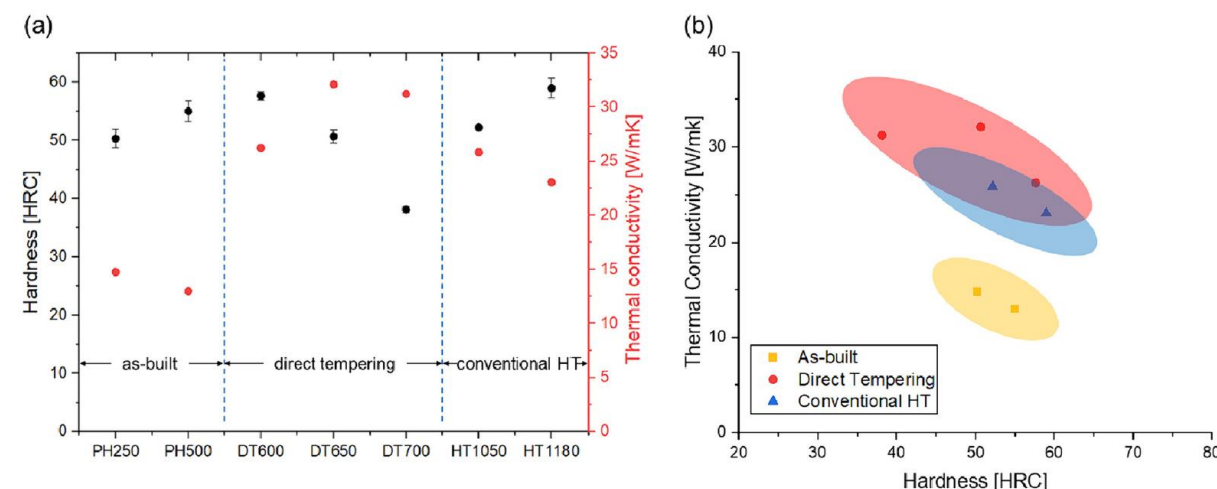


Figure 12. Relationship between thermal conductivity and hardness.

Thank you!



TECHNICAL WORKSHOP

Optimising steels microstructure and surface integrity to face new challenges in Additive Manufacturing



Funded by
the European Union

The NewAIMS project has received funding from the European Union's Research Fund for Coal and Steel (RFCS): project num. 101112371





PREdictive simulation of finishing operations
in steel **Additive Manufacturing** for optimal
SURface integrity

Heat treating Additive Manufacturing Alloys

PRESENTER NAME: MIGUEL VARELA [IDONIAL]

EMAIL: Miguel.Varela@idonial.com

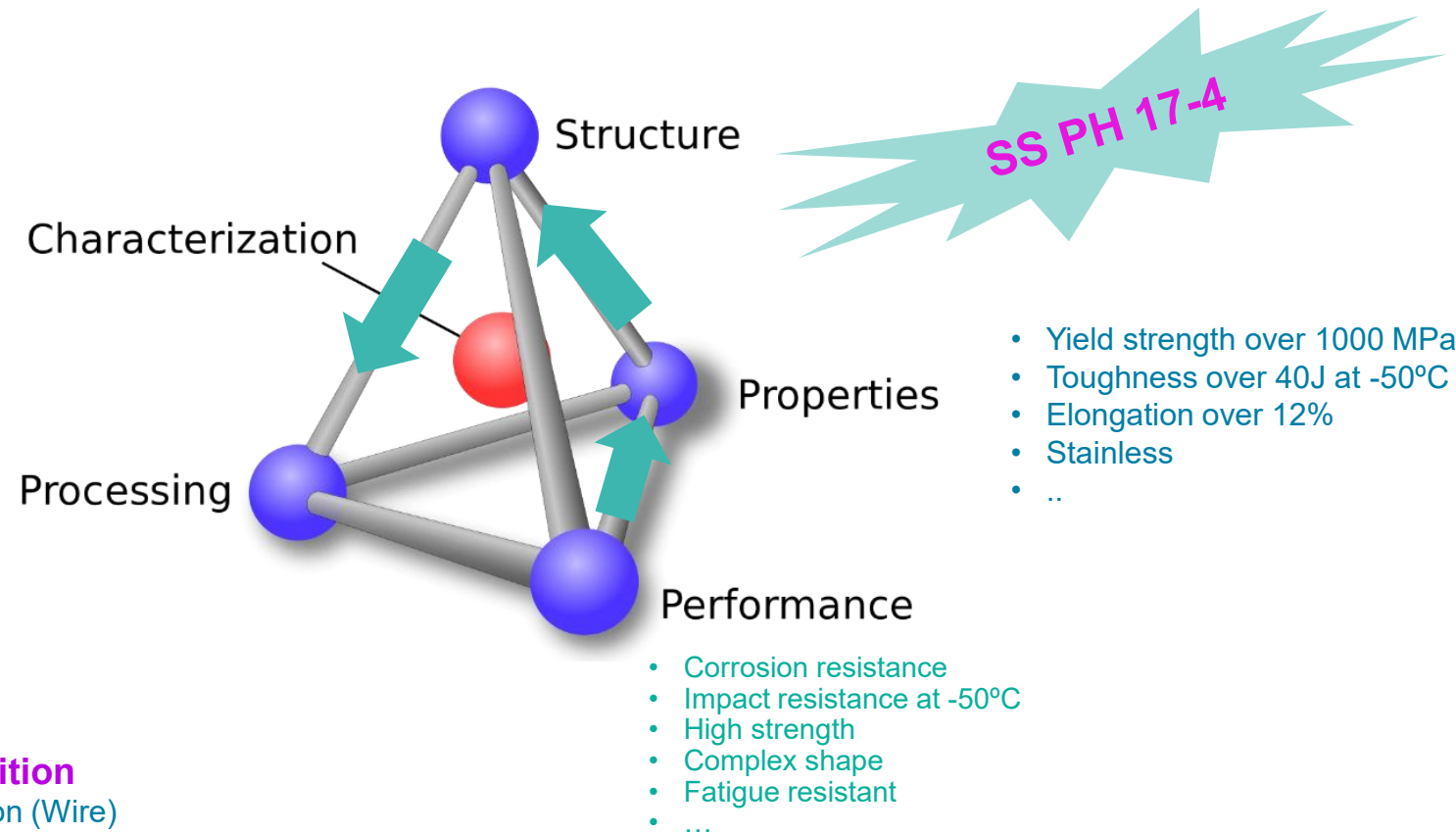
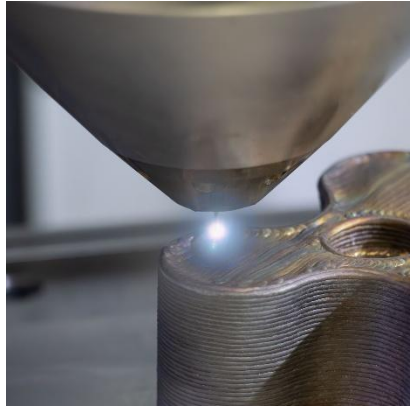
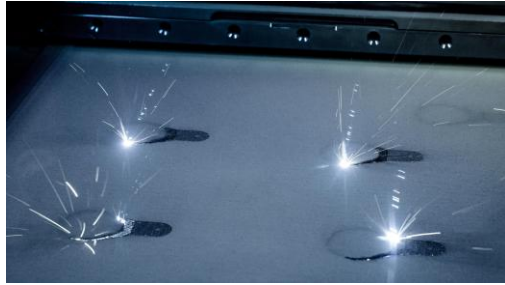
DATE: 07/10/2025



Funded by
the European Union

How a heat treatment works?

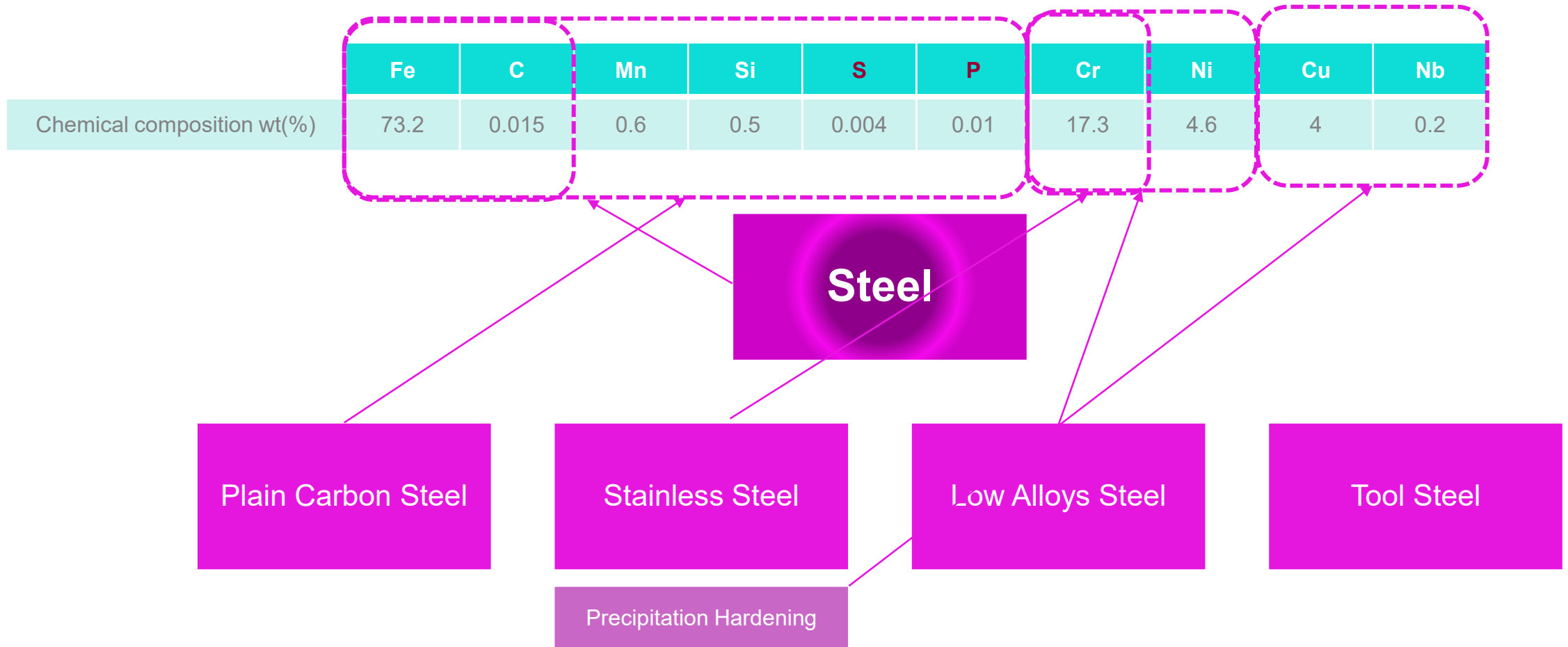
- Martensitic
- Precipitation Hardening (PH)



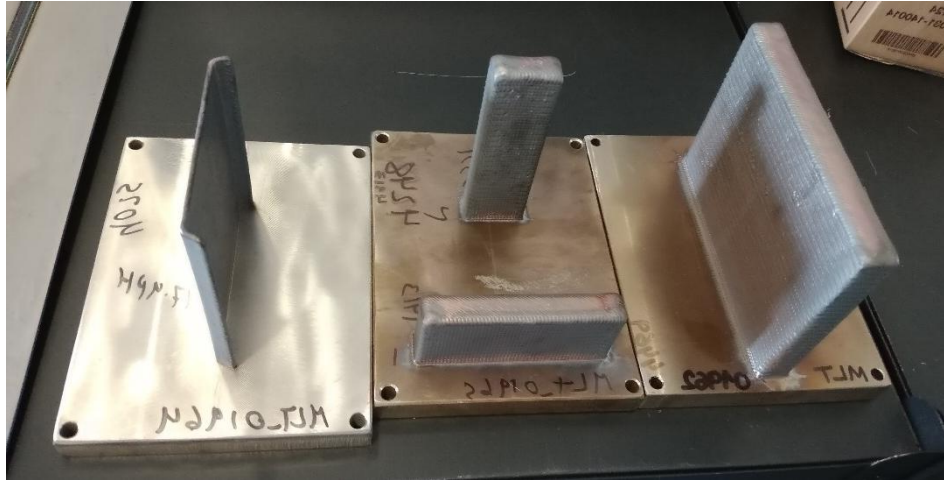
- **Chemical composition**
- Raw material production (Wire)
- AM technology (L-DED) manufacturing
- **Heat treatment**

Chemical Composition

Stainless Steel PH 17- 4 a.k.a ER 630 / 1.4542 / UNS S17400



As-Built



Single Wall (SW)

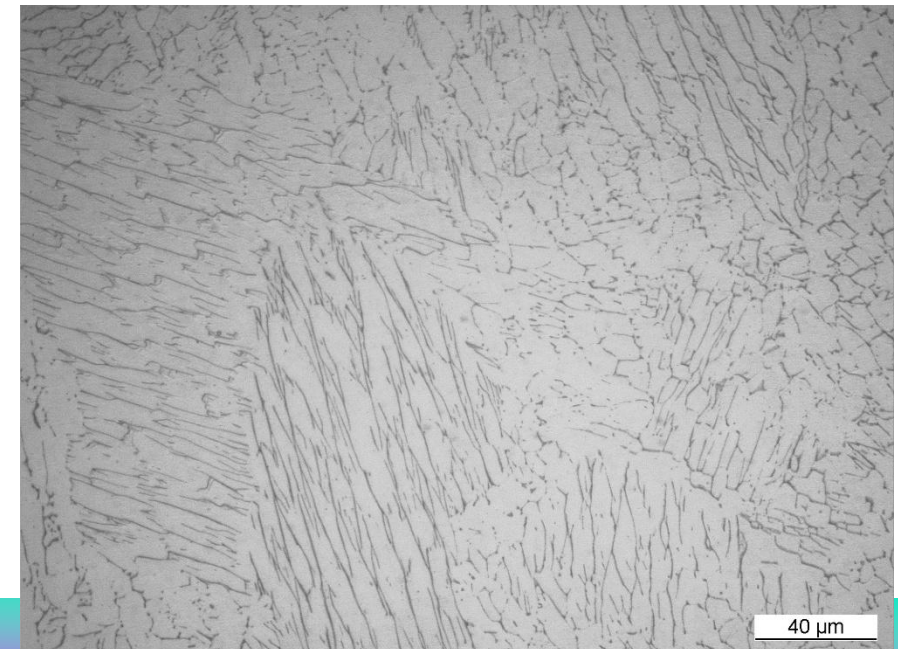
Massive Wall (MW)

Super Massive Wall (MW)

- [BCT Matrix] Moderately soft martensitic (carbon-free) matrix
- [Cu-Rich] Precipitation of nm size coherent particles that block dislocation movement

PH17-4 DED AM Tensile Test **without** heat treatment

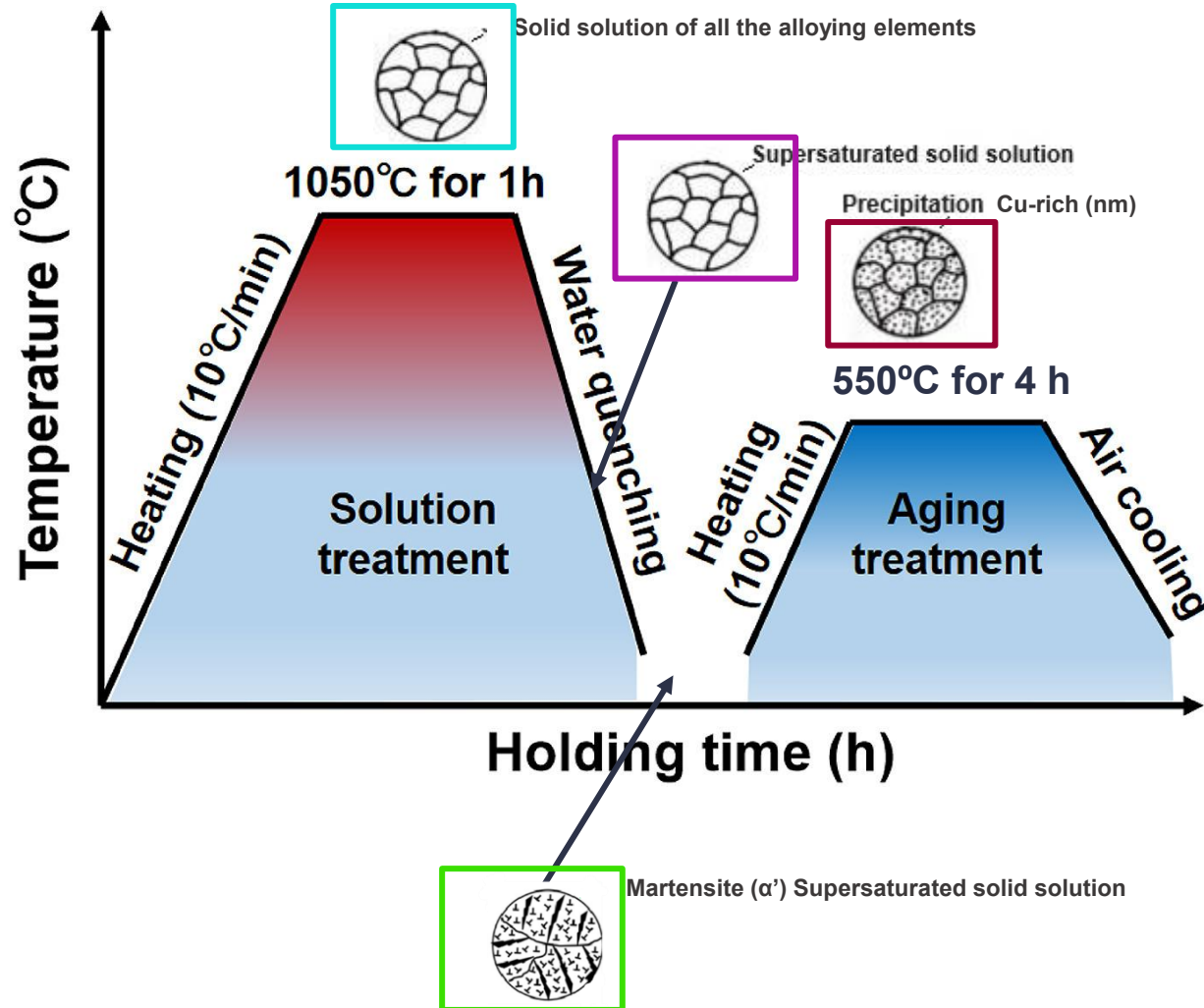
Cod	Ys (MPa)	UTS (MPa)	E(%)
Ref PH17-4 HT	1000	1070	12
SW V	506	978	15
MW V	969	1209	9
MW H	824	1132	17
SMW V	539	1149	18
SMW H	534	1128	21



Heat Treatment

GOALS

- Fully austenitic solid solution (Ni balance Cr)
- Quench a supersaturated solid solution without diffusion transformations (Cr and Mn)
- Strong but ductile martensitic matrix (Low C)
- Well dispersed coherent nano-precipitates to increase strength (Cu)



Heat Treatment

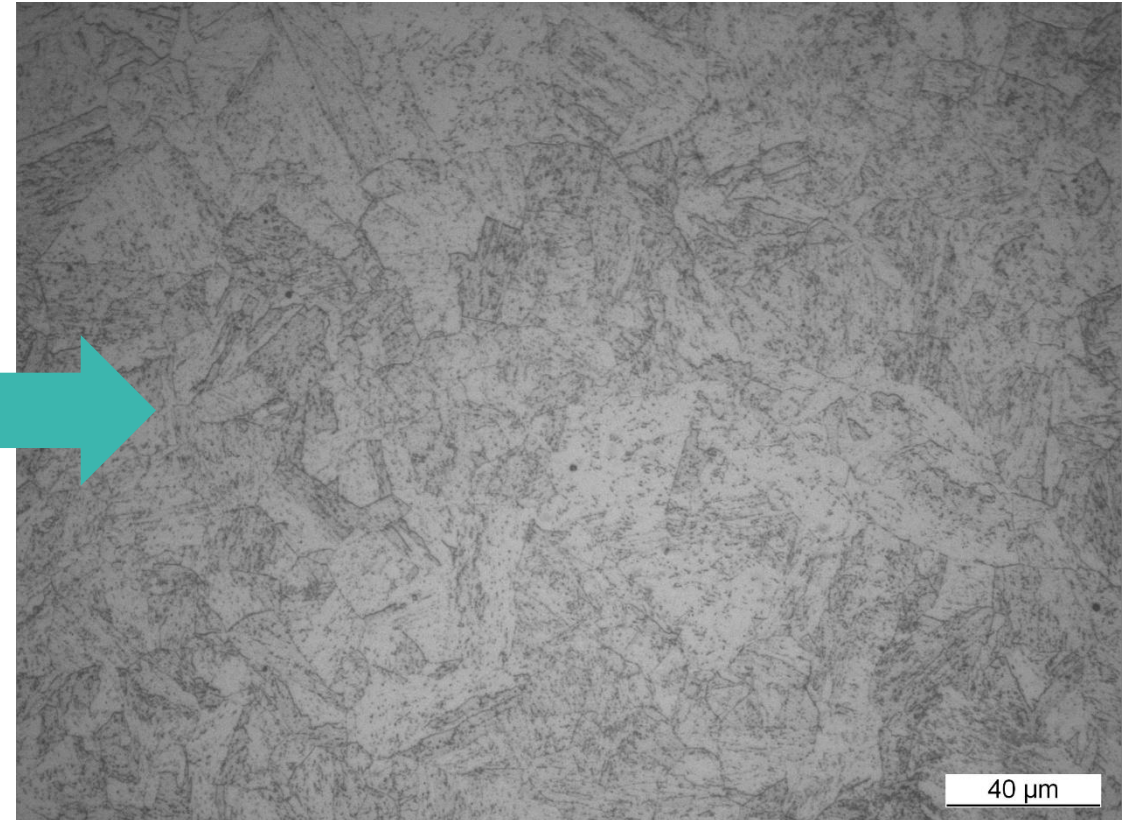
PH17-4 DED AM Tensile Test **with** heat treatment (H1025)

Cod	Ys (MPa)	UTS (MPa)	E(%)
Ref PH17-4 HT	1000	1070	12
SW V HT	992	1092	12.5
MW V HT	1039	1114	15
MW H HT	1066	1130	15
SMW V HT	1002	1088	12
SMW H HT	997	1066	23

ok!

40 µm

PH17-4 DED AM **Without** heat treatment



40 µm

PH17-4 DED AM **With** heat treatment



A project coordinated by:

eurecat

PREdictive simulation of finishing operations in steel **Additive Manufacturing** for optimal **SUR**face integrity

Thank you!

The SuPreAM project has received funding from the European Union's Research Fund for Coal and Steel (RFCS): project num. 101112346. Funded by the European Union. Views and opinions expressed are however those of the author(s) only and do not necessarily reflect those of the European Union or REA. Neither the European Union nor the granting authority can be held responsible for them.



**Funded by
the European Union**



Funded by
the European Union

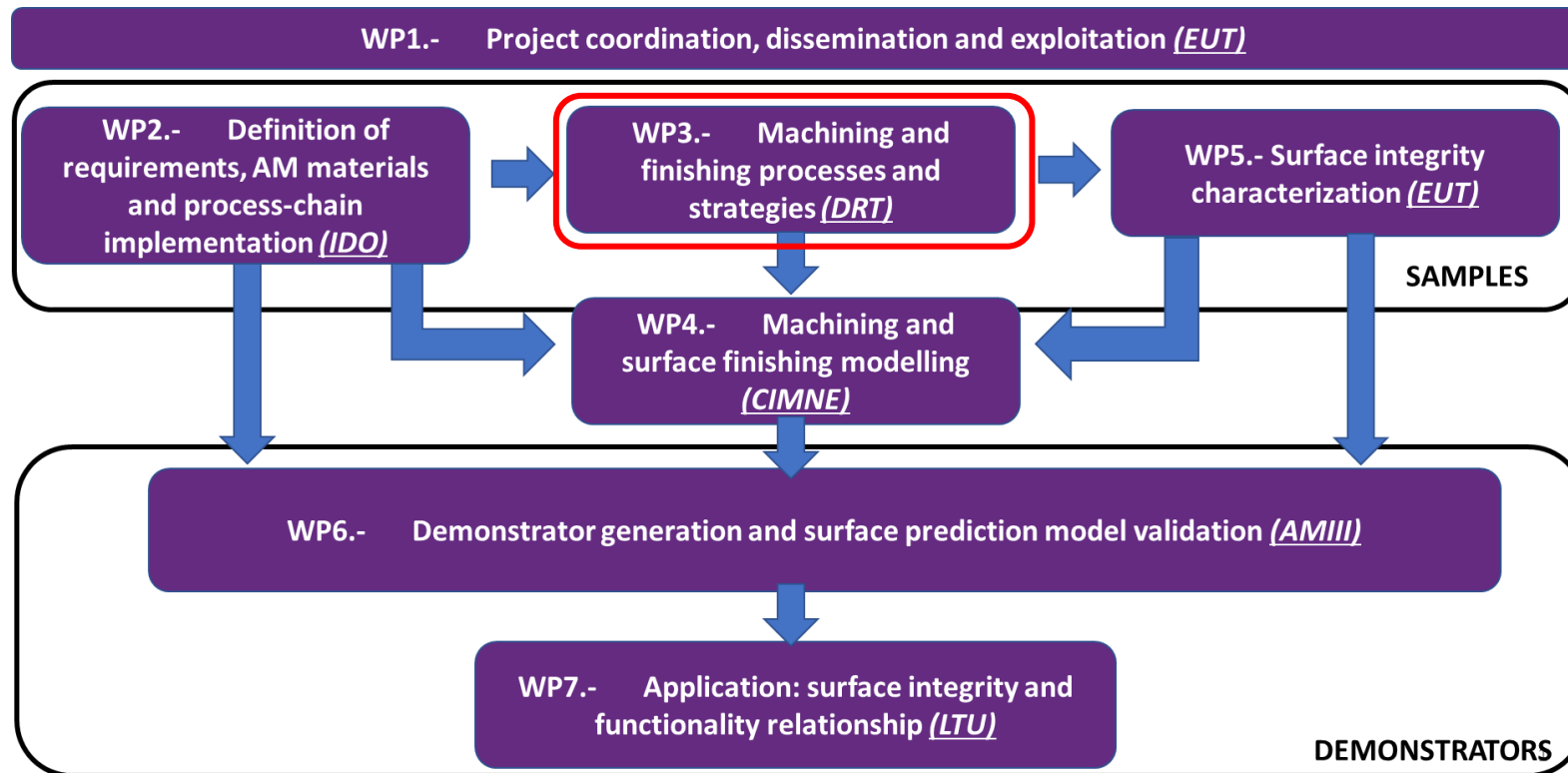
Predictive simulation of finishing operations in steel Additive Manufacturing for optimal Surface integrity

Machining and finishing processes and strategies for injection

Marco Dias
Researcher, DRT Group
marco.dias@drt-group.com



PERT chart of SuPreAM



OBJECTIVES

- Machining and Finishing **processes selection** for AMed machining
- Machining and finishing **process strategies** & tests development **for surface integrity optimization**
- Techniques **demonstration** through **surface integrity optimized samples**



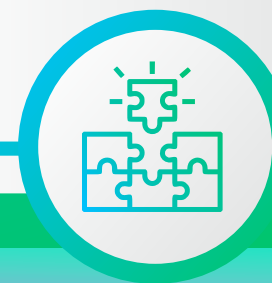
VALUE PROPOSITION

- State-of-the-art review
- **Sensitive parameters** identification
- AMed machined sample parts for injection mould application
- Improvement of finishing surface of **plastic parts produced** from samples optimized in the **AMed machining process**



WORKPACKAGE IMPORTANCE

- Processes definition for **concept validation**
- Strategy protocol design for AMed steel components, based on **sustainable methodologies** and processes
- Interconnection with WP4 & WP5 for **continuous investigation** and **results achievement**



Use cases domains



DRT GROUP

Additive Manufactured
injection mould



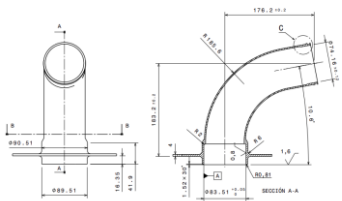
GRUPO SEVILLA CONTROL

Additive Manufactured
structural component
for aerospace application

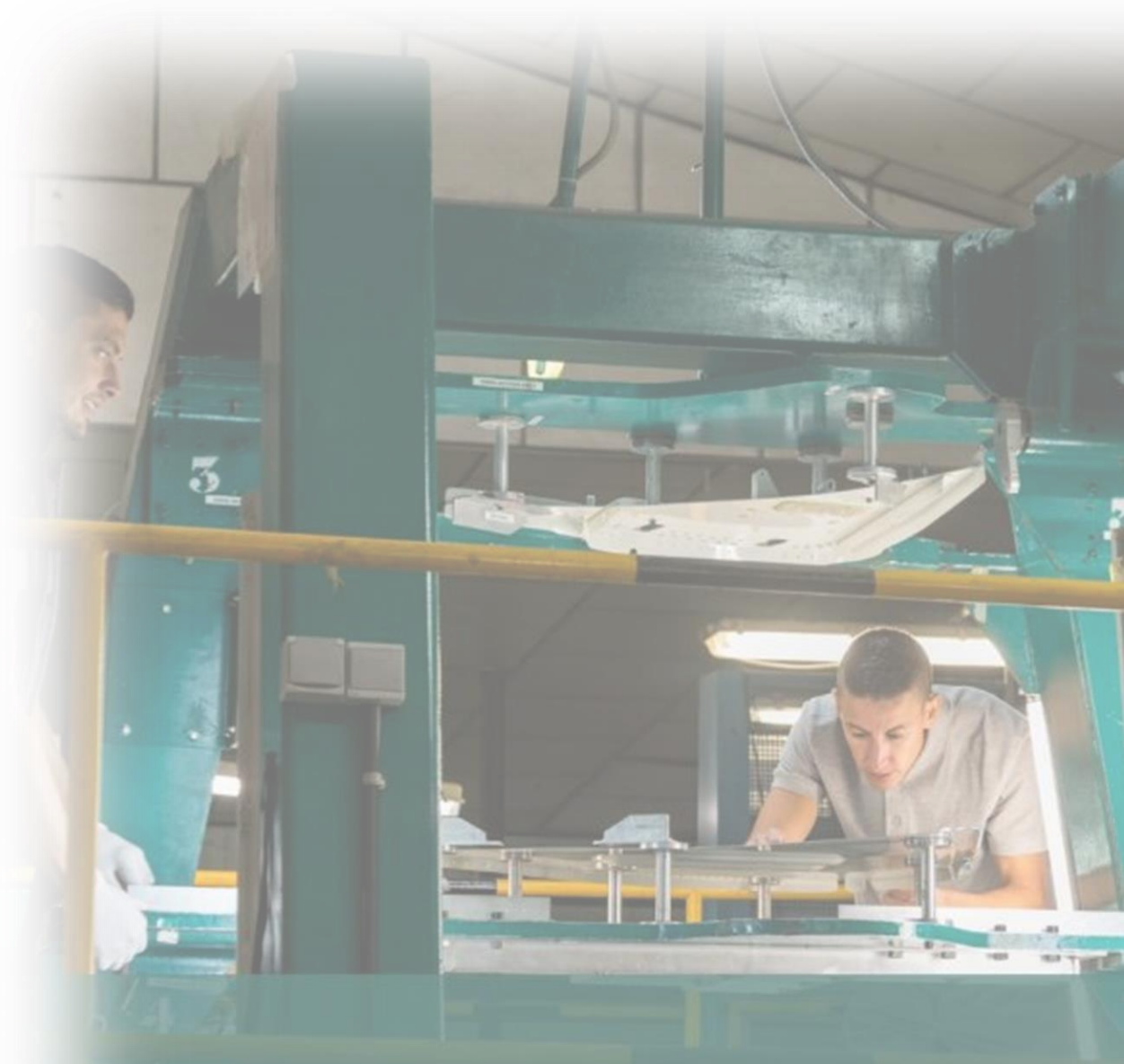




Grupo Sevilla Control (GSC) is a company specialising in the **manufacturing of machined components and assemblies for the aerospace** sector. With more than 40 CNC machining centres and an advanced technological infrastructure, GSC supplies high-precision, high-quality parts, ranging from conventional materials to advanced alloys used in aeronautical and defence applications.



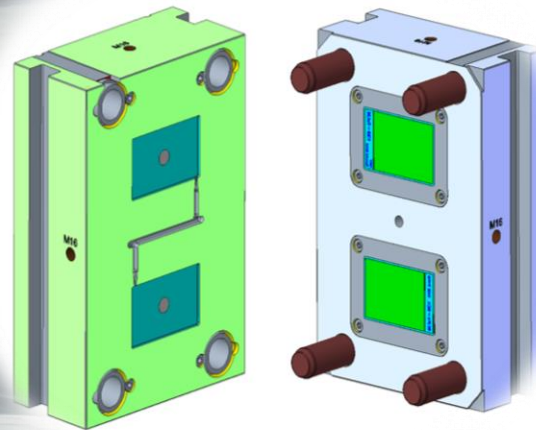
Within the SuPreAM project, GSC actively participates in the evaluation and development of innovative **strategies to optimize the machining of critical components.**



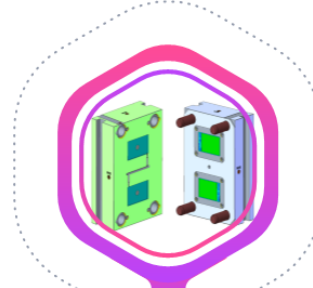


DRT
GROUP

DRT MOLDS (DRT Group) is a Portuguese company that developed **expertise** in different areas related to the **design, fabrication, marketing and after-sales service of molds and plastics**, working for OEMs, namely with the VW Group (automotive sector) as a Supplier Club member.



In the context of the SuPreAM project, DRT aimed to develop **new approaches to improving the surfaces of inserts** as a constituent part of the molds it manufactures, with focus on **EDM Erosion** and **Polishing hand process**.



Trial Mold



EDM



Polishing

EDM Strategy Protocol

2 electods dedicated to cutting at Ra = 12,5

1 electrode for cutting sequence at RA = 3,2



2x Conventional

Material: **2343 ESU**
2738 HH

Roughness: **Ra = 3,2**
Ra = 12,5

Cooling: **Conventional**

Polymer: **PC - Black**



2x Additive Manufacturing

Material: **MSI**

Roughness: **Ra = 3,2**
Ra = 12,5

Cooling: **Conformal**

Polymer: **PC - Black**

DRT
GROUP



2x Conventional (EDM)

Material: **2343 ESU**
2738 HH

Roughness: **Ra = 0,025**
Ra = 0,05

Cooling: **Conventional**

Polymer: **PC - Cristal**



2x Additive Manufacturing

Material: **MSI**

Roughness: **Ra = 0,025**
Ra = 0,05

Cooling: **Conformal**

Polymer: **PC - Cristal**

Polishing Strategy Protocol

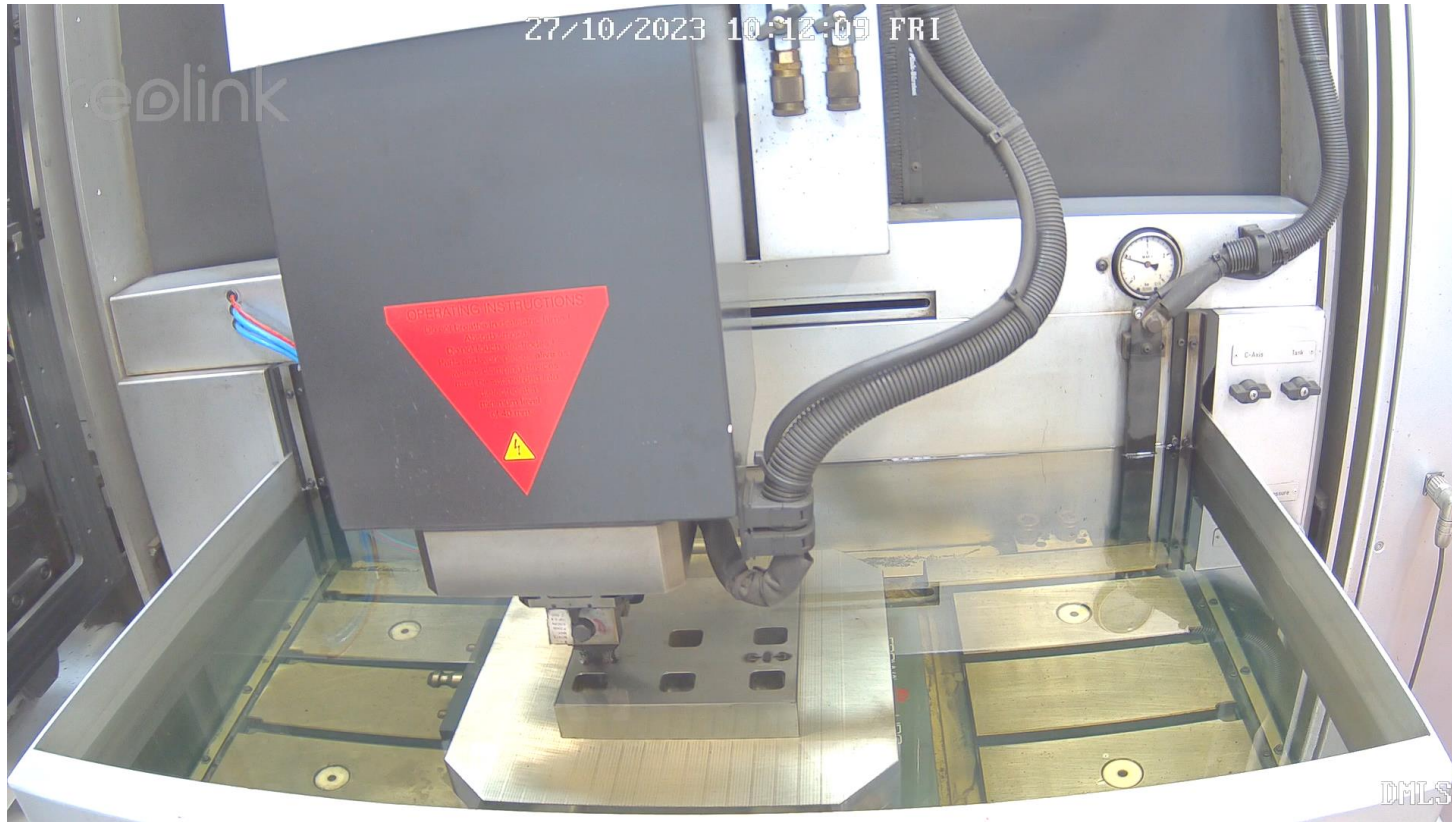
. Sandpaper 240, 600, 800, 2000

. Diamond paste 10μ, 5μ, 3,5μ, 1,5μ, 0,5μ

. Wooden Lapping Sticks – soft+hard



Electrical Discharge Machining (EDM)



EDM, also known as spark erosion, is a precise manufacturing process that utilizes **electrical discharges to shape metal components**. This technique is particularly valuable in the production of injection mold tools, enabling the creation of intricate and accurate mold components that are challenging to achieve with traditional machining methods.

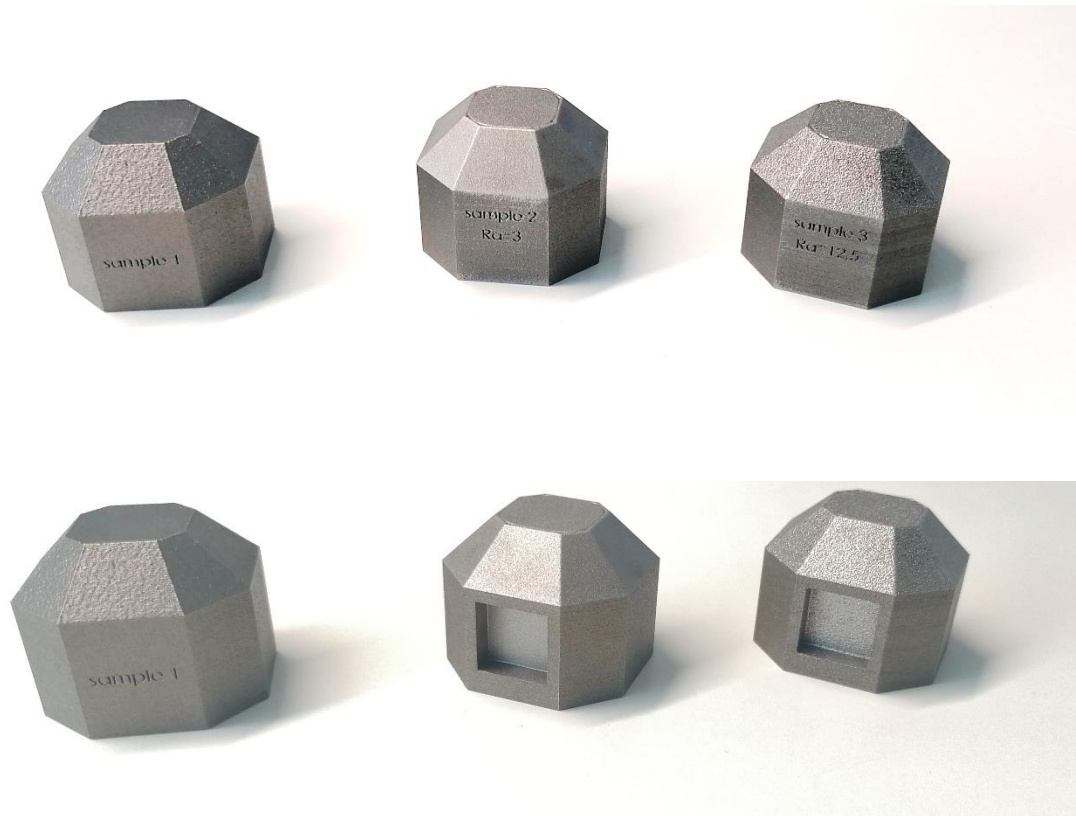
” **Sinker EDM** employs a specifically shaped electrode, often made of graphite or copper, which is submerged alongside the workpiece in a dielectric fluid.

Polishing hand process

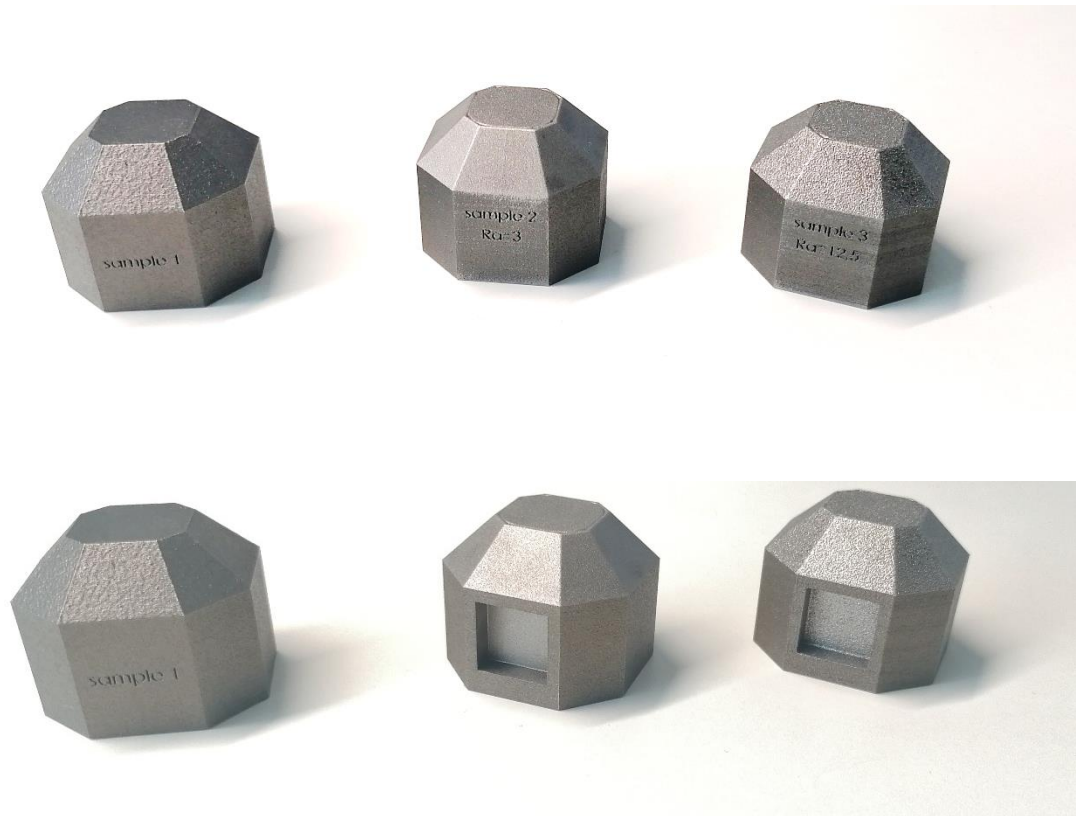


Polishing in injection mold manufacturing is a finishing process used to **refine the mold's surface by removing machining marks, tool marks, and imperfections.** This process involves using abrasive stones, diamond compounds, and specialized polishing tools to achieve the desired surface finish.

EDM Sample Characterization

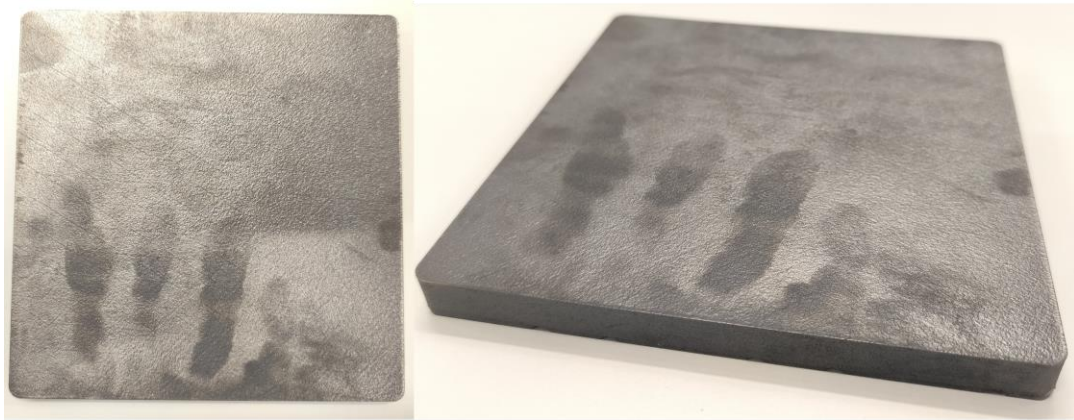


EDM Sample Characterization



EDM Sample Characterization

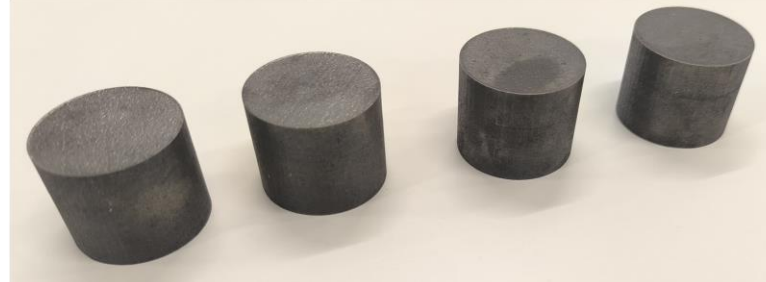
TASK



TASK



TASK



EDM Sample Characterization

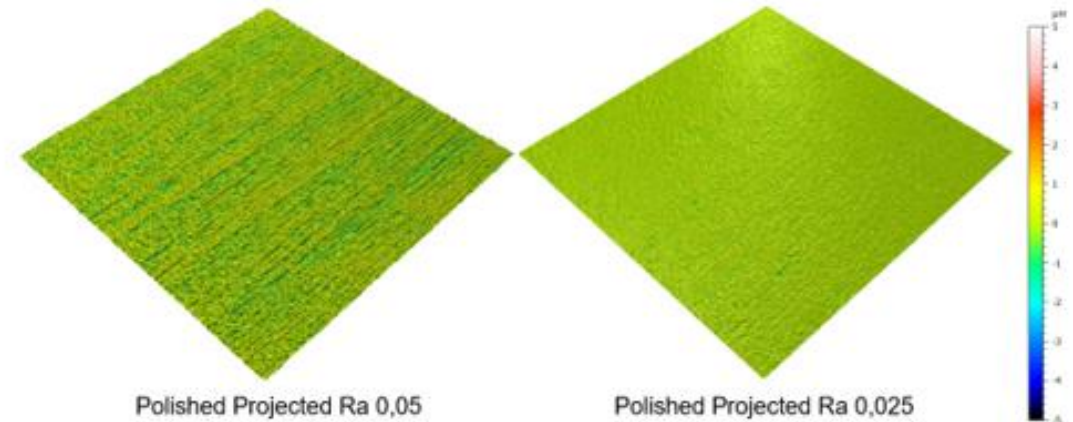


Polishing Sample Characterization



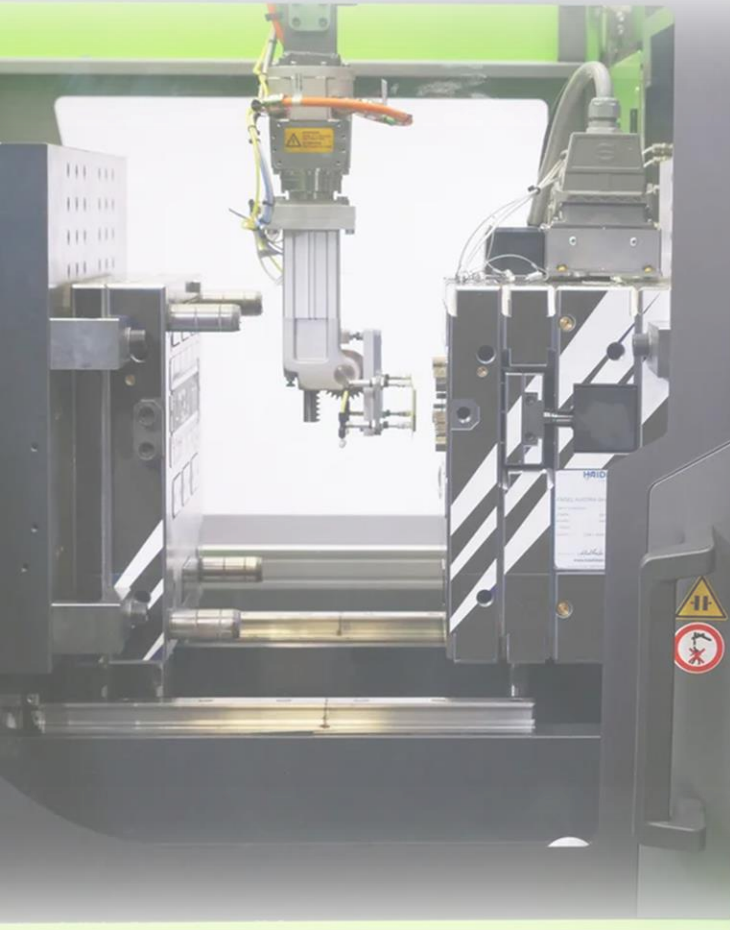
RA= 0,025
« mirror-like»

RA= 0,05
« high-gloss»



Sample	Measured Ra [μm]	Measured Sa [μm]
Ra 0.05	0.177	0.246
Ra 0.025	0.040	0.072

Plastic Injection Impact



Surface Defects on Parts

Poor Demolding

Inconsistent Gloss or Texture

Weld Line Visibility

Higher Reject Rate

Accelerated Mold Wear

Contamination Risk

Dimensional Inaccuracy



TECHNICAL WORKSHOP

Optimising steels microstructure and surface integrity to face new challenges in Additive Manufacturing



Funded by
the European Union

SuPreAM project has received funding from the European Union's
Research Fund for Coal and Steel (RFCS): project num. 101112346



Funded by
the European Union

Predictive simulation of finishing operations in steel Additive Manufacturing for optimal Surface integrity

Machining and CNC monitoring for AM steels – Aerospace use case

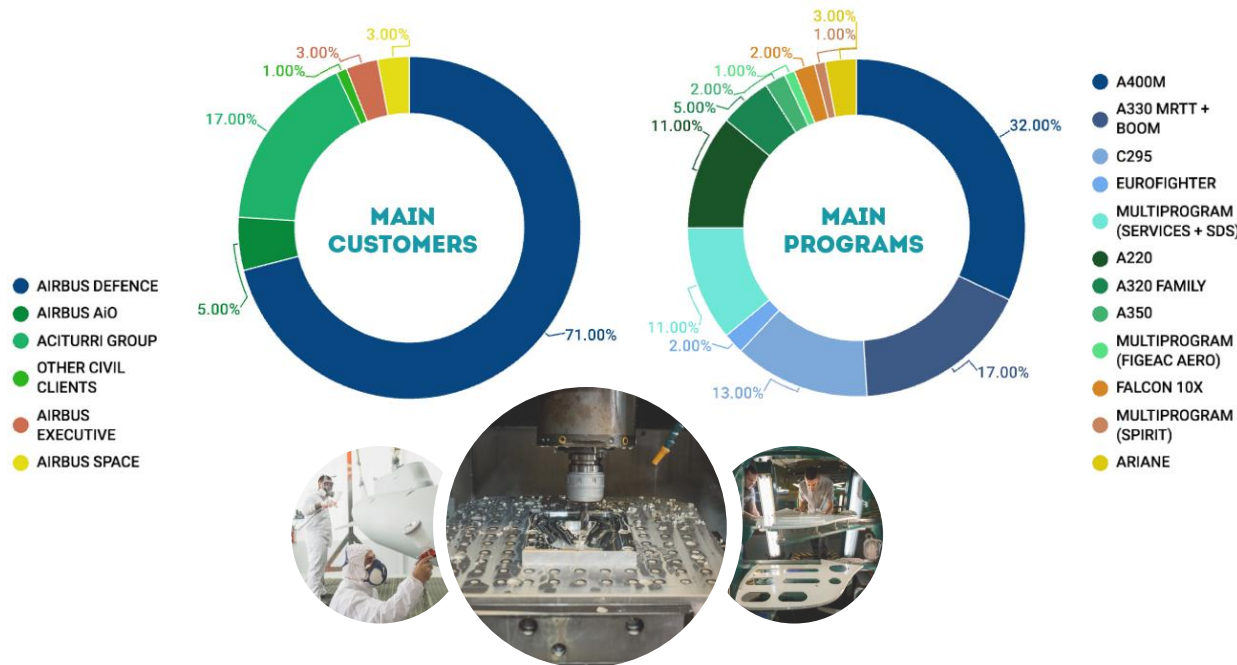
Luciano Villarreal
R&D Engineer, Sevilla Control
Luciano.villarreal@gsc-aero.com



Why SuPreAM is strategic for GSC?

Grupo Sevilla Control - Aerospace use case

A company fully committed to metallic manufacturing and assembly for the aerospace industry.



What challenges does Sevilla Control face and how does AM provide solutions?



Aerospace parts need high precision and reliability.



Many parts have different and some complex geometries.



Current machining strategies need optimization for AM materials



Aerospace use case

First goal: Evaluation and consolidation of steel additive technologies for manufacturing of complex aeronautical components.



Real use case involving a part of the refueling boom used in air-to-air refueling, belonging to the Airbus MRTT program.

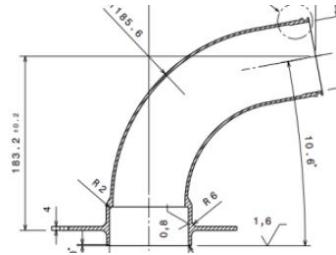
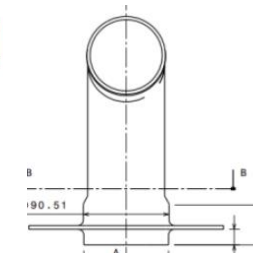
Why is this component a key focus?

COMPLEX GEOMETRIES

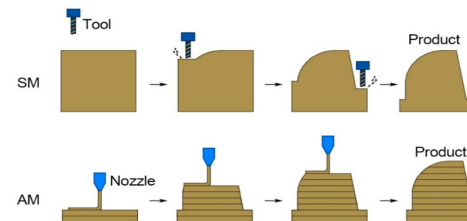
MEDIUM DIMENSION
(250 x 370 mm)

LOW RATES

HIGH COST MATERIAL



Compare both strategies

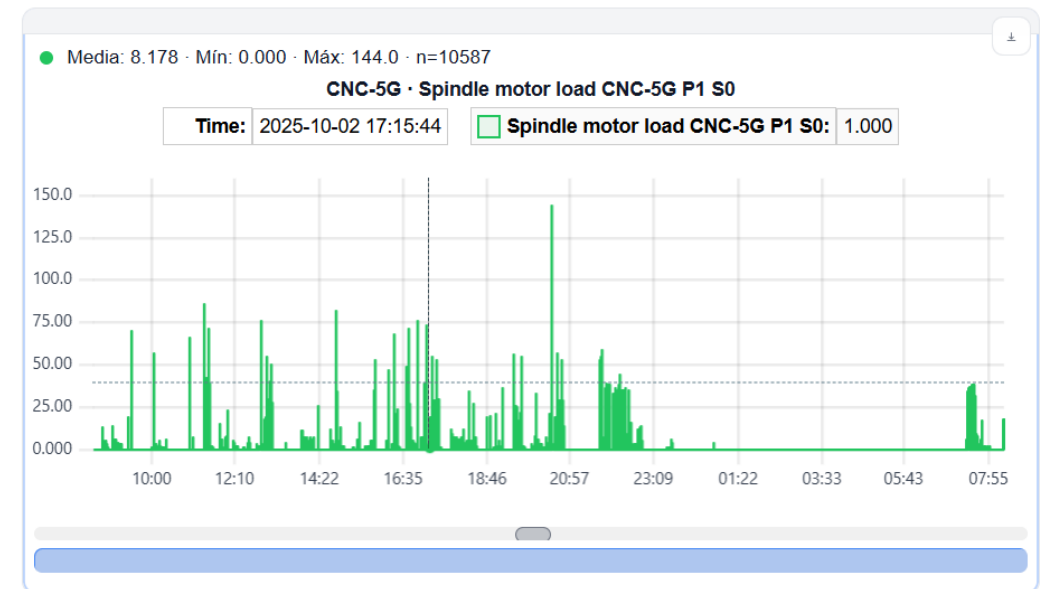
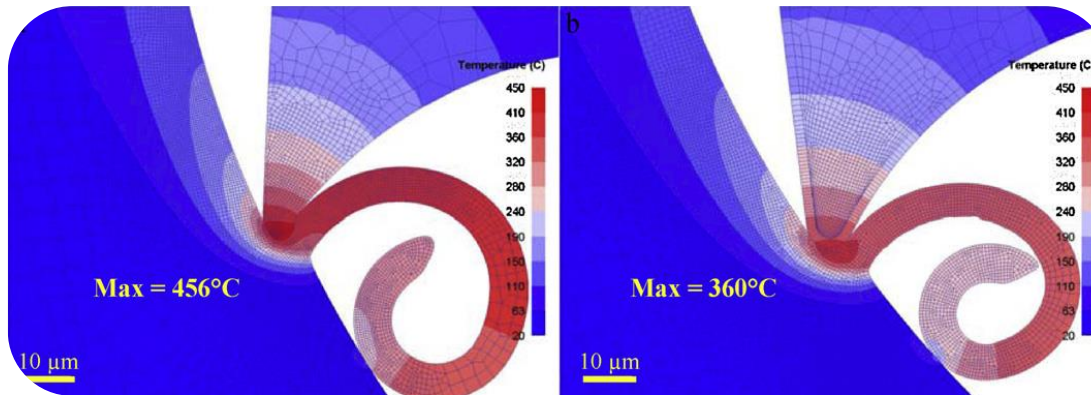


Indicator	Current Process	Planned Process	Advantages AM vs CNC
Final part weight (kg)	2,513	2,513	-
Initial material weight (kg)	141,40	3,00	97,88%
Buy-to-Fly ratio	98,22%	16,23%	83,47%
Machining time	3120,00	90,00	97,12%
Material cost (€)	4.242,00 €	360,00 €	91,51%

Aerospace use case

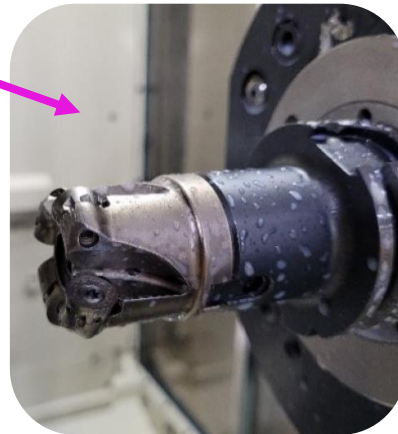
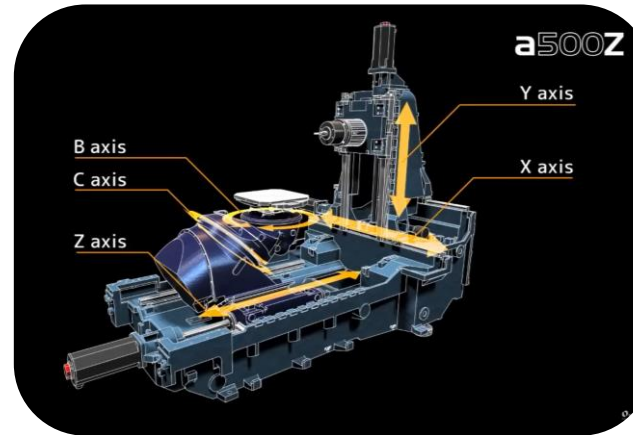
Second goal: Enhance predictive simulation models for machining processes.

During machining of test specimens, we collect data using our MTLINKi monitoring system from Fanuc, enabling precise process control and model validation.



Machining and finishing processes and strategies

Definition of machining condition and strategies and machining of sample parts

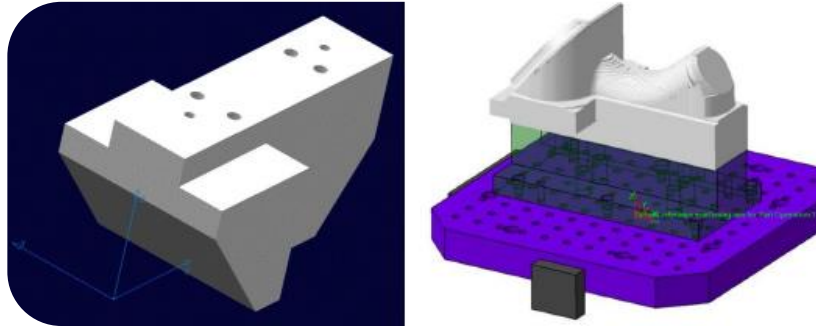


Design, AM and quality control of demonstrator: Redesign of geometry

Machining of test samples allows analysis of tool and material behavior, crucial for redesigning the elbow.



Current manufacturing process



Next steps:

- Analyse machining setup to minimize vibration impact.
- Evaluate adding supports if vibration control via strategy is insufficient.
- GSC will develop internal programming and machining strategies to optimize the process.

Vibrations, especially axial loads, are key factors affecting machining quality and tolerances.



TECHNICAL WORKSHOP

Optimising steels microstructure and surface integrity to face new challenges in Additive Manufacturing



Funded by
the European Union

SuPreAM project has received funding from the European Union's
Research Fund for Coal and Steel (RFCS): project num. 101112346



TECHNICAL WORKSHOP

Optimising steels microstructure and surface integrity to face new challenges in Additive Manufacturing



Funded by
the European Union

SuPreAM project has received funding from the European Union's
Research Fund for Coal and Steel (RFCS): project num. 101112346



Funded by
the European Union

Predictive simulation of finishing operations in steel Additive Manufacturing for optimal Surface integrity

New Materials and Processes in Additive Manufacturing: From LPBF to wire-DED

LAURA DEL RÍO FERNÁNDEZ
ARCELORMITTAL GLOBAL R&D
laura.delriofernandez@arcelormittal.com

ANA VELA MORENO
ARCELORMITTAL GLOBAL R&D
ana-gracia.vela@arcelormittal.com



- 01** Who we are
- 02** What we do
- 03** ArcelorMittal contribution to SuPreAM Project
- 04** Wire Laser Additive Manufacturing
- 05** New Steel powders for Additive Manufacturing: SAM1

ArcelorMittal Additive Manufacturing Area

Who we are



20 Full time Researchers

out of **240** Researchers in ArcelorMittal Global R&D SPAIN
and **1650** in Global R&D



■ Master/Engineers (65%)
■ Doctors (35%)



■ Male (65%)
■ Female (35%)

1 Department Director
1 Portfolio Leader
1 Area Leader
1 Scientist
7 Senior Researchers
12 Researchers



Strong Scientific Network with other R&D centers,
universities, and industrial partners worldwide.

What we do



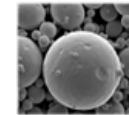
Multidisciplinary team within the Product and Process
Development Department, focus on bridging
advanced research with industrial steel applications.



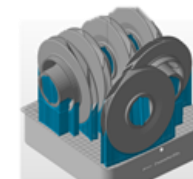
Materials development



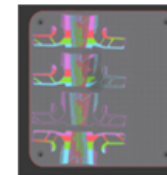
Powder production



Design



**Computational
and AI**



**Process development
& optimization**



**Co-engineering and technical
support to customers**

What we do

Material development

- All main steel families under study.
- New concepts and optimization of commercial ones.
- Material (in powder and in wire format)—process—property relationships.
- 12 patents granted on differentiated products (powders).

Atomization

- Two equipment: to develop our own alloys and optimize the process, but also for developments for specific applications and atomization on demand.
- 7 patents granted.

Design

- Additively Manufactured Spare Parts implemented in ArcelorMittal plants.
- Extensive experience on Additive Manufacturing Design for Automotive Applications.
- 5 patents granted.

Printing and post processing

- Process development on a wide range of machines.
- Process optimization in terms of repeatability, accuracy, timing, etc.
- Simulate, test and optimize in real conditions, iterating with design.

Characterization

- Specific Labs ISO 9001 certified.
- Built-in for internal development and technical support to customers.
- Global R&D internal network equipment for detailed characterization and end-use properties.

Computational and AI

- Processes optimization.
- Multiscale modeling and data processing.
- Generative design: from production to areas of concern (stress, tolerances...) and how to adapt parameters.
- 1 Patent + Industrial Secrets.



ArcelorMittal contribution to SuPream Project

Injection mold



Aerospace structural component



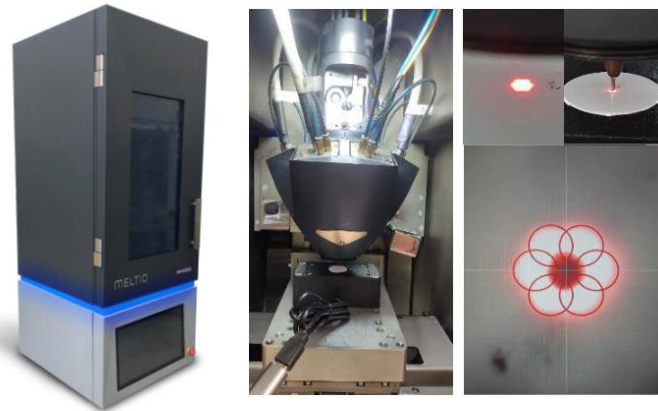
- To develop the optimal process for each steel grade and Additive Manufacturing Technology in order to avoid part defects and to achieve the optimal part properties.
- To design and implement new steels for Additive Manufacturing
- To redesign and optimize the additive manufacturing processes (LB-PBF & DED) for use-case components.

Wire Laser Additive Manufacturing

Wire-DED: ArcelorMittal capabilities

Meltio M450

Several units dedicated to material processing and process optimization.



Configuration Laser Head assembly with 3 axis cartesian
Build volume 150 x 170 x 425mm
Laser Power 1.2 kW – 6 Diode laser Beams (0,2 kW each one) – $\lambda = 976$ nm
Wire diameter 0.8-1.6 mm Ø wire
Software Open Source (Cura, Simplify) or License (Powermill, Meltio Horizon,...)

Capability to induce **Hot-wire** preheating to increment productivity and quality enhancement.

Multirobot cell

Large manufacturing plant with the possibility of using 16 movement axis at the same time, dedicated to complex parts.

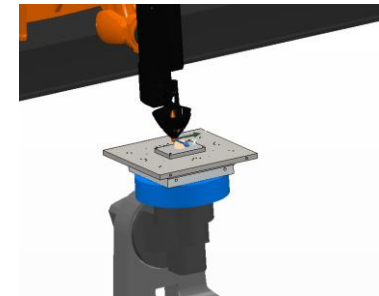


Configuration Laser Head assembly with Robot arm
Build volume 1000 x 1000 x 1000 mm
Laser Power 1.2 kW – 6 Diode laser Beam (0.2 kW per laser)
Wire diameter 0.8-1.2 mm Ø wire
Software Open Source (Cura) or Licensed (Powermill, Meltio Space, NX CAM)

Capability to induce **Hot-wire** preheating to increment productivity and quality enhancement.

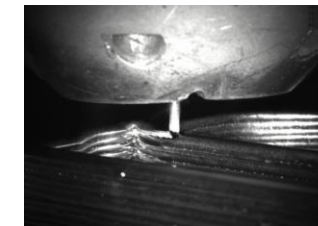
Digital Twin

- Programming complex sequence
- Non-planar multirobot printing
- Collision check
- Distortion simulation & correction



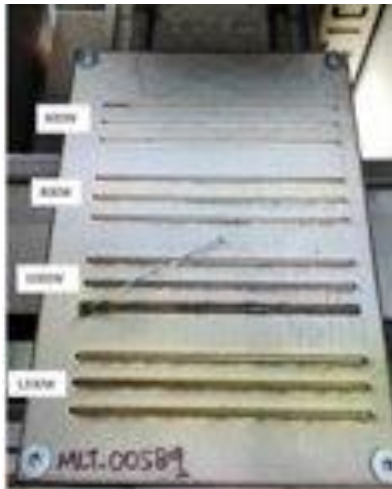
Process Monitoring

- Thermal Camera SWIR
- Quality assurance
- Monitoring on-fly

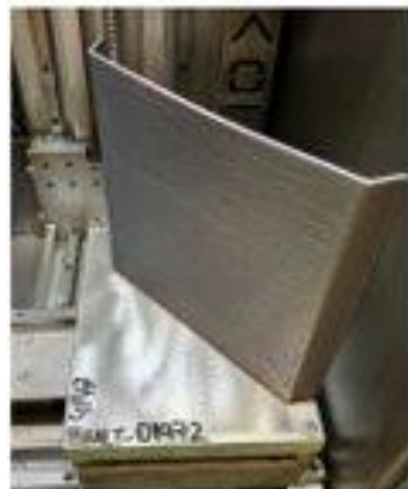


Process development 17-4PH steel grade: Methodology

Single tracks



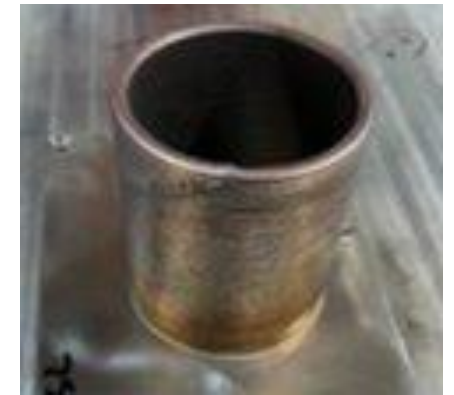
Hollow parts



Massive parts



Complex parts

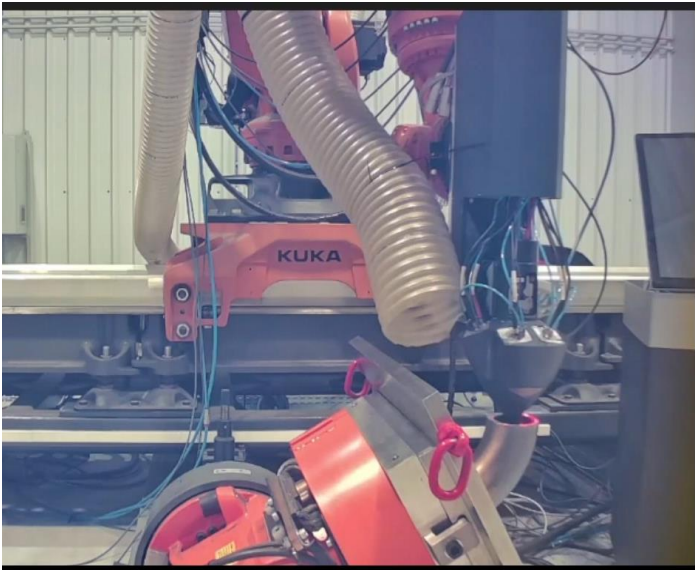


Process parameters wire-DED	Recommended values
Laser Power [W]	800 - 1200
Process Speed [mm/s]	8 - 12
Wire feed Speed [mm/s]	12 - 20
Shielding gas Flow [L/min]	15 - 20

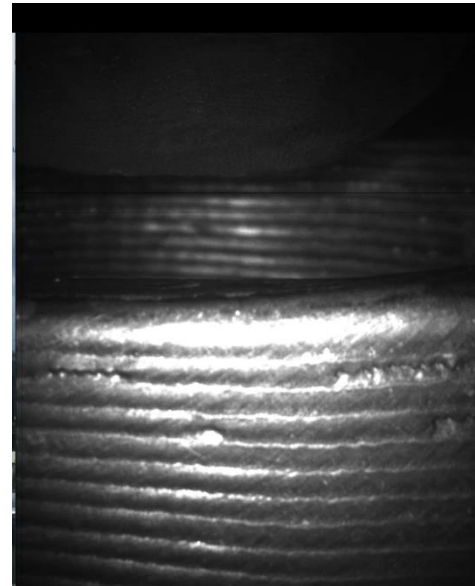
Geometry and printing strategy parameters	Recommended values
Layer Height [mm]	0.6 - 1.2
Hatch distance [mm]	0.8 - 1.4
Toolpath Strategy	Raster pattern, offset pattern..

Demonstrator generation

Objective: near shape part approach



6+2 axis path strategy
Non constant layer height



Adaptative Feed speed control
algorithm



Near to shape part
validation

New Steel powders for Additive Manufacturing

AdamiQ™ SAM 1. The Cobalt-Free sustainable replacement of M300

Motivation for creating the material / Industry need

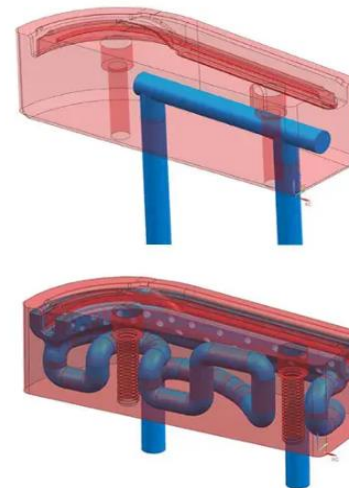
Lean maraging steels were developed to mimic the corrosion resistance of stainless steels. Their corrosion resistance is similar to that of maraging stainless alloys and significantly better than that of high-nickel (Ni) maraging steels. These alloys could be suitable for applications in mildly corrosive environments such as the food industry, pulp and paper, and oil & gas sectors. The chemical composition of lean maraging steels is optimized to achieve high strength compared to the conventional 18Ni300 maraging steel, which contains high amounts of cobalt (Co) and nickel (Ni).

Key Characteristics:

- Cobalt-free
- High printability
- Comparable mechanical properties to 18Ni300
- Enhanced corrosion resistance, similar to 17-4PH

Applications:

- Medium-low corrosion environments
- Aerospace
- Conformal-cooled mould tooling and Rubber Tyres mould (sipes)
- Oil and gas
- Thin gauge rolling



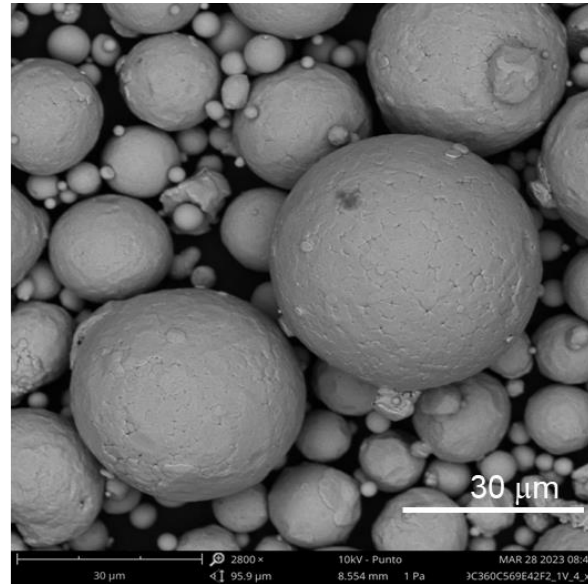
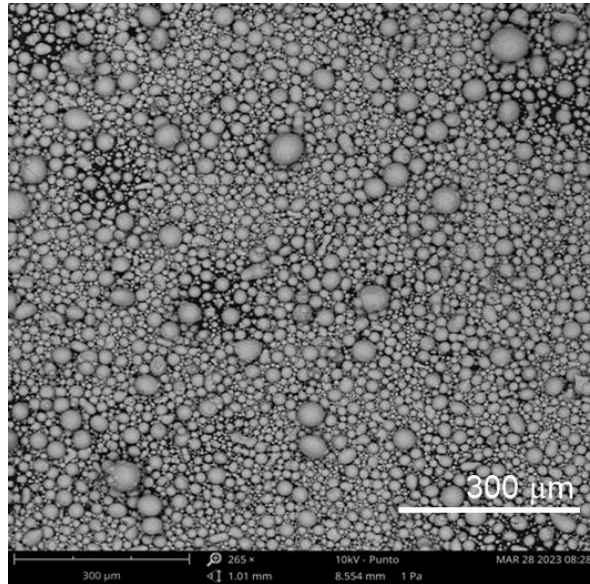
Conformal cooling insert mould.
Source: [Linear AMS](#)



Rubber Tyres mould (sipes)
Source: [AddUp / Michelin](#)

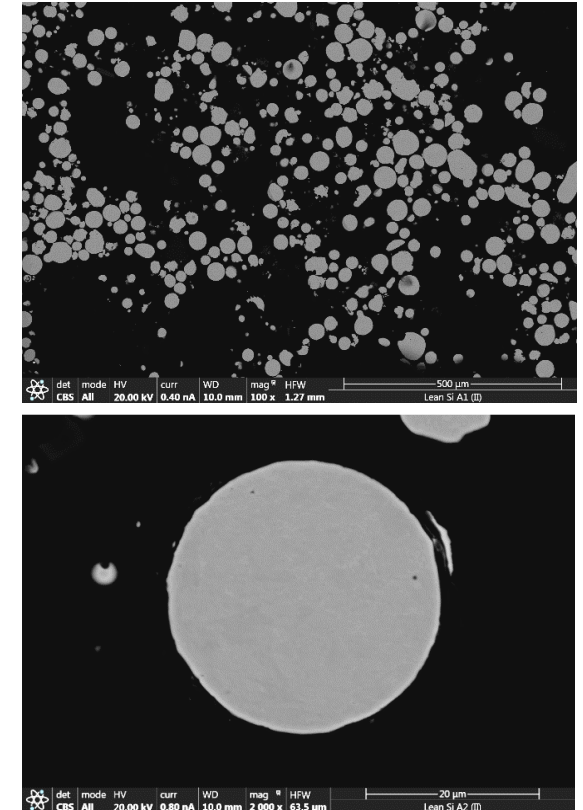
AdamiQ™ SAM 1. The Cobalt-Free sustainable replacement of M300

Powder morphology



Secondary Electron Microscopy (SEM) images of SAM1 powder with particle size between 20 and 63 microns.

- AdamiQ™ SAM 1 Steel powder is characterized by a spherical morphology and high packing density, which confer good flow properties.
- AdamiQ™ SAM 1 Steel powder is free of pores or voids as can be observed by LOM analysis.



Light Optical Microscope (LOM) images of powder cross section.

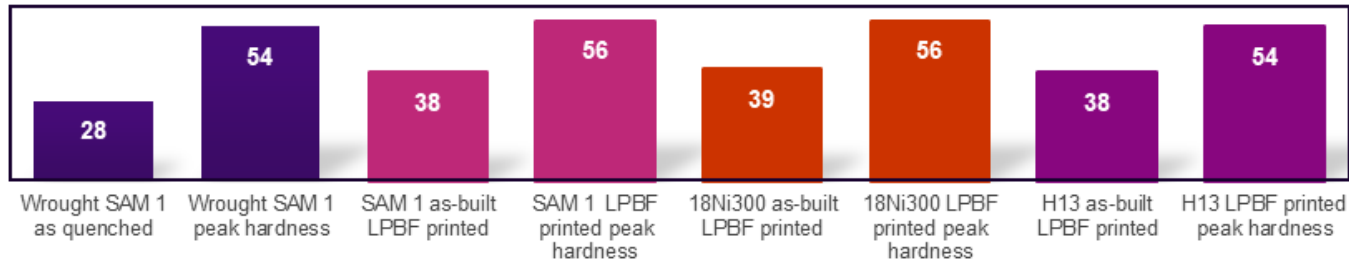
Our Steel Powders



- ✓ Cobalt risks removed
- ✓ Easy to print
- ✓ Corrosion Resistance similar to 17-4PH
- ✓ Hardness in the range of M300

Powder Chemical Composition

C	Ni	Cr	Si	Ti	Cu	P	S	O	N	Others
< 0.04	6 - 7.5	5 - 8.5	0.50 - 1.5	0.50 - 1.5	0.50 - 1	< 0.02	< 0.02	< 0.10	< 0.20	<1.5

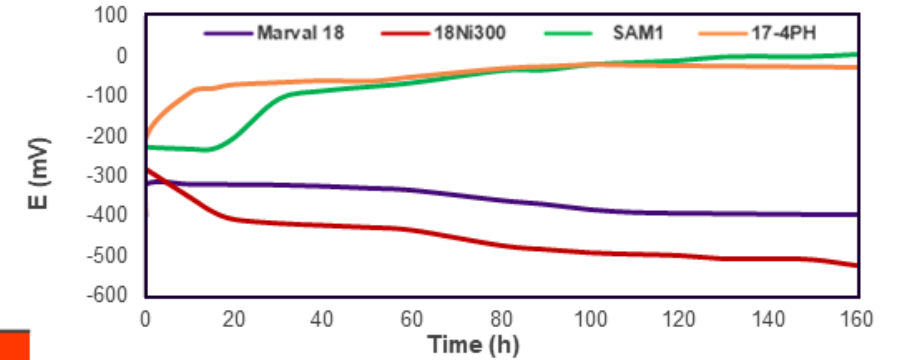


Peak Hardness HRC values comparison between SAM 1 (both the Wrought and the LPBF-printed experimental data), 18Ni300 and 17-4PH in the as-built and aged conditions.

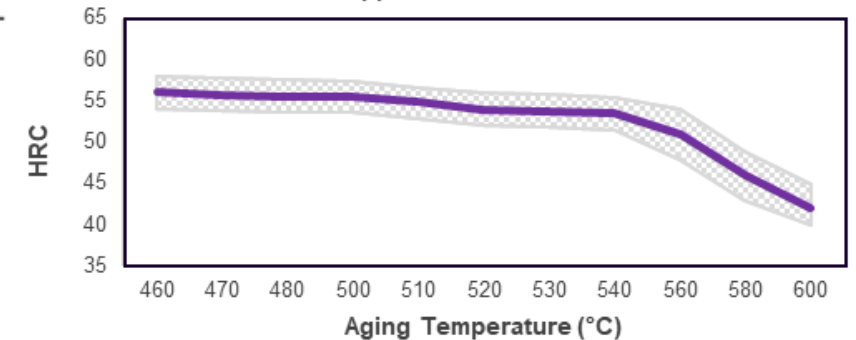
Mechanical properties As-Built machined samples (vertical orientation)

Yield Strength $R_{0.2}$ [MPa]	Tensile Strength R_m [MPa]	Elongation A [%]	Impact CVN at 20°C [J]	Impact CVN at -60°C [J]
961	1069	25	153	38

AdamIQ™ SAM 1 COBALT-FREE SUSTAINABLE REPLACEMENT OF M300



Open circuit potential evolution during 1 week immersion in 1000 ppm Cl⁻ at 20°C.



Aging temperature effect on hardness for LPBF-printed AdamIQ™ SAM1 composition.

Thank you



TECHNICAL WORKSHOP

Optimising steels microstructure and surface integrity to face new challenges in Additive Manufacturing



Funded by
the European Union

SuPreAM project has received funding from the European Union's
Research Fund for Coal and Steel (RFCS): project num. 101112346